WHOI-88-22

Woods Hole Oceanographic Institution
Massachusetts Institute of Technology

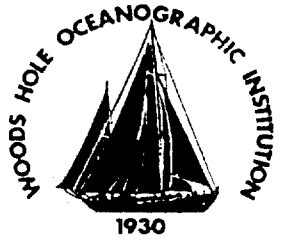

Joint Program
in Oceanography
and
Oceanographic Engineering

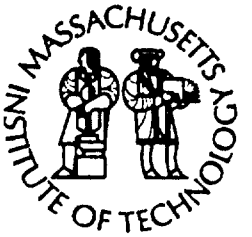

DOCTORAL DISSERTATION

The Kinetics and Thermodynamics of Copper Complexation in Aquatic Systems

by

Janet G. Hering

June 1988

WHOI-88-22

The Kinetics and Thermodynamics of Copper Complexation in Aquatic Systems

by

Janet G. Hering

Woods Hole Oceanographic Institution
Woods Hole, Massachusetts 02543

and

The Massachusetts Institute of Technology
Cambridge, Massachusetts 02139

June 1988

Doctoral Dissertation

Funding was provided through the Massachusetts Institute of Technology by NOAA; the National Science Foundation; and by the Office of Naval Research.

 This thesis should be cited as:
Janet G. Hering, 1988. The Kinetics and Thermodynamics of Copper Complexation in Aquatic Systems.
Ph.D. Thesis. MIT/WHOI, WHOI-88-22.

Approved for publication; distribution unlimited.

Approved for Distribution:

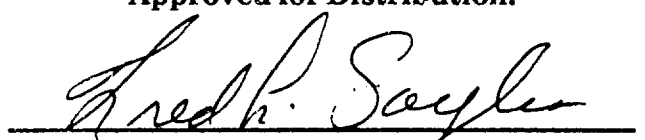

Frederick L. Sayles, Chairman
Department of Chemistry

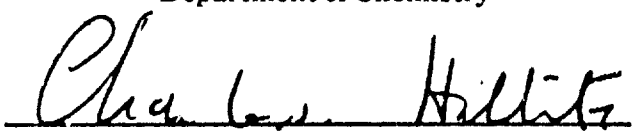

Charles D. Hollister
Dean of Graduate Students

THE KINETICS AND THERMODYNAMICS OF COPPER COMPLEXATION IN AQUATIC SYSTEMS

by

JANET GORDON HERING

A.B., Cornell University
(1979)
A.M., Harvard University
(1981)

Submitted in partial fulfillment of the
requirements for the degree of

DOCTOR OF PHILOSOPHY

at the

MASSACHUSETTS INSTITUTE OF TECHNOLOGY

and the

WOODS HOLE OCEANOGRAPHIC INSTITUTION

May 1988

Signature of Author _____
Joint Program in Oceanography,
Massachusetts Institute of Technology/
Woods Hole Oceanographic Institution

Certified by _____
François M.M. Morel
Thesis Supervisor

Accepted by _____
John Edmond
Chairman, Joint Committee for Chemical Oceanography
Massachusetts Institute of Technology/
Woods Hole Oceanographic Institution

THE KINETICS AND THERMODYNAMICS OF COPPER COMPLEXATION IN AQUATIC SYSTEMS

by

JANET GORDON HERING

ABSTRACT

Copper complexation is ubiquitous in natural waters. Yet, many questions remain on the chemistry and biogeochemistry of naturally-occurring complexing agents. This thesis examines the sources and extent of biological cycling of such complexing agents and also the physical-chemical nature of their interactions with copper.

Investigations of copper complexation in coastal ponds and coordinated laboratory studies suggest that both labile, biogenic and refractory ligands contribute to the observed copper complexation. Culture and incubation experiments demonstrate ligand production associated with phytoplankton photosynthetic activity and suggest microbial degradation of complexing agents. However in the coastal ponds studied, the biological cycling of natural complexing agents is obscured possibly due to contributions of refractory ligands to the observed copper complexation, mixing of pond waters with coastal seawater, or to the natural balance between biological production and degradation.

The physical-chemical nature of interactions of humic acids with copper was studied by examining both the thermodynamics and kinetics of these interactions. Extensive studies of the kinetics of metal- and ligand-exchange reactions with well-defined ligands under natural water conditions (i.e.- low concentrations of reacting species and the presence of competing metals and ligands) provide a mechanistic framework for examining the kinetics of metal-humate complexation reactions.

Study of the kinetics of copper-for-calcium metal-exchange reactions and metal titration experiments (individual metal titrations

with calcium or copper and copper titrations in the presence of calcium as a competing metal) show that alkaline earth and transition metals do not compete for the same humate metal-binding sites.

Ligand exchange reactions between humate-bound copper and a fluorescent complexing agent proceed both through dissociation of the initial copper-humate species and by direct attack of the incoming ligand on the initial copper complex. The relative importance of these mechanisms is dependent on the copper-to-humate loading. Both of these mechanisms should contribute to overall ligand exchange reactions at the copper-to-humate loadings typical of estuarine and coastal waters.

The observed kinetics of ligand exchange reactions with copper-humate species is consistent with the reaction of copper bound at discrete humate metal-binding sites. Apparent saturation of the strong copper-binding site (i.e.- slow-reacting copper-humate species) at high copper-to-humate loadings allows estimation of the strong copper-binding site density ($\approx 10^{-7}$ mol/mg humic acid) and of the conditional stability constant for copper binding at that site ($\approx 10^{10.1}$).

Investigations of ligand-exchange reactions of humate-bound copper in the presence of seawater concentrations of calcium demonstrate that the kinetics of metal coordination reactions under natural water conditions cannot be neglected. Even at high copper-to-humate loadings, the formation of CuEDTA on addition of copper to a mixture of humic acid and EDTA (0.01 M Ca, pH = 7.3) proceeded over the course of several hours as compared with immediate formation of CuEDTA in the absence of calcium. Based on these results, equilibrium for this reaction in seawater at environmental copper-to-humate-loadings and lower EDTA concentrations is predicted to occur on a time scale of months to years.

The kinetics of coordination reactions with humic acids may be interpreted to provide information on the nature of metal-humate interactions. This information complements equilibrium studies of such interactions. In the field, the study of the interactions of metals with naturally-occurring complexing agents is complicated by the presence of mixtures of labile, biogenic and refractory ligands. Finally, this work indicates that the assumption of fast equilibration of metals and ligands (i.e.- pseudoequilibrium) in seawater is not valid.

"At a certain point you say to the woods, to the sea, to the mountains, the world. Now I am ready. Now I will stop and be wholly attentive. You empty yourself and wait, listening. After a while you hear it: there is nothing there. There is nothing but those things only, those created objects, discrete, growing or holding, or swaying, being rained on or raining, held, flooding or ebbing, standing, or spread. You feel the world's word as a tension, a hum, a single chorused note everywhere the same. This is it: this hum is the silence. Nature does utter a peep- just this one. The birds and the insects, the meadows and swamps and rivers and stones and mountains and clouds: they all do it; they all don't do it. There is a vibrancy to the silence, a suppression as if someone were gagging the world. But you wait, you give your life's length to the listening, and nothing happens. The ice rolls up, the ice rolls back, and still that single note obtains. The tension, or lack of it, is intolerable. The silence is not actually suppression; instead, it is all there is."

Annie Dillard
Teaching a Stone to Talk

"But no matter whether my probings made me happier or sadder, I kept on probing to know."

Zora Neale Hurston
Dust Tracks on a Road

"What we see depends mainly on what we look for."

Salada Tea bag

ACKNOWLEDGEMENTS

Certainly it is impossible in a few words of acknowledgement to describe fully the contributions of family, friends, and colleagues to this work or to express fully my thanks for the support, encouragement, and instruction so freely given.

My parents have from my earliest memory encouraged my intellectual development and have unstintingly supported my academic career. I thank them for their love and the many opportunities they have afforded me.

My brothers and friends have provided the balance of fun and support necessary to survive graduate work. For their friendship I thank Lou and Jim, Deb Backhus, Liz Sikes, Lynn Roberts, Kathleen Newman, Anne Carey, Ginger Armbrust, Susan Silverstein, Rita Long, Kay Stone, and Lyn Rossano.

On a practical level, I would like to acknowledge the assistance of several individuals and agencies. I thank Dave Kulis for help in culturing phytoplankton and both him and Ann Michaels for help in field sampling. I thank Margie Roulier for her library research. And I thank Susan Chapnick, Paula Rosener, and Ed Boyle for instruction in trace metal analysis. This thesis work was financially supported by NOAA (grant NA79 AA-D-00077), NSF (grants OCE-8317532 and OCE 8615545), ONR (grant N00014-86-K-0325), and the International Copper Research Association (INCRA Project No. 364A).

Finally, I would like to acknowledge the feed-back, criticism, and instruction provided by my colleagues at MIT and WHOI. I thank the many students and post-docs who have listened to and commented on my ongoing work in research group meetings, especially Bill Fish, David Waite, David Dzombak, Gail Harrison, Kathleen Newman, Gary Jones, Brian Palenik, Steve Cabaniss, and Bob Hudson. I owe special thanks to the members of my thesis committee, Cindy Lee, Don Anderson and Ed Boyle, for their insight, advice and criticism and particularly to Francois Morel whose scientific understanding guided and shaped my research work and whose friendship and encouragement made the completion of this thesis possible.

TABLE OF CONTENTS

LIST OF FIGURES

PAGE

CHAPTER TWO

CHAPTER THREE

CHAPTER FOUR

CHAPTER FIVE

CHAPTER SIX

PAGE

APPENDIX A

APPENDIX B

LIST OF TABLES

PAGE

APPENDIX A.

APPENDIX B

CHAPTER 1

INTRODUCTION

Organic complexation of transition metals in natural waters has a profound influence on metal biogeochemistry. Metal speciation influences biological availability of metals (Anderson and Morel, 1978; Sunda and Guillard, 1976; Anderson and Morel, 1982) as well as chemical processes such as sorption (Dalang et al., 1984; Davis and Leckie, 1978, 1979), precipitation/dissolution (Campbell and Tessier, 1984), and oxidation/reduction (Waite and Morel, 1984, Finden et al., 1984). Metal complexation appears to be ubiquitous in the aquatic environment, occuring in fresh (Sunda and Hanson, 1979; Cabaniss and Shuman, in press) and saline (Hering et al., 1987 and ref. cit.) and under both pristine (Sunda and Ferguson, 1983; Coale and Bruland, submitted) and polluted regimes (Hering et al., 1987). For copper, the extent of complexation is close to 100%.

Many questions on metal complexation in natural waters remain unresolved. The sources, structures, and extent of biological cycling of naturally-occuring complexing agents are largely unknown. Some of the metal complexation is natural waters is likely due to complexation by humic substances. Humic substances isolated from natural waters have been shown to bind many metals (Hering and Morel, submitted; Fish, 1984; Sunda et al., 1984; Cabaniss and Shuman, 1984) and are present in whole waters at concentrations sufficient to contribute significantly to the observed metal complexation. Metal complexation by biogenic ligands in

natural waters has been inferred from observed production of complexing agents in cultures of phytoplankton (McKnight and Morel, 19980; Imber and Robinson, 1983; Trick et al. 1983), bacteria (Neilands, 1981; Actis et al, 1986), fungi (Neilands, 1984), and some higher organisms (Fish and Morel, 1983). However, evidence from the field supporting biological production of complexing agents is more tenuous. It is not clear to what extent the biota, through production and degradation of complexing agents, influences metal speciation in the environment nor what proportion of metal complexing agents in natural waters are labile, biogenic compounds rather than refractory geopolymers such as humic substances.

The interactions of metals and natural complexing agents have been modeled by analogy with the interactions of well-defined organic ligands (or polymers) and metals. There has been a proliferation of models describing metal-humate (or metal-natural complexing agents) interactions largely because the available data has not been sufficient to discriminate between models (Fish et al., 1986; Dzombak et al., 1986; Cabaniss and Shuman, 1988). Thus the models cannot provide information as to the structure of natural complexing agents or the nature of their interactions with metals.

The models applied to metal complexation all assume equilibrium (or pseudo-equilibrium) between complexing agents and dissolved metal species and rapid re-equilibration of the system after any perturbation of metal speciation. However there have been relatively few investigations of the kinetics of metal coordination reactions under environmentally representative conditions (pH, major cations, trace

metal and ligand concentrations, etc.) and, for the most part, the assumption of rapid equilibration of metal and ligand species remains untested.

This thesis investigates several of the questions raised above. Chapter 2 reports on a comparison of laboratory and field studies examining biological cycling of natural complexing agents. Culture and incubation experiments show production of complexing agents associated with phytoplankton photosynthetic activity and microbial degradation. Trends in copper complexation observed in the field in a diel study are consistent with this hypothesis although overall changes in copper complexation are quite small. This chapter is to be submitted as a research paper with Dr. C. Lee as a co-author. Her suggestions on experimental design and editorial comments were a substantial contribution to this work.

Copper and calcium complexation by isolated humic substances are described in chapter 3. The comparison of individual metal titrations and competition experiments provide additional constraints for modeling metal-humate interactions.

Chapters 4-6 report on the investigations of the kinetics of metal coordination reactions. Relatively simple systems are examined in chapters 4 and 5 to determine factors controlling the rates of metal-exchange (chapter 4) and ligand-exchange (chapter 5) reactions. The focus is on measuring rates of reactions under environmentally appropriate conditions and on relating the observed kinetics with the thermodynamics of metal-ligand interactions. In chapter 6, more complex systems (mixtures of competing metals and ligands) are investigated. A

model system is studied to demonstrate the conditions under which slow coordination reactions may be expected. Experiments with humic substances and a strong synthetic ligand show that the assumption of rapid equilibration of ligands and metals under natural or analytical conditions with low concentrations of metals and ligands and seawater calcium concentrations is not valid.

The appendices describe some additional work on measurement of copper and ligand speciation and provide ancillary data to chapters 4 and 5. A field comparison of methods for determination of copper complexation is described in Appendix A. This paper was published in Marine Chemistry and was co-authored by Drs. R. Ferguson, W. Sunda and F. Morel. Drs. Ferguson and Sunda provided the bacterial bioassay data. Drs. Sunda and Morel assisted in editing the manuscript. Appendix B describes an analytical method for the determination of ligand speciation using a fluorescent ligand. This appendix provides some of the background for chapter 5. Data from the kinetics experiments discussed in Chapters 4 and 5 are given in appendices C and D.

Chapter 7 consists of a brief summary of the conclusions of the other chapters.

REFERENCES

Actis, L.A., W. Fish, J.H. Crosa, K. Kellerman, S.R. Ellenberger, F.M. Hauser and J. Sanders-Loehr (1986) J. Bacteriol. 167: 57-65.

Anderson, D.M. and F.M.M. Morel (1978) Limnol. Oceanog. 23: 283-95.

Anderson, M.A. and F.M.M. Morel (1982) Limnol. Oceanog. 27: 789-813.

Cabaniss, S.E. and M.S. Shuman (1988) Geochim. Cosmochim. Acta 52: 185-93.

Campbell, P.G.C. and A. Tessier (1984) in Trace Metal Complexation in Natural Waters, ed. C.J.M. Kramer and J.C. Duinker. The Hague: Martinus Nijhoff/ Dr. W. Junk Pub. pp. 67-81.

Coale, K.H. and K.W. Bruland submitted to Limnol. Oceanog.

Dalang, F., J. Buffle, W. Haerdi (1984) Environ. Sci. Technol. 18: 135-41.

Davis, J.A. and J.O. Leckie (1978) Environ. Sci. Technol. 12: 1309-15.

Davis, J.A. and J. O. Leckie (1979) Environ. Sci. Technol. 13: 1289-91.

Dzombak, D.A., W. Fish and F.M.M. Morel (1986) Environ. Sci. Technol. 20: 669-75.

Finden, D.A.S., E. Tipping, G.H.M. Jaworski, C.S. Reynolds (1984) Nature 309: 782-3.

Fish, W. (1984) Ph.D. Thesis, Massachusetts Institute of Technology, Cambridge, MA.

Fish, W. and F.M.M. Morel (1983) Can. J. Fish. Aquat. Sci. 40: 1270-7.

Fish, W., D.A. Dzombak and F.M.M. Morel (1986) Environ. Sci. Technol. 20: 676-83.

Hering, J.G, W.G. Sunda, R.F. Ferguson and F.M.M. Morel (1987) Mar. Chem. 20: 299-312.

Hering J.G. and F.M.M. Morel, submitted to Environ. Sci. Technol.

Imber, B.E. and M.G. Robinson (1983) Mar. Chem. 14: 31-41.

McKnight, D.M. and F.M.M. Morel (1979) Limnol. Oceanog. 24: 823-37.

McKnight, D.M. and F.M.M. Morel (1980) Limnol. Oceanog. 25: 62-71.

Neilands, J.B. (1981) Ann. Rev. Biocem. 50: 715-31.

Neilands, J.B. (1984) Microbial Sciences 1: 9-14.

Sunda, W.G. and R.F. Ferguson (1983) in Trace Metals in Seawater, ed. C.S. Wong, E. Boyle, K.W. Bruland, J.D. Burton, and E.D. Goldberg. New York: Plenum Press, pp. 871-891.

Sunda, W.G. and R.R. Guillard (1976) J. Mar. Res. 34: 511-29.

Sunda, W.G. and P.J. Hanson (1979) in Chemical Modeling in Aqueous Systems, ed. E.A. Jenne. Washington: ACS. pp. 147-80.

Sunda, W.G., D. Klaveness, A.V. Palumbo (1984) in Trace Metal Complexation in Natural Waters, ed. C.J.M. Kramer and J.C. Duinker. The Hague: Martinus Nijhoff/ Dr. W. Junk Pub. pp. 399-409.

Trick, C.G.. R.J. Andersen, A. Gillam, P.J. Harrison (1983) Science 219: 306-8.

Waite, T.D. and F.M.M. Morel (1984) Environ. Sci. Technol. 18: 860-8.

CHAPTER TWO

SOME EFFECTS OF BIOLOGICAL ACTIVITY ON COMPLEXATION OF COPPER

ABSTRACT

Seasonal and diel measurements of copper complexation in two salt ponds are compared with laboratory studies of copper complexation in phytoplankton cultures and incubation experiments. Laboratory studies suggest that the biota may be involved in the cycling of naturally-occurring copper complexing agents. However, in the field, only small changes in copper complexation were observed even with large changes in photosynthetic activity (in a diel study) and copper complexation was not correlated with phytoplankton abundance (in a seasonal study). The lack of an effect of phytoplankton activity on measured copper complexation in the field may be due to tight coupling between biological production and degradation processes resulting in a steady-state concentration of complexing agents and to a significant contribution of refractory ligands, such as humic materials, to overall copper complexation.

INTRODUCTION

Complexation of copper occurs in a wide variety of aquatic environments from the oligotrophic open ocean (Coale and Bruland, submitted; Sunda and Ferguson, 1983) to more productive coastal waters (Hering, et al., 1987; Kramer and Duinker, 1984; Moffett and Zika, 1987;

Wood et al., 1983; van den Berg, 1984a,b; Huizenga and Kester, 1983; Mackey, 1983). The extent of complexation in surface waters is close to 100% complexation for Cu. Observed metal complexation has been largely attributed to the presence of organic complexing agents and has been described in terms of equilibrium association of metals with natural ligands (following Stumm and Morgan, 1981; Morel, 1983).

The presence and importance of organic complexing agents has been inferred from several lines of evidence. Metal complexing or buffering capacity is removed by UV-oxidation of water samples (Sunda et al., 1984; Anderson et al. 1984). Organic material isolated from natural waters (i.e.- humic materials) has been shown to bind many metals (Hering and Morel, submitted and ref. cit.). Humic materials are present in whole waters at concentrations (up to 1.2 mg/L in seawater and up to 8.0 mg/L in freshwaters, Thurman, 1986) sufficient to contribute significantly to observed metal complexation. A correlation between DOC and metal complexation has also been shown (Newell and Sanders, 1986). In addition, biological production of metal complexing agents has been observed in cultures of phytoplankton (McKnight and Morel, 1979,1980; Trick et al., 1983a,b; Imber and Robinson, 1983; Swallow et al. 1978; Serriti et al. 1986), bacteria, and fungi (Neilands, 1981,1984; Actis et al., 1986) as well as some higher organisms (Fish and Morel, 1983). Although adsorption of metals onto inorganic colloids might contribute to the overall complexing ability of the "dissolved" fraction of natural waters, the surfaces of particles found in natural waters are coated with organic material (Hunter and

Liss, 1982). Thus the interactions of metals with colloidal particulates may be dominated by the nature of the surficial organic matter.

Recently, it has been suggested that the apparent complexation of ambient copper in surface waters may be due in part to the presence of collloidal copper sulfides (Luther et al., 1976; Luther and Swartz, 1988). The presence of free sulfide in oxic waters has also been postulated (Elliott et al., 1988). It is unlikely, however, that sufficient free sulfide to account for the observed strong complexation of copper added to natural water samples, up to ≈ 50 nM copper (Hering et al., 1987), is present in oxic waters.

Complexation of trace metals by naturally-occurring organic ligands may reflect the influence of the biota on the chemistry of the aquatic environment. In oceanic systems, the vertical profile of complexing agents also suggests a biological source for the ligands (Kramer 1985, Coale and Bruland, submitted). However, efforts to demonstrate a direct link between biological activity and metal complexation have been mostly inconclusive. Metal complexation has been correlated with phytoplankton abundances in enclosure experiments (Imber and Robinson, 1983) but not in tidal ponds or coastal waters (Anderson et al.,1984).

This paper presents results of seasonal and diel studies of metal complexation in two coastal ponds and compares field measurements with phytoplankton culture and incubation experiments. Although production of complexing agents was observed in laboratory cultures and changes in Cu complexation occured on incubation of natural water samples,

relatively constant Cu complexation was observed in field samples. The stability of metal buffering capacity in these environments may be due to the contribution of relatively refractory ligands, possibly terrestrial humic materials (as suggested by Anderson et al., 1984), or to a steady-state between biological production and consumption of more labile natural complexing agents.

EXPERIMENTAL SECTION

Field samples were taken from two shallow salt ponds in Falmouth, MA. Both Salt and Perch Ponds are small (Salt Pond 29 ha, Perch Pond 66 ha), shallow (<6 m), eutrophic salt ponds on Vineyard Sound in Falmouth, MA. Perch Pond is connected to Vineyard Sound through Great Pond by shallow inlets and is subjected to restricted tidal flushing (as described by Garcon et al., 1986) Salt Pond is an enclosed marine glacial basin which is highly stratified with an oxygen-depleted epilimnion and an anoxic, more saline hypolimnion (Kim and Emery, 1971). At our sampling site, H_2S concentrations in the anoxic waters are high (5 mM); the depth below which H_2S is present varies seasonally from 3 m in the summer to 5 m in the winter (Wakeham et al., 1984). Salinities at both sites were approximately 25^{o}/oo; the salinity at Perch Pond ranged from 23 to 28^{o}/oo over the study period.

Field samples were collected in acid-washed polyethylene bottles using an all-polyethylene collection system as described by Anderson et al. (1984). Amperometric titrations of Salt Pond samples were begun within 1 h of sample collection. For the diel study, samples were

collected from Salt Pond over an 18-h period on October 9-10, 1985. The sampling depth was 3 m, the depth of the chl a maximum. Samples for amperometric titration were stored in polyethylene at 4^{o} C until analysis (analyses were performed within 24 h of sampling except for analyses of replicate samples taken on Nov. 14 and Feb. 1). For the seasonal study, depth-integrated samples were taken (as described by Anderson et al, 1984) from Perch Pond from November 1984 to April 1985. All samples were collected between 1100 and 1400h. Samples for incubation experiments were collected from Perch Pond on Feb. 26, 1985. Depth-integrated samples, either filtered (0.45 μm Nuclepore) or unfiltered, were stored in acid-washed polyethylene containers. Light incubated samples were subject to constant illumination at 200 $\mu Em^{-2}sec^{-1}$. All unfiltered, incubated samples were filtered through 0.45 μm Nuclepore filters immediately prior to titrations.

During the seasonal study, the dinoflagellate Heterocapsa triquetra was counted in Perch Pond samples by microscopic examination. Under bloom conditions, H. triquetra was essentially the only algal species observed. Before and after the bloom (Nov. 14 and Apr. 24), approximately 20% of the mixed phytoplankton population was H. triquetra.

For the culture study, Heterocapsa triquetra was grown in uni-algal, axenic cultures under different metal regimes. Cultures were grown from a single cell isolate (HT 984) from Perch Pond (L. Brand). An axenic culture was obtained by treatment with antibiotics. Cultures were maintained in f/2 medium (Guillard and Ryther, 1962) prepared with

coastal seawater. For ligand production experiments a culture was grown in f/2 major nutrients with 10^{-7} M Fe_T (no other metals or EDTA added). Media was sterilized by autoclaving and spiked with ferric chloride stock solution immediately before inoculation. The inoculum culture, in exponential growth, was diluted 1:50 into fresh f/2 media containing no added Fe, 10^{-8}, 10^{-7}, or 10^{-6} M Fe with no other metals or EDTA added. Cultures were grown at 20° C under continuous light (200 $\mu Em^{-2}sec^{-1}$). Cells were counted using a Coulter Counter. Inoculation of culture media into marine bacterial broth showed no bacterial contamination. Examination of culture media by light microscopy (with Newmarski interference optics) one week after stationary phase showed very few or no bacteria. Stationary phase cultures were filtered through 0.45 μm Nuclepore filters under low pressure. Culture medium was stored frozen for amperometric titrations.

Amperometric titrations were performed on both filtered and unfiltered samples as described in Hering et al. (1987). Briefly, the method measures reduction of Cu(II) to Cu(I) at ambient pH at 90 mV (relative to Ag/AgCl). Natural water samples were equilibrated with added Cu for 10 min before amperometric measurements were begun. Electrode response was calibrated using UV-oxidized seawater or seawater diluted into electrolyte solutions (0.5 M NaCl, 2 mM $NaHCO_3$) for titrations of diluted culture media. The theory and application of the method (Waite and Morel, 1983) and the electrode system (Matson et al., 1977) have been described in detail elsewhere.

RESULTS AND DISCUSSION

In the cultures of H. triquetra grown on different concentrations of iron, higher additions of iron to the culture media resulted in increased cell densities (Fig. 1a). The production of Cu complexing agents by H. triquetra is seen in measurements of Cu complexation in the culture medium (Figure 1b). Increased Cu complexation (i.e.- lower concentration of inorganic Cu) is correlated with stationary phase cell density. This can be seen more clearly by qualitatively translating individual curves to a single value using the fraction of added Cu measured as inorganic Cu at a given added Cu concentration (in this case 106 nM added Cu). Figure 1c shows that the %inorganic Cu is roughly proportional to cell density. Since the production of Cu complexing agents did not increase in reponse to iron limitation it is unlikely that these phytoplankton exudates are siderophores, specific metabolites involved in iron acquisition and transport. Siderophore production by phytoplankton is markedly enhanced in iron-depleted medium (Trick et al, 1983, McKnight and Morel, 1980). Since copper does not commonly stimulate ligand production by phytoplankton (McKnight and Morel, 1980; Clarke et al., 1987), the presence of metal complexing agents observed in H. triquetra culture media may not be directly related to the metal nutritional status of the organism.

Incubation studies on water samples from Perch Pond over a 4 to 15 day period under varied conditions resulted in changes in measured Cu comlexation by the samples (Figure 2). Cu complexation in unfiltered samples increased for samples incubated in the light and decreased for

Figure 1. Culture studies (a) growth curve for H. triquetra cultures grown in f/2 medium with (○) no added Fe, (△) 10^{-8} M, (□) 10^{-7} M, (▽) 10^{-6} M Fe_T; (b) Cu titrations of diluted culture medium from stationary phase H. triquetra cultures grown under different Fe_T (symbols as above). Dilution: (○) 2% culture medium in electrolyte (0.5 M NaCl, 2mM$NaHCO_3$), (△,□,▽) 3% culture medium in electrolyte (c) % inorganic Cu (at 106 nM added Cu) as a function of stationary phase cell densities of H. triquetra grown under different Fe_T (symbols as above). [Note that decreased % inorganic Cu corresponds to increased Cu complexation by the medium.]

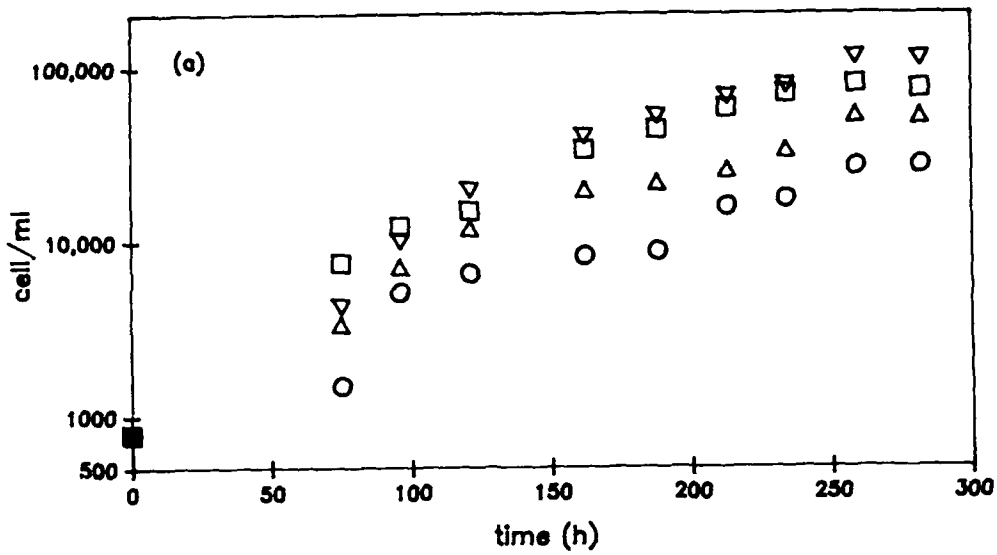
(a)
100,000
10,000
1000
500
cell/ml
0
50
100
150
200
250
300
time (h)

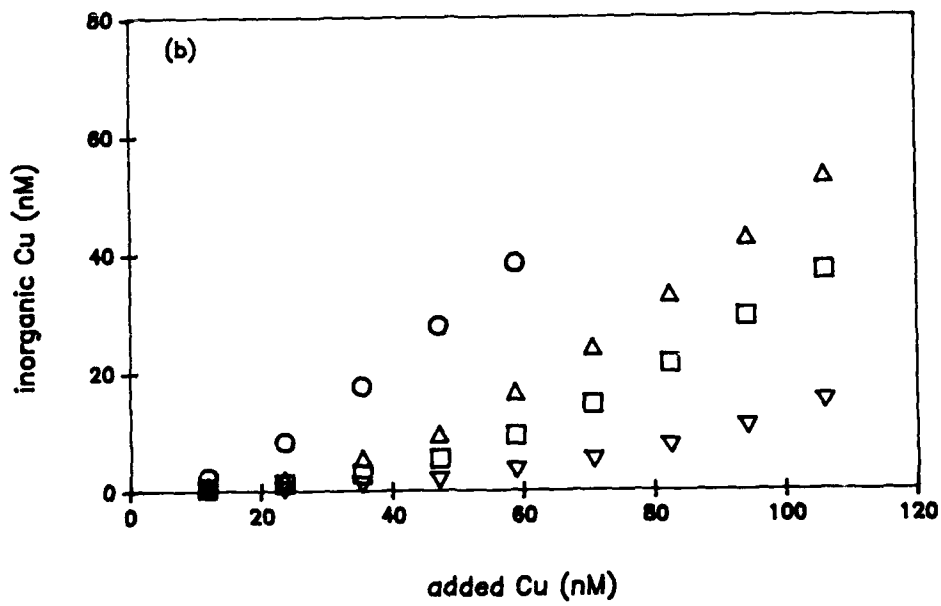
(b)
80
60
40
20
0
inorganic Cu (nM)
0
20
40
60
80
100
120
added Cu (nM)

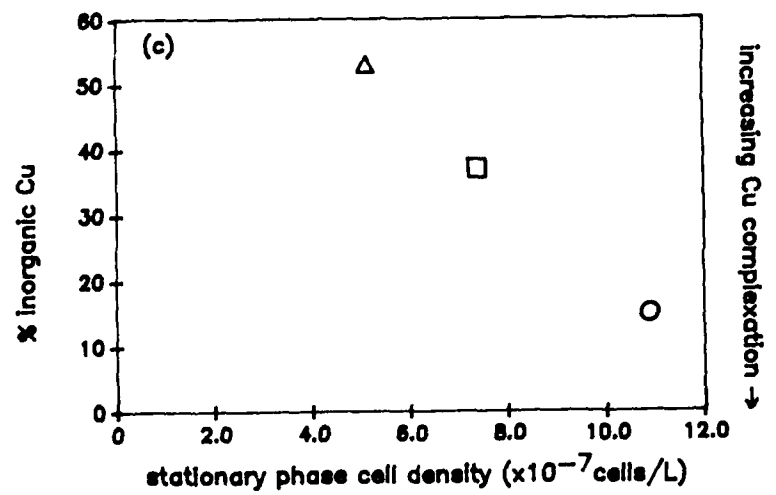
(c)
60
50
40
30
20
10
0
% inorganic Cu
increasing Cu complexation →
0
2.0
4.0
6.0
8.0
10.0
12.0
stationary phase cell density (x10⁻⁷cells/L)

Figure 2. Results of Cu titrations of incubated samples from Perch Pond. Amperometric data (a, b) (●) initial sample, pH= 8.27 (a) incubation of filtered samples (○) 20° C, dark, 4 d, pH=8.10; (△) 20° C, light, 5d, pH= 8.26; (□) 5° C, dark, 9d, pH=7.92; (▽) 20° C, dark, 14d, pH=8.02; (b) incubation of unfiltered samples (○) 20° C, light, 4d, pH= 8.72; (△) 20° C, dark, 6d, pH= 7.96; (▽) 5° C, dark, 7d, pH= 7.93; (□) 20° C, light, 15 d, pH= 8.09; (c) the % inorganic Cu (at 106 nM added Cu) shown for filtered and unfiltered samples incubated under light (□) or dark (▨) conditions. Note: all samples incubated without filtration were filtered immediately before titrations.

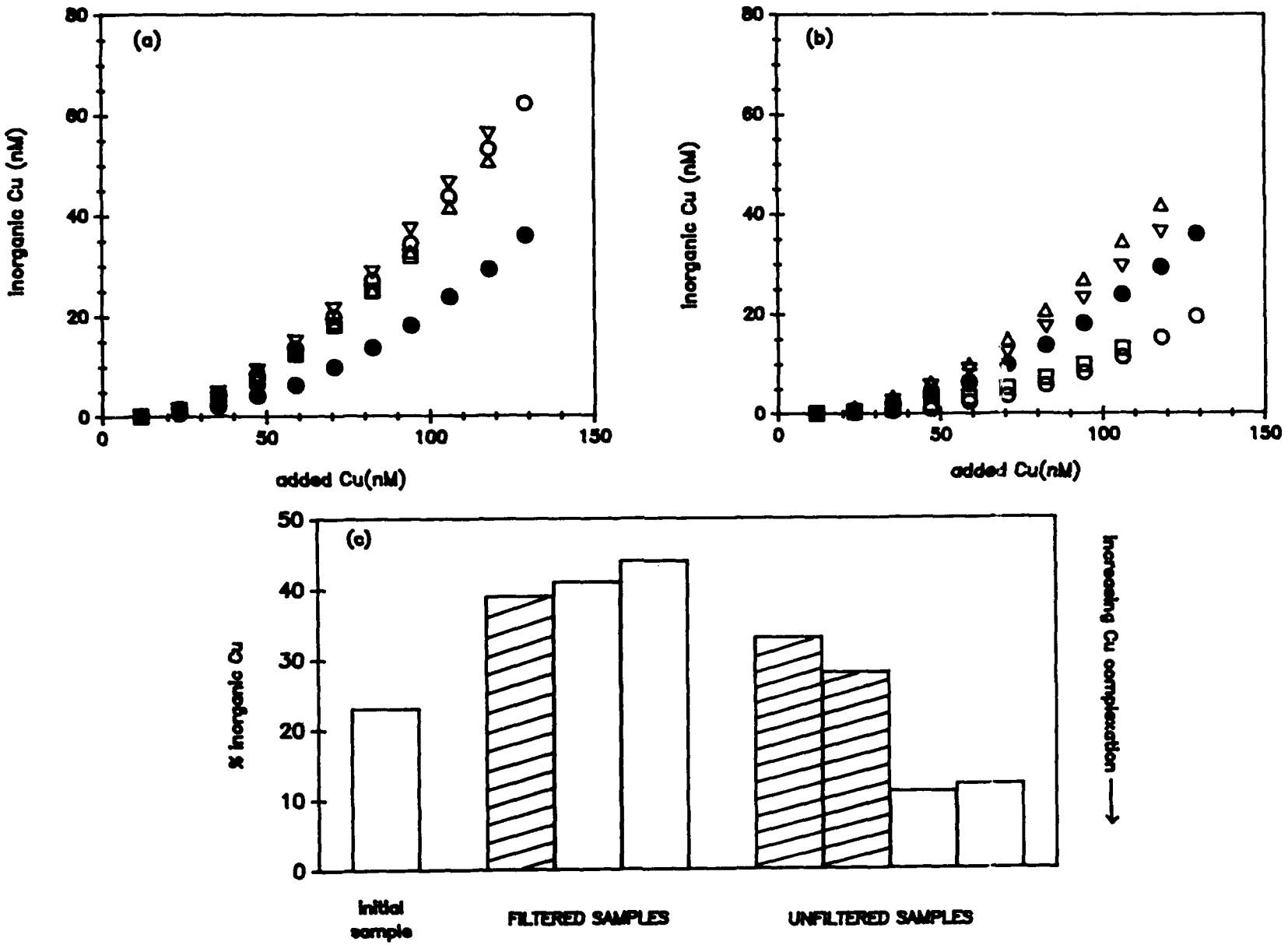
(a)
Inorganic Cu (nM)
added Cu(nM)
0
20
40
60
80
0
50
100
150
(b)
Inorganic Cu (nM)
added Cu(nM)
(c)
% Inorganic Cu
0
10
20
30
40
50
Initial sample
FILTERED SAMPLES
UNFILTERED SAMPLES
Increasing Cu complexation

dark-incubated samples suggesting production of ligands during growth of photosynthetic organisms. In contrast, decreased Cu complexation was observed in all filtered samples regardless of light or temperature regimes. Since our filtering process removes phytoplankton but not all the bacteria, this decrease in complexation is consistent with microbial degradation of ligands. However, sorptive loss of complexing agents to container walls may also contribute to the observed decrease in Cu complexation. Although some fraction of the Cu complexing agents appear to be labile on time scales of a few days, relatively refractory ligands must also contribute to the observed Cu complexation as only a slight additional decrease in Cu complexation occured between 4 and 15 days of incubation.

Enclosure of samples for incubation studies in containers is likely to have perturbed the natural biota; nevertheless, these results suggest active biological cycling of Cu complexing agents. Since samples were incubated in polyethylene (low wavelength light effectively excluded), it is unlikely that the light effect on unfiltered samples was due to abiotic photochemistry. Sorptive loss of Cu to the container walls would be expected to result in a uniform increase in apparent Cu complexation. Thus, we attribute the decrease in Cu complexation to bacterial degradation of complexing agents and the light-associated increase in Cu complexation to phytoplankton activity. Since dark-incubated unfiltered samples showed decreased Cu complexation, death, lysis or degradation of phytoplankton or zooplankton in the dark apparently do not contribute to observed Cu complexation. Only slight

Cu complexation by zooplankton body fluids has been observed in a previous study (Fish and Morel, 1983).

In field studies, the effect of phytoplankton activity on Cu complexation is not dramatic. Only small changes in Cu complexation were observed in unfiltered samples in the diel study (Figure 3a). However, the slight trend of increased Cu complexation in the afternoon and decreased Cu complexation through the evening and night is consistent with the production of complexing agents linked to photosynthetic activity.

Relative to the total complexation capacity of Salt Pond waters, the changes we observed with time are quite small (Figure 3b). This might at first suggest that there is only a small contribution from labile, biogenic ligands to overall metal buffering capacity, the major contribution being from refractory ligands (possibly humic materials). However, this is not necessarily the case. Turnover of amino acids and polyamines were also measured in the pond during the course of this study (Lee et al., in prep.). Results from measurements earlier in the summer during a phytoplankton bloom showed short turnover times and large diel changes in concentrations of these biologically labile compounds. By the time of our October Cu complexation measurements however, production and consumption processes in the pond were more balanced. Even though turnover of the compounds was rapid, the concentration of the labile compounds was maintained in a very narrow range. Thus, we cannot discount the importance of labile compounds as complexing agents as seen in the incubation experiments.

Figure 3. (a) Cu titrations of Salt Pond water. Samples collected Oct. 9 (○) 1040h, (△) 1530h, (□) 1945h, Oct. 10 (▽) 0440h. (b) % inorganic Cu (at 100 nM added Cu) for Salt Pond water as a function of time.

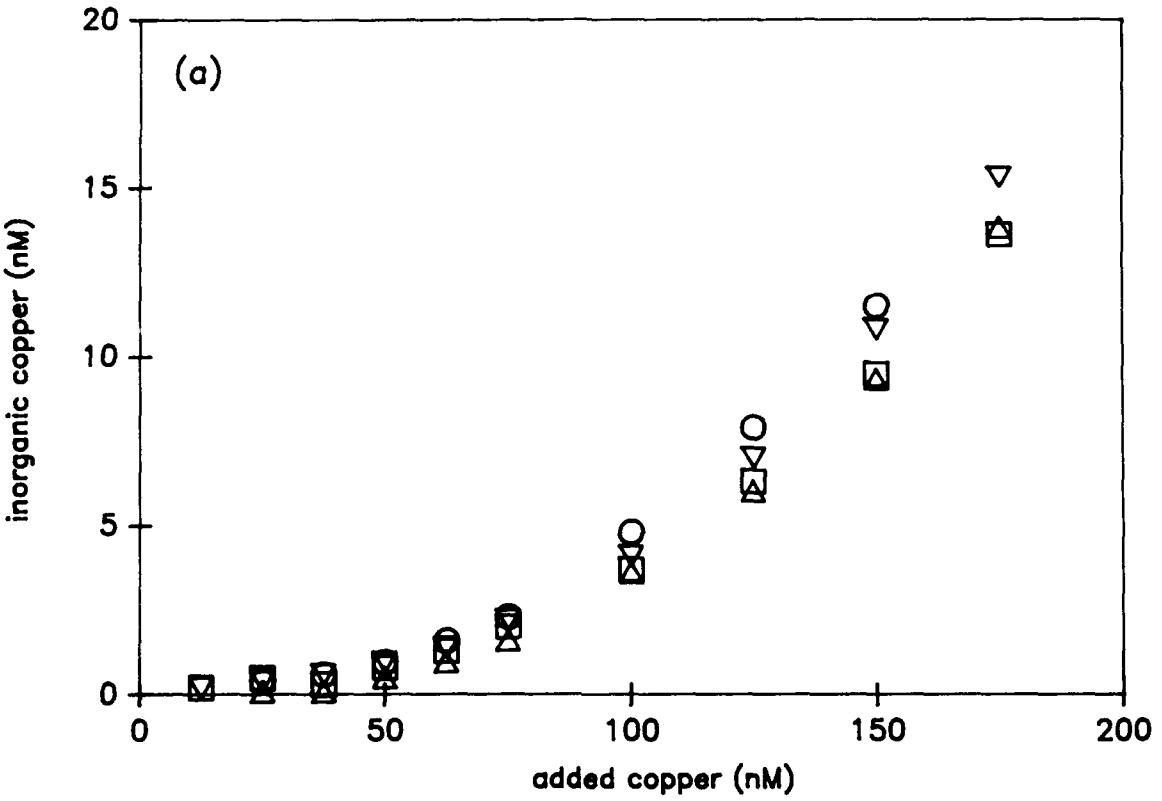
(a)
inorganic copper (nM)
added copper (nM)
0
5
10
15
20
0
50
100
150
200

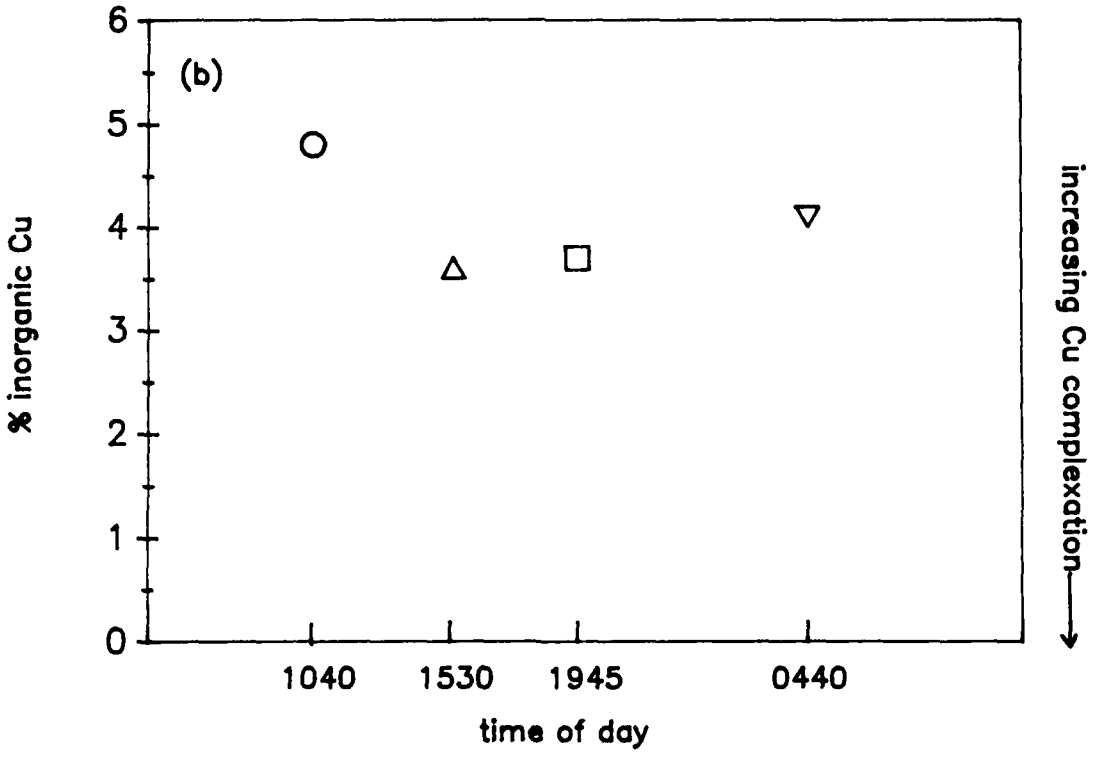
(b)
% inorganic Cu
time of day
increasing Cu complexation
0
1
2
3
4
5
6
1040
1530
1945
0440

Measurement of Cu complexation in Perch Pond waters were made from Nov. 1984 to April 1985 (Figure 4). Although it is not clear exactly when in December the onset of the bloom occurred, changes in Cu complexation observed between samples taken at low H. triquetra densities and samples taken during the phytoplankton bloom were on the same order as the variability observed during the bloom. However, increased Cu complexation was observed as phytoplankton cell numbers decreased in April, perhaps suggesting production of complexing agents as a result of phytoplankton senescence.

The potential influence of the dinoflagellate bloom in Perch Pond on Cu complexation may be assessed by comparison of culture and field studies. Stationary phase cell densities obtained in culture were much higher than those observed in the field even under bloom conditions. However as Cu titrations of culture media were done with highly diluted samples, the diluted culture media from H. triquetra grown under 10^{-7} and 10^{-6} M Fe_T correspond to effective cell densities of 2-3 $x10^6$ cell/L (roughly equal to field cell densities under bloom conditions). Based on the production of ligand observed in the culture experiments, we would predict that the dinoflagellate population would have contributed significantly to the total concentration of Cu complexing agents in its environment at naturally-occuring cell densities.

Both incubation and culture studies indicate that production of Cu complexing agents is associated with phytoplankton photosynthetic activity. However, consistent with previous observations, only small effects due to photosynthetic activity or phytoplankton abundance were

Figure 4. H. triquetra cell densities and % inorganic Cu (at 106 nM added Cu) in Perch Pond over sampling period Nov. 1984 through April 1985 (O) log [cell/L], (▲) % inorganic Cu for filtered samples, (■) % inorganic Cu for unfiltered samples.

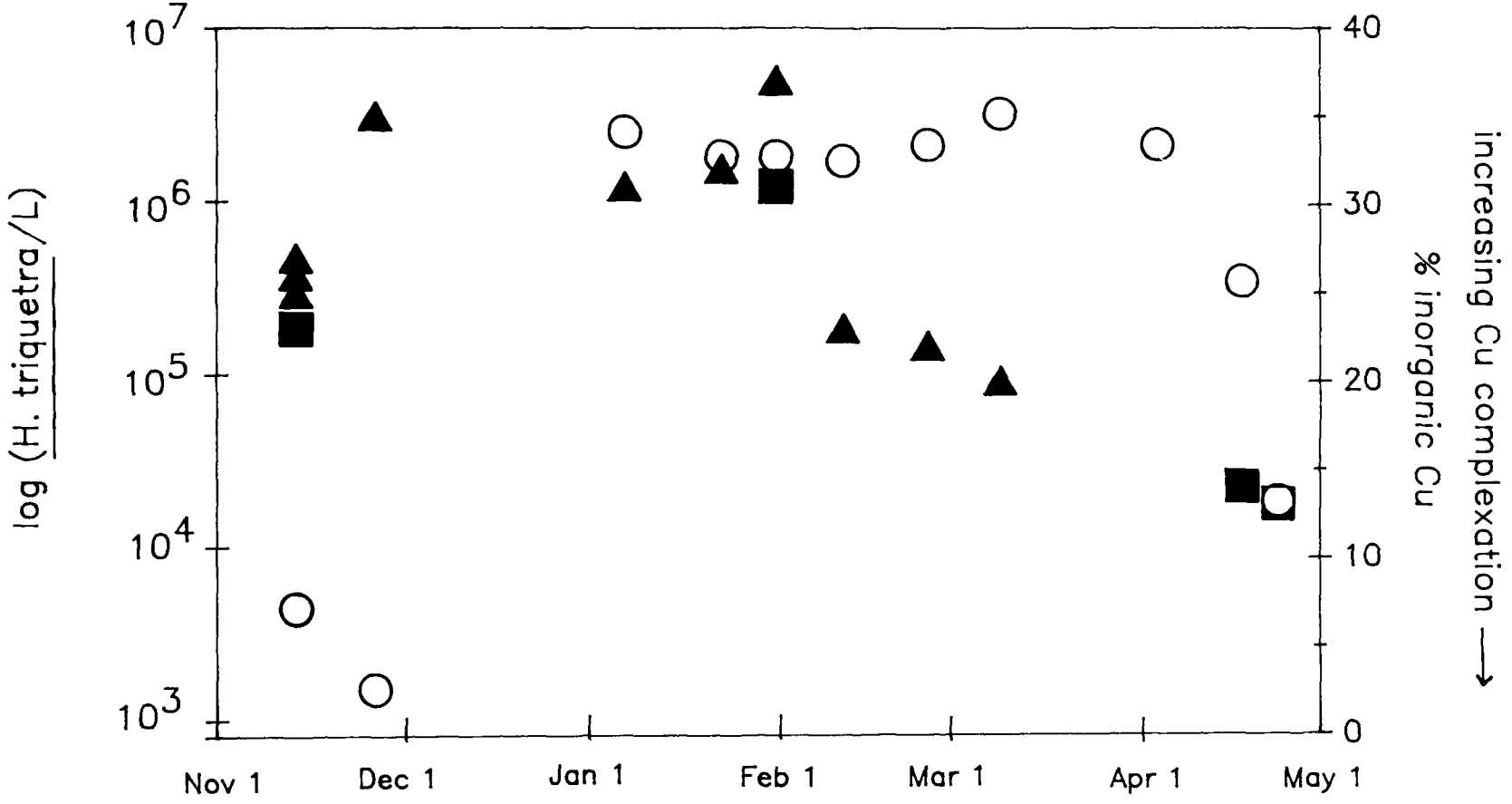
log (H. triquetra/L)
10^7
10^6
10^5
10^4
10^3
Nov 1
Dec 1
Jan 1
Feb 1
Mar 1
Apr 1
May 1
40
30
20
10
0
% inorganic Cu
increasing Cu complexation

observed. This lack of strong correlation between phytoplankton activity and Cu complexation observed in diel and seasonal studies may be due to several factors. At both sites, phytoplankton production and bacterial degradation of labile, biogenic ligands may be tightly coupled so that ligand concentration remains relatively constant as discussed earlier. A significant fraction of the observed Cu complexation may also be due to refractory ligands such as humic acids. In Perch Pond water, mixing with coastal seawater may reduce the importance of phytoplankton-bloom produced ligands relative to more resistant ligands possibly present in coastal waters. Our culture experiments may be biased by different physiological conditions of H. triquetra in culture (at stationary phase) and in the field which could result in very different ligand release rates. The increased Cu complexation observed in light-incubated, unfiltered samples of Perch Pond water suggests that, at field densities, phytoplankton activity can increase Cu complexation in the presence of bacteria. However, the physiological conditions of the phytoplankton may have been severely perturbed during incubation studies upsetting the balance between production and degradation.

Laboratory studies suggest that metal speciation in natural water may be influenced by biological production and degradation of complexing agents. However in coastal ponds, which are likely to be subject to large inputs of terrigenous materials, measurements of Cu complexation (analogous to bulk measurements of biological substrates) are insufficient to resolve the mechanisms controlling the concentrations of naturally-occuring complexing agents.

REFERENCES

Actis, L.A., W. Fish, J.H. Crosa, K. Kellerman, S.R. Ellenberger, F.M. Hauser and J. Sanders-Loehr (1986) J. Bacteriol. 167: 57-65.

Anderson, D.M., J.S. Lively, R.F.Vaccaro (1984) J. Mar. Res. 42: 677-95.

Clarke, S.E., J. Stuart, and J. Sanders-Loehr (1987) Appl. Environ. Microbiol. 53: 917-22.

Coale, K.H. and K.W. Bruland, Limnol. Oceanogr., submitted

Elliott, S., E. Lu, and F.S. Rowland (1988) presented at AGU/ASLO Ocean Sciences Meeting., Jan. 18-22.

Fish, W. and F.M.M. Morel (1983) Can. J. Fish. Aquat. Sci. 40: 1270-7.

Garcon, V.C., K.D. Stolzenbach, D.M. Anderson (1986) Estuaries 9: 179-87.

Guillard, R.R.L. and J.H. Ryther (1962) Can. J. Microbiol. 8: 229-39.

Hering, J.G, W.G. Sunda, R.F. Ferguson and F.M.M. Morel (1987) Mar. Chem. 20: 299-312.

Hering J.G. and F.M.M. Morel, submitted to Environ. Sci. Technol.

Huizenga, D.L. and D.R. Kester (1983) Mar. Chem. 13: 281-91.

Hunter, K.A. and P.S. Liss (1982) Limnol. Oceanog. 27: 322-35.

Imber, B.E. and M.G. Robinson (1983) Mar. Chem. 14: 31-41.

Kim, C.M. and K.O. Emery (1971) Salt Pond: Topography, Sediments, and Water. Salt Pond Areas Bird Sanctuaries, Inc. Annual Report, Falmouth, MA.

Kramer, C.J.M. and J.C. Duinker (1984) in Complexation of Trace Metals in Natural Waters, ed. C.J.M. Kramer and J.C. Duinker. The Hague: Nijhoff/ Dr. W. Junk Publishers, pp. 217-238.

Kramer, C.J.M. (1984) Thesis. Rijksuniveriteit te Gronigen. Amsterdam. The Netherlands.

Luther, G.W., Z. Wilk, R.A. Ryan and A.L. Myerson (1986) Mar. Poll. Bull. 17: 535-42.

Luther, G.W. and C.B. Swartz (1988) presented at AGU/ASLO Ocean Sciences Mtg., Jan. 18-22.

Mackey, D.J. (1983) Mar. Chem. 14: 73-87.

Matson, W., E. Zink, R. Vitukevitch (1977) Am. Lab. 9: 59-73.

McKnight, D.M. and F.M.M. Morel (1979) Limnol. Oceanog. 24: 823-37.

McKnight, D.M. and F.M.M. Morel (1980) Limnol. Oceanog. 25: 62-71.

Moffett, J.W. and R.G. Zika (1987) Mar.Chem. 21: 303-13.

Morel, F.M.M. (1983) Principles of Aquatic Chemistry, New York: Wiley-Interscience.

Neilands, J.B. (1981) Ann. Rev. Biochem. 50: 715-31.

Neilands, J.B. (1984) Microbial Sciences 1: 9-14.

Newell, A.D. and J.G. Sanders (1986) Environ. Sci. Technol. 20: 817-21.

Serriti, A., D. Pellegrini, E. Morelli, C. Barghiani, R. Ferrara (1986) Mar. Chem. 18: 351 .

Stumm, W and J.J. Morgan (1981) Aquatic Chemistry, New York: Wiley-Interscience.

Sunda, W.G. and R.F. Ferguson (1983) in Trace Metals in Seawater, ed. C.S. Wong, E. Boyle, K.W. Bruland, J.D. Burton, and E.D. Goldberg. New York: Plenum Press, pp. 871-891.

Sunda, W.G., D. Klaveness, A.V. Palumbo (1984) in Trace Metal Complexation in Natural Waters, ed. C.J.M. Kramer and J.C. Duinker. The Hague: Martinus Nijhoff/ Dr. W. Junk Pub. pp. 399-409.

Swallow, K.C., J.C. Westall, D.M. McKnight, F.M.M. Morel (1978) Limnol. Oceanogr. 23: 538-42.

Thurman, E.M. (1986) Organic Geochemistry of Natural Waters. Dordrecht: Martinus Nijhoff/ Dr. W. Junk Pub.

Trick, C.G.. R.J. Andersen, A. Gillam, P.J. Harrison (1983) Science 219: 306-8.

Trick, C.G., R.J. Andersen, N.M. Price, A. Gillam, P.J. Harrison (1983) Mar. Biol. 75: 9-17.

van den Berg, C.M.G. (1984) Mar. Chem. 15: 1-18.

van den Berg, C.M.G. (1984) Mar. Chem. 14 :201-12.

Waite, T.D. and F.M.M. Morel (1983) Anal. Chem. 55: 1268-74.

Wakeham, S.G., B.L. Howes, and J.W.H. Dacey (1984) Nature 310: 770-2.

Wood, A.M., D.W. Evans, J.J. Alberts (1983) Mar. Chem. 13: 305-26.

CHAPTER THREE

HUMIC ACID COMPLEXATION OF CALCIUM AND COPPER

Abstract

High affinity metal binding by isolated humic acids has been observed for both copper and calcium in metal titration experiments. Results of titrations of humic acids with a single metal (either calcium or copper) are consistent with a discrete ligand site model of humate-metal binding. However copper titrations in the presence of excess calcium do not show competitive effects predicted by such a model. Hence, different ligand sites must be involved in calcium and copper binding or a binding mechanism other than discrete ligand binding must be operative.

Introduction

Metal complexation by naturally-occurring ligands has been reported for a wide variety of aquatic environments. It has been suggested that such natural ligands control the speciation of transition metals and thus the bioavailability of transition metals in natural waters. Humic substances (i.e.- humic and fulvic acids) constitute from 10-30% of dissolved organic carbon in seawater to 70-90% in wetland waters (1). Metal binding by humic acids has been demonstrated for materials isolated from a variety of sources. Thus it appears that at least some of the metal complexation observed for natural waters may be attributed to humic substances.

The extent and nature of the association of natural ligands with the major cations (particularly the alkaline earth metals calcium and magnesium) are predicted to affect the affinity of such ligands for transition metals. Models of the speciation of humic substances and of transition metals in natural waters suggest that for some metals (e.g.- copper and mercury) metal-humate complexes should predominate in freshwaters. Organic complexation is predicted to be less important in seawater; the decreased importance of humic substances in controlling the speciation of transition metals in seawater is a consequence of the increased complexation of the humic substances by alkaline earth metals (2,3,4). Such models assume competition between calcium and copper for discrete binding sites.

Metal-humate interactions have been modeled by describing the humic acid as a mixture of discrete ligands. Such models successfully describe titrations of humic (or fulvic) acids with a single metal (5,6,7,8) or with two transition metals (9). However the discrete ligand representation does not provide a unique description of titration data and thus is not necessarily descriptive of the chemical reality. Alternative models are also consistent with experimental observations (6,10,11,12,13).

Herein, we report the results of calcium and copper titrations of humic acids. The results of titrations with either metal alone can be described with a discrete ligand model. Strong humic-copper binding was observed consistent with previous results (7,14,15). However observed calcium-binding was significantly stronger than has been reported

(2,16,17,18), a difference we attribute to the higher ligand-to-metal concentration ratios we examined. Little or no competition by calcium was observed in copper titrations. This lack of competition suggests either that calcium and copper are bound selectively at different sites or that different mechanisms of binding are operative for alkaline earth and transition metals.

Experimental Section

Humic acid preparation. Following a modification of the procedure described by Nash and Choppin (19), humic acid (obtained as the Na salt from Aldrich Chemical Co.) was dissolved in water (Millipore Q-H_2O) and precipitated by the addition of concentrated HCl. The supernatant was removed after centrifugation and the solid was resuspended in 3 M HCl. The supernatant gave an intense red color on addition of KSCN solution indicating Fe(III) contamination. The procedure was repeated 10 times with acid and twice with a water rinse. The solid was resuspended in water and transferred to a loosely covered culture dish. The sample was dried at 80°C for 2 days. [This material is referred to in the text as acid-washed Aldrich humic acid.]

The Aldrich humic acid was also cleaned more gently by precipitating with acid followed by water-washing (3 times as described above) and drying (referred to in the text as water-washed Aldrich humic acid). Pre-treatment was necessary to eliminate the significant calcium contamination observed in a titration of untreated Aldrich humic acid.

Calcium titrations of Reference Suwannee Stream Humic Acid (USGS) were performed on untreated and acid-washed humic material.

Elemental analysis shows significant differences between the two humic acids used in this study. The nitrogen content of Aldrich humic acid (0.51% after purification to the H^+- form) reported by Malcolm and MacCarthy (20) is lower than the value of 1.1% for Suwannee Stream reference humic acid provided by the USGS. The average molecular weight of Suwannee Stream humic acid is approximately 1100 Da (G. Aiken, pers. comm.). It is likely that the average molecular weight of the commercial material is considerably higher as it is derived from sedimentary sources. Based on ^{13}C-NMR data, Malcolm and MacCarthy (20) have concluded that commercial humic acids are not representative of aquatic or soil humic acids. However comparison of calcium titration data for Aldrich and Suwannee Stream humic acids (vide infra) indicates that use of re-precipitated commercial humic acid in preliminary studies of metal complexation is not inappropriate.

Solutions of humic acid for calcium titrations were prepared in the appropriate electrolyte from dried samples. Base was added to dissolve the humic acid, the pH was adjusted to 8.2 and the samples were equilibrated for at least 2 hours before titrations. For copper titrations, dilute solutions of the humic acid in electrolyte were prepared from a slightly alkaline concentrated solution. The stock solution was stored at 4^oC in the dark.

Calcium titrations. Analytical grade reagents were used without further purification. Calcium titrations were performed by addition of stock solutions of $CaCl_2$ to 100 mL of solutions of humic acid (at ~0.2, 1.0, and 2.0 g/L) in 0.08 M KCl, 2mM $NaHCO_3$. Solutions were bubbled

with air during the titrations. Free calcium ion concentrations were measured with an Orion 93-20 calcium ion selective electrode with an Orion 701A pH meter. A constant pH of 8.20 ± 0.05 was maintained during the titration by the addition of base. Titrations were performed at 22 ± 2°C. Calibration curves were run in the same electrolyte solution immediately preceding each sample titration and the final point of the calibration curve was rechecked after the sample titration. Response of the calcium electrode was Nernstian above $(Ca^{2+}) = 10^{-5}$M. Below this value, the relationship between $\log(Ca^{2+})$ and the potential was obtained from empirical calibration curves at low total calcium as recommended by the manufacturer (cf. ref. 21). The non-Nernstian response of the electrode in this range most probably results from competitive ion exchange of protons or K^+ in place of Ca^{2+} (22). The detection limit for the calcium ion selective electrode is 10^{-7} M (manufacturer's specifications).

Inorganic complexation of calcium by carbonate or hydroxide is not calculated to be important in these solutions based on the constants for calcium complexation given by Smith and Martell (23). [Constants were adjusted for ionic strength as in ref. 4.] At the end of the titrations, the solutions are super-saturated with respect to calcite. However, calibration curves do not indicate precipitation of any solid calcium phase. Precipitation of inorganic calcium minerals is therefore disregarded in further discussion.

Copper titrations. Copper titrations were performed by the addition of stock solutions of $CuCl_2$ (2.0×10^{-5} M freshly prepared from

$10^{-2.0}$ M solutions) to 160 mL of solutions of humic acids (at 0.3 and 0.6 mg/L) in 0.5 M NaCl, 2 mM $NaHCO_3$. The initial pH of humic acid solutions were in the range 8.2 to 8.3. Changes in pH during the titration were less than 0.05 pH units. Calibration curves were run in the same electrolyte solution immediately preceding each sample titration. Inorganic copper concentrations were measured by fixed-potential amperometry at 90 mV relative to Ag/AgCl. Application of this amperometric method for determination of inorganic copper in seawater has been described previously (24,25). Amperometric measurements were made with an Environmental Science Associates Model 3040 Charge Transfer Analyzer equipped with a pyrolytic graphite working electrode, Pt counter-electrode, and Ag/AgCl, saturated NaCl reference electrode. The Charge Transfer Analyzer and electrode systems have been described in detail by Matson et al. (26).

Modeling. Metal titration curves were fit assuming complexation by discrete ligands. The optimization of stability constants (K_i) and ligand concentrations (L_{iT}) for individual titrations was done using FITEQL (27). Subsequent iterations to adjust constants for calcium and copper titrations simultaneously were done by hand. The equation describing the discrete ligand fit is:

$$M_T = (M^{2+}) \left[\frac{1}{\alpha} + \sum_i \frac{K_i L_{iT}}{1 + K_i (M^{2+})} \right]$$

where α describes inorganic complexation of the metal (α is the ratio of the M^{2+} concentration to the concentration of inorganic complexes of the metal) (14). For calcium no inorganic complexation was included; for

copper the inorganic species $CuOH^+$, $CuCO_3^o$, and $Cu(CO_3)_2^{2-}$ were considered.

Precipitation of a calcium-humate solid phase is not considered in modeling the titration data although some aggregation of the humic material was observed at the end of the calcium titrations. The calcium titration curves can be modeled without considering any solid Ca-humate phase and do not show obvious control of calcium ion concentrations by a solid (i.e.- constant (Ca^{2+}) in the presence of excess humates). In such a complex system, however, the consistency of a fit that neglects Ca solids with the titration data does not prove that Ca speciation is unaffected by any precipitation of Ca-humate.

Results and Discussion

Calcium titrations of acid-cleaned Aldrich humic acid (concentrations 2.0, 1.0, and 0.26 g/L) and of Suwannee Stream humic acid (concentrations 1.0 and 0.22 g/L) clearly show decreased free calcium ion concentration with an increase in total humic acid concentration at lower values of total calcium (Fig. 1a and b). The solid curves shown in all figures are generated from discrete ligand model fits (vide infra). It is this region of the curve (i.e.- low metal-to-ligand ratios) from which the existence of high affinity metal-binding sites present at low concentrations may be deduced.

Although pre-treatment of the Aldrich humic acid was required to remove calcium contamination, the water-washed humic acid showed only slightly less calcium binding than the acid-washed samples. Titrations

Fig.1. Calcium titration data shown with model fits using ligands in Table I (solid curves) (a) Aldrich humic acid (◇) 2.0 g/L, (□) 1.0 g/L, (△) 0.26 g/L, (○) 0.26 g/L (b) Suwanee Stream humic acid (□) 1.0 g/L, (○) 0.22 g/L.

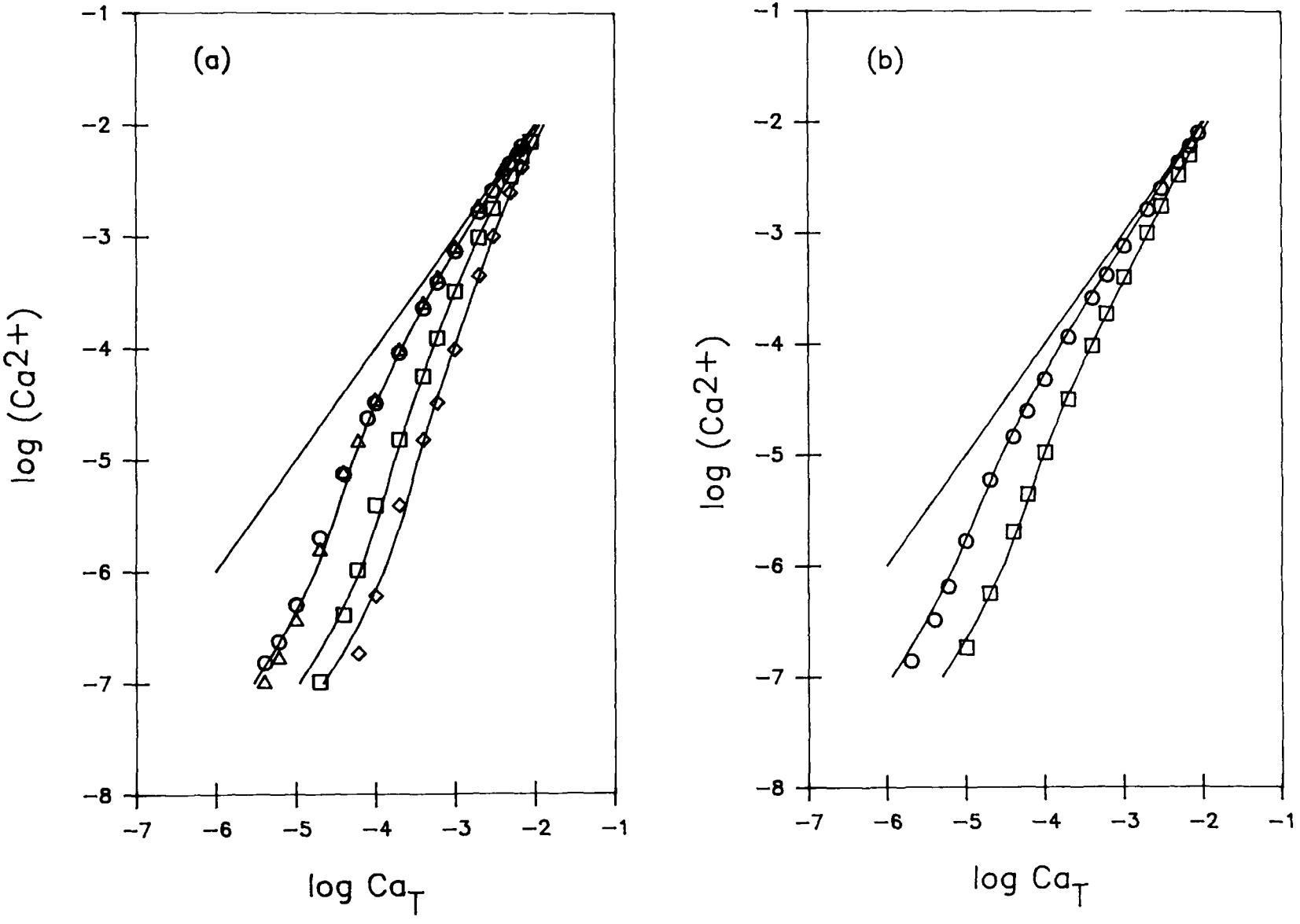
(a)
(b)
log (Ca2+)
log Ca$_T$
−1
−2
−3
−4
−5
−6
−7
−8

of Suwannee Stream humic acid re-precipitated and washed with acid showed no significant difference in calcium binding from untreated samples (Figure 2a,b). This similarity indicates that the washing treatment does not affect the intrinsic calcium binding ability of the humic acid and is suitable for removing contaminating metals.

Copper titration of Suwannee Stream humic acid (0.0003 and 0.0006 g/L) also show significant metal complexation (Fig. 3). Little or no effect of calcium (at 10^{-2} M) was observed on copper titrations (Fig. 4a,b). In contrast, the presence of 10^{-2} M Ca has a marked effect on copper complexation by a well-defined ligand, nitrilotriacetic acid, in agreement with thermodynamic predictions (Fig. 4c).

Calcium titrations of both Suwannee Stream and Aldrich humic acids were fit using a discrete ligand model with 3 ligands (i.e.- 3 different sites for Cu-binding on the humic acid) (Table I). The fitting routine was constrained by using the same stability constants (K_i) for both types of humic acids and adjusting the ligand concentrations (L_{iT}). A single set of ligands (normalized for amount of humic acid) is consistent with all titration data over a 10-fold range in humic acid concentration.

Both the calcium and copper titrations of Suwannee Stream humic acid were modeled by assuming a single set of ligand concentrations (in mole sites/ g humic acid). The stability constants obtained with this constraint are roughly 10^4-10^5-fold stronger for copper than for calcium (Table II). Some caution should be exercised in applying this model over such a large range in humic acid concentrations. Aggregation of

Fig. 2. Effect of pre-treatment on calcium titration data (a) Aldrich humic acid 1.0 g/L (○) water-washed, (△) acid-washed (b) Suwanee Stream humic acid 0.22 g/L (□) untreated, (▽) acid-washed.

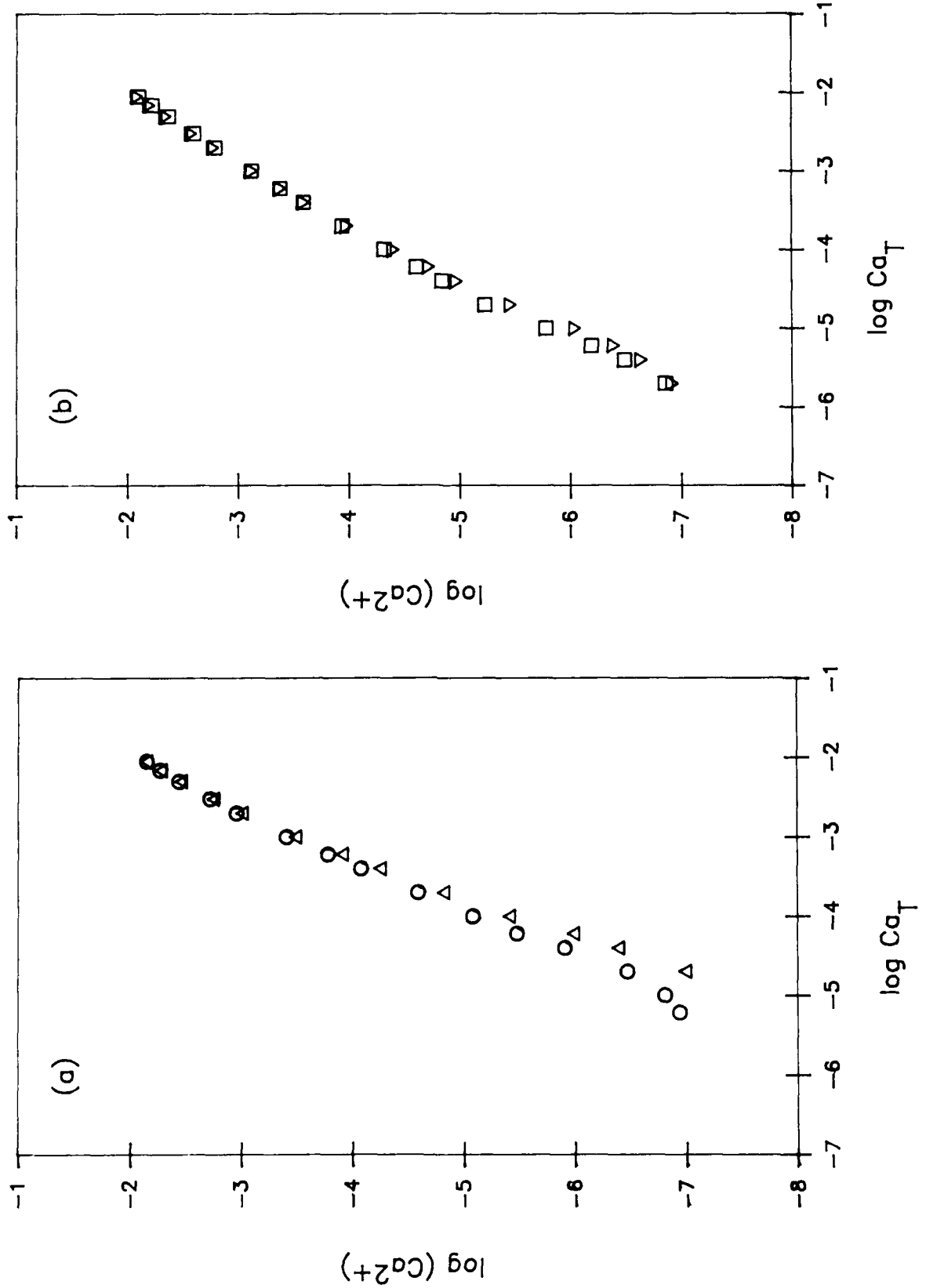
(a)
(b)
log (Ca2+)
log Ca_T
-1
-2
-3
-4
-5
-6
-7
-8

Fig. 3. Copper titrations of Suwanee Stream humic acid with model fits using ligands in Table II (solid curves) (○) 0.3 mg/L (average of 4 titrations), (▽) 0.6 mg/L (average of two titrations).

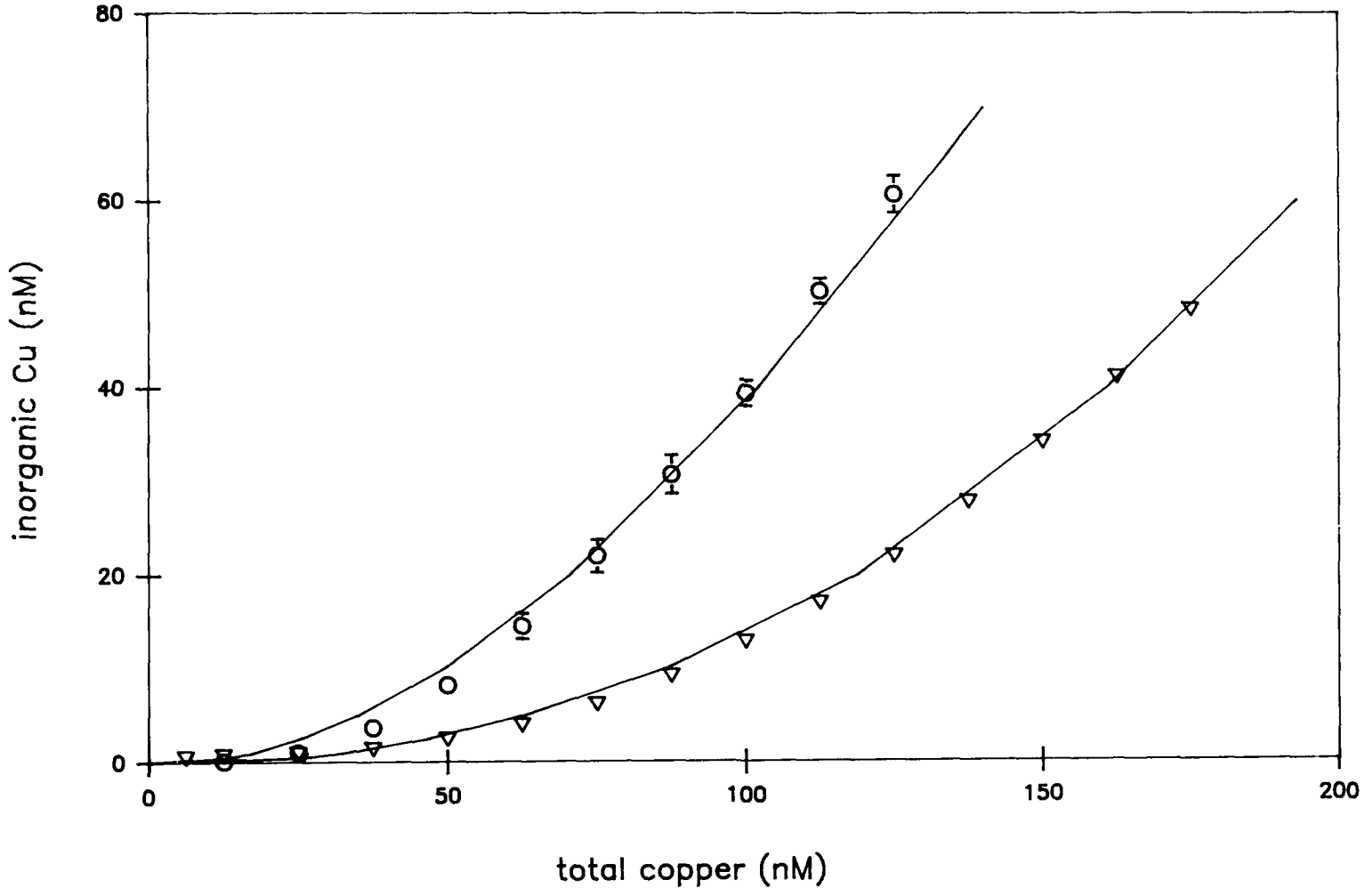
80
60
40
20
0
inorganic Cu (nM)
0
50
100
150
200
total copper (nM)

Fig. 4. Effect of calcium on copper titrations of SSHA (a) 0.3 mg/L (□) no Ca, (▽) 10^{-2} M Ca (b) 0.6 mg/L (○) no Ca, (△) 10^{-2} M Ca and of NTA (c) (○) no Ca, (◇) 10^{-2} M Ca (solid curves are predicted values). [N.B.- The deviation of observed and predicted values for 10^{-2} M Ca at high added Cu may be due to lability of the CuNTA complex under these conditions (cf. ref. 24).]

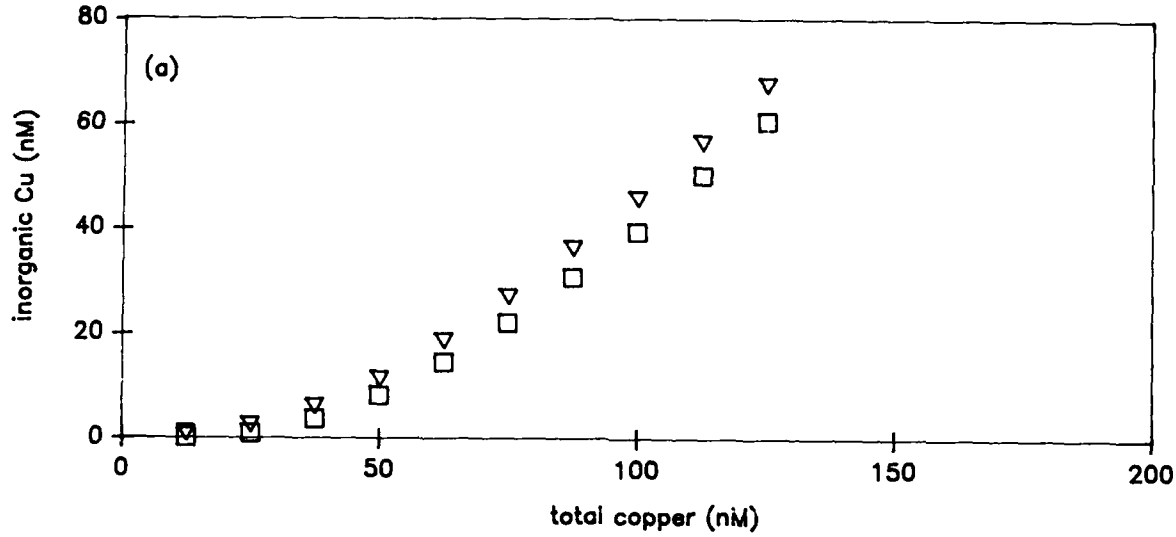
(a)
inorganic Cu (nM)
total copper (nM)
0
20
40
60
80
0
50
100
150
200

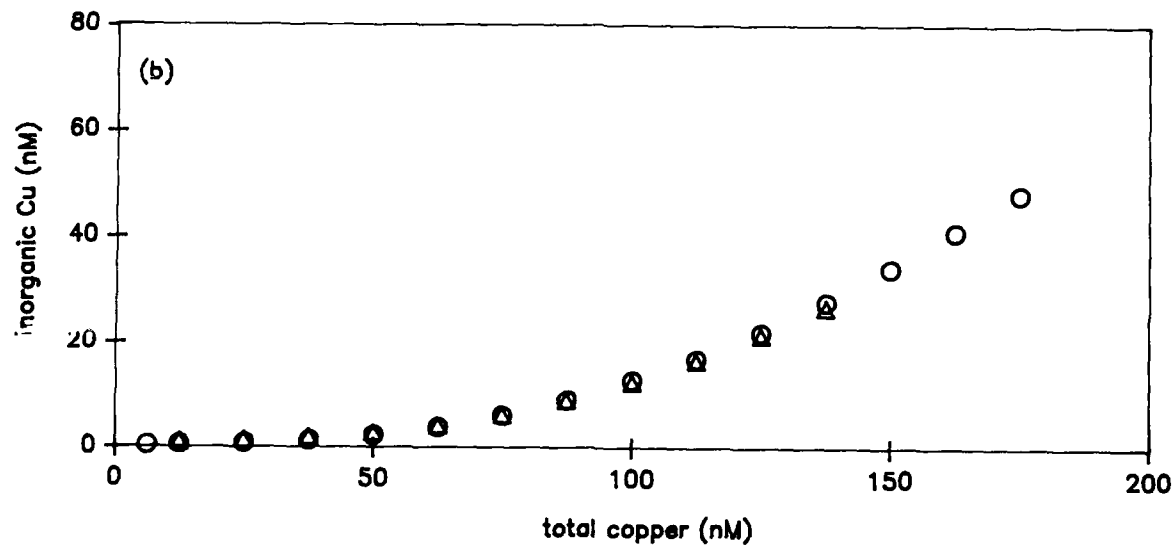
(b)
inorganic Cu (nM)
total copper (nM)
0
20
40
60
80
0
50
100
150
200

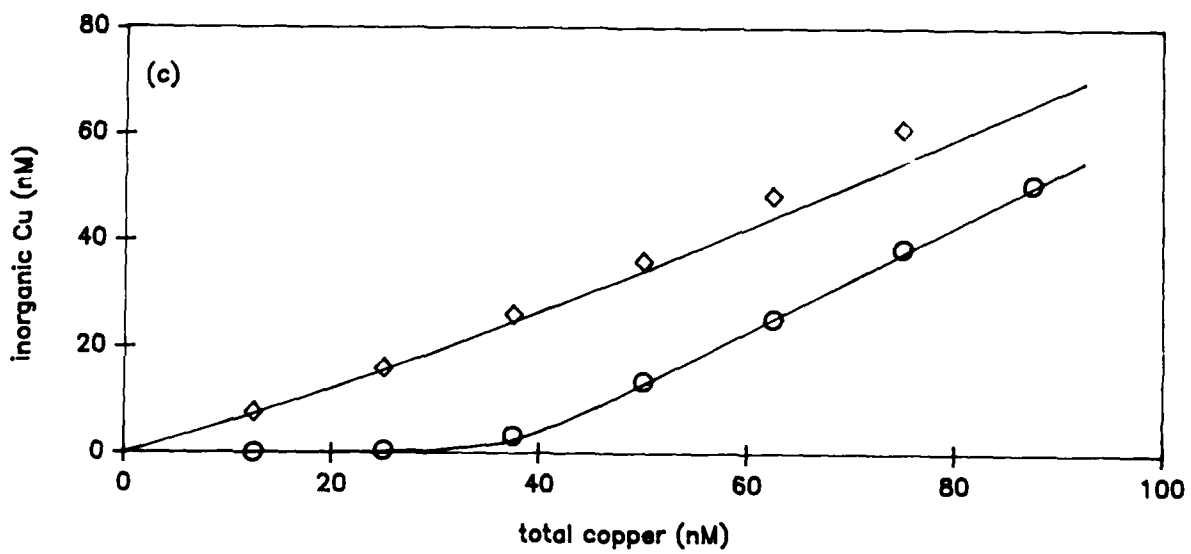
(c)
inorganic Cu (nM)
total copper (nM)
0
20
40
60
80
0
20
40
60
80
100

Table I. Discrete-ligand model fit for Suwanee Stream and Aldrich humic acids (values for stability constants are constrained)

$\log K_{CaL}$	L_T (mole site/g humic acid)	
	SSHA	Aldrich
6.0	5.0×10^{-5}	1.2×10^{-4}
4.1	2.0×10^{-4}	4.1×10^{-4}
2.9	1.8×10^{-3}	1.2×10^{-3}

Table II. Discrete ligand model fit for calcium and copper titration data of SSHA (values for total ligand concentrations are constrained)

L_T (mole site/ g humic acid)	log K_{CaL}	log K_{CuL}
5.0×10^{-5}	6.0	>11
2.0×10^{-4}	4.1	9.2
1.8×10^{-3}	2.9	6.6

humic and fulvic acids at high concentrations has been shown to contribute to copper complexation; however, aggregation is considered to be less likely to influence calcium binding (28,29).

The congruence of the discrete ligand representations for calcium and copper titrations of Suwanee Stream humic acid (over >1000- fold range in humic acid concentrations) may be taken to imply that the same ligand sites are involved in complexation of both alkaline earth and transition metals. This interpretation would predict direct competition between copper and calcium for high affinity binding sites. However such competitive behavior is not observed. Cabaniss and Shuman (5) and Sunda and Hanson (14) have reported only slight competition between calcium and copper in fulvic acid titrations. Recent observations by McKnight and Wershaw (30) show decreasing copper complexation by fulvic acid with an increase in calcium concentration from 10^{-5} to 10^{-3} M (with $Ca(NO_3)_2$ as the sole supporting electrolyte). However, no further decrease in copper complexation was observed for 10^{-2} M calcium. This behavior was attributed to structural heterogeneity of humate copper-binding sites and competition of copper and calcium for only a portion of the binding sites with no competition for other sites. The lack of a competitive effect of calcium in our copper titration experiments is consistent with our observations that the kinetics of copper complexation by Suwannee Stream humic acid is unaffected by the presence of calcium; in contrast, copper complexation by EDTA is kinetically hindered in seawater (31).

However convenient and descriptive the discrete ligand model is for fitting titrations of humic or fulvic acids with a single metal, it requires separate ligand sites to predict the observed lack of competition between calcium and copper. Assumptions of competitive effects in complexation models are likely to result in underestimation of transition metal complexation in seawater.

It is also possible that this data fitting model does not correspond to the physical-chemical reality of metal binding by humates. Mechanisms other than discrete ligand binding, such as electrostatic or territorial binding, may govern complexation of alkaline earth and transition metals. Data on interactions of humic acids with several metals and particularly on competitive interactions serves to constrain models of metal-humate interactions.

Literature Cited

(1) Thurman, E.M. *Organic Geochemistry of Natural Waters*, Martinus Nijhoff/ Dr. W. Junk: Dordrecht, 1985.

(2) Mantoura, R.F.C.; Dickson, A.; Riley, J.P. *Est. Coast. Mar. Sci.* **1978**, *6*, 387.

(3) Stumm, W.; Morgan, J.J. *Aquatic Chemistry*, Wiley-Interscience: New York, 1981.

(4) Morel, F.M.M. *Principles of Aquatic Chemistry*, Wiley-Interscience: New York, 1983.

(5) Cabaniss, S.E.; Shuman, M.S. *Geochim. Cosmochim. Acta* **1988**, *52*, 185.

(6) Turner, D.R.; Varney, M.S.; Whitfield, M.; Mantoura, R.F.C.; Riley, J.P. *Geochim. Cosmochim. Acta*, **1985**, *50*, 289.

(7) Fish, W.; Dzombak, D.A.; Morel, F.M.M. *Environ. Sci. Tech.* **1986**, *20*, 676.

(8) McKnight, D.M.; Feder, G.K.; Thurman, E.M.; Wershaw, R.L.; Westall, J.C. *Sci. Tot. Environ.* **1983**, *28*, 65.

(9) Fish, W. Ph.D. Thesis, Mass. Instit. of Technol., Cambridge MA, 1984.

(10) Dzombak, D.A.; Fish, W.; Morel, F.M.M. *Environ. Sci. Technol.* **1986**, *20*, 669.

(11) Cabaniss, S.E.; Shuman, M.S.; Collins, B.J. in *Complexation of Trace Metals in Natural Waters* ed. C.J.M. Kramer and J.C. Duinker, Martinus Nijhoff/ Dr. W. Junk: The Hague, 1984.

(12) Perdue, E.M.: Lytle, C.R. *Environ. Sci. Technol.* **1983**, *17*, 654.

(13) Ephraim, J.; Marinsky, J.A. *Environ. Sci. Technol.* **1986**, *20*, 367.

(14) Sunda, W.G.; Hanson, P.J. in *Chemical Modeling in Aqueous Systems: Speciation, Sorption, Solubility, and Kinetics*, ed. E.A. Jenne, ACS Symposium Series no. 93, 1979.

(15) Sunda, W.G.; Klaveness, D.; Palumbo, A.V. in *Trace Metal Complexation in Natural Waters*, ed C.J.M. Kramer and J.C. Duinker, Martinus Nijhoff/ Dr. W. Junk: The Hague, 1984.

(16) Dempsey, B.A.; O'Melia, C.R. in *Aquatic and Terrestrial Humic Materials*, ed. R.F. Christmann and E.T. Gjessing, Ann Arbor Science: Ann Arbor, MI, 1983.

(17) Choppin,G.R.; Shanbag, P.M. J. *Inorg. Nucl. Chem.* **1981**, *43*, 921.

(18) Sposito, G.; Holtzclaw, K.M.; Le Vesque-Madore, C.S. *Soil Sci. Am. J.* **1978**, *42*, 600.

(19) Nash, K.L.; Choppin, G.R. *J. Inorg Nucl. Chem.* **1980**, *42*, 1045.

(20) Malcolm, R.L.; MacCarthy, P. *Environ. Sci. Technol.* **1986**, 20, 904.

(21) Thomas, J.D.R. *Lab. Practice* **1978**, *27*, 857.

(22) Buck, R.P. in *Ion-Selective Electrodes in Analytical Chemistry*, vol. 1, ed. H. Freiser, Plenum Press: New York, 1978.

(23) Smith, R.M.; Martell, A.E. *Critical Stability Constants*, vol. 4, Plenum Press: New York, 1976.

(24) Waite, T.D.; Morel, F.M.M. *Anal. Chem.* **1983**, *55*, 1268.

(25) Hering, J.G.; Sunda, W.G.; Ferguson, R.L.; Morel, F.M.M. *Mar. Chem.* **1987**, *20*, 299.

(26) Matson, W.R.; Zink, E.; Vitekevitch, R. *Am. Lab.*, **1977**, *55*, 1268.

(27) Westall, J.C. Technical Report, Dept. of Chem., Oregon State Univ., Corvallis OR, 1982.

(28) Underdown, A.W.; Langford, C.H.; Gamble, D.S. *Environ. Sci. Technol.* **1985**, *19*, 132.

(29) Gamble, D.S.; Langford, C.H.; Underdown, A.W. *Org. Geochem.* **1985**, *8*, 35.

(30) McKnight, D.M.; Wershaw, R.L. in *Humic Substances in the Suwannee River, Georgia: Interactions, Properties, and Proposed Structures*, ed. J.A. Leenheer and R.C. Averett, U.S. Geological Survey, Water-Supply Paper, in press.

(31) Hering, J.G.; Morel, F.M.M., submitted to *Environ. Sci. Technol.*

CHAPTER FOUR

KINETICS OF TRACE METAL COMPLEXATION: THE ROLE OF ALKALINE EARTH METALS

Abstract

The formation reactions of metal complexes are known to be intrinsically fast for most metals. However, at the high alkaline earth concentrations of seawater, a dramatic reduction in the rate of copper complexation by the model ligand ethylenediaminetetraacetic acid (EDTA) is observed. For example, the (pseudo first-order) half-life for inorganic copper reacting with EDTA in seawater is ~2 h at 10^{-7} M EDTA, ~20 h at 10^{-8}M EDTA, etc. This kinetic hindrance to the formation of the thermodynamically-favored CuEDTA species results from several factors: (1) the preponderance of the calcium complex in the speciation of EDTA, (2) the competition of calcium and copper for reaction with any free EDTA formed by the dissociation of CaEDTA, and (3) the slow kinetics of direct attack of Cu on CaEDTA compared to reaction with free or protonated EDTA species. If metal complexing agents in natural waters behave as discrete ligands, then the reaction of a metal at strong binding sites may also be kinetically hindered at high alkaline earth concentrations. In contrast with the reaction of EDTA, however, the rate of complexation of Cu by humic acid is not observably affected by high calcium concentrations.

At environmentally representative metal and ligand concentrations, the reaction of CaEDTA with Cu proceeds through two types of mechanisms, an indirect pathway involving dissociation (partly acid-catalyzed) of the initial alkaline earth metal complex and a direct pathway involving

formation of an intermediate dinuclear complex with both metals partially bound to the ligand. The direct pathway is increasingly favored at high Ca and Mg concentrations. Rate constants are given for both pathways.

The observed rate constants can be related to specific attributes of the reacting ligands and metals. Rates of reactions through both indirect and direct pathways are governed by the affinity of the ligand for the alkaline earth metal. The stability of the protonated complex determines the importance of the acid-catalyzed indirect pathway. The rate of indirect exchange is inversely proportional to the alkaline earth metal concentration and is accelerated at low pH. Thus, for a given ligand, environmental factors (alkaline earth metal concentrations and pH) will determine which pathway for metal exchange predominates. The slowest exchange kinetics will occur under high alkaline earth and pH conditions (i.e.- seawater). Rates of metal exchange reactions are predicted for a series of ligands and the implications of these results for metal exchange reactions of naturally-occuring ligands are examined.

Introduction

Chemical reactions (e.g.- oxidation-reduction, complexation, or precipitation) occurring in the aquatic environment have often been modeled by assuming equilibrium or steady-state conditions. Several recent reviews have focused on the validity of such assumptions and compared the time-scales (or half-lives) of chemical reactions with those of appropriate physical processes such as mixing. (1-4)

This paper focuses on the kinetics of trace metal complexation reactions. The effects of complexation on bioavailability and toxicity

(5-7), sorption (8-10), precipitation/dissolution (11) and oxidation/reduction of metals (12,13) have been widely demonstrated. Disequilibrium between metals and complexing ligands in natural waters may result from changes in either reactant concentration. Changes in metal concentrations may arise from mixing of water masses, upwelling of deep waters (14-17), photochemical dissolution of oxides (12,13,18), or anthropogenic inputs (19). Biological production (20-29) and anthropogenic inputs (30,31) may both contribute to changes in ligand concentrations. Such perturbations may have significant ecological consequences if the rate of re-establishment of chemical equilibrium is slow compared to rates of competing processes (such as biological metal uptake).

The kinetics of metal complexation reactions may also have important implications for analytical measurements of metal complexation. Most methods for the determination of metal complexation in natural waters involve metal additions to water samples. Times chosen for the equilibration of added metal with the sample vary as do observations of the effects of equilibration times. These effects may arise from other processes (e.g.- metal adsorption to container walls or biological transformations) as well as from slow complexation reactions (32-34). The results of analytical methods involving ligand-exchange process (i.e.- equilibrium with added ligands) may also be influenced by the kinetics of complexation reactions (35-37).

In addition to the nature and concentrations of the metal and ligand, the kinetics of complexation in aquatic systems are likely to be influenced by the concentrations of alkaline earth metals and pH. In

natural waters, particularly in seawater, alkaline earth metals are predicted to control the speciation of naturally-occuring ligands (38-40). Thus the kinetics of complexation of transition metals added to natural waters may be governed by the rate of exchange with alkaline earth metals complexed to natural ligands. The net result can be a dramatic retardation of complexation reactions which are otherwise expected to be rapid. This has been observed in artificial seawater where the slow equilibration of added copper to a phytoplankton culture containing artificial chelators resulted in initially high toxicity (5).

Due to the complexity and heterogeneity of natural ligands, the kinetics of metal-exchange reactions involving such ligands are extremely difficult to study. We have chosen, therefore, to investigate the rates and mechanisms of exchange reactions with well-defined ligands (EDTA and NTA) under conditions of environmental interest (i.e.- environmentally-representative ligand and metal concentrations, pH, ionic strength, and a range of alkaline earth metal concentrations). The objective of such a study is to correlate the observed rates of metal exchange reactions with the reactivity of the metals and ligands and with environmental parameters to provide a conceptual framework for the kinetics of metal exchange reactions with both natural and artificial ligands in natural waters.

Background

Metal-exchange reactions of the type:

$$AL + M \longrightarrow A + ML$$

Here: A = Ca or Mg and M = Cu

have been shown to proceed through two types of mechanisms: an indirect pathway involving dissociation (partially acid-catalyzed) of the initial alkaline earth metal complex and a direct pathway involving formation of an intermediate dinuclear complex with both metals bound to the ligand. The mechanisms of transition metal exchange reactions (e.g.- A = Ni, M = Cu) of EDTA have been reviewed by Margerum (41) and Margerum et al. (42). Such reactions proceed predominantly via a direct pathway. For reactions of alkaline earth complexes both indirect (43) and direct (44-47) pathways have been demonstrated. Although reactions of CaEDTA with Pb (43) and Cd (44) have been described mechanistically, the studies were conducted with the transition metal in excess of the alkaline earth metal (Pb exchange) and with millimolar or greater ligand concentrations (Cd exchange). Metal-exchange experiments conducted under more realistic conditions (ligand and metal concentrations 10^{-8} to 10^{-7} M) by Raspor et al. (45-47) were not conducted under the range of conditions (i.e.- in Ca and H^+ concentrations) necessary for the determination of mechanistic pathways.

In this paper, the mechanistic description of metal-exchange reactions of alkaline earth complexes of EDTA is used as a basis for relating observed reaction rates to a thermodynamic description of metal-ligand interactions (see also ref. 4) and environmental parameters such as pH and alkaline earth metal concentrations. This approach allows for extrapolation to other ligands and conditions pertinent to natural waters. The implications of these studies for the complexation reactions of natural ligands is discussed.

Theory

Results of the kinetics experiments are interpreted based on a reaction mechanism involving both direct and indirect pathways. [Terms and definitions are given in Table I.] The choice of reaction pathways is based on our empirical (i.e.- hindsight) observations of reaction rates under varying initial reactant concentrations and on previous work (vide supra). Rate expressions are derived for indirect, proton-catalyzed indirect, and direct pathways assuming steady-state concentrations of intermediate species and negligible back-reaction of products (48). Previous work (41, 44) has demonstrated no significant acid-catalyzed direct pathway. Such a pathway is therefore neglected in this discussion. The mechanistic pathways are outlined below and the rate expressions (for conditions of excess alkaline earth metals [i.e.- (A) >> (Cu)] are given.

Indirect mechanism:

$$AL \underset{k_1}{\overset{k_{-1}}{\rightleftharpoons}} A + L \quad ; \quad K_{AL} = k_1/k_{-1}$$

$$Cu + L \xrightarrow{k_2} CuL \quad ; \quad k_{Cu}^{L} = k_2$$

$$\frac{-d(Cu)}{dt} = \frac{k_{-1}k_2}{k_1}\frac{(AL)(Cu)}{(A)} = \frac{k_{Cu}^{L}\,(AL)(Cu)}{K_{AL}\,(A)} \qquad (1)$$

Acid-catalyzed indirect mechanism:

$$AL + H \underset{k_{-3}}{\overset{k_3}{\rightleftharpoons}} ALH$$

$$ALH \underset{k_4}{\overset{k_{-4}}{\rightleftharpoons}} A + HL$$

Table I. Terms and Definitions

A.....an alkaline earth metal, either Ca or Mg

k_M^L or k_{Cu}^L.....intrinsic rate constant for the formation of complex ML or CuL by reaction of M or Cu with ligand L

k_{Cu}^{HL}.....intrinsic rate constant for the formation of complex CuL by reaction of Cu with the protonated ligand HL (H^+ is displaced by the incoming metal)

k_{Cu}^{AL}.....intrinsic rate constant for direct attack of Cu on complex AL to give the product CuL

k_{Cu}^{A--L}.....rate constant for reaction of Cu with partially-dissociated complex A---L to give the dinuclear complex ALCu

k^{Cu-H_2O}.....rate constant for water-loss from the inner coordination sphere of Cu

K_{AL} or K_{HL}.....equilibrium stability constant for complex AL or HL

$K^{\#}$.....stability constant for the complex AL with respect to the partially-dissociated complex A---L, thus $K^{\#} = [AL]/[A---L]$

$$HL + Cu \underset{k_{-5}}{\overset{k_5}{\rightleftharpoons}} CuLH \qquad ; \; k_5 = k_{Cu}^{HL}$$

$$CuLH \xrightarrow{k_6} CuL + H$$

Assuming $k_{-5} << k_6$ and introducing $(k_3/k_{-3})/(k_4/k_{-4}) = K_{HL}/K_{AL}$, leads to the rate expression

$$\frac{-d(Cu)}{dt} = \frac{k_5 k_3 k_{-4}}{k_{-3} k_4} \frac{(Cu)(AL)(H)}{(A)} = \frac{k_{Cu}^{HL} K_{HL}}{K_{AL}} \frac{(AL)(Cu)(H)}{(A)} \qquad (2)$$

Direct mechanism:

$$AL + Cu \underset{k_{-a}}{\overset{k_a}{\rightleftharpoons}} ALCu$$

$$ALCu \xrightarrow{k_{-b}} A + CuL$$

$$\frac{-d(Cu)}{dt} = \frac{k_{-b} k_a}{k_{-a} + k_{-b}} (AL)(Cu) = k_{Cu}^{AL} (AL)(Cu) \qquad (3)$$

In view of the much greater affinity of the ligand for the transition metal Cu than for the alkaline earth metal A, it is reasonable to assume $k_{-b} >> k_{-a}$. The rate constant for the direct pathway then reduces simply to k_a, the rate of formation of the dinuclear complex.

The direct reaction may be written to include explicitly the partial dissociation of the initial complex required for the formation of the dinuclear complex:

$$AL \underset{k_0}{\overset{k_{-0}}{\rightleftharpoons}} A\text{---}L \qquad ; \; K^{\#} = k_0 / k_{-0}$$

$$A\text{---}L + Cu \xrightarrow{k_f} ALCu \qquad ; \; k_f = k_{Cu}^{A\text{--}L}$$

Then for a steady-state concentration of A---L,

$$\frac{-d(Cu)}{dt} = k_a (AL)(Cu) = \frac{k_{-0}k_f}{k_0}(AL)(Cu) = \frac{k_{Cu}^{A--L}}{K^{\#}}(AL)(Cu) \quad (4)$$

For all the above mechanisms, the overall rate law is:

$$\frac{-d(Cu)}{dt} = \left[\left(\frac{k_{Cu}^{L}}{K_{AL}} + \frac{k_{Cu}^{HL} K_{HL}(H^+)}{K_{AL}} \right) \frac{1}{(A)} + \frac{k_{Cu}^{A--L}}{K^{\#}} \right] (AL)(Cu) \quad (5)$$

The alkaline earth-dependent component of the observed rate constant corresponds to the term $[k_{Cu}^{L} + k_{Cu}^{HL} K_{HL}(H^+)]/ K_{AL}$ and the alkaline earth independent component of the observed rate constant to the term $(k_{Cu}^{A--L})/ K^{\#}$. The contribution of these pathways may be evaluated by observing the dependence of the overall second-order rate "constant" (i.e.- rate = $k_{obs}(AL)(Cu)$) as a function of the concentration of alkaline earth metals in solution and pH.

For the prediction of the half-life of Cu reacting with AL, the pseudo first-order rate constant is equal to the overall second-order rate constant (at specified pH and alkaline earth concentrations) multiplied by the total ligand concentration AL (which is assumed to be constant). Metal half lives for reaction via indirect or direct pathways are predicted by including only the appropriate terms in the rate equation. Thus for the indirect pathway, the pseudo first-order rate constant is:

$$\frac{k_{Cu}^{L} \quad k_{Cu}^{HL} K_{HL}(H^+)}{K_{AL}} \quad (AL) \quad (6)$$

$$(A)$$

and the pseudo first-order half life for Cu is simply ln2/rate constant. For the direct pathway, the pseudo first-order rate constant is:

$$\frac{k_{Cu}^{AL}(AL)}{K^{\#}} \quad (7)$$

It must be emphasized that these mechanisms and rate equations apply only in the case where the speciation of the ligand is dominated by the alkaline earth metal A. If the alkaline earth complex is not the major ligand species, then the rate of complexation is controlled by the rate of reaction of Cu with the free or protonated ligand. Under these conditions, fast reactions (< minutes) are expected (vide infra).

Experimental Section

All chemicals were analytical grade and most were used without further purification. However, in preparation of the electrolyte solutions (0.5 M NaCl), 5 M NaCl solutions were treated with Chelex 100 to remove trace metals and then diluted with Milli-Q water. [Chelex 100 resin was cleaned with 3 M NH_4OH, rinsed extensively and reconverted to the Na^+-form before use to minimize leaching of organic chelators from the resin.] Suwanee River humic acid obtained from the U.S. Geological Survey was cleaned by re-precipitation from acid solution. The precipitated humic acid was water-washed and dried.

Kinetics experiments. Reactions of alkaline earth metal complexes of EDTA (or NTA) with Cu were followed by measuring concentrations of inorganic copper over time. Inorganic copper concentrations were related to the current measured over 35 sec at 90 mV relative to Ag/AgCl in a well-stirred solution as Cu(II) was reduced to Cu(I). [Current measured without stirring was subtracted to account for non-mass transport-limited phenomena.] Application of this amperometric method for the determination of inorganic copper in seawater has been described previously (49, 50).

Amperometric measurements were made with an Environmental Science Associates Model 3040 Charge Transfer Analyzer equipped with a pyrolytic graphite working electrode, Pt counter-electrode, and Ag/AgCl, saturated NaCl reference electrode. The Charge Transfer Analyzer and electrode systems have been described in detail by Matson et al. (51).

Copper was added to electrolyte (either UV-oxidized Sargasso seawater or solutions of 0.5 M NaCl, 2 mM $NaHCO_3$ with varying concentrations of Ca or Mg) and equilibrated with the electrode system. Aliquots of pre-formed alkaline earth metal complexes of EDTA (i.e.- EDTA pre-equilibrated with excess Ca or Mg) were added and the decrease in concentration of inorganic copper was measured over time. [The experiments were performed by adding ligands rather than metals to the solution because the electrode responds much faster to decreases than to increases in inorganic copper.] Figure 1a shows the electrode response to copper additions and to addition of a large excess of ligand. Response of the electrode system to a decrease in inorganic copper concentration either by complexation (with excess ligand as in the figure) or by dilution was instantaneous on the time scale of the amperometric measurement (~1 min). For each run, electrode response to copper additions (after equilibration) in the absence of any ligands was used as a calibration curve (as in Figure 1b). [N.B.- At high Ca concentrations, the solutions were formally super-saturated with respect to calcite. However, measurement of free Ca^{2+} concentrations with a calcium ion-selective electrode showed no precipitation of any solid calcium phase.]

Data treatment. Inorganic copper concentrations were plotted against time after ligand additions to obtain kinetic parameters. For most of the

Figure 1. Amperometric determination of inorganic copper in 0.5 M NaCl, 0.01 M $CaCl_2$, 0.002 M $NaHCO_3$ (a) Response (counts) to addition of 12.5 nM Cu at t=0, 810, and 1620 sec and to addition of 63 μM CaEDTA at t=4800 sec (b) Calibration curve for response vs. added Cu.

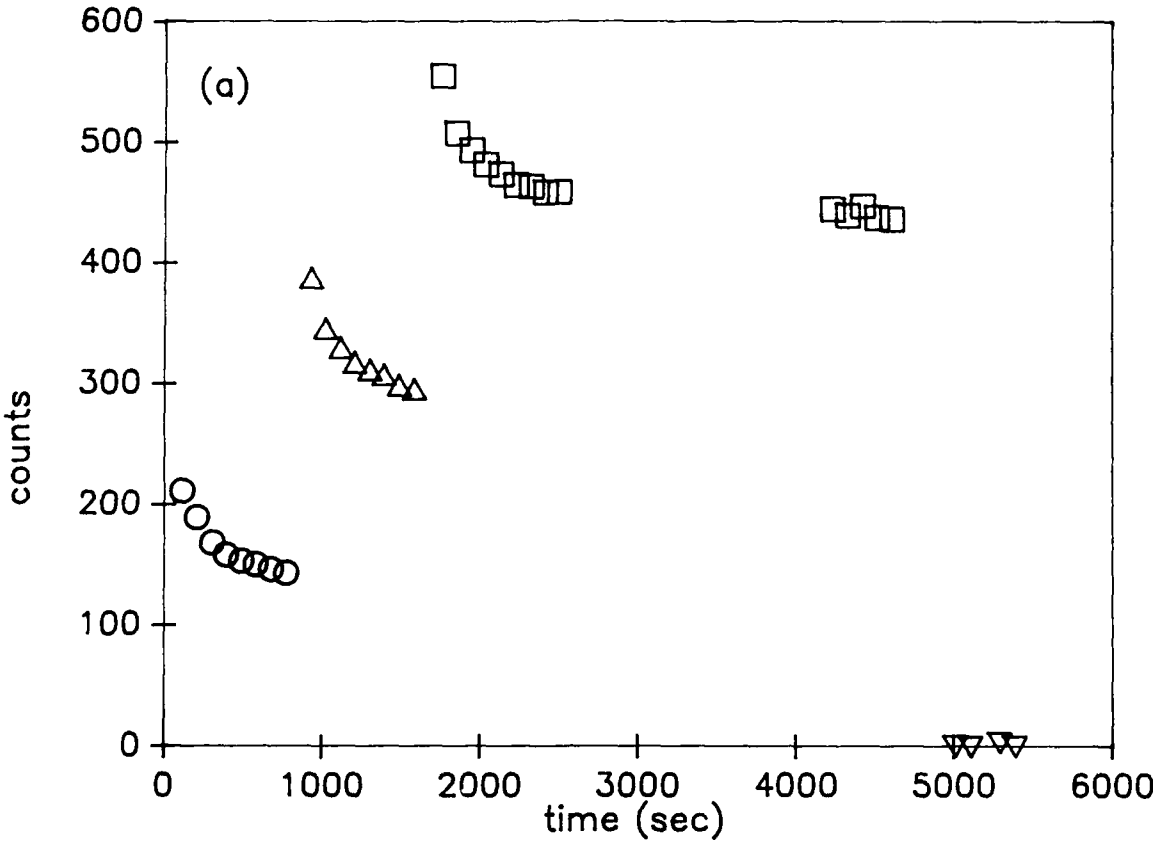
(a)
600
500
400
300
200
100
0
counts
0
1000
2000
3000
4000
5000
6000
time (sec)

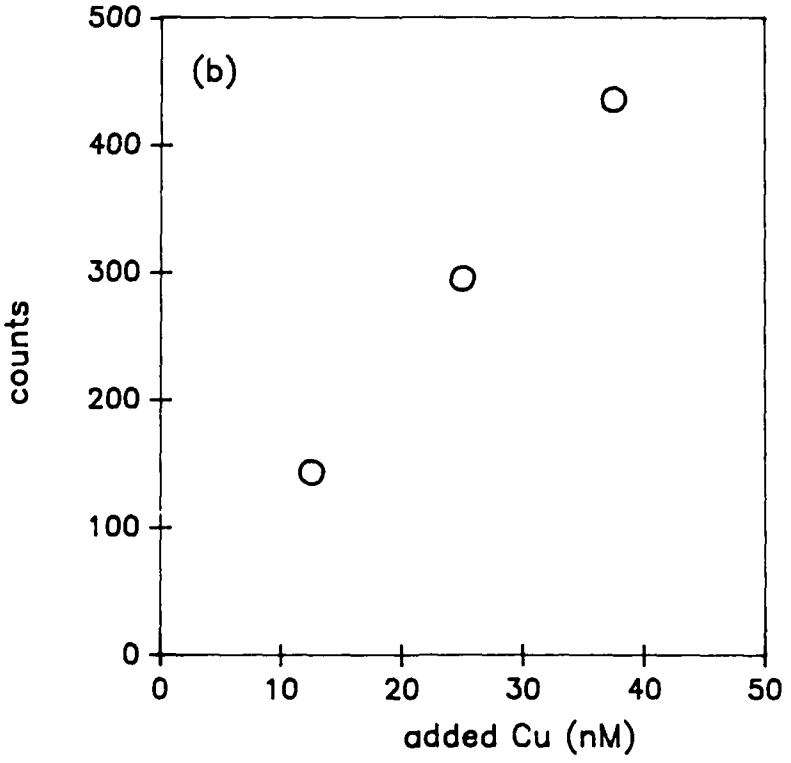
(b)
500
400
300
200
100
0
counts
0
10
20
30
40
50
added Cu (nM)

CaEDTA experiments the change in $(CaEDTA)_{init}$ was small (<5% for the initial reaction). In these cases, $\ln[(Cu)_{init}/(Cu)_t]$ was plotted against time. The resulting pseudo-first order rate constant was divided by $(CaEDTA)_{init}$ to obtain the second order rate constant k_{obs} i.e.-

$$-d(Cu)/dt = k_{obs}\,(CaEDTA)(Cu)$$

For the MgEDTA experiments and some of the CaEDTA experiments, the second order rate constants were obtained directly from

$$\frac{1}{(a-b)} \ln \frac{b(a-x)}{a(b-x)} = kt \qquad \text{for } a = (MgEDTA)_{init} \quad b = (Cu)_{init}$$

x = change in Cu concentration

It should be noted that the rates of some of the MgEDTA experiments were at the upper limit of determination by this method, the reaction having proceeded to more than 50% completion by the first measurement. The rate constants determined from these experiments should be considered minimum estimates.

For all but three of the experiments, the change in inorganic copper concentration was followed to at least 50% reaction. Some deviation from first order behavior in Cu concentration was observed at longer reaction times possibly due to the heterogeneous nature of the measurement system.

Results

The rate of reaction of the (pre-formed) CaEDTA complex with copper depends on the background concentration of calcium in the solution. For example, Figure 2 illustrates that the rate of reaction is significantly faster with 10^{-5} M background Ca than with 10^{-2} M Ca.

The rate of reaction is first order in inorganic copper concentration and first order in the concentration of CaEDTA (Figure 3). The rate

Figure 2. Concentrations of inorganic Cu over time after additions of 125 nM CaEDTA at t=0 in 0.5 M NaCl, 0.002 M $NaHCO_3$ and (○) 10^{-5} M Ca_T or (□) 10^{-2} M Ca_T. Initial concentration of inorganic Cu 37.5 nM (▲).

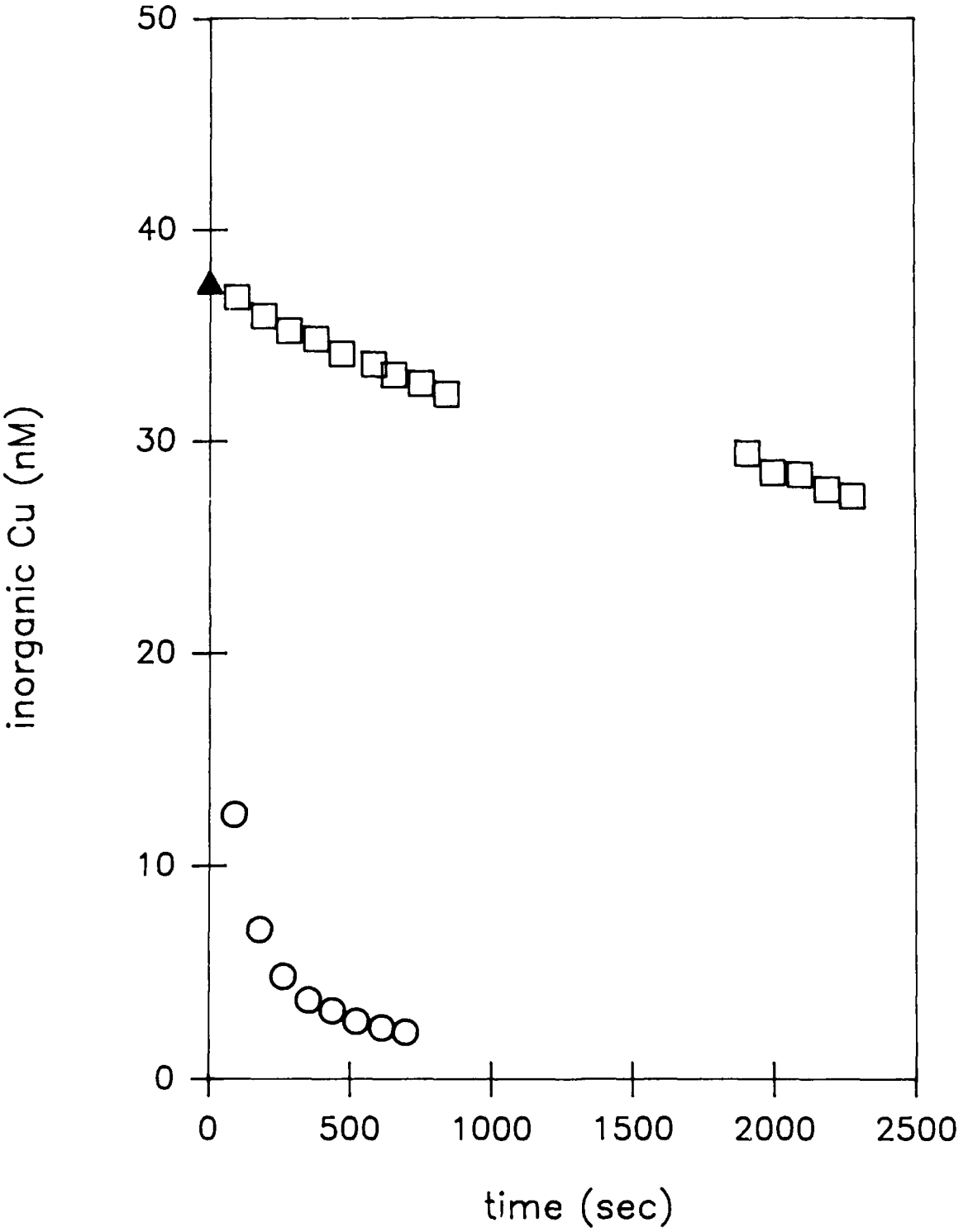
50
40
30
20
10
0
inorganic Cu (nM)
0
500
1000
1500
2000
2500
time (sec)

Figure 3. Logarithmic transform of inorganic Cu concentration vs. time after addition of (∇) 1250 nM CaEDTA or (Δ) 125 nM CaEDTA. Electrolyte: 0.5 M NaCl, 0.01 M $CaCl_2$, 0.002 M $NaHCO_3$.

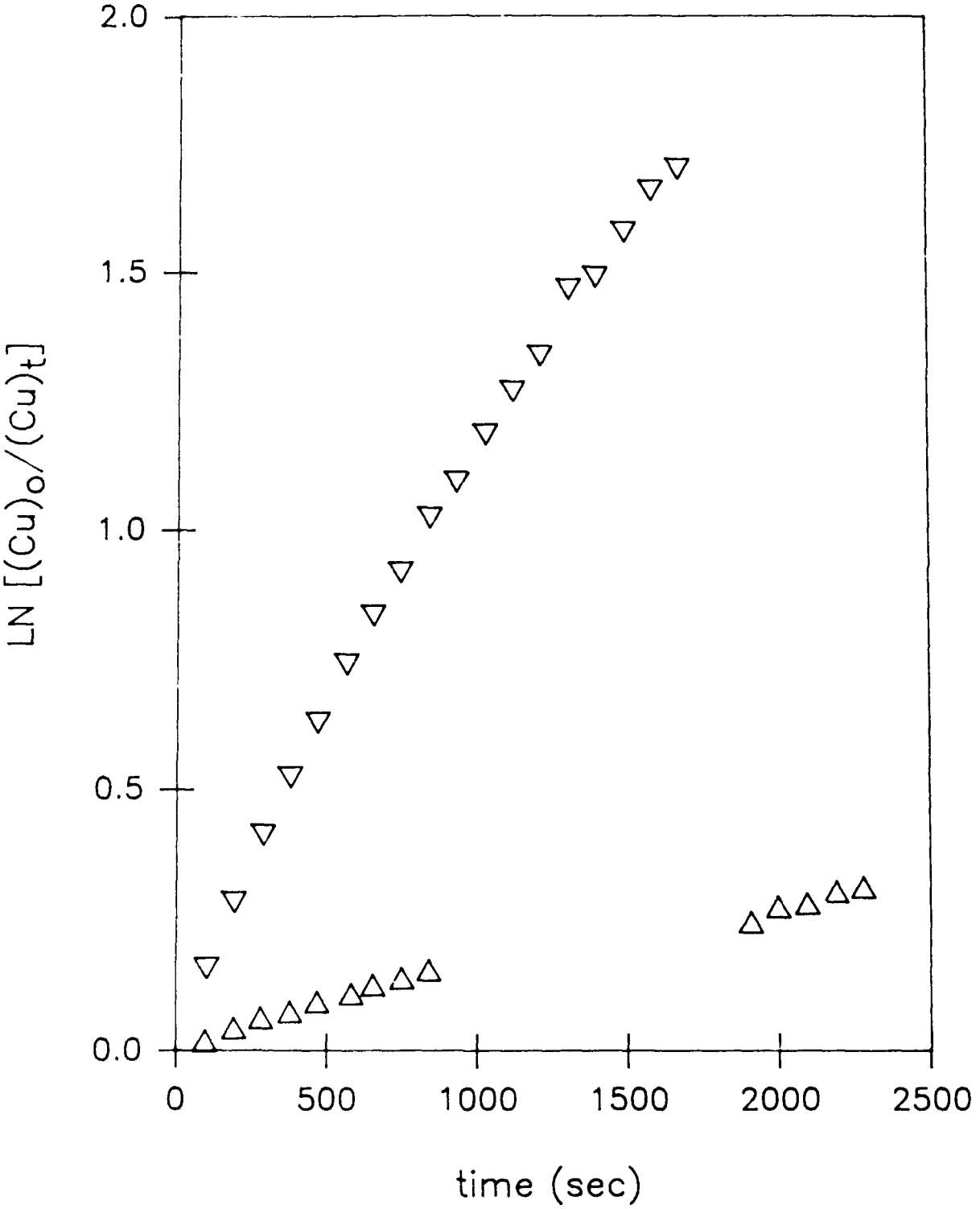
2.0
1.5
1.0
0.5
0.0
LN [(Cu)o/(Cu)t]
0
500
1000
1500
2000
2500
time (sec)

constants are independent of initial metal or ligand concentrations (Table II). The two experiments run in Sargasso seawater indicate that the presence of Mg (at seawater concentrations) does not affect the observed rate of reaction of CaEDTA with Cu. This is to be expected since MgEDTA is not the dominant equilibrium EDTA species under seawater conditions.

The effect of the calcium concentration on the rate of Cu complexation is not constant over the experimental range in calcium concentrations. The observed rate is inversely proportional to Ca concentration up to $(Ca^{2+}) \sim 10^{-3.5}$ M. Above this value, the rate is observed to be independent of the Ca concentration (Figure 4). The observed rate coefficient (k_{obs}) can be expressed as the combination of Ca-independent and Ca-dependent terms, thus

$$\frac{-d(Cu)}{dt} = k_{obs}(CaEDTA)(Cu) = \left[\frac{0.55\ sec^{-1}}{(Ca)} + 970\ M^{-1}sec^{-1}\right](CaEDTA)(Cu)$$

Values for the Ca-dependent rate constant ($0.55 \pm 0.07\ sec^{-1}$) and the Ca-independent rate constant ($970 \pm 50\ M^{-1}\ sec^{-1}$) were obtained by plotting k_{obs} vs. $1/(Ca)_T$ (Figure 5).

The Ca-dependent term is a conditional constant, valid for a fixed pH. A dependence of this constant on pH (due to the contribution of protonated ligand intermediates to the overall reaction) is predicted from theory. Although the behavior of this term over a large pH range was not determined, some pH dependence was observed. Thus

$$\text{Ca-dependent rate constant} = 0.12\ sec^{-1} + 5.0 \times 10^{7} M^{-1}sec^{-1}\ (H^{+})$$

Table II. CaEDTA experiments. Reaction conditions and values of log [second-order rate constant ($M^{-1}sec^{-1}$)] for $-d(Cu)/dt = k_{obs}$ (CaEDTA) (Cu).

log Ca_T	pH	$(Cu)_{init}$ (nM)	$(CaEDTA)_{init}$ (nM)	log k_{obs} ($M^{-1}sec^{-1}$)
-2.0*	8.3	37.5	1250	3.02
-2.0	8.2	25.0	750	2.98
-2.0*	8.3	37.5	125	3.05
-2.0	8.3	25.0	113	3.06
-2.5	8.2	37.5	750	3.04
-3.0	8.3	25.0	113	3.22
-3.0	8.2	25.0	750	3.11
-3.43	8.2	37.5	750	3.46
-3.8	8.2	37.5	375	3.71
-3.95	8.3	37.5	750	3.77
-4.5	8.2	37.5	150	4.25
-4.9	7.9	25.0	150	4.73
-5.0	8.5	25.0	113	4.44
-5.0	7.9	37.5	128	4.88
-5.0	8.2	37.5	75	4.74

(* in UV- oxidized Sargasso seawater)

Figure 4. Log of second-order rate constant ($M^{-1}sec^{-1}$) [for $-d(Cu)/dt = k(EDTA_T)(Cu)$] vs. log alkaline earth metal concentration for (Δ) A-Mg, (□) A-Mg point omitted in data-fitting, and (O) A-Ca. (——) Fit for empirical constants as given in text, (---) contribution of indirect pathway and (....) contribution of direct pathway to overall rate constant.

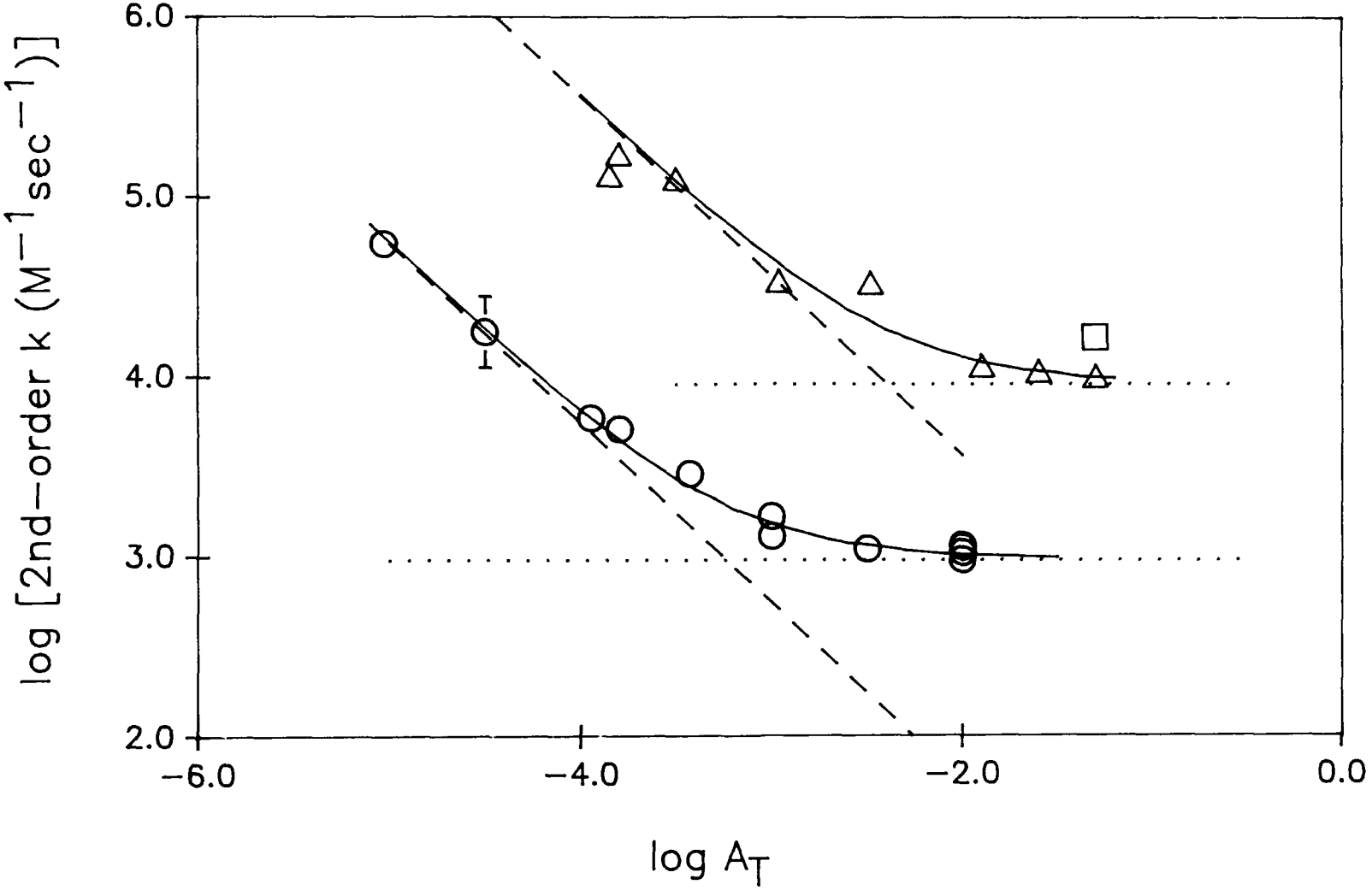
6.0
5.0
4.0
3.0
2.0
−6.0
−4.0
−2.0
0.0
log [2nd−order k (M⁻¹sec⁻¹)]
log A_T

Figure 5. Linear plot of second-order observed rate constant ($M^{-1}sec^{-1}$) [for $-d(Cu)/dt = k(CaEDTA)(Cu)$ vs. $1/Ca_T$. (——) Fit for empirical rate constants in text derived from weighted linear regression. [Inset shows data for high Ca concentrations on expanded scale.]

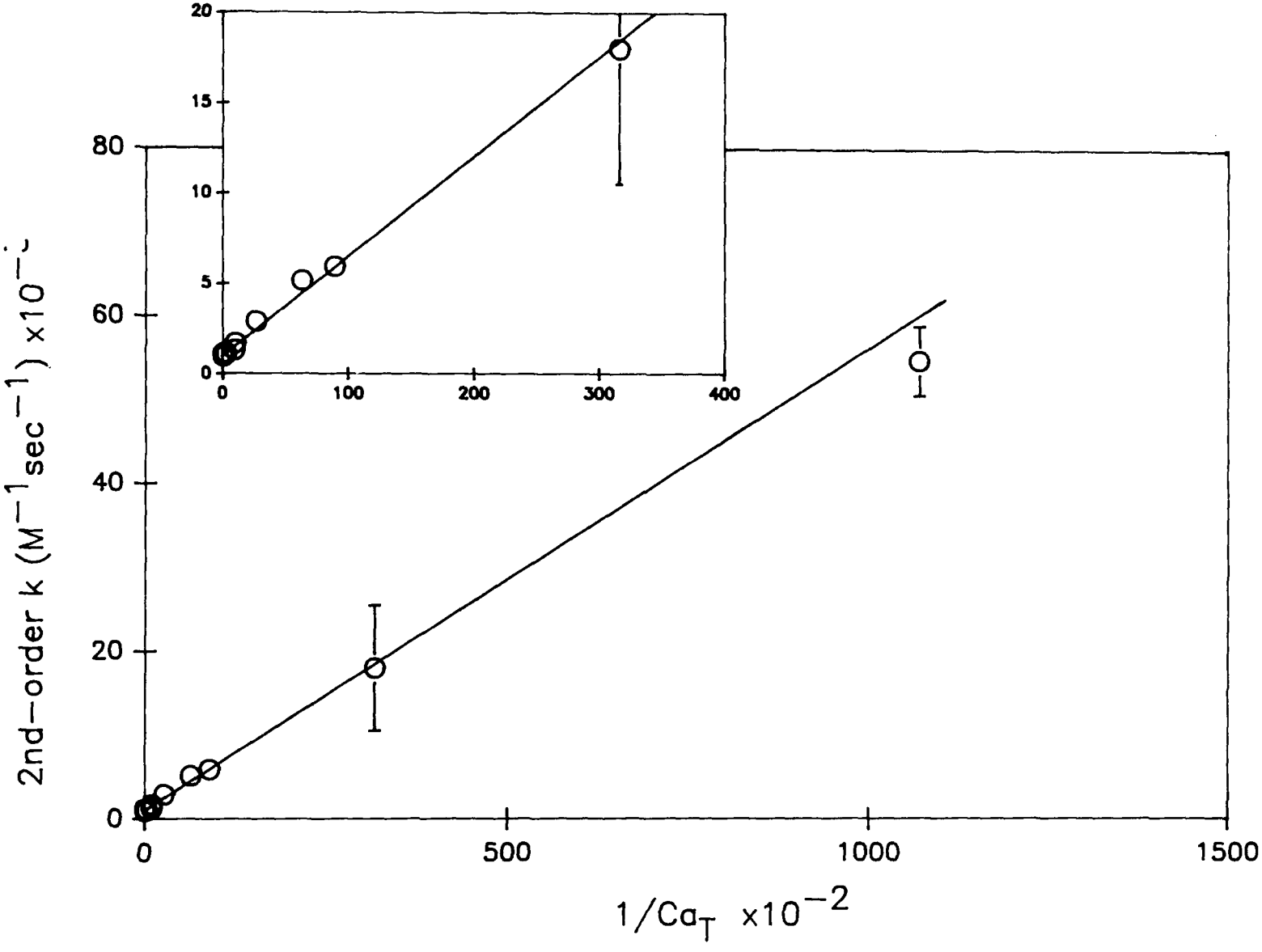
2nd-order k ($M^{-1}sec^{-1}$) x10^{-2}
1/Ca_T x10^{-2}
0
20
40
60
80
500
1000
1500
5
10
15
100
200
300
400

A plot of the Ca-dependent rate constant (i.e.- $(Ca)k_{obs}$ at low (Ca) vs. (H^+) (shown in Figure 6) gave values for the (H^+)-independent term ($0.12 \pm 0.04\ sec^{-1}$) and the (H^+)-dependent term ($5.0 \pm 0.9 \times 10^7\ M^{-1}\ sec^{-1}$).

The overall rate of reaction of CaEDTA with inorganic copper may be described as

$$\frac{-d(Cu)}{dt} = \left[\frac{[0.12 + 5.0 \times 10^7 (H^+)]}{(Ca)} + 9.7 \times 10^2 \right] (CaEDTA)(Cu)$$

The various empirical rate constants can be related to fundamental kinetic and thermodynamic parameters (see Theory- eqn. 5 and Table III).

Similar behavior is observed for the reaction of MgEDTA with Cu in the presence of excess Mg. The rate of reaction of MgEDTA is faster than that of CaEDTA at corresponding concentrations of excess alkaline earth metals (Table IV, Figure 4). Due to the analytical uncertainties involved in determining the fast reaction rates observed at low Mg, the Mg-dependent rate can only be approximated as $36 \pm 10\ sec^{-1}$. The Mg-independent rate constant is $9.2 \pm 0.8 \times 10^3\ M^{-1}\ sec^{-1}$.

In an analogous experiment with the synthetic chelator nitrilotriacetic acid (NTA), the formation of CuNTA in seawater was virtually instantaneous (95% of the calculated equilibrium value within 2 min). A Cu titration of NTA in seawater showed good agreement with the calculated equilibrium values. Kinetic effects were not observable on the time scale (i.e.- minutes) of this experiment (52).

The rate of reaction of Suwannee River humic acid with Cu was also observed to be fast and unaffected by the presence of 10^{-2} M Ca. Reaction of humic acid with copper resulted in the same decrease in inorganic Cu concentration at 0 and 10^{-2} M Ca_T (Figure 7). Cu titrations of humic

Figure 6. Linear plot of the Ca-dependent rate constant (in sec^{-1}) as a function of (H^+) for (O) reaction of Cu with CaEDTA and (Δ) for reaction of Cd with CaEDTA based on the results of Kuempel and Schaap. [N.B.- Data analysis by Kuempel and Schaap assumed reaction of $HEDTA^{3-}$ only, the data was re-interpreted to include explicitly the reaction of $EDTA^{4-}$.]

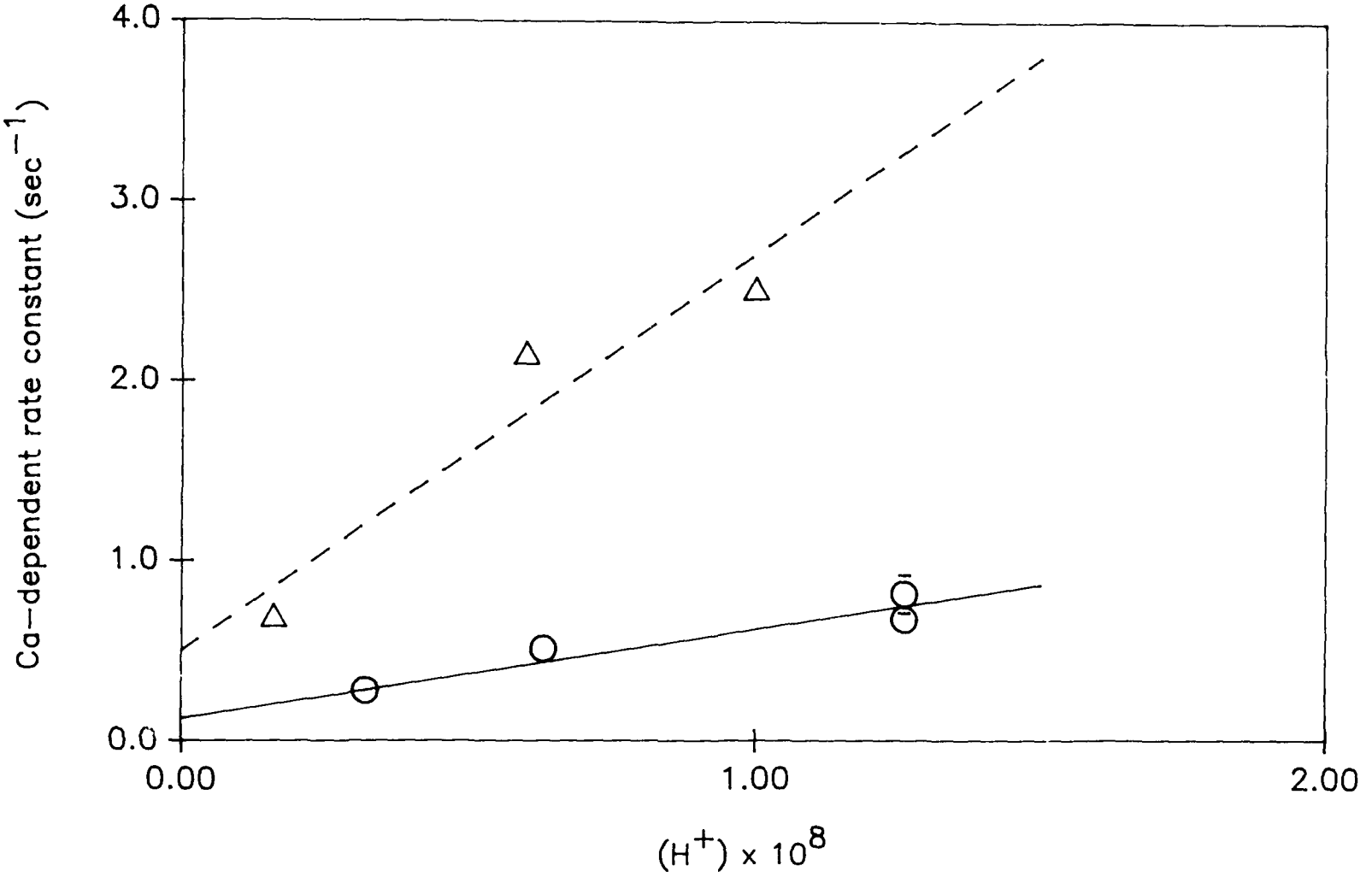
4.0
3.0
2.0
1.0
0.0
0.00
1.00
2.00
Ca-dependent rate constant (sec^{-1})
(H$^+$) x 10^8

Table III. (a) Rate constants for the reaction of Cu with CaEDTA

empirical rate constants description	value	calculated fundamental rate constants
Ca-dependent H^+-independent	0.12 sec^{-1}	$k_{Cu}^{L} = 0.12\ K_{CaL} = 2.3 \times 10^{9}\ M^{-1}sec^{-1}$
Ca-dependent H^+-dependent	$5.0 \times 10^{7}\ M^{-1}sec^{-1}$	$k_{Cu}^{HL} = 5.0 \times 10^{-7} K_{CaL}/K_{HL} = 5.7 \times 10^{7}\ M^{-1}sec^{-1}$
Ca-independent	970 $M^{-1}sec^{-1}$	$k_{Cu}^{CaL} = 970\ M^{-1}sec^{-1}$

[log K_{CaL}=10.28, log K_{HL}= 10.22, μ= 0.5, T=25°C (ref 43)]

(b) Rate constants for the reaction of Cd with CaEDTA from re-interpreted results of Kuempel and Schaap.

empirical rate constants description	value	calculated fundamental rate constants
Ca-dependent H^+-independent	0.50 sec^{-1}	$k_{Cd}^{L} = 2.4 \times 10^{9}\ M^{-1}sec^{-1}$
Ca-dependent H^+-dependent	$2.19 \times 10^{8}\ M^{-1}sec^{-1}$	$k_{Cd}^{HL} = 1.7 \times 10^{8}\ M^{-1}sec^{-1}$

[log K_{CaL} =9.68, log K_{HL}= 9.8, μ =1.0, T=25°C (ref. 44)]

TABLE IV. MgEDTA experiments. Reaction conditions and log [second-order rate constant ($M^{-1}sec^{-1}$)] for $-d(Cu)/dt = k_{obs}$ (MgEDTA) (Cu).

log Mg_T	pH	$(Cu)_{init}$ (nM)	$(MgEDTA)_{init}$ (nM)	log k_{obs} ($M^{-1}sec^{-1}$)
-1.3	8.2	37.5	62.5	4.00
-1.3	8.0	"	"	4.22#
-1.6	8.3	"	"	4.03
-1.9	8.3	"	"	4.06
-2.48	8.2	"	"	4.52
-2.96	8.3	"	"	4.53*
-3.51	8.2	"	"	5.10*
-3.8	8.2	"	"	5.24*
-3.85	8.2	"	"	5.12*

(* Probably minimum estimate of rate)
(# omitted in determination of empirical rate constants)

Figure 7. Concentrations of inorganic Cu in 0.5 M NaCl, 0.002 M $NaHCO_3$ over time after addition of Suwannee Stream humic acid (final concentration 0.3 mg/L) for background calcium concentrations of (O) 0 or (□) 0.01 M Ca_T (for (□) humic acid was pre-equilibrated with 0.001 M Ca_T).

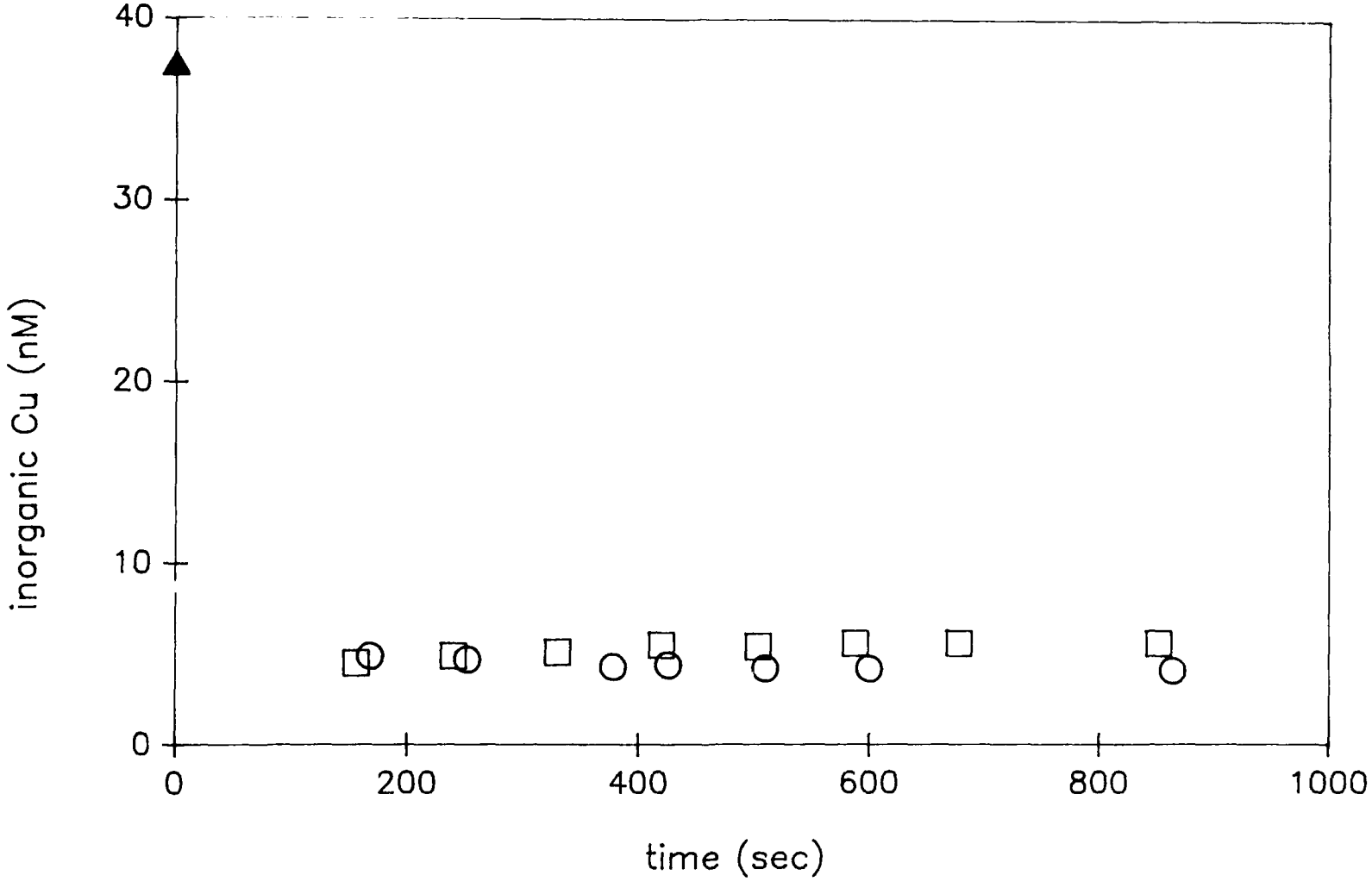
40
30
20
10
0
inorganic Cu (nM)
0
200
400
600
800
1000
time (sec)

acid also showed no competition between Cu and Ca for humic acid metal-binding sites (52).

Discussion

Reaction mechanisms and rate expressions. Our experiments as well as previous work suggest that both indirect and direct pathways are important in metal-exchange reactions between alkaline earth complexes of EDTA and transition metals. In experiments with CaEDTA and Cu, the observed dependence of the rate on Ca concentration suggests that both mechanisms contribute to the overall reaction. At low Ca concentrations, the rate is inversely proportional to Ca_T consistent with the indirect mechanism; at high Ca, the rate is Ca independent as predicted by the direct mechanism (Figure 4). Thus for the reactions of CaEDTA with Cu, the Ca concentration is the parameter that determines which mechanism will predominate at a given pH. The observed pH dependence of the indirect rate constant is consistent with reaction of the protonated ligand intermediate.

The validity of the proposed mechanisms and derived rate expression is supported by the comparison of the reactions of Ca- and MgEDTA complexes. According to the rate expression, the indirect rate constant (i.e.- the Ca- or Mg-dependent term) is determined by the affinity of the ligand for the alkaline earth metal and for protons and by the intrinsic forward rate constant for the formation of CuL (or CuLH). If the reactions of CaEDTA and MgEDTA with Cu are compared, the terms involving the incoming metal (k_{Cu}^{L} and k_{Cu}^{HL}) are eliminated and the ratio of the indirect rate constants should be related to be the ratio of the stability

constants. [N.B.- Stability constants are taken from Martell and Smith (53) for ionic strength of 0.1 M. Ionic strength correction terms do not appear since the same corrections apply to both Ca and Mg constants.]

$$\frac{\text{Mg-dependent k}}{\text{Ca-dependent k}} = \frac{K_{CaL}}{K_{MgL}} = \frac{10^{10.61}}{10^{8.83}} = 60$$

Despite the uncertainty in the value of the Mg-dependent rate constant, the observed ratio (66 ± 26) is comparable to the predicted value.

The prediction of the ratio of Mg- and Ca-independent rate constants from theory involves considerably more assumptions. If the direct pathway is controlled by the rate of formation of the dinuclear intermediate ALCu, the ratio of alkaline earth indepedent rate constants for the reaction of Cu with MgEDTA and CaEDTA is

$$\frac{\text{Mg-independent k}}{\text{Ca-independent k}} = \frac{k_{Cu}^{Mg--L}}{k_{Cu}^{Ca--L}} \frac{K_{Ca}^{\#}}{K_{Mg}^{\#}}$$

The stability constant for the alkaline earth metal complex relative to the partially-dissociated complex, $K^{\#}$, may be estimated by using MIDA (methyliminodiacetic acid) as a model for the EDTA fragment (41). Then

$$K^{\#} = K_{A\text{-}EDTA} / K_{A\text{-}MIDA}. \qquad (8)$$

If rates of reaction of a single metal, Cu, with the partially-dissociated complexes Mg---L and Ca---L are taken to be equal, the relative interchange rates of reaction of Cu with MgEDTA vs. CaEDTA is predicted to be

$$\frac{\text{Mg-independent k}}{\text{Ca-independent k}} = \frac{K_{MgMIDA}\ K_{CaEDTA}}{K_{MgEDTA}\ K_{CaMIDA}} = \frac{10^{3.48}10^{10.61}}{10^{8.83}10^{3.79}} = 32$$

The observed ratio (10 ± 1) is somewhat less than the predicted value.

This difference may be due to an inaccurate estimation of the stability constant for the intermediate.

The assumption that the direct pathway is controlled by the rate of formation of the dinuclear complex is also supported by the similarity in the rates of reaction of CaEDTA with different transition metals (Cu, Cd, Zn, and Pb) (Table V). For such reactions, the interchange rate constant reflects the kinetic reactivity of the metals toward the partially-dissociated complex. The rate of formation of the dinuclear complex is related to the lability of solvent (i.e.- H_2O) molecules in the inner coordination sphere of the incoming metal (54-56). The rate constants for reaction by direct attack of CaEDTA with Cu, Cd, Zn, and Pb are roughly proportional to the water-loss rate constants for the different metals consistent with the rate-limiting formation of the dinuclear intermediate. If the stability of the dinuclear intermediate controlled the rate of the direct reaction, variations in rate constants by factors of up to 10^4 would be predicted based on the affinities of the metals for MIDA (as a model of the intermediate) (Table V) (41).

Comparison with literature values. The observed pH-dependence of the indirect rate constant leads to an estimate of the formation rate constants for reactions of Cu with $EDTA^{4-}$ and $HEDTA^{3-}$: k_{Cu}^{L} and k_{Cu}^{HL}. These constants are similar to those that fit the data of Kuempel and Schaap for the reaction of CaEDTA with Cd (Figure 6, Table III). The formation rate constants k_M^L and k_M^{HL} may be estimated by assuming that, in accordance with the "Eigen mechanism", the rate-determining step is loss of water from the inner-coordination sphere of the metal ion after an outer sphere complex between the metal and ligand has been formed (54-56).

TABLE V. Rate constants for metal exchange by direct pathway with CaEDTA

metal	rate constant ($M^{-1}sec^{-1}$)	ref.	k^{M-H_2O} (from ref. 42)	K_{M-MIDA} (from ref. 53)
Zn	300*	45	$3x10^7$ $7.2x10^7$	$4.6x10^7$
Cd	230 300*	44 45	$1.6x10^8$ $2.5x10^8$	$5.9x10^6$
Cu	970	this work	$2x10^8$ $5x10^8$ $>10^8$ $\sim 5x10^9$	$1.2x10^{11}$
Pb	3000*	45	$2.5x10^9$ $7.5x10^9$	$1.0x10^8$

(* These rate constants include both direct and indirect reaction)

Thus k_M^L should depend chiefly on the nature of the metal ion. The similarity in values of k_M^L for Cu and Cd is consistent with the reported water-loss constants (see Table V) though a range of values for $k^{Cu\text{-}H_2O}$ has been reported. Variations might arise from inorganic complexation of the metal, varying ionic strength, or reactions with ligands of different charge (54-56). As can be seen in Table VI, there is reasonable agreement in reported values of k_M^L although there is wide variation in reported values for the rate constants k_M^{HL}.

Prediction of metal exchange rates. For the model ligand EDTA, the rate of reaction of the calcium complex with copper may be predicted from the rate expression

$$\frac{-d(Cu)}{dt} = \left[\left(\frac{k_{Cu}^L + k_{Cu}^{HL} K_{HL}(H^+)}{K_{CaL}} \right) \frac{1}{(Ca)} + k_{Cu}^{CaL} \right] (CaEDTA)(Cu)$$

as a function of the solution parameters Ca_T and pH (for a given and constant concentration of CaEDTA). As shown in Figure 8 (for (CaEDTA) = 10^{-7} M), both high pH and high Ca concentrations increase the (pseudo first-order) half-life of uncomplexed copper. The relative contributions of the direct and indirect pathways to the overall rate are also determined by pH and Ca_T. The indirect pathway is favored at low pH and low Ca_T (e.g.- in freshwater), the direct pathway at high pH and high Ca_T (e.g.- in seawater). Also shown on Figure 8 are the values of pH and Ca_T for which the contribution of both pathways to the overall rate are equal.

The rate of metal exchange reaction with alkaline earth complexes of other ligands can be predicted based on the stability constants of the calcium and protonated ligand complexes and the abovementioned considerations. This, of course, assumes that the mechanisms governing

TABLE VI. Formation rate constants

metal	ligand	k_M^L ($M^{-1}sec^{-1}$)	k_M^{HL} ($M^{-1}sec^{-1}$)	ref
Cu	$EDTA^{4-}$	$2.3x10^9$	$5.7x10^7$	this work
			*$6x10^8$ to $2x10^9$	57 and ref cit
			*$1.3x10^8$	42
			$8.4x10^7$	58
Cd	$EDTA^{4-}$	#$2.4x10^9$	#$1.7x10^8$	44
			*$2.6x10^8$ to $3.7x10^9$	44 and ref cit
Ca	$EDTA^{4-}$	$6x10^9$	$3.5x10^7$	59
		$2.4x10^{10}$	$1.7x10^7$	43
			$2.3x10^7$	60
Cu	IDA^{2-}	$3.0x10^9$	$1.2x10^4$	61
	$MIDA^{2-}$	$7.4x10^9$	$1.1x10^4$	61

(* assumes no reaction of $EDTA^{4-}$)

(# re-interpreted to include reaction of $EDTA^{4-}$)

Figure 8. Log [(pseudo first-order Cu half-life (sec)] with respect to reaction with 10^{-7} M CaEDTA as a function of pH and log Ca_T. Also shown is the line defining the values of pH and log Ca_T for which the indirect and direct mechanisms contribute equally to the reaction of Cu with CaEDTA.

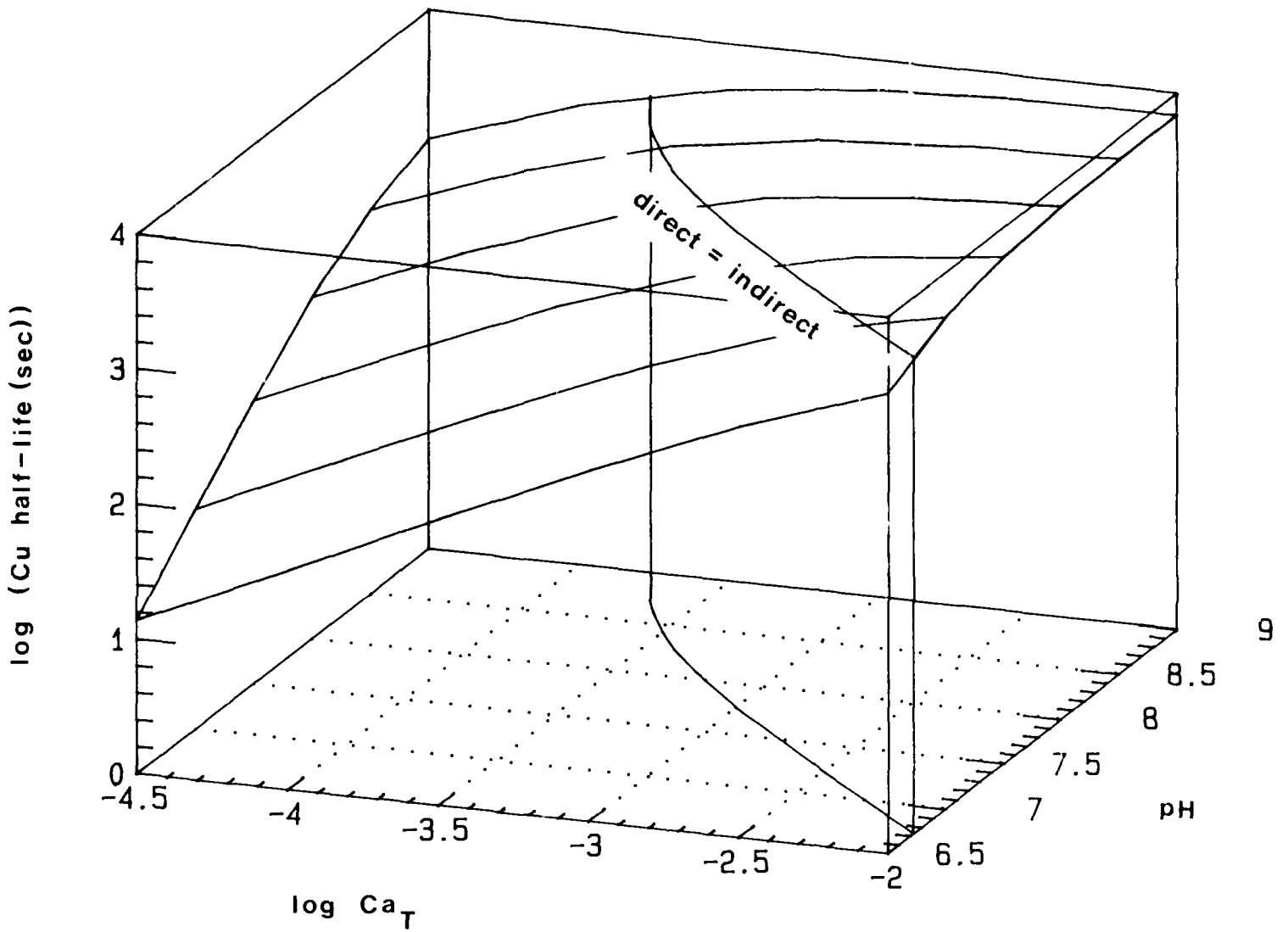
log (Cu half-life (sec))
4
3
2
1
0
direct = indirect
-4.5
-4
-3.5
-3
-2.5
-2
log Ca_T
6.5
7
7.5
8
8.5
9
pH

the metal exchange reactions of EDTA are also appropriate for other ligands.

It must be remembered that these predictions hold only if the alkaline earth metal complex of the ligand is thermodynamically favored over protonated forms of the ligand. In the limiting case where the ligand occurs as L or HL, metal complexation reactions are predicted to be extremely fast even at environmental metal and ligand concentrations.

The (pseudo first-order) half-life of inorganic Cu with respect to metal exchange reactions with Ca complexes of well-defined ligands (see Table VII) are predicted below for conditions favoring (i) indirect (low Ca_T) and (ii) direct (high Ca_T and high pH) pathways for ligand concentrations of 10^{-7} M. [N.B.- For lower ligand concentrations, proportionately longer half-lives would be predicted.]

(i) Indirect reaction (freshwater system): Rate constants may be predicted from the stability constants K_{AL} and K_{HL} and the formation constants k_{Cu}^{L} and k_{Cu}^{HL}. The value of k_{Cu}^{L} is ca. 3×10^{9} M^{-1} sec^{-1} (Table VI). However the effect of ligand protonation is significantly greater than simple electrostatics would predict and k_{Cu}^{HL} varies widely depending on ligand structure (41, 62). Due to the difficulty in estimating k_{Cu}^{HL}, it is only possible to predict limits for the indirect rate constant. A lower limit for the indirect rate constant may be predicted by assuming $k_{Cu}^{L} \ll k_{Cu}^{HL}$ (i.e.- no contribution of the protonated ligand to the rate). Calculation of an upper limit for this constant assumes $k_{Cu}^{L} \sim k_{Cu}^{HL}$ (see eqn. 6).

Figure 9a shows the predicted pseudo first-order half-lives for Cu (for $(CaL) = 10^{-7}$ M and $Ca_T = 0.37$ mM) at pH = 6.5 and 8.2 for a series of

Table VII. Ligands used in Figures 9 and 10

1 NTA

2 trimethylenedintrilotetraacetic acid (TMDTA)

3 N-(2-hydroxyethyl) ethylenedinitrilo,N,N',N' triacetic acid (HEDTA)

4 meso-(1,2dimethylethylene) dinitrilotetraacetic acid

5 EDTA

6 DL-(methylethylene)dinitrilotetraacetic acid (PDTA)

7 DL-(1,2dimethylethylene)dinitriloteraacetic acid

8 trans-1,2-cyclohexylenedinrilotetraaceticacid (CDTA)

Figure 9. Predicted values for log [Cu half-life (sec)] for reaction of Cu with calcium-bound ligands (at 10^{-7} M L_T) as a function of the calcium stability constants of the ligands. Values for K_{CaL} from ref. 53 for μ= 0.1, T=20° C for compounds 1-8 [see Table VII].

(a) freshwater system: indirect reaction for Ca_T= 0.37 mM, pH = 6.5 (□) or 8.2 (Δ). Half-lives are predicted from rate constants for the indirect pathway

$$k=(k_{Cu}^{L} + k_{Cu}^{HL} K_{HL}(H^+))/ K_{CaL}Ca_T \qquad T_{1/2}= \ln 2/ kL_T$$

for (○) k_{Cu}^{L}= 3 x 10^9 $M^{-1}sec^{-1}$, k_{Cu}^{HL} ~ 0 and (□, Δ) k_{Cu}^{L} = k_{Cu}^{HL} = 3 x $10^9 M^{-1}sec^{-1}$. Cu half-life for reaction of CaEDTA based on empirical rate constants (■) pH=6.5, (▲) pH=8.2.

(b) Seawater system: direct reaction. Half-lives predicted from rate constants for the direct pathway

$$k = k_{Cu}^{Ca--L} K_{CaMIDA}/ K_{CaL} \qquad T_{1/2} = \ln 2/ k L_T$$

K_{CaMIDA}= $10^{3.79}$. The rate constant k_{Cu}^{Ca--L} is taken to be equal to K_{Cu}^{L} = 3 x 10^9 M^{-1} sec^{-1}. This may be an overestimate of the actual rate constant thus underestimating the half-life.

(◆) Cu half-life for reaction with CaEDTA based on empirical rate constants.

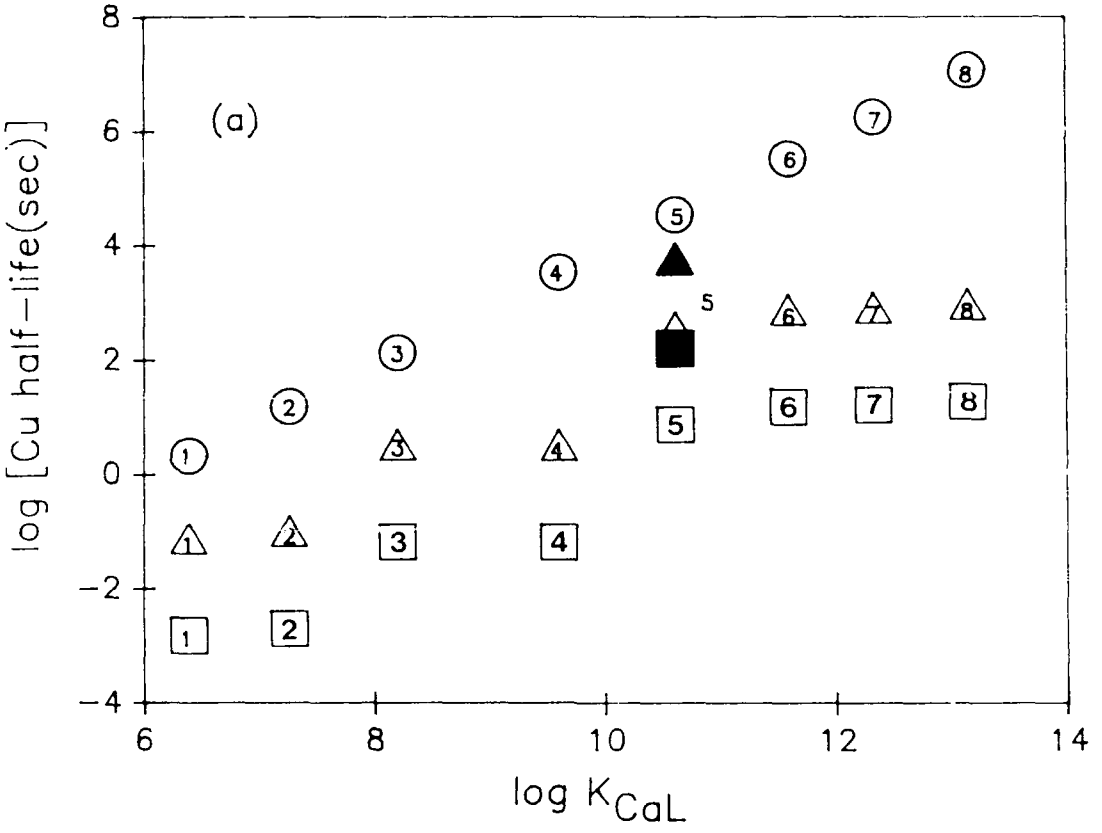
(a)
log [Cu half-life(sec)]
log K_{CaL}
8
6
4
2
0
−2
−4
6
8
10
12
14

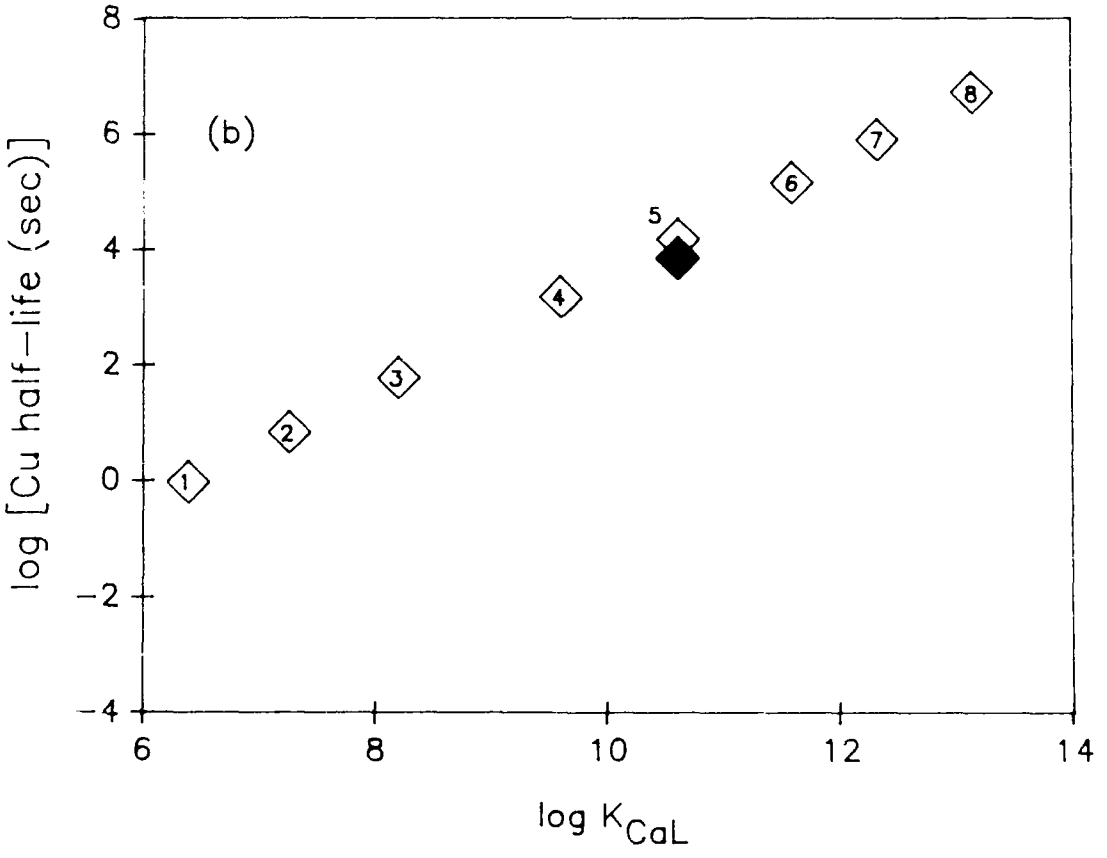
(b)
log [Cu half-life (sec)]
log K_{CaL}
8
6
4
2
0
−2
−4
6
8
10
12
14

well-defined ligands as a function of the stability constant for the calcium complexes. A large uncertainty in the predicted half-lives arises from uncertainty in the contribution of the acid-catalyzed pathway particularly at low pH. The Cu half-life for reaction with EDTA based on empirical results suggests that the acid-catalyzed pathway predominates at pH 6.5 resulting in fast metal-exchange reactions. At pH 8.2, acid catalysis is significantly less important for EDTA and the Cu half-life predicted ignoring acid-catalysis is within an order of magnitude of the observed value.

(ii) Direct reaction (seawater system): Results of EDTA experiments suggest that the rate for metal exchange by direct attack is controlled by the relative stabilities of the alkaline earth metal complex and the partially-dissociated complex. For EDTA, the ligand MIDA can be used as a model for the EDTA ligand fragment. This model for the ligand fragment may be applied to a series of ligands with the same chelating functionalities as EDTA. Figure 9b shows predicted half-lives for uncomplexed copper with respect to metal exchange by the direct pathway (see eqns. 7 and 8).

It must be emphasized that the predicted rate constants (and half-lives) for the direct pathway are dependent on the model for the ligand fragment. The calcium stability constant for the ligand fragment determines the steady-state concentration of the partially-dissociated complex, which is accessible to attack by the incoming metal. Thus for a given K_{CaL}, the predicted direct rate constant will be directly proportional to the calcium stability constant for the chosen model of the ligand fragment. Although MIDA is a reasonable model for the EDTA ligand

fragment, it may not be so for natural ligands.

For the reaction with alkaline earth complexes of NTA, the predicted half-life by either the indirect or direct pathway is only a few seconds. This is consistent with our observations of extremely fast reaction of NTA and Cu in seawater.

Application to natural ligands. There is little doubt that in most natural waters soluble copper is bound to organic ligands with strong effective affinities for the metal. As demonstrated in the EDTA study, the rates of Cu complexation may be quite slow in the presence of Ca or Mg if the ligand speciation is controlled by Ca or Mg and the alkaline earth metal directly competes with the incoming metal for ligand binding sites Thus if some or all of the observed Cu complexation in natural waters can be ascribed to discrete ligands, absolute and relative rates of copper complexation should depend primarily on their affinities for alkaline earths, particularly calcium. Relatively few determinations of calcium complexation by natural ligands have been made however and usually not in a concentration range which allows quantitation of the effect on ligand speciation. Reported values for effective stability constants for isolated humic and fulvic materials are of the range ~10^2-10^4 (pH range 2-8) (38, 63-65). Recent work in our laboratory indicates a somewhat higher affinity Ca binding by humic acids (52). Based on these results, it is unlikely that Ca complexation is important to natural ligand speciation in freshwaters (at low pH and Ca_T). Conversely in seawater (high pH and Ca_T), Ca complexation is predicted to control ligand speciation. It is not possible to translate these results directly into reaction half-lives (as in Figure 9, for example) because we do not know

the actual Ca constants, only effective values, valid at a given pH. Predicted half-lives as a function of effective constants of known ligands are shown in Figure 10 for indirect (10a: pH = 6.5; Ca_T = 0.37 mM) and direct (10b: pH = 8.2) exchange.

Based on the available data on calcium binding by humic and fulvic materials, the half-life for copper with respect to metal exchange in freshwaters should be fast (i.e.- on the order of minutes). Extrapolation of experiments with EDTA to low pH indicate that even ligands with high affinity for calcium react quickly under these conditions.

Under seawater conditions the direct pathway for metal exchange should predominate. Since the half-lives predicted for reaction via this pathway are dependent on the value chosen for the stability constant for the partially-dissociated calcium complex, a better understanding of the natural ligand structure is necessary to predict metal half-lives accurately. For example, catechol, which has been proposed as a model for the chelating functionality of humic materials, has a greater affinity for alkaline earth metals than does MIDA (K_{MgL} for catechol is $10^{5.7}$). A faster rate of exchange via the direct pathway would be predicted using catechol rather than MIDA to model the ligand fragment.

Analytical considerations. The complexation of copper that is measured through Cu titration is necessarily rapid compared to the measurement techniques - typically minutes to hours. The remaining question is whether such complexation measurements may be missing some of the strong binding ligand fraction that reacts slowly. Our model studies with EDTA suggest that ligands with high affinity for both Cu and Ca may be underestimated in determinations of trace metal complexation in natural

Figure 10. Predicted values of log [Cu half-life (sec)] as a function of effective Ca stability constants [$K^{eff}_{CaL} = K_{CaL} / K_{HL}(H^+)$] for (a) freshwater system: indirect pathway exchange conditions as in Figure 9a for pH=6.5 (○) maximum half-lives computed assuming no acid-catalysis, (□) minimum half-lives including acid-catalysis, (■) empirically-derived half-life for reaction with CaEDTA and

(b) seawater system: direct pathway reaction conditions as in Figure 9b for pH=8.2, (◆) empirically derived half-life for reaction with CaEDTA.

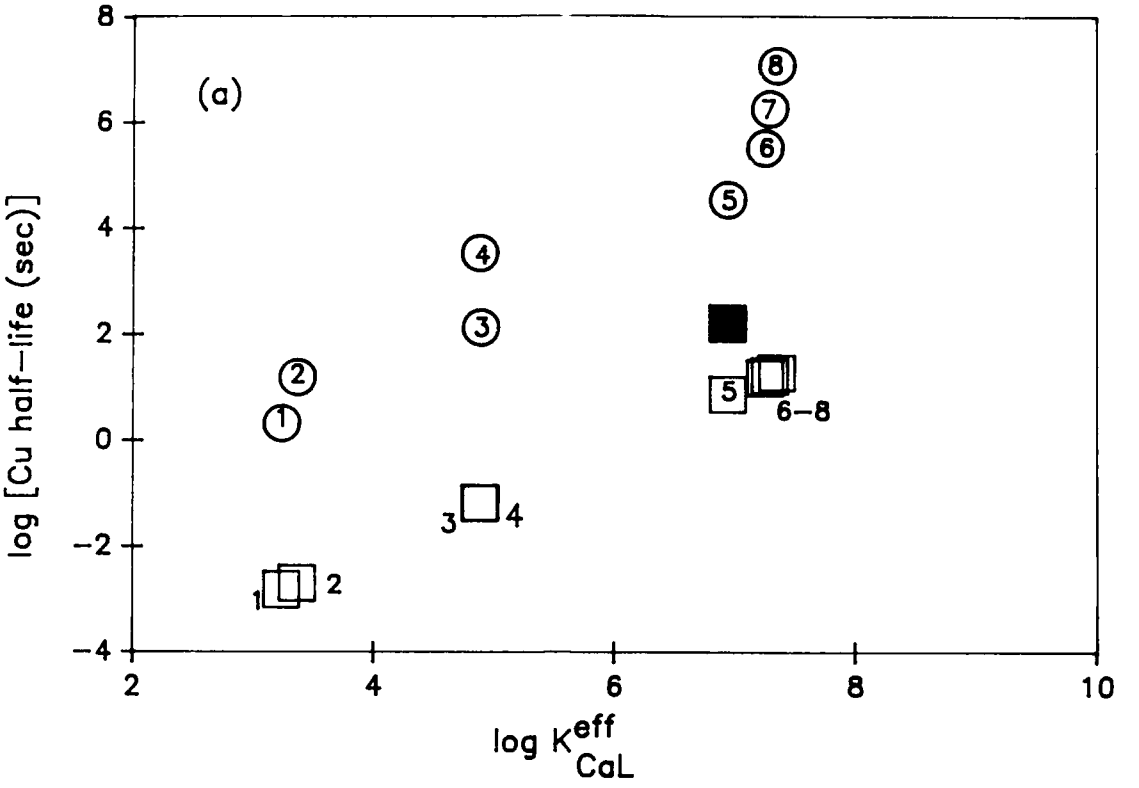
(a)
log [Cu half-life (sec)]
log K^eff CaL
8
6
4
2
0
−2
−4
2
4
6
8
10
1
2
3
4
5
6–8

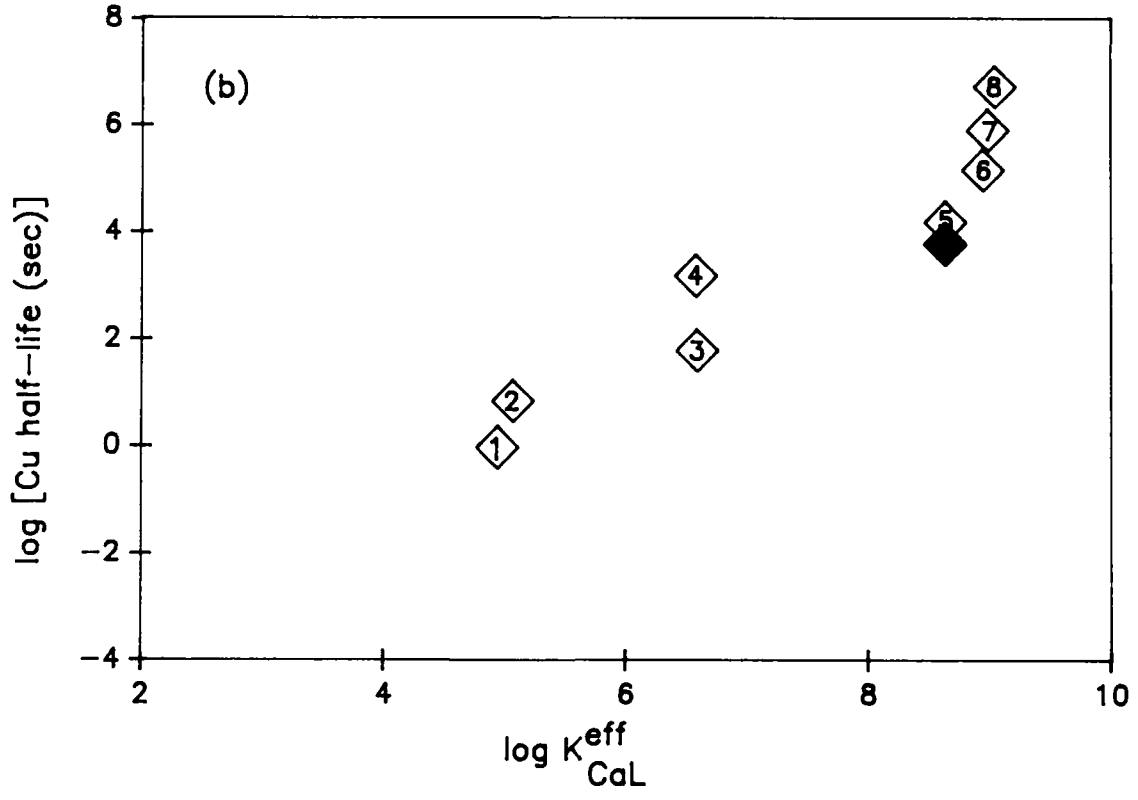
(b)
log [Cu half-life (sec)]
log K^eff CaL
8
6
4
2
0
−2
−4
2
4
6
8
10
1
2
3
4
5
6
7
8

waters which involve metal additions. This effect may be particularly dramatic if the added copper reacts initially with weaker faster-reacting ligands and further reaction with the stronger ligands involves both metal and ligand exchange ($CaL_1 + CuL_2 \longrightarrow CuL_1 + CaL_2$) (66). Such strong ligands would be inefficient at buffering metal additions on short (min-hr) time scales although they might strongly influence long term equilibrium concentrations of free metal ions.

The above argument is predicated on the hypothesis that calcium and copper actually compete for the same binding sites as would be the case for a well-defined discrete ligand. However it is not clear that this condition applies to humic and fulvic compounds which account for part if not all of the organic complexation of transition metals in natural waters. The few reported studies of the effects of calcium on copper binding by humic substances (67, 68) show little competition effects and we have observed essentially none (52). This is consistent with our result showing no measurable kinetic effect of calcium on copper complexation by isolated humates (Figure 7). If indeed calcium and copper do not compete for binding sites in humic molecules, then our model with EDTA is not applicable to humics and the kinetics of copper complexation by humics should be fast even in high calcium media.

Influence of the incoming metal on rates of metal exchange. For both direct and indirect mechanisms the rate of metal exchange reactions is directly dependent on the kinetic reactivity of the incoming metal. This metal reactivity is related to the lability of solvent molecules in the inner-coordination sphere of the metal (i.e.- the water-loss constants). Relative rates of metal-exchange reactions for the reaction of different

transition metals with a given alkaline earth metal complex would be expected to parallel the water-loss constants of the metals such that $Cr^{3+} << Fe^{3+} < Ni^{2+} < Co^{2+} \sim Fe^{2+} < Zn^{2+} < Mn^{2+} < Cd^{2+} < Cu^{2+} < Hg^{2+} < Pb^{2+}$ (42, 54-56). Thus for some metals, particularly Cr^{3+}, Fe^{3+}, and Ni^{2+}, reactions with calcium-bound ligands should proceed significantly slower than reactions of the same ligands with Cu (Figure 11).

Conclusion

Experiments with EDTA suggest that for discrete, multidentate ligands with high affinity for alkaline earth metals, the rate of complexation reactions may be strongly decreased by binding with Ca and Mg in hard waters. This effect of alkaline earth metals is due to the competition between alkaline earth and transition metals for reaction with free ligand formed by dissociation of the initial alkaline earth metal complex and to the very slow direct attack of transition metals on ligands complexed with alkaline earth metals as compared with the reaction with free or protonated ligand species. Thus, the concentrations of such ligands in seawater would be underestimated by analytical techniques for measurement of metal complexation that involve metal additions. The nature of the incoming metal (i.e.- the kinetic lability of bound solvent) also determines whether kinetic effects will be important on environmental time scales. The same relative decrease in the rate of complexation reactions may be important for intrinsically slow-reacting metals (Cr^{3+}, Fe^{3+}, or Ni^{2+}) and not for fast-reacting metals (Cu^{2+} or Pb^{2+}).

Determinations of trace metal complexation in natural waters by a wide array of analytical methods demonstrate the occurrence of ligands

Figure 11. Scale of predicted half-lives for metals relative to Cu half-life for metal-exchange reactions.

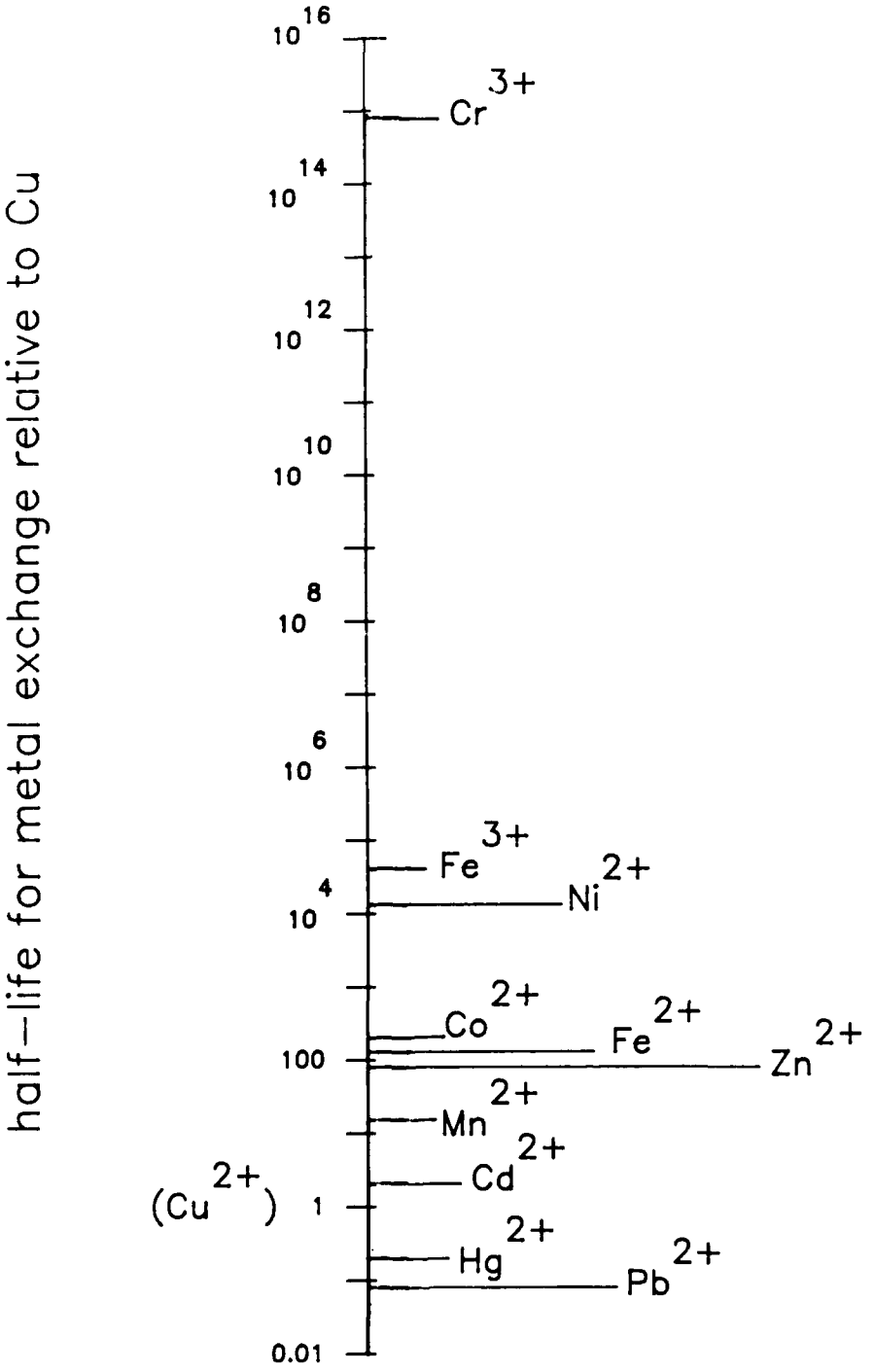
half–life for metal exchange relative to Cu
10^{16}
10^{14}
10^{12}
10^{10}
10^{8}
10^{6}
10^{4}
100
1
0.01
Cr^{3+}
Fe^{3+}
Ni^{2+}
Co^{2+}
Fe^{2+}
Zn^{2+}
Mn^{2+}
Cd^{2+}
(Cu^{2+})
Hg^{2+}
Pb^{2+}

that react quickly with added metals even at seawater concentrations of alkaline earth metals. Consistent with such observations, the rate of copper complexation by isolated humic acid was found not to be retarded in the presence of seawater calcium. This result contrasts with those observed for EDTA and may reflect the fact that Cu and Ca do not compete for the same binding sites in the humic molecules.

Literature Cited

1. Pankow, J.F.; Morgan, J.J. *Environ. Sci. Technol.* **1981**, *15*, 1155.
2. Pankow, J.F.; Morgan, J.J. *Environ. Sci. Technol.* **1981**, *15*, 1306.
3. Morgan, J.J.; Stone, A.T. in *Chemical Processes in Lakes* ed. W. Stumm, Wiley-Interscience: New York, 1985.
4. Hoffmann, M.R. *Environ. Sci. Technol.* **1981**, *15*, 345.
5. Anderson, D.M.; Morel, F.M.M. *Limnol. Oceanog.* **1978**, *23*, 283.
6. Sunda, W.G.; Guillard, R.R. *J. Mar. Res.* **1976**, *34*, 511.
7. Anderson, M.A.; Morel, F.M.M. *Limnol. Oceanog.* **1982**, *27*, 789.
8. Dalang, F.; Buffle, J.; Haerdi, W. *Environ. Sci. Technol.* **1984**, *18*, 135.
9. Davis, J.A.; Leckie, J.O. *Environ. Sci. Technol.* **1978**, *12*, 1309.
10. Davis, J.A.; Leckie, J.O. *Environ. Sci. Technol.* **1979** *13*, 1289.
11. Campbell, P.G.C.; Tessier, A. in *Trace Metal Complexation in Natural Waters* ed. C.J. Kramer and J.C. Duinker, Martinus Nijhoff/ Dr. W. Junk Pub.: The Hague, 1984.
12. Waite, T.D.; Morel, F.M.M. *Environ. Sci. Technol.* **1984**, *18*, 860.
13. Finden, D.A.S.; Tipping, E.; Jaworski, G.H.M.; Reynolds, C.S. *Nature* **1984**, *309*, 783.
14. Bruland, K.W. *Earth Planet. Sci. Lett.* **1980**, *47*, 176.
15. Boyle, E.; Sclater, F.R.; Edmond, J. *Earth Planet. Sci. Lett.* **1977**, *37*, 38.
16. van Geen,A.; Rosener, P.; Boyle, E. *Nature*, in press.
17. Sunda, W.G.; Barber, R.T.; Huntsman, S.A. *J. Mar. Res.* **1981**, *39*,567.
18. Sunda, W.G.; Huntsman, S.A.; Harvey, G.R. *Nature* **1983**, *301*, 234.
19. Morel, F.M.M.; Schiff, S.L. in *Ocean Disposal of Municipal Wastewater: Impacts on the Coastal Environment* vol. I ed. E.P. Myers, MIT Seagrant: Cambridge, 1983.
20. Imber, B.; Robinson, M.G.; Pollehne, F. in *Trace Metal Complexation in Natural Waters* ed. C.J. Kramer and J.C. Duinker, Martinus Nijhoff/ Dr. W. Junk Pub.: The Hague, 1984.
21. Seritti, A.; Pellegrini, D.; Morelli, E.; Barghiani, C.; Ferrara, R. *Mar. Chem.* **1986**, *18*, 351.
22. Estep, M.; Armstrong, J.E.; van Baalen, C. *App. Microbiol.* **1975**, *30*, 186.
23. Murphy, T.P.; Lean, D.R.S.; Nalewajko, C. *Science*, **1976**, *192*, 900.
24. Trick, C.G.; Andersen, R.J.; Gillam, A.; Harrison, P.J. *Science*, **1983** *219*, 306.
25. Imber, B.E.; Robinson, M.G. *Mar. Chem.* **1983**, *14*, 31.
26. Trick. C.G.; Andersen, R.J.; Price, N.M.; Gillam, A.; Harrison, P.J. *Mar. Biol.* **1983**. *75*, 9.
27. McKnight, D.M.; Morel, F.M.M. *Limnol. Oceanog.* **1980**, *25*, 62.
28. McKnight, D.M.; Morel, F.M.M. *Limnol. Oceanog.* **1979**, *24*, 823.
29. Swallow, K.C.; Westall, J.C., McKnight, D.M., Morel, F.M.M. *Limnol. Oceanog.* **1978**, *23*, 538.
30. Jardim, W.F.; Allen, H.E. in *Trace Metal Complexation in Natural Waters* ed. C.J. Kramer and J.C. Duinker, Martinus Nijhoff/ Dr. W. Junk Pub.: The Hague, 1984.
31. Sposito, G.; Holtzclaw, K.M.; Le Vesque-Madore, C.S. *Soil Sci. Soc. Am. J.* **1979**, *43*, 1148.

32. Buckley, P.J.M.; van den Berg, C.M.G. *Mar. Chem.* **1986**, *19*, 281..
33. Kramer, C.J.M.; Duinker. J.C. in *Trace Metal Complexation in Natural Waters* ed. C.J. Kramer and J.C. Duinker, Martinus Nijhoff/ Dr. W. Junk Pub.: The Hague, 1984.
34. Chau, Y.K.; Gachter, R.; Lum-Shue-Chan, K. *J. Fish. Res. Board Can.* **1974**, *31*, 1515..
35. Moffitt, J.W.; Zika, R.G. *Mar. Chem.* **1987**, *21*, 301.
36. Sunda, W.G.; Hanson, A.K. *Limnol. Oceanog.* **1987**, *32*, 537.
37. Sunda, W.G. *Mar. Chem.* **1984**, *14*, 365.
38. Mantoura, R.F.C.; Dickson, A.; Riley, J.P. *Est. Coast. Mar. Sci.* **1978**, *6*, 387.
39. Stumm, W.; Morgan, J.J. *Aquatic Chemistry* Wiley-Interscience: New York, 1981.
40. Morel, F.M.M. *Principles of Aquatic Chemistry* Wiley-Interscience: New York, 1983.
41. Margerum, D.W. *Rec. Chem. Prog.* **1963**, *24*, 237.
42. Margerum, D.W.; Cayley, G.R.; Weatherburn, D.C.; Pagenkopf, G.K. in *Coordination Chemistry*, vol. 2 ed. A. Martell, ACS Monograph 174, 1978.
43. Carr, J.D.; Swartzfager, D.G. *J. Am. Chem. Soc.* **1975**, *97*, 315.
44. Kuempel, J.R.; Schaap, W.B. *Inorg. Chem.* **1968**, *7*, 2435.
45. Raspor,B.; Nurnberg, H.W.; Valenta, P.; Branica, M. *J. Electroanal. Chem.* **1980**, *115*, 293.
46. Raspor,B.; Nurnberg, H.W.; Valenta, P.; Branica, M. *Limnol. Oceanog.* **1981**, *26*, 54.
47. Raspor, B.; Valenta, P.; Nurnberg, H.W.; Branica, M. *Thal. Jugoslav.* **1977**, *13*, 79.
48. Moore, J.W.; Pearson, R.G. *Kinetics and Mechanism*, 3rd ed., Wiley-Interscience: New York, 1981.
49. Waite, T.D.; Morel, F.M.M. *Anal. Chem.* **1983**, *55*, 1268.
50. Hering, J.G.; Sunda, W.G.; Ferguson, R.L.; Morel, F.M.M. *Mar. Chem.* **1987**, *20*, 299.
51. Matson, W.R.; Zink, E.; Vitukevitch, R. *Am. Lab.* **1977**, *9*, 59.
52. Hering, J.G.; Morel, F.M.M. *Environ. Sci. Technol*, in press.
53. Martell, A.E.; Smith, R.M. *Critical Stability Constants*, vol. 1, Plenum Press: New York, 1974.
54. Eigen, M.; Kruse, W.; Maass, G.; De Maeyer, L. *Prog. React. Kin.* **1964**, *2*, 285.
55 Eigen, M. *Pure Appl. Chem.* **1963**, *6*, 97.
56. Eigen, M.; Wilkins, R.G. in *Mechanisms of Inorganic Reactions*, ed. R. Kent Murmann, R.T.M. Fraser, and J, Bauman, ACS Adv. in Chem. Ser. 1965, 49, 55.
57. Tanaka, N.; Osawa, H.; Kamada, M. *Bull. Chem. Soc. Jpn.* **1963**, *36*, 530.
58. Ackermann, H.; Schwarzenbach, G. *Helv. Chim. Acta* **1952**, *35*, 485.
59. Bryson, A.; Fletcher, I.S. *Aust. J. Chem.* **1970**, *23*, 1095.
60. Rechnitz, G.A.; Lin, Z.F. *Anal. Chem.* **1968**, *40*, 696.
61. Roche, T.S.; Wilkins, R.G. *J. Am. Chem. Soc.* **1974**, *96*, 5082.
62. Cassatt, J.C.; Wilkins R.G. *J. Am. Chem. Soc.* **1968**, *90*, 6045.
63. Dempsey, B.A.; O'Melia, C.K. in *Aquatic and Terrestrial Humic Materials*, ed. R.F. Christmann and E.T. Gjessing, Ann Arbor Science: Ann Arbor, MI, 1983.

64. Choppin, G.R.; Shanbag, P.M. *J. Inorg Nucl. Chem.* **1981**, *43*, 921.
65. Sposito, G.; Holtzclaw, K.M., Le Vesque-Madore, C.S. *Soil. Sci. Soc. Am. J.* **1978**, *42*, 600.
66. Hering J.G.; Morel, F.M.M. in prep.
67. Cabaniss, S.E.; Shuman, M.S. *Geochim. Cosmochim. Acta*, **1988**, *52*, 185.
68. Sunda, W.G.; Klaveness, D.; Palumbo, A.V. in *Trace Metal Complexation in Natural Waters* ed. C.J. Kramer and J.C. Duinker, Martinus Nijhoff/ Dr. W. Junk Pub.: The Hague, 1984.

CHAPTER FIVE

THE KINETICS OF TRACE METAL COMPLEXATION: LIGAND EXCHANGE REACTIONS

ABSTRACT

Ligand exchange reactions of CuNTA and Cu-humate complexes with a fluorescent complexing agent were examined. Results with the model system demonstrate that the overall reaction occurs both via complete dissociation of the initial CuNTA complex (indirect pathway) and by direct attack of the fluorescent ligand on CuNTA (direct pathway). Both of these pathways are also involved in ligard exchange reactions of humate-bound Cu at the Cu-to-humate loading typical of estuarine and coastal waters. At higher Cu-to-humate loadings, the overall reaction is dominated by the indirect pathway. The relationship between observed rate constants for this mechanism and conditional stability constants for Cu-humate interactions is discussed.

INTRODUCTION

The speciation of trace metals in natural waters is determined by the reactivity of the metals toward a complex (and varying) mixture of inorganic anions, organic ligands, reactive chemical species (e.g.- H_2O_2), surfaces and organisms. Concentrations of (operationally defined) "dissolved" metals may include fine colloidal species, organic and inorganic metal complexes.

Both metal speciation and biological availablity (or toxicity) are functions of the tendency of the metal to react (as quantified by the

free metal ion activity) under (pseudo) equilibrium conditions. For metals ocurring as organic complexes, pseudo-equilibrium conditions may be maintained only if the rates of metal complexation reactions are fast compared with rates of metal uptake. However if complex dissociation and ligand exchange rates are slow compared to biological uptake, the rate of metal incorporation into the biota will be limited by abiotic chemical kinetics.

The apparent rate of other processes (precipitation, reduction, adsorption) will be similarly influenced by the rates of metal complexation reactions if (1) the reacting metal occurs predominantly as an organic complex and (2) the process of interest requires removal of the metal from the initial complex.

In this study, we have investigated rates of complex dissociation and ligand exchange for copper under environmentally relevant conditions of pH and metal and ligand concentrations. The objective of this work was to determine how the nature and concentrations of the ligands involved in exchange reactions influence the mechanistic pathways through which the reactions proceed and to use results obtained with well-defined ligands to aid in interpretation of ligand exchange reactions of copper-humate complexes.

BACKGROUND

Classical kinetic studies of ligand exchange reactions of transition metals (as reviewed by Margerum et al., 1978) have shown the reactions to proceed by direct attack of the incoming ligand on the initial metal complex and (usually) rate-determining dissociation of the

ternary complex thus:

$$ML + L' \underset{}{\overset{\text{fast}}{\rightleftharpoons}} LML' \xrightarrow{\text{slow}} L + ML' \qquad (1)$$

The observed rate constants are influenced by steric and electrostatic factors and by protonation of the incoming ligand. Some rate constants for ligand exchange reactions of well-defined ligands are given in Table I. A mechanism involving the rate-limiting formation of a ternary complex and subsequent fast reaction to products has also been proposed by Sweigart and DeWit (1969) to explain their observation that to some extent the reaction was independent of the concentration of the incoming ligand.

In contrast, Shuman and co-workers have observed that ligand exchange reactions of Cu-DOC complexes proceed via dissociation of the copper complexes and have measured dissociation rates for these complexes by electrochemical methods (Shuman and Michael, 1978; Shuman et al., 1983; Olson and Shuman, 1983). Other studies of reactions of metal-fulvates or of reactions of metals with fulvic acids have focused on different metals- Fe (Langford and Khan, 1975; Langford et al., 1977, 1981; Waite and Morel, 1984), Al (Mak and Langford, 1982; Plankey et al., 1986), and Ni (Lavigne et al., 1987).

In this work, we compare the kinetic behavior of well-defined ligands with humic acids in ligand exchange reactions. Reactions with well-defined ligands are examined at environmentally realistic ligand and metal concentrations. Previous studies (as in Table I) have been conducted at high ligand and metal concentrations ($\sim 10^{-4}$ to 10^{-2} M). The extrapolation to environmental concentrations is complicated by changes in the importance of 1:2 metal-ligand complexes over such

TABLE I. Rate constants for ligand exchange reactions ($ML + Y \longrightarrow L + MY$)

(from Margerum et al., 1978)

ML	Y	k_Y^{ML} ($M^{-1}sec^{-1}$)
$Cu(NTA)^-$	MNT^{2-}	1.6×10^3
	$H_2(tetren)^{2+}$	2.1×10^8
	$H_3(tetren)^{3+}$	6.1×10^4
$Ni(NTA)^-$	BT^{3-}	3.27×10^4
	$H(BT)^{2-}$	58
	CAL^{3-}	2.5×10^5
	$H(CAL)^{2-}$	1.67×10^3
	$DTPA^{5-}$	910
	$H(DTPA)^{4-}$	306
	$H_2(DTPA)^{3-}$	1.78
	$EDTA^{4-}$	1.5×10^3
	$H(EDTA)^{3-}$	4.14, 233
	$H_2(EDTA)^{2-}$	0.443
	$H(HEEDTA)^{2-}$	1.96
	$H_2(HEEDTA)^-$	0.427
	NTA^{3-}	3×10^{-5}
	H(PAR)	420
$Co(NTA)^-$	CAL^{3-}	6.5×10^5
	$H(CAL)^{2-}$	2.6×10^5
	$CyDTA^{4-}$	65, 85
	$H(CyDTA)^{2-}$	0.34, 0.58
$Zn(NTA)^-$	$CyDTA^{4-}$	7.5
	$H(CyDTA)^{3-}$	5.4×10^{-2}
	NTA^{3-}	2.0×10^6
	$H(NTA)^{2-}$	530

ML	Y	k_Y^{ML} ($M^{-1}sec^{-1}$)
$Pb(NTA)^-$	NTA^{3-}	6.6×10^7
	$H(NTA)^{2-}$	3.1×10^3
$Cd(NTA)^-$	NTA^{3-}	1.8×10^7
	$H(NTA)^{2-}$	290
$Cu(CyDTA)^{2-}$	$H(trien)^+$	2.5
	$H_2(trien)^{2+}$	0.04
	En	0.12
	Dien	15
	$H(dien)^+$	3.4
	Tetren	5.0
	$H(tetren)^+$	4.7
	$H_2(tetren)^{2+}$	0.2
	$H_3(tetren)^{3+}$	0.007
	Trien	5.4
$Cu(EDTA)^{2-}$	$EDTA^{4-}$	0.174
	$H(EDTA)^{3-}$	1.5×10^{-2}
	MNT^{2-}	7.6×10^3
	Penten	1.7×10^4
	$H(penten)^+$	1.6×10^4
	$H_2(penten)^{2+}$	3×10^3
	$H_3(penten)^{3+}$	1.5×10^3
	Tetren	2.2×10^5
	$H(tetren)^+$	3.7×10^5
	$H_2(tetren)^{2+}$	6.7×10^3
	$H_3(tetren)^{3+}$	34

ML	Y	k_Y^{ML} ($M^{-1}sec^{-1}$)
$CuEDTA^{2-}$	Trien	4.3×10^5
		9.1×10^5
	$H(trien)^+$	3.5×10^4
		1.8×10^4
	$H_2(trien)^{2+}$	2.1×10^4
		360
	$H_3(trien)^{3+}$	44
$Cu(EGTA)^{2-}$	PAR^-	300
	H(PAR)	1.8

ABBREVIATIONS

BT	Eriochrome Black T
CAL	1-(hydroxy-4-methyl-2-phenylazo)-2-napthol-4-sulfonate
CyDTA	cyclohexylenediaminetetraacetic acid
dien	diethylenetriamine
EDTA	ethylenediaminetetraacetic acid
EGTA	ethyleneglycolbis(2-aminoethyl ether)-tetraacetic acid
en	ethylenediamine
HEEDTA	hydroxyethylethylenediaminetetraacetic acid
MNT	maleonitriledithiolate
NTA	nitrilotriacetic acid
PAR	4-(2-pyridylazo)resorcinol
penten	N,N,N',N'-tetra(2-aminoethyl)ethylenediamine
tetren	tetraethylenepentamine
trien	triethylenetetramine

concentration ranges. The mechanistic pathways elucidated with well-defined ligands are consistant with the equilibrium stability constants of the metal complexes. The kinetics of ligand exchange reactions of humic acids are interpreted in light of the mechanisms applicable to well-defined ligands.

THEORY

The kinetic behavior of ligand exchange reactions was examined to determine the mechanistic pathways for these reactions. Terms and definitions are given in Table II. The mechanisms are written below with reaction of the protonated ligands included in the overall rate constants, which are pH-dependent, and rate expressions are derived assuming steady-state concentrations of intermediate species (i.e.- Cu and LCuD) and neglecting back reaction of the product CuD. For each mechanism, contributions of the protonated species to the rate constants can be expressed explicitly if equilibration of protonated species is assumed to be rapid. Thus for the indirect mechanism:

$$CuL_T \underset{k_{Cu}}{\overset{k_{CuL_T}}{\rightleftharpoons}} Cu + L_T \qquad (2)$$

$$Cu + D_T \underset{k_{CuD_T}}{\overset{k_{Cu}^{D_T}}{\rightleftharpoons}} CuD_T \qquad (3)$$

$$\frac{-d(D)}{dt} = \left[\frac{k_{CuL_T}\, k_{Cu}^{D_T}}{k_{Cu}^{D_T} (D_T) + k_{Cu}^{L_T} (L_T)} \right] (CuL)\ (D_T) \qquad (4)$$

where

TABLE II. Terms and Definitions

k_{CuL} or k_{CuD}.....intrinsic rate constants for dissociation of complex CuL or CuD

k^{H}_{CuL} or k^{H}_{CuD}.....intrinsic rate constant for acid-catalyzed dissociation of complex CuL or CuD or for dissociation of the protonated complex CuLH or CuDH (these are mathematically identical)

k^{L}_{Cu} or k^{D}_{Cu}.....intrinsic rate constant for formation of the complex CuL or CuD by reaction of Cu with D or L

k^{HL}_{Cu} or k^{HD}_{Cu}.....intrinsic rate constant for formation of complex CuL or CuD by reaction of Cu with HL or HD (H^+ is displaced by the incoming metal)

k^{CuL}_{D} or k^{CuL}_{HD}.....intrinsic rate constant for direct attack of D or HD on complex CuL to give the product CuD

k_{CuD_T} or k_{CuL_T}.....overall rate constant (at fixed pH) for dissociation (including acid-catalyzed dissociation) of complex CuD or CuL

$k^{L_T}_{Cu}$ or $k^{D_T}_{Cu}$.....overall rate constant (at fixed pH) for formation of complex CuL or CuD by reaction of Cu with all L or D

α.....ratio of rate constants for reaction of Cu with D_T and L_T, $k^{D_T}_{Cu} / k^{L_T}_{Cu}$

$k^{CuL}_{D_T}$.....overall rate constant for reaction of all D species with complex CuL to give the product CuD

k_{ind}.....rate constant for reaction via indirect pathway

k_{dir}.....rate constant for reaction via direct pathway

K_{HD} or K_{HL}.....equilibrium stability constant for complex HD or HL

K_{CuD}^{cond}.....conditional stability constant (pH-dependent) for complex CuD

P_m.....fitting parameter used to account for imperfect mixing in kinetics experiments

Hum_T.....total humic acid concentration

HumX.....concentration of humate binding site X (X= 1,2 for 2 binding site types)

CuHumX.....concentration of Cu bound at humate site X

S.....site density of Cu humate binding sites/ mg humic acid

k_{H1}^{ind} or k_{H1}^{dir}.....rate constant for reaction of CuHum1 with D by indirect or direct pathway

k_{H2}.....rate constant for reaction of CuHum2 with D

k_{CuHum_T}.....rate constant for dissociation of CuHum

$k_{Cu}^{Hum_T}$.....rate constant for reaction of Cu with Hum

$$k_{CuL_T} = k_{CuL} + k^{H}_{CuL}(H^+) \qquad (5) \qquad k^{L_T}_{Cu} = \frac{k^{HL}_{Cu} K_{HL}(H^+) + k^{L}_{Cu}}{1 + K_{HL}(H^+)} \qquad (6)$$

$$k^{D_T}_{Cu} = \frac{k^{HD}_{Cu} K_{HD} (H^+) + k^{D}_{Cu}}{1 + K_{HD} (H^+)} \qquad (7)$$

[N.B. k_{CuD_T} is neglected in consideration of the reaction as written above. It is shown here for future discussion of the reverse reaction (i.e.- CuD + L $\longrightarrow$ D + CuL).]

For the direct reaction:

$$CuL + D \rightleftharpoons LCuD \rightleftharpoons L + CuD$$

$$\frac{-d(D)}{dt} = k^{CuL}_{D_T} (CuL)(D_T) \qquad (9) \qquad k^{CuL}_{D_T} = \frac{k^{CuL}_{D} + K^{CuL}_{H} K_{HD} (H^+)}{1 + K_{HL} (H^+)} \qquad (10)$$

In this study, the rate constants for the formation and dissociation of the ternary complex, which is assumed to be at steady-state, were not resolved and so are expressed as a single term ($k^{CuL}_{D_T}$).

These two types of mechanisms can be distinguished experimentally based on the observed effect of the free L concentration on the rate. In the presence of excess L the overall rate is:

$$\frac{-d(D)}{dt} = \left[\frac{k_{CuL_T} k^{D_T}_{Cu}}{k^{D_T}_{Cu}} \frac{1}{(L_T)} + k^{CuL}_{D_T} \right] (CuL) (D_T)$$

The importance of the indirect pathway should be strongly influenced by the relative concentrations of D and L. For (L) >> (D), competitive behavior is predicted and the rate should be inversely proportional to (L). For (L) << (D), "trapping" behavior is predicted and the rate should be dependent only on the intrinsic rate constant for dissociation

of the initial metal complex (k_{CuL_T}). In contrast the apparent rate constant for direct attack of D on CuL should be unaffected by the concentration of free L or the L:D ratio.

EXPERIMENTAL SECTION

Materials: Analytical grade reagents were used without further purification except for NaCl. Solutions of 5 M NaCl, prepared with analytical grade salts, were treated with Chelex 100 to remove trace metals and then diluted with Milli-Q water. [Chelex 100 resin was cleaned with 3 M NH_4OH, rinsed extensively and then reconverted to the Na^+-form before use to minimize leaching of organic chelators from the resin.] Humic acid (Aldrich) was obtained as the Na-salt and cleaned before use by re-precipitation from acid solution (as described in Hering and Morel, submitted (a)). The fluorescent reagent, Calcein, (herein referred to as dye or D) was used as received from Sigma.

All kinetics experiments (except for the study of the reverse reaction of NTA with CuD) were performed on 0.1 M NaCl and 10^{-3} M PO_4 (pH= 7.4 ± 0.2) at room temperature. The experiment on the reverse reaction was done in 0.1 M NaCl buffered to pH 7.3 with 5 mM HEPES (N-2-hydroxyethylpiperazine-N'-2-ethanesulphonic acid). Experiments were routinely conducted using acid-washed (dilute HCl) polyethylene and sample handling was done in a laminar flow hood.

Measurement of the fluorescent reagent: Calcein is fluorescent over the pH range of ~3-11. The fluorescence is quenched on formation of complexes with paramagnetic transition metals, in this case Cu^{2+} (Pribil, 1982 and ref. cit.). The determination of speciation of the

dye in the presence of Cu by fluorescence quenching is described in detail in Appendix B. Fluorescence was measured with a Perkin-Elmer LS-5 fluorescence spectrophotometer at an excitation wavelength of 492 nm and an emmission wavelength of 511 nm. The fluorescence-dye concentration relationship was calibrated for all kinetics experiments in the presence of NTA or EDTA. For experiments with humic acid, the dye fluorescence was calibrated at each humic acid concentration. At high concentrations of humic acid, apparent fluorescence of the humic acid is decreased probably due to absorption of the fluoresced light by the humic acid in solution.

Kinetics experiments: All kinetics experiments (again excepting the NTA reverse reaction experiment) were performed by mixing approximately equal volumes of reagent solutions using a dual syringe assembly. Thus for reactions of CuNTA with dye, reagent solutions (either Cu premixed with NTA in buffer, or dye in buffer) were drawn into two syringes. At t=0, the reagents were mixed by dispensing them from the syringes through tubing joined by a T-connection into a fluorescence cuvette. Fluorescence signals were integrated over 4 sec. The first fluorescence reading was obtained at ~20 sec and thereafter at ~10 sec intervals. Fluorescence was measured for between 10 and 30 min. The extent of reaction occurring over this time varied considerably depending on the reaction conditions. For the NTA reverse reaction, the reaction was initiated by spiking a solution of the pre-equilibrated Cu/dye in buffer in 100 mL volumetric flasks with a small aliquot of 0.01 M NTA. The solutions were mixed and aliquots removed for fluorescence measurements. The first fluorescence measurement was

obtained at ~4 min. The experiment was performed in duplicate. Each flask was sampled at ~10 min intervals for the first hour. The reaction was followed to equilibrium (~4 h).

Data treatment and modeling: In all kinetics experiments, measured fluorescence was related to free dye concentration by calibration curves obtained immediately following the kinetics experiments. No other dye species (i.e- than free or protonated D) was considered to contribute to observed fluorescence. Quenched fluorescence was attributed solely to the formation of a 1:1 CuD species. Thus from the total concentrations of reagents, the (assumed) stoichiometry of the complexes, and the observed fluorescence, the concentrations of free D and CuD over time could be calculated.

For kinetics experiments performed with the dual syringe assembly, the approximate nature of the mixing procedure affects the initial concentrations of the reagents. A fitting parameter P_m, P_m = apparent $(D)_o$/[1/2 undiluted $(D)_o$], was introduced in the data analysis to account for imperfect mixing as described below.

The method of extraction of rate constants from kinetic data varied depending on the concentrations of reactants. For reactions of CuNTA with dye (NTA in excess), an observed second-order rate constant (i.e.- rate = - d(D)/ dt = k_{obs} (CuNTA)(D)) was obtained in one of two ways. For (CuNTA) >> (D), a pseudo-first order rate constant was obtained from and exponential fit to the concentration of free dye over time. The extrapolated value of $(D)_o$ was used to calculate the mixing parameter P_m then

$$\text{2nd-order rate constant} = \frac{\text{pseudo 1st-order rate constant}}{(\text{CuNTA})}$$

where the concentration of CuNTA is corrected for the mixing inefficiency. For (CuNTA) ≈ (D), the second-order rate constant was obtained explicitly by plotting

$$\frac{1}{(\text{CuNTA})_o - (\text{D})_o} \ln\left[\frac{(\text{D})_o\,[(\text{CuNTA})_o - x]}{(\text{CuNTA})_o\,[(\text{D})_o - x]}\right] \qquad (12)$$

where x is the amount reacted (Moore and Pearson, 1981). The mixing parameter P_m in this case was also obtained from the ratio of the apparent initial dye concentration (again extrapolated from a simple exponential fit) to the expected initial concentration.

For the reaction of CuNTA with dye (NTA not in excess), the data was modeled applying the rate constants for the indirect [(k_{CuL_T} $k_{Cu}^{D_T}/k_{Cu}^{L_T}$) and direct ($k_{D_T}^{CuL_T}$) mechanisms obtained from experiments with NTA in excess. For each data set, the fit was optimized using two fitting parameters, α (the ratio of $k_{Cu}^{D_T}/k_{Cu}^{L_T}$) and P_m, by comparing the observed (D) over time with the predicted values based on the following model. For CuNTA + D ⟶ NTA + CuD,

$$\frac{-d(\text{D})}{dt} = \left[\frac{k_{CuL_T}\,k_{Cu}^{D_T}}{k_{Cu}^{L_T}(\text{NTA}) + k_{Cu}^{D_T}(\text{D})} + k_{D_T}^{CuL_T}\right](\text{CuNTA})(\text{D}) \qquad (13)$$

let $(\text{D})_t = y$, then amount reacted is $(\text{D})_o - y$ and from stoichiometry

$$(\text{CuNTA})_t = (\text{CuNTA})_o - (\text{D})_o + y$$

$$(\text{NTA})_t = (\text{NTA})_o + (\text{D})_o - y$$

then

$$\frac{-dy}{dt} = \left(\frac{k_{CuL_T} k_{Cu}^{D_T}}{k_{Cu}^{L_T}\,[(NTA)_o + (D)_o - y] + k_{Cu}^{D_T}\, y} + k_{D_T}^{CuL_T} \right) \cdot \left((CuNTA)_o - (D)_o + y \right) y \qquad (14)$$

or

$$\left(\frac{\alpha\, k_{CuL_T}}{(\alpha-1)y + (NTA)_o + (D)_o} + k_{D_T}^{CuL_T} \right) \left([(CuNTA)_o - (D)_o]\, y + y^2 \right) \qquad (15)$$

and

$$(y)_{t+\Delta t} = (y)_t - \left(\left[\frac{\alpha\, k_{CuL_T}}{(\alpha-1)y + (NTA)_o + (D)_o} + k_{D_T}^{CuL_T} \right] \cdot \left[[(CuNTA)_o - (D)_o] y + y^2 \right] \right) \Delta t. \qquad (16)$$

The mixing parameter P_m affects the initial values of all concentrations such that

$$\text{apparent } (D)_o = \text{undiluted } (D)_o\ (P_m)$$

$$\text{apparent } (NTA)_o = \text{undiluted } (NTA)_o\ (1-P_m)$$

$$\text{apparent } (Cu)_o = \text{undiluted } (Cu)_o\ (1-P_m).$$

Because there are two fitting parameters in this model, α and P_m, there is a large uncertainty in the value of α. Figure 1 shows the difficulty in constraining the value for α with the available data. [N.B.- the sensitivity of the fit to the value for α varies depending on the ratio of reactants.]

For the reaction of CuD with excess ligand (either NTA or EDTA), the data was analyzed as pseudo-first order reaction in CuD. Thus for CuD + L $\longrightarrow$ D + CuL (excess L), the pseudo first-order rate constant for the indirect pathway is

Figure 1. Free dye concentration over time for CuNTA + D $\longrightarrow$ NTA + CuD (at approximate concentrations $D_T \approx 40$ nM, $Cu_T \approx 50$ nM, $NTA_T \approx 60$ nM). Model fit to data for (——) $\alpha = 0.7$, $P_m = 0.49$; (---) $\alpha = 1.1$, $P_m = 0.47$; (...) $\alpha = 0.3$, $P_m = 0.52$.

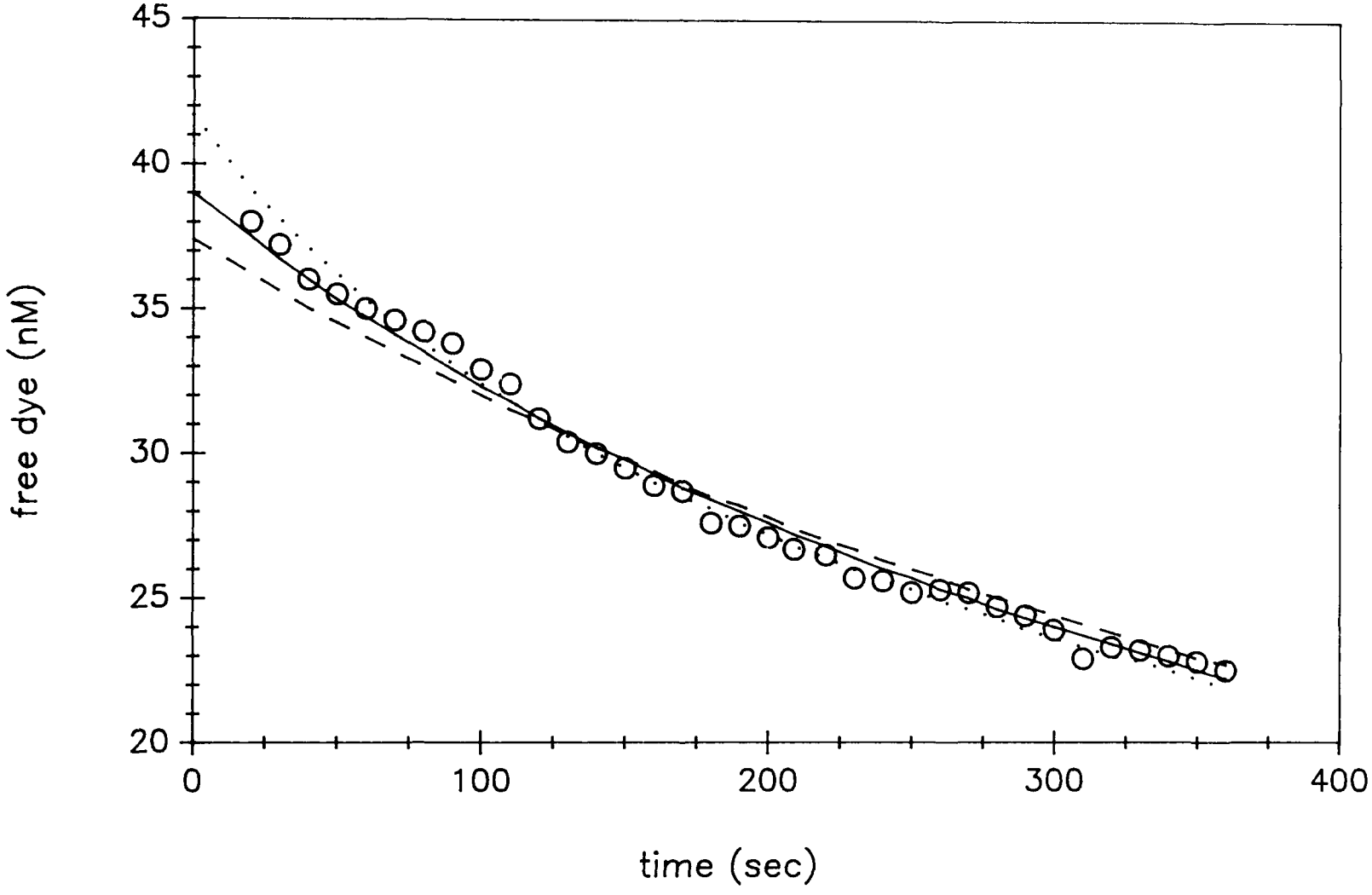
45
40
35
30
25
20
free dye (nM)
0
100
200
300
400
time (sec)

$$\frac{k_{CuD_T}\, k_{Cu}^{L_T}(L)}{k_{Cu}^{L_T}(L) + k_{Cu}^{D_T}(D)} = k_{CuD_T} \qquad \text{for } (L) >> (D) \qquad (17)$$

and the pseudo first-order rate constant for the direct pathway is

$$k_{L_T}^{CuD}(L)$$

for

$$\frac{-d(CuD)}{dt} = \left(k_{CuD_T} + k_{L_T}^{CuD}(L) \right) (CuD). \qquad (18)$$

For experiments with EDTA, a value for P_m based on the apparent concentration of $(D)_o$ was applied as a correction to all concentrations. In these cases the effect of the formation of Cu_2D on the expected $(D)_o$ was also included in the calculation (see Appendix B). However the reaction of $Cu_2D + L \longrightarrow CuD + CuL$ is neglected in the kinetic analysis as it does not result in any fluorescence change.

RESULTS

Model system: Ligand exchange reactions between the fluorescent dye and synthetic ligands were studied for

$$CuL + D \longrightarrow L + CuD \qquad L = NTA$$

(herein referred to as the "forward" reaction) and for

$$CuD + L \longrightarrow D + CuL \qquad L = NTA, EDTA$$

(referred to as the "reverse" reaction). [Rate constants obtained for these reactions are summarized in Table III.] For the forward reaction of the dye with CuNTA, the ligand exchange was inhibited by free NTA as shown in Figure 2. For experiments with a sufficient excess of NTA (free NTA: dye > 5), indirect pathway (NTA-dependent) and direct pathway

TABLE III. Summary of rate constant for ligand exchange reactions (model system- L = NTA).

indirect mechanism

$$CuL \underset{k_{Cu}^{L_T}}{\overset{k_{CuL_T}}{\rightleftharpoons}} Cu + L$$

$$Cu + D \underset{k_{CuD_T}}{\overset{k_{Cu}^{D_T}}{\rightleftharpoons}} CuD$$

$k_{Cu}^{L_T} = 9 \pm 4 \times 10^{7}\ M^{-1}\ sec^{-1}$

$k_{CuL_T} = 2 \pm 1 \times 10^{-3}\ sec^{-1}$

$k_{Cu}^{D_T} = 5.2 \pm 0.3 \times 10^{7}\ M^{-1}\ sec^{-1}$

$k_{CuD_T} = 3.6 \pm 1.6 \times 10^{-5}\ sec^{-1}$

$$K_{CuD}^{cond} = \frac{k_{Cu}^{D_T}}{k_{CuD_T}} = 10^{12.2 \pm 0.2}$$

direct mechanism

$$CuL \rightleftharpoons LCuD \rightleftharpoons L + CuD$$

$k_{D_T}^{CuL} = 4.8 \pm 1.0 \times 10^{3}\ M^{-1}\ sec^{-1}$

$k_{L_T}^{CuD} = 25 \pm 2\ M^{-1} sec^{-1}$

$$\frac{K_{CuD}^{cond}}{K_{CuL}^{cond}} = \frac{k_{D_T}^{CuL}}{k_{L_T}^{CuD}} = 10^{2.3 \pm 0.1}$$

$$K_{CuD}^{cond} = 10^{12.9 \pm 0.1}$$

Figure 2. Free dye concentration over time for CuNTA + D $\longrightarrow$ NTA + CuD at varying NTA concentrations. Approximate concentrations: $D_T \approx 10$ nM, $Cu_T \approx 50$ nM, $NTA_T \approx 60$ (○, △), 80 (□), 120 (▽), or 200 (◇).

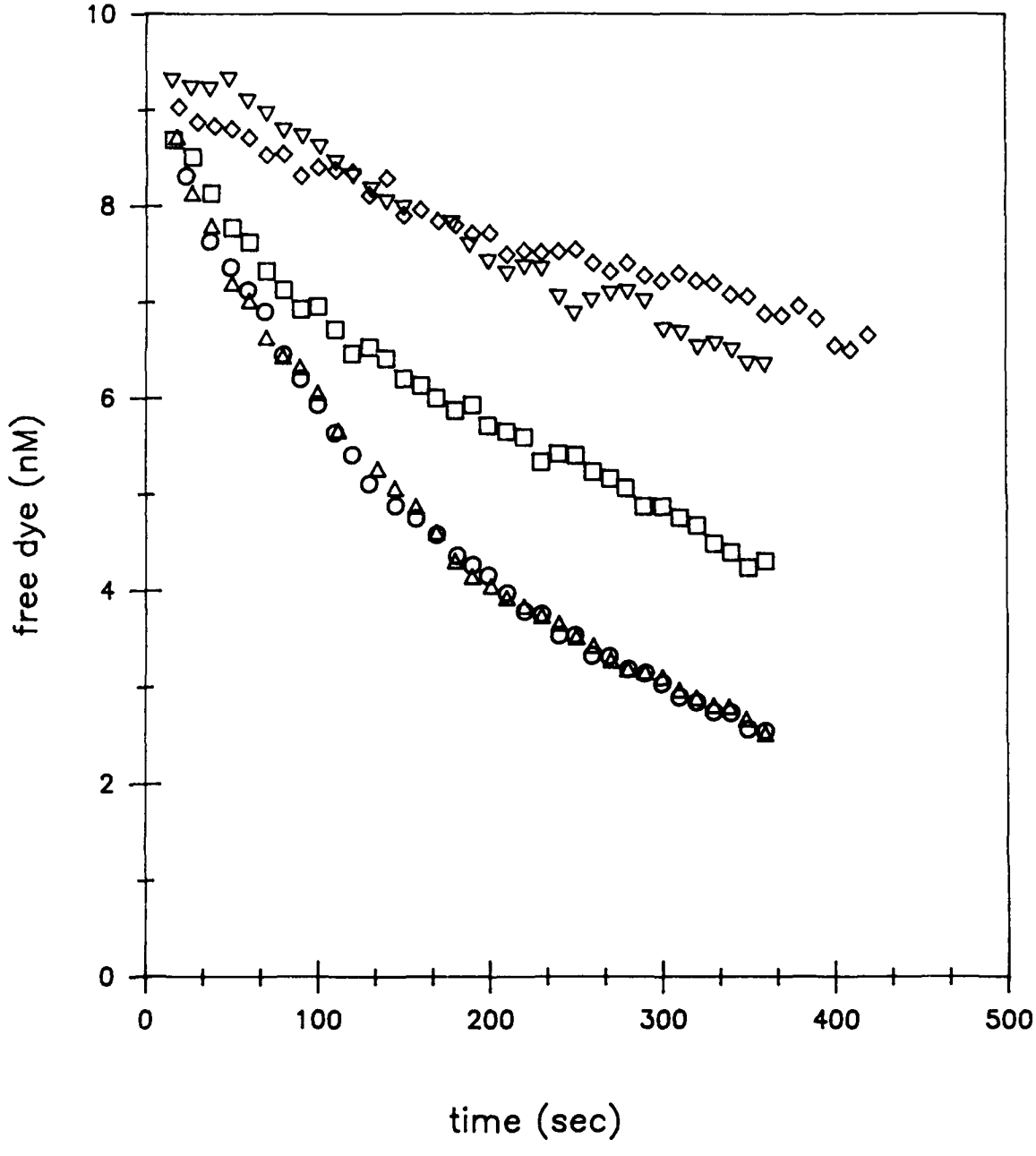
10
8
6
4
2
0
free dye (nM)
0
100
200
300
400
500
time (sec)

(NTA-independent) rate constants were extracted from a plot of observed second-order rate constant (i.e.- rate = $-d(D)/dt = k_{obs}\,(CuNTA)(D)$) as a function of 1/(free NTA) as shown in Figure 3. The non-zero intercept indicates that at high free NTA concentrations the dominant pathway for ligand-exchange does not involve (complete) dissociation of the CuNTA complex. From Figure 3, the following rate constants are obtained:

for the indirect mechanism, the NTA-dependent rate constant is

$$\frac{k_{CuL_T}\,{}^{D_T}k_{Cu}}{{}^{L_T}k_{Cu}} = 1.31 \pm 0.07 \times 10^{-3}\ sec^{-1}$$

and for the direct mechanism, the NTA-independent rate constant is

$${}^{CuL}k_{D_T} = 4.8 \pm 1.0 \times 10^{3}\ M^{-1}\ sec^{-1}$$

For these conditions (i.e.- excess free NTA), the contributions of the two pathways are equal at a free NTA concentration of ~270 nM. The ratio ${}^{L_T}k_{Cu} / k_{CuL_T}$ corresponds to the conditional stability constant for CuNTA ($K^{cond}_{CuNTA} = 10^{10.6}$, pH = 7.3, μ = 0.1). Thus

$${}^{D_T}k_{Cu} = \frac{k_{CuL_T}\,{}^{D_T}k_{Cu}}{{}^{L_T}k_{Cu}}\,K^{cond}_{CuNTA} = 5.2 \pm 0.3 \times 10^{7}\ M^{-1}\ sec^{-1}$$

For ligand exchange experiments under conditions for which the free NTA was not in excess of the dye the observed indirect (NTA-dependent) rate constant is

$$\frac{k_{CuL_T}\,{}^{D_T}k_{Cu}}{{}^{L_T}k_{Cu}(L) + {}^{D_T}k_{Cu}(D)} \qquad (19)$$

and the ratio of ${}^{D_T}k_{Cu} / {}^{L_T}k_{Cu}$ may be obtained. For 32 experiments

Figure 3. Observed second-order rate constants vs 1/(NTA) for CuNTA + D $\longrightarrow$ NTA + CuD [$-d(D)/dt = k_{obs}(CuNTA)(D)$ and $k_{obs} = k_{ind}/(NTA) + k_{dir}$].

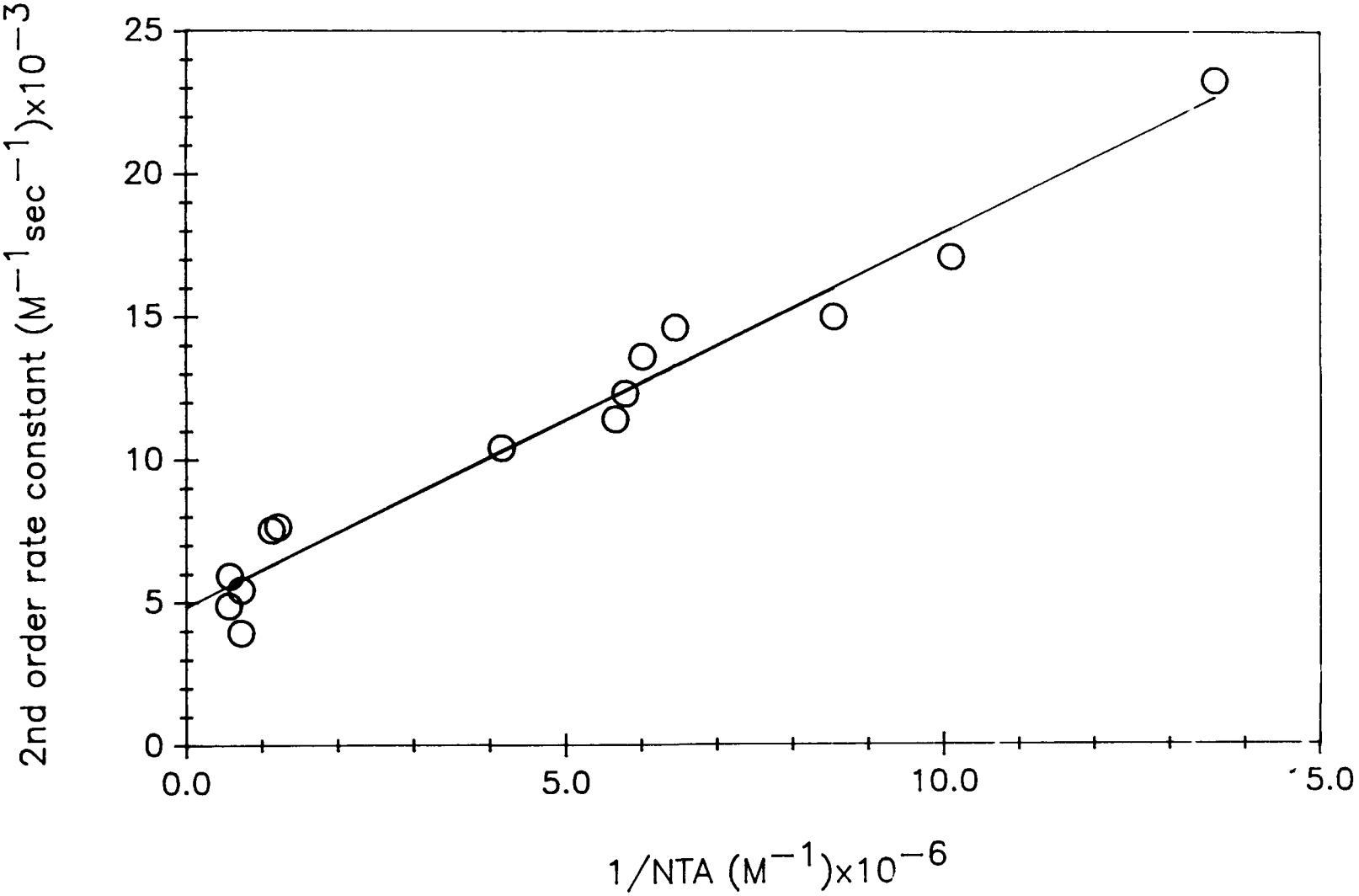
2nd order rate constant ($M^{-1}sec^{-1}$)x10^{-3}
25
20
15
10
5
0
0.0
5.0
10.0
5.0
1/NTA (M^{-1})x10^{-6}

(conditions shown in Table IV), the experimental results are consistent with a value of this ratio of 0.6 ± 0.3 (shown for a sample data set in Figure 1). The large uncertainty in this value allow only rough estimates of $k_{Cu}^{L_T}$ and k_{CuL_T}. Thus

$$\kappa_{CuL_T} = \frac{k_{CuL_T}}{k_{Cu}^{D_T}} \; k_{Cu}^{D_T} = \frac{1.31 \times 10^{-3}}{0.6} = 2 \pm 1 \times 10^{-3} \text{ sec}^{-1}$$

and

$$k_{Cu}^{L_T} = K_{CuNTA}^{cond} \; k_{CuL_T} = 10^{10.6} \; (2 \times 10^{-3}) = 9 \pm 4 \times 10^{7} \text{ M-1 sec}^{-1}.$$

An independent estimate of $k_{Cu}^{L_T}$ may be obtained from the work of Maguire (1974) in which the effect of pH on the rate of CuNTA formation was studied. For the reactions

$$Cu + NTA \xrightarrow{k_{Cu}^{NTA}} CuNTA$$

and

$$Cu + HNTA \xrightarrow{k_{Cu}^{HNTA}} CuNTA + H^+$$

the observed rate constant for reaction of Cu with both NTA species ($k_{Cu}^{NTA_T}$) is

$$\frac{k_{Cu}^{NTA} + k_{Cu}^{HNTA} \; K_{HNTA}(H^+)}{1 + K_{HNTA}(H^+)} \; . \qquad (20)$$

Values for the rate constants k_{Cu}^{NTA} (7.1×10^9 $M^{-1}sec^{-1}$) and k_{Cu}^{HNTA} (1.0×10^5 $M^{-1}sec^{-1}$) were obtained from a plot of $k_{Cu}^{NTA_T}[1 + K_{HNTA}(H^+)]$ vs. (H^+) as shown in Fig. 4. The predicted value for $k_{Cu}^{NTA_T}$ at pH= 7.3 (i.e.- for $k_{Cu}^{L_T}$ in our experiments) is 2.0×10^7 $M^{-1}sec^{-1}$.

TABLE IV. Kinetic parameter derived for experiments with (NTA) ≈ (D)

for $CuNTA + D \longrightarrow NTA + CuD$ $\quad \alpha k_{CuL_T} = 1.31 \times 10^{-3}$

$k_{D_T}^{CuL} = 4.8 \times 10^{3}$

concentration before dilution (nM)			α	P_m
Cu_T	NTA_T	D_T		
100	120	20	0.6	0.47
"	"	20	0.8	0.45
"	"	40	0.8	0.46
"	"	80	0.7	0.49
"	"	200	0.4	0.56
"	"	200	0.6	0.52
"	"	300	1.0	0.55
"	"	400	0.6	0.52
"	"	500	0.9	0.53
100	140	200	0.5	0.46
"	"	300	0.6	~ 50
"	"	300	0.5	0.49
"	"	400	0.4	0.50
"	"	400	0.3	0.50
"	"	500	0.8	0.48
100	160	20	1.0	0.41
"	"	20	0.9	0.43
"	"	40	0.4	0.50
"	"	40	1.0	0.54
"	"	80	0.6	0.48
"	"	100	0.4	0.52
"	"	200	0.7	0.51
"	"	200	0.6	0.51
100	240	40	0.1	0.46
"	"	80	0.5	0.48
"	"	200	0.5	0.50

concentration before dilution (nM)			α	P_m
Cu_T	NTA_T	D_T		
100	400	200	0.2	0.51
200	280	200	0.1	0.49
"	280	300	0.2	0.50
"	280	400	0.2	0.47
"	280	400	0.4	0.48
"	280	500	0.2	0.51

Figure 4. Effect of pH on formation of CuNTA based on work of Maguire (1974). For the reaction $Cu + NTA_T \longrightarrow CuNTA$,

$$k_{Cu}^{NTA_T} = \frac{k_{Cu}^{NTA} + k_{Cu}^{HNTA} K_{HNTA} (H^+)}{1 + K_{HNTA} (H^+)} .$$

Thus, the intrinsic rate constants k_{Cu}^{NTA} and k_{Cu}^{HNTA} can be extracted from a plot of $k_{Cu}^{NTA_T} [1 + K_{HNTA} (H^+)]$ vs. (H^+).

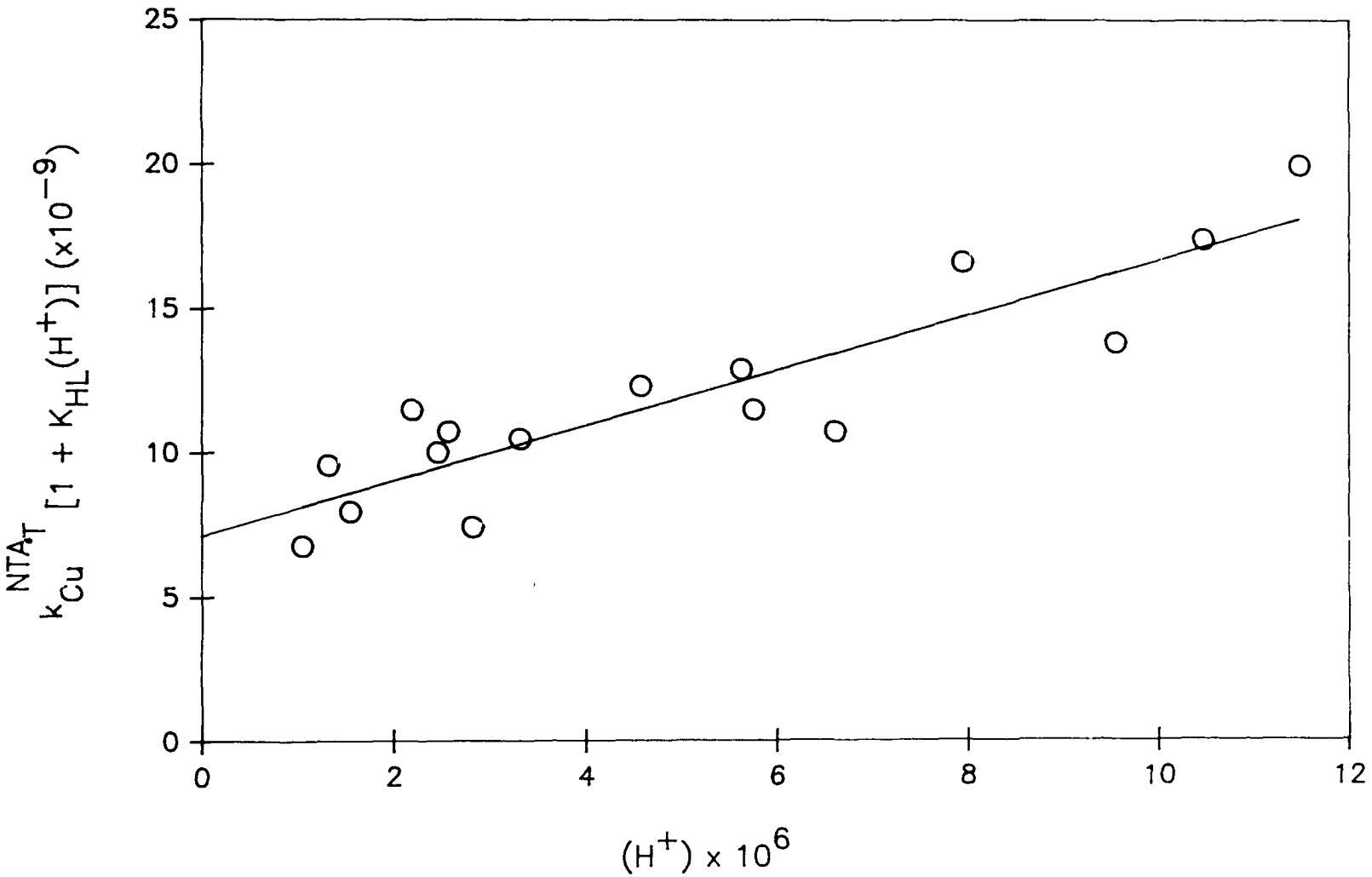
25
20
15
10
5
0
0
2
4
6
8
10
12
$k_{Cu}^{NTA_T}$ [1 + $K_{HL}(H^+)$] ($\times 10^{-9}$)
$(H^+) \times 10^6$

The reverse reaction (i.e.- CuD + L) was studied for L = NTA with a very large excess of NTA and for L = EDTA over a range of EDTA concentrations. From the reaction with NTA the constant for the direct pathway was determined.

$$k_{L_T}^{CuD} = 25 \pm 2\ M^{-1}\ sec^{-1}$$

For the reaction of CuD with EDTA (EDTA in excess), contributions of indirect and direct pathways to the overall rate could be assessed by plotting a pseudo-first order rate constant against EDTA concentration (Fig. 5). Thus for

$$\text{rate} = \frac{d(D)}{dt} = k_{obs}\ (CuD) = \left[k_{CuD_T} + k_{L_T}^{CuD}\ (EDTA) \right] (CuD). \qquad (21)$$

The rate constant for the direct pathway is

$$k_{L_T}^{CuD} = 33.0 \pm 3.5\ M^{-1}\ sec^{-1}. \qquad (L = EDTA)$$

For the indirect mechanism (for "trapping" conditions, i.e. with excess EDTA)

$$k_{CuD_T} = 3.6 \pm 1.6 \times 10^{-5}\ sec^{-1}.$$

The consistency of the kinetic data may be assessed by comparison of kinetic and equilibrium constants. The ratio of the indirect rate constants $k_{Cu}^{D_T} / k_{CuD_T}$ is the conditional stability constant for CuD, then

$$\frac{k_{Cu}^{D_T}}{k_{CuD_T}} = K_{CuD}^{cond} = \frac{5.2 \pm 0.3 \times 10^{7}}{3.6 \pm 1.6 \times 10^{-5}} = 10^{12.2 \pm 0.2}$$

The ratio of the rate constants for reaction by direct attack corresponds to the ratio of the conditional stability constants for CuD and CuNTA

Figure 5. Observed first-order rate constant for reverse reaction

$CuD + EDTA \longrightarrow D + CuEDTA$ [$-d(CuD)/dt = k_{obs}(CuD)$ and

$k_{obs} = k_{CuD_T} + k_{L_T}^{CuD_T}(EDTA)$].

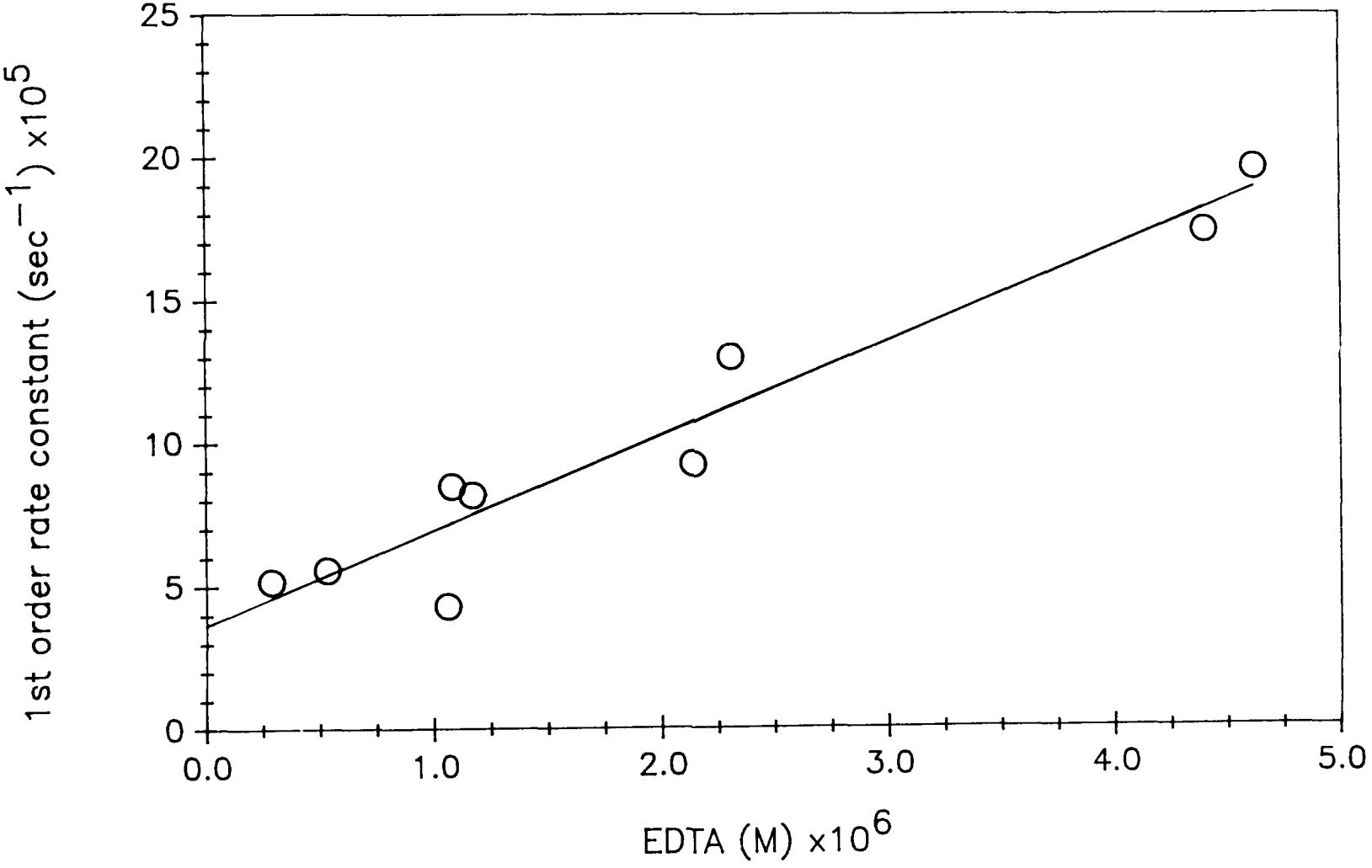
25
20
15
10
5
0
0.0
1.0
2.0
3.0
4.0
5.0
1st order rate constant (sec^{-1}) x10^{5}
EDTA (M) x10^{6}

$$\frac{k_{D_T}^{CuL}}{k_{L_T}^{CuD}} = \frac{K_{CuD}^{cond}}{K_{CuNTA}^{cond}} = \frac{4.8 \pm 1.0 \times 10^3}{25 \pm 2} = 190 \pm 40$$

for $K_{CuNTA}^{cond} = 10^{10.6}$, $K_{CuD}^{cond} = 10^{12.9 \pm 0.1}$.

Some of the discrepancy between estimates for K_{CuD}^{cond} may be due to the involvement of minor species (see Discussion). From equilibrium studies (see Appendix B), the best estimate of K_{CuD}^{cond} is $10^{12.8}$ in reasonable agreement with the values obtained from kinetics experiments.

Humic acid ligand exchange: The reaction of the dye with Cu-humate complexes was studied at several different humic acid concentrations. For the reaction

$$CuHum + D \longrightarrow Hum + CuD$$

a general decrease in the ligand exchange rate is observed with increasing humic acid concentrations (Figure 6). For the ligand exchange reaction with 5.4 or 10.8 mg/L humic acid, each reaction could be fit with a single rate constant as shown in Figure 7a. However, for lower concentrations of humic acid (1.1 mg/L) two rate constants were required (Figure 7b). Values obtained for the rate constants are summarized in Table V). As discussed for the model system the contributions of the indirect and direct mechanisms may be estimated from the relation between the observed second-order rate constants and the free humic acid concentration (i.e.- Hum_T - CuHum). For 5.4 and 10.8 mg/L humic acid, the humic acid Cu-binding sites should be sufficiently in excess of Cu_T (50 nM) that free humic ≈ total humic. However for 1.1 mg/L humic acid the necessity for two kinetic rate constants suggests that the Cu concentration is not negligible compared to the concentration of strong binding sites. Thus the data for 1.1

Figure 6. Free dye over time for CuHum + D $\longrightarrow$ Hum + CuD for approximate concentrations $Cu_T \approx 50$ nM and $D_T \approx$ 20 nM (a) or 50 nM (b). Total humic acid $\approx$ 1.1 mg/L (O), 5.4 mg/L (Δ), and 10.8 mg/L ($\square$).

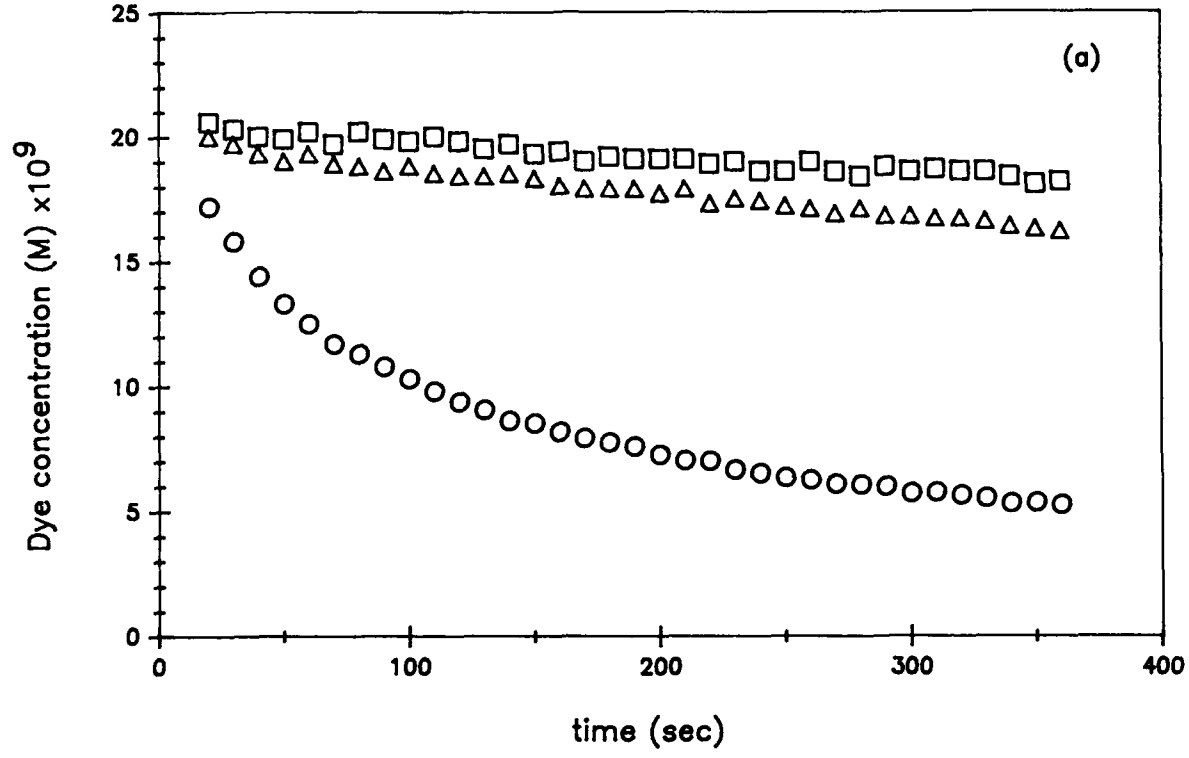
(a)
Dye concentration (M) x10^9
25
20
15
10
5
0
0
100
200
300
400
time (sec)

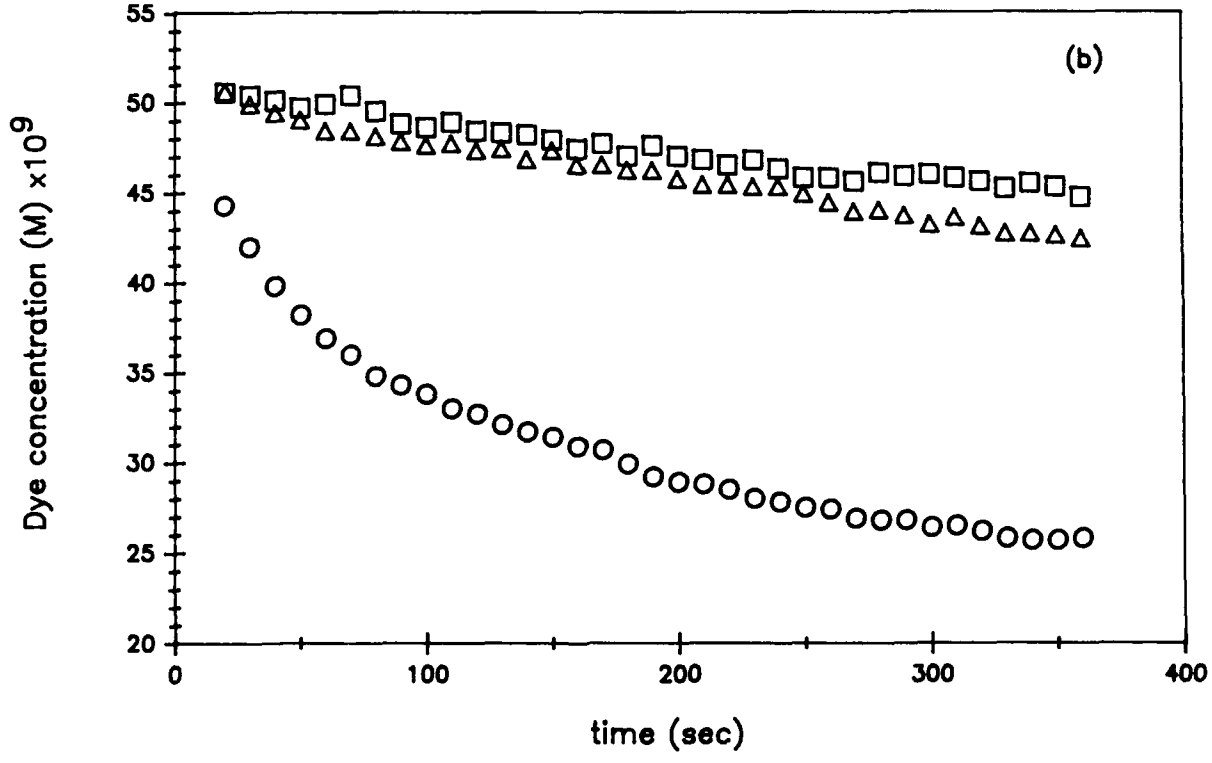
(b)
Dye concentration (M) x10^9
55
50
45
40
35
30
25
20
0
100
200
300
400
time (sec)

Figure 7. Logarithmic transform of the free dye over time (normalized to apparent $(D)_o$) for CuHum + D $\longrightarrow$ Hum + CuD. With (CuHum)>(D), the reaction is pseudo-first order in D. Approximate concentrations: $Cu_T \approx 50$ nM, $D_T \approx 20$ nM, (a) $Humic_T \approx 5.4$ mg/L (Δ), and 10.8 mg/L ($\square$) and (b) $Humic_T \approx 1.1$ mg/L.

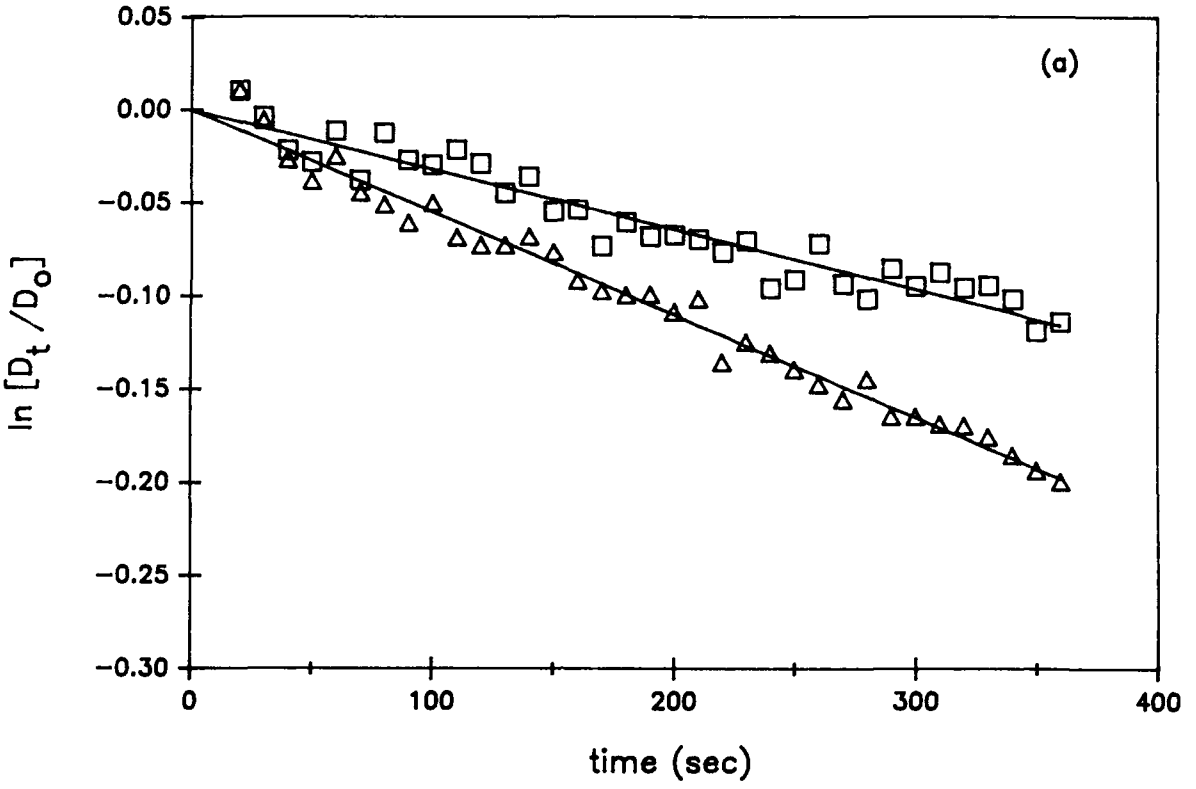
(a)
0.05
0.00
−0.05
−0.10
−0.15
−0.20
−0.25
−0.30
ln [D_t / D_o]
0
100
200
300
400
time (sec)

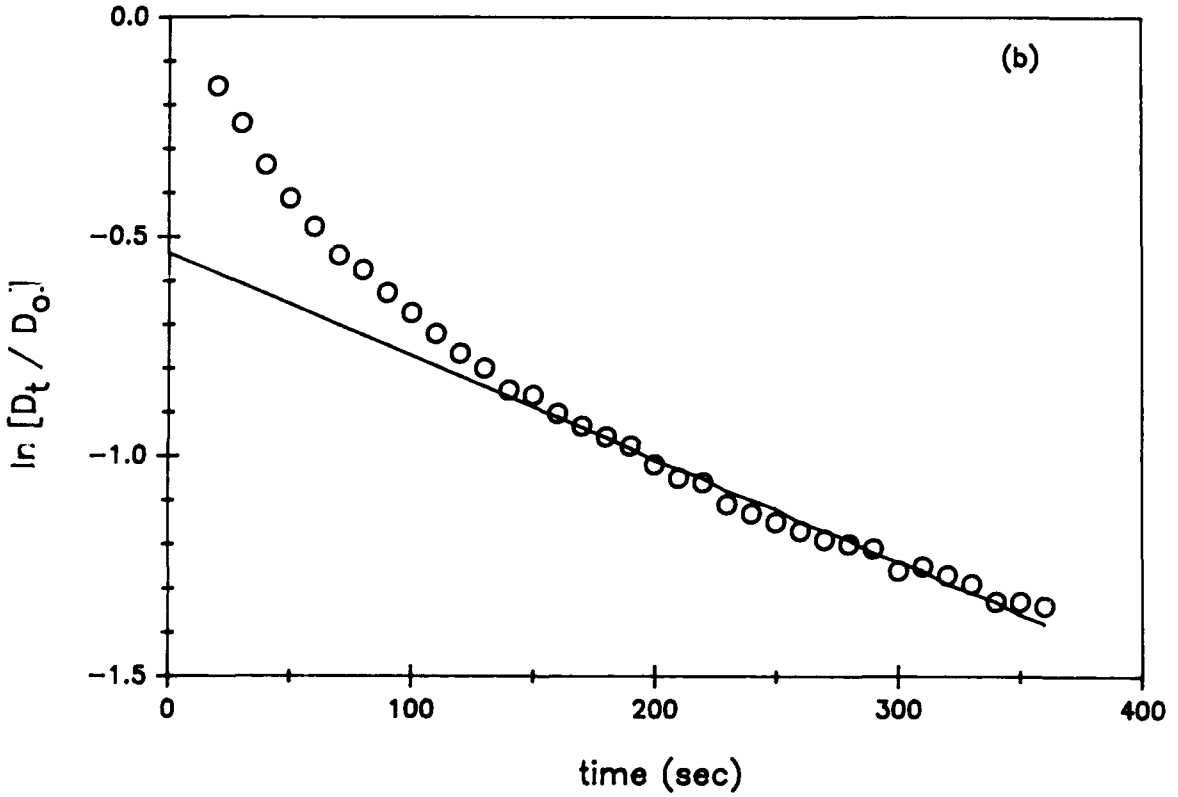
(b)
0.0
−0.5
−1.0
−1.5
ln [D_t / D_o]
0
100
200
300
400
time (sec)

TABLE V. Summary of rate constant for ligand exchange reactions (humic acid)

approximate concentration		obs. second-order rate constant
Dye (nM)	Hum_T (mg/L)	($M^{-1}sec^{-1}$)
20	10.8	6.58×10^3
50	10.8	7.39×10^3
20	5.4	1.09×10^4
50	5.4	1.03×10^4
20	1.1	(early) 9×10^5
		(late) 6.0×10^4

mg/L is omitted from Fig. 8a which shows the second-order rate constant vs. the reciprocal of the humic acid concentration (in mg/L). Figure 8b shows the rate constant for later reaction of the 1.1 mg/L experiment with the corresponding value of 1/free humic used in subsequent modeling of this reaction. Again by analogy with the model system we expect that for

$$\text{rate} = -\frac{d(D)}{dt} = k_{obs}\,(\text{CuHum})(D) \qquad (22)$$

$$k_{obs} = k_{ind}\,\frac{1}{(\text{Hum})} + k_{dir}. \qquad (23)$$

From Figure 8,

$$k_{ind} = 3.95 \pm 0.63 \times 10^{4}\ \text{mg mol}^{-1}\ \text{sec}^{-1} \quad \text{and}$$

$$k_{dir} = 3.3 \pm 0.6 \times 10^{3}\ \text{M}^{-1}\ \text{sec}^{-1}.$$

These results indicate the contribution of both indirect and direct pathways to the observed reaction.

For the experiments with 1.1 mg/L humic acid, the apparent change in the rate constants over the course of the reaction indicated that the amount of Cu bound was not negligible compared to the concentration of strong Cu binding sites. If, for the reaction with 20 nM dye, it is assumed that the observed rate constant (for the later part of the reaction) conforms to the equation determined for the reaction at higher humic acid concentrations [i.e.- $k_{obs} = 3300 + (39{,}500)*(1/\text{free humic})$], then the concentration of free humic at 1.1 mg/L total humic acid and 50 nM Cu_T can be calculated. For $k_{obs} = 60{,}000$, the calculated free humic concentration is 0.7 mg/L and the Cu-bound humic concentration is 0.4 mg/L. The amount of Cu bound to this site is ~42 nM (since some of the total 50 nM of Cu is bound in the faster reacting site- see Appendix).

Figure 8. Plot of second-order rate constant vs 1/(free humic) for $CuHum + D \longrightarrow Hum + CuD$, $-d(D)/dt = k_{obs}(CuHum)(D)$, $k_{obs} = k_{diss}/(\text{free humic}) + k_{int}$. (a) experimental results for 5.4 and 10.8 mg/L humic acid (with the assumption that free humic ≈ total humic) (b) experimental values for 5.4 and 10.8 mg/L and extrapolated value for 1.1 mg/L Hum_T used in calculations for Fig. 9.

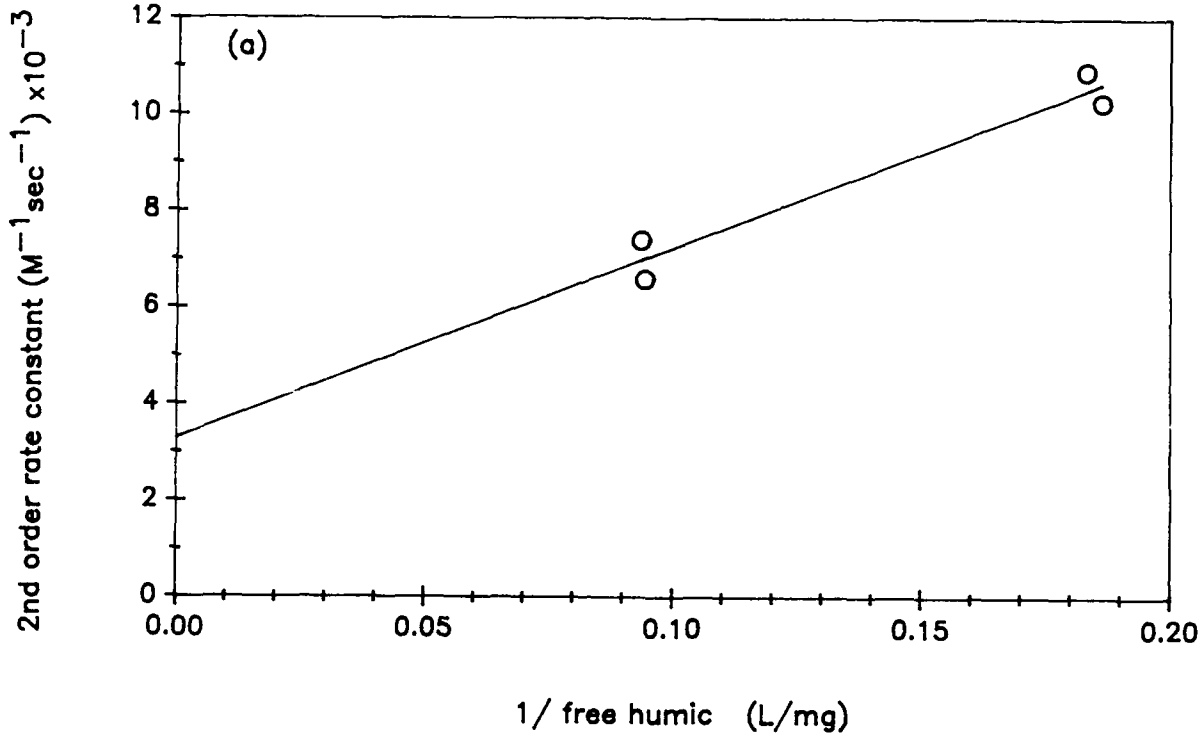
(a)
12
10
8
6
4
2
0
0.00
0.05
0.10
0.15
0.20
2nd order rate constant ($M^{-1}sec^{-1}$) x10^{-3}
1/ free humic (L/mg)

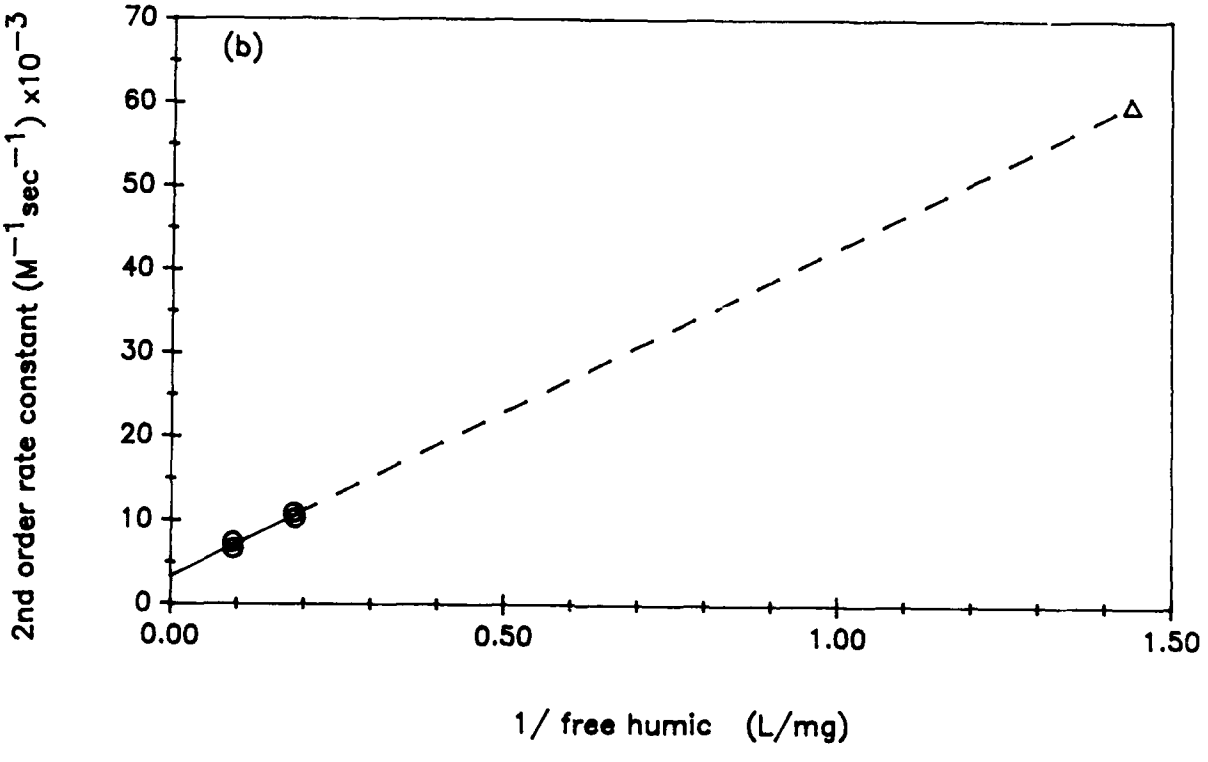
(b)
70
60
50
40
30
20
10
0
0.00
0.50
1.00
1.50
2nd order rate constant ($M^{-1}sec^{-1}$) x10^{-3}
1/ free humic (L/mg)

Thus the site density is

$$\frac{42 \text{ nM Cu/L}}{0.4 \text{ mg/L}} \approx 10^{-7} \frac{\text{mol Cu-binding site}}{\text{mg humic acid}} .$$

For the experiemnt with 50 nM dye and 1.1 mg/L humic acid, extraction of rate constants is complicated by the non-negligible change in Cu-humate concentration as compared with the change in the dye concentration. However these results may be compared with other ligand exchange experiments with humic acids using the following model. [A complete description of the model is given in the Appendix.] In this model, the dye reacts with Cu bound at 2 humate sites (i.e.- with CuHum1, the slow-reacting species, and CuHum2, the fast-reacting species). The initial concentrations of these Cu-humate species (for $Cu_T \approx 50$ nM, $Hum_T \approx 1.1$ mg/L) is taken from the experiments with 20 nM dye. The reaction of the dye with CuHum1 is described with the 2 rate constants, for ligand exchange via indirect and direct pathways, obtained from Fig. 8. The reaction of the dye with CuHum2 is described with a single rate constant. The value for this rate constant is optimized from the model fit for the experiment with 20 nM dye, 1.1 mg/L humic acid. Then for

$$\text{Dye} + \text{CuHum2} \xrightarrow{k_{H2}} \text{CuDye} + \text{Hum2}$$

$$\text{Dye} + \text{CuHum1} \xrightarrow{k_{H1}} \text{CuDye} + \text{Hum1} \qquad \text{where } k_{H1} = \frac{k_{H1}^{ind}}{(\text{Hum1})} + k_{H1}^{dir}$$

$$\frac{-d(\text{Dye})}{dt} = k_{H2}\,(\text{CuHum2})(\text{Dye}) + \left(\frac{k_{H1}^{ind}}{(\text{Hum1})} + k_{H1}^{dir} \right) (\text{CuHum1})(\text{Dye}) \qquad (24)$$

where

$$(\text{Hum1})\ [\text{mg/L}] = Hum_T\ [\text{mg/L}] - \frac{(\text{CuHum1})\ [\text{mol/L}]}{\text{site density } [\text{mol/mg}]} . \qquad (25)$$

The site density (10^{-7}mol/mg) is obtained from the 20 nM, 1.1 mg/L Hum_T experiment as described above. The model fit to the data is shown for experiments with 1.1 mg/L Hum_T, 50 nM Cu_T and both 20 and 50 nM Dye_T in Figure 9 (note that there are no adjustable parameters in the fit to the 50 nM Dye experiment). The deviation of the model fit from the data at longer times may indicate that the system is approaching equilibrium. The general agreement of the model with the data demonstrates the consistency of ligand exchange experiments with 1.1, 5.4, and 10.8 mg/L Hum_T.

DISCUSSION

The results obtained in model systems (with well-defined ligands) demonstrate that the kinetics of ligand exchange reactions are consistent with a relatively simple interpretation. In this interpretation, ligand exchange reactions at high concentrations of the out-going ligand are dominated by direct attack of the incoming ligand on the initial metal-ligand complex. This result is consistent with previous observations. However at low concentrations of the outgoing ligand (in this case NTA), an indirect pathway becomes important. Based on this model, kinetic constants can be derived from the data. The agreement of the rate constant for the formation of CuNTA (at pH=7.3) derived from ligand exchange experiments with the value predicted from the work of Maguire supports our interpretation of the ligand exchange kinetic data. The validity of the model chosen for the reaction mechanism(s) may also be assessed from the concordance of kinetic and equilibrium stability constants.

Figure 9. Model fit for reaction of Dye with 2 Cu-humate species (solid lines) and data for ligand exchange reaction of Dye with Cu/humic acid ($Cu_T \approx 50$ nM, $Hum_T \approx 1.1$ mg/L) $Dye_T \approx 20$ (O) or 50 (Δ) nM.

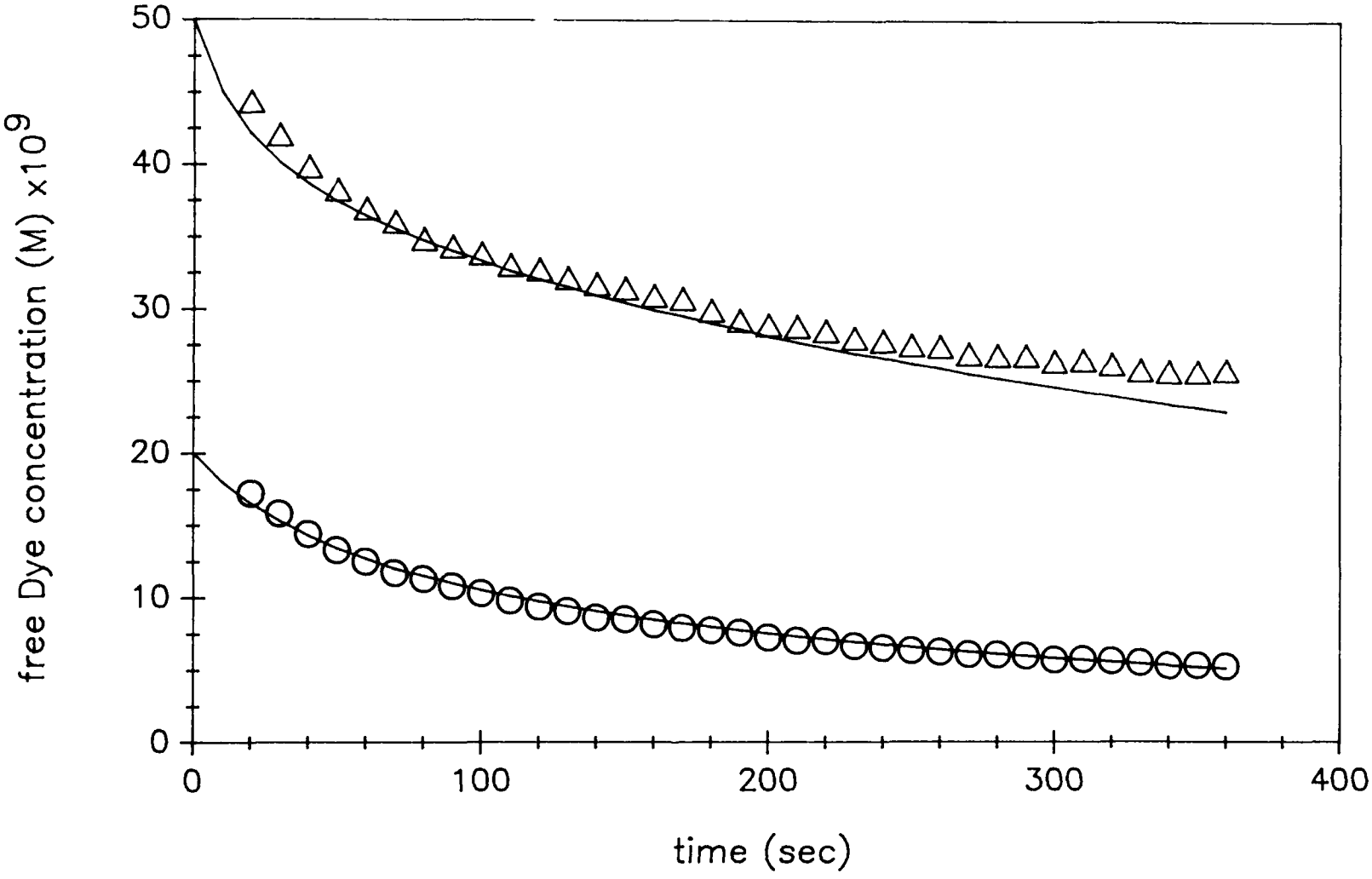
50
40
30
20
10
0
0
100
200
300
400
free Dye concentration (M) x10^9
time (sec)

Although this mechanistic model for ligand exchange reactions is reasonably consistent with kinetic and equilibrium observations, it is nonetheless an oversimplification of the actual system. Equilibrium experiments (see Appendix B) show that some minor species, particularly the dinuclear species Cu_2D, are not negligible. The presence of a stable ternary complex, NTACuD, is also indicated by equilibrium experiments. However with only the available information on the concentration of reacting species, a more detailed mechanism cannot be defined.

Based on results from the model system, ligand-exchange reactions of the fluorescent reagent with Cu-humate may be interpreted using the same models. These results suggest both direct and indirect pathways for the ligand exchange reactions. The contributions of the two mechanisms to the overall reaction are approximately equal at a free humic acid concentration of ~13±4 mg/L with 50 nM Cu_T or at a Cu-to-humate loading of ~4 x 10^{-3} μmol Cu/ mg humic acid.

To assess the contributions of these pathways in natural waters, this value for Cu-to-humate loading may be compared with Cu_T/DOC ratios measured in the environment. In Table VI, the value obtained from kinetic experiments (expressed now in terms of μmol Cu_T/ mg-C humic) is compared with values reported by Newell and Sanders (1986) and Anderson et al. (1984). Since the Cu-to-DOC loading in natural waters is very similar to the Cu-to-humate carbon loading for which the indirect and direct mechanisms are equally important in ligand exchange reactions, it may be concluded that both of these types of mechanisms must also be important under natural conditions. In comparison, the experiments of

TABLE VI. Cu-to-humate or DOC loadings

		μmol Cu/ mg C
Cu-to-humate loading for which direct and indirect pathways contribute equally to ligand exchange reactions (from kinetic experiments)		$\sim 8 \times 10^{-3}$
Cu-to-DOC ratios found in natural waters		
Newell and Sanders (1986)	Sal	
	5.4	6.6×10^{-3}
	10.9	1.4×10^{-2}
	13.9	1.3×10^{-2}
Anderson et al. (1984)		
tidal pond	23-28	$7\pm3 \times 10^{-3}$
coastal	32	$7\pm2 \times 10^{-3}$

Shuman et al. (1983), in which only an indirect pathway for ligand exchange was observed, were conducted at much higher Cu-to-DOC loadings (0.34 μmol Cu/ mg DOC).

The rate constant for ligand exchange reactions by the indirect pathway of Cu-humate complexes with the fluorescent dye provides information on Cu-humate binding. By analogy with the model system, for the ligand exchange reaction

$$CuHum + D \longrightarrow Hum + CuD$$

by an indirect mechanism

$$CuHum \underset{k_{Cu}^{Hum_T}}{\overset{k_{CuHum_T}}{\rightleftharpoons}} Cu + Hum \qquad (26)$$

$$Cu + D \xrightarrow{k_{Cu}^{D_T}} CuD \qquad (27)$$

the observed humic-dependent rate constant is

$$k_{ind} = \frac{k_{CuHum_T}\, k_{Cu}^{D_T}}{k_{Cu}^{Hum_T}} = 3.95 \pm 0.63 \times 10^4 \text{ mg mol}^{-1} \text{ sec}^{-1}.$$

From the model study, $k_{Cu}^{D_T} = 5.2 \pm 0.3 \times 10^7 \text{ M}^{-1} \text{ sec}^{-1}$, then

$$\frac{k_{CuHum_T}}{k_{Cu}^{Hum_T}} = \frac{3.95 \times 10^4}{5.2 \times 10^7} = 7.6 \pm 1.3 \times 10^{-4} \text{ mg/L}$$

or $k_{Cu}^{Hum_T} / k_{CuHum_T} = 1.3 \pm 0.2 \times 10^3$ L/mg. This ratio is related to a more conventionally expressed conditional stability constant for CuHum by the Cu-binding site density (in mol/ mg humic acid). Thus

$$k_{Cu}^{Hum_T} / k_{CuHum_T} = 10^{3.12} = K_{CuHum}^{cond} \left[\text{L/mol}\right] \text{ site density } \left[\text{mol/mg}\right] \qquad (28)$$

As discussed previously, the site density (i.e.- mol Cu binding sites/ wt humic acid) may be calculated for the slow-reacting site (Huml) from ligand exchange experiments with 20 nM Dye, 50 nM Cu_T, and 1.1 mg/L Hum_T. The calculated site density is ~10^{-7}mol/mg. The corresponding stability constant for Cu binding at this site (K_{CuHuml}) is $10^{10.1}$.

The results of ligand exchange experiments with humic acids demonstrate the crucial role of metal-to-humate loading in kinetics experiments. Only at low Cu-to-humate loadings (approximately environmental values) can the contribution of the direct mechanism be discerned. At higher Cu-to-humate loadings, more than one rate constant is required to fit the data. This is consistent with the previous observation of Shuman and co-workers who found that three rate constants were required to model the reaction of CuDOC with PAR, 4-(2-pyridylazo)resorcinol, (at 0.34 μmol Cu/ mg DOC) and also of Lavigne et al. (1987) who again found three rate constants to be required in this case to model the reaction of Ni-fulvate with PAR (at 0.12 to 1.1 μmol Ni/ mg fulvic acid).

For ligand-exchange reactions at low Cu-to-humate ratios, the requirement for only a single rate constant for the indirect mechanism does not necessarily indicate involvement of only one type of humate binding site. The apparent "saturation" of the site(s) at 1.1 mg/L humic acid puts an upper bound on the site density and thus a lower bound on the Cu-humic stability constant. However the involvement of stronger sites at correspondingly lower site densities cannot be eliminated.

CONCLUSION

The ligand exchange reactions of Cu-humate species with the fluorescent reagent can be interpreted based on the model used for the reaction of this reagent with CuNTA. Experiments with well-defined ligands demonstrate that the concentration range and relative concentrations of the reactants chosen for study determines whether the contributions of different mechanisms can be discerned. Ligand exchange reactions of Cu complexes with well-defined ligands and with humic acid proceed by mechanisms involving both dissociation of the initial Cu complex and direct attack of the incoming ligand on the initial complex. Both pathways are likely to be important at Cu-to-humate loadings occuring in natural waters. The rate constants observed for the indirect reaction of Cu-humate species may be further interpreted to provide information on equilibrium stability constants for Cu-humate interactions.

REFERENCES

Anderson, D.M., J.S. Lively, R.F.Vaccaro (1984) J. Mar. Res. 42: 677-95.

Hering J.G. and F.M.M. Morel, submitted to Environ. Sci. Technol.

Langford, C.H. and T.R. Khan (1975) Ca. J. Chem. 53: 2979-84.

Langford, C.H. and M. Parris (1972) in Comprhensive Chemicial Kinetics vol 7, ed. C.H. Bamford and C.F.H. Tipper. Amsterdam: Elsevier Publishing Co.

Langford, C.H., R. Kay, G.W. Quance, T.R. Khan (1977) Anal. Lett. 10: 1249-60.

Langford, C.H., S.M. Wong, A.L. Underdown (1981) Can. J. Chem. 59: 181-6.

Lavigne, J.A., C.H. Langford and M.K.S. Mak (1987) Anal. Chem. 59: 2616-20.

Mak, M.K.S. and C.H. Langford (1982) Can. J. Chem. 60: 2023-8.

Margerum, D.W., G.R. Cayley, D.C. Weatherburn, and G.K. Pagenkopf (1974) in Coordination Chemistry vol 2, ed. A. Martell. ACS Monograph 174.

Moore, J.W. and R.G. Pearson (1981) Kinetics and Mechanism 3rd ed. New York: Wiley-Interscience.

Newell, A.D. and J.G. Sanders (1986) Environ. Sci. Technol. 20: 817-21.

Olson, D.L. and M.S. Shuman (1983) Anal. Chem 55: 1103-7.

Plankey, B.J., H.H. Patterson, C.S. Cronan (1986) Environ. Sci. Technol. 20: 160-5.

Pribil, R. (1982) Applied Complexometry, Oxford: Pergammon Press.

Shuman, M.S. and L.C. Michael (1978) Environ. Sci. Technol. 12: 1069-72.

Shuman, M.S., B.J. Collins, P. J. Fitzgerald, D.L. Olson in Aquatic and Terrstrial Humic Materials ed. R.F. Christmann and E.T. Gjessing. Ann Arbor, MI: Ann Arbor Science.

Sweigart, D.A. and D.G. DeWit (1969) Inorg. Chem. 9: 1580-2.

Waite, T.D. and F.M.M. Morel (1984) Anal. Chim. Acta 162: 263-74.

APPENDIX: Model used for reaction of Dye with Cu/humic acid (50 nM Cu_T, 1.1 mg/L humic acid).

Dye reacts with Cu bound at 2 humate sites (i.e.- CuHum1, slow-reacting species, and CuHum2, fast-reacting species).

$$D + CuHum2 \xrightarrow{k_{H2}} CuD + Hum2$$

$$D + CuHum1 \xrightarrow{k_{H1}} CuD + Hum1 \qquad k_{H1} = \frac{k_{H1}^{diss}}{(Hum1)} + k_{H1}^{int}$$

Then species concentrations over time are predicted from:

$$(D)_{t+\Delta t} = (D)_t - \left[\left(k_{H2}(CuHum2)_t(D)_t + \left(\frac{k_{H1}^{diss}}{(Hum1)} + k_{H1}^{int}\right)(CuHum1)_t\right)(D)\right]\Delta t$$

$$(CuHum2)_{t+\Delta t} = (CuHum2)_t - \left[k_{H2}(CuHum2)_t(D)_t\right]\Delta t$$

$$(CuHum1)_{t+\Delta t} = (CuHum1)_t - \left[\left(\frac{k_{H1}^{diss}}{(Hum1)} + k^{int}\right)(CuHum1)_t(D)_t\right]\Delta t$$

and

$$(Hum1)_{t+\Delta t} = Hum1_T - \frac{(CuHum1)_{t+\Delta t}}{S}$$

The input parameters to this model are:

k_{H1}^{ind} = 39,500 mg mol^{-1} sec^{-1}

k_{H1}^{dir} = 3,300 $M^{-1}sec^{-1}$

k_{H2} = 9 x 10^5 M^{-1} sec^{-1}

Hum_T = 1.1 mg/L

$(D)_o$ = 20 or 50 nM

$(CuHum1)_o$ = 42 nM

$(CuHum2)_o$ = 8 nM

S = 10^{-7} mol/mg

Δt = 10 sec

The rate constants k_{H1}^{dir} and k_{H1}^{ind} are obtained from analysis of ligand exchange experiments conducted with high humic acid concentrations as shown in Figure 8. The rate constant k_{H2} is optimized from the model fit for the experiment with 20 nM Dye, 50 nM Cu_T, 1.1 mg/L Hum_T.

The initial concentrations of CuHum1 and CuHum2 and the site density S are calculated as follows: For the experiment with 20 nM Dye, 50 Nm Cu_T, 1.1 mg/L, ln(D) is plotted vs time (shown in Figure 7b). The extrapolation of the line fit to this data (for $t \geq 130$ sec) to zero time gives the concentration of Dye (at t = 0) reacting with CuHum1 (the slow-reacting Cu-humate species). The remainder of the Dye is taken to have reacted with CuHum2. Thus

D_T - extrapolated value of $(D)_o$ = (CuHum2)

Cu_T - $(CuHum2)_o$ = $(CuHum1)_o$.

The site density, S, is calculated as described in the text under Results.

CHAPTER SIX

SLOW COORDINATION REACTIONS IN AQUATIC SYSTEMS

ABSTRACT

The rates of reaction of transition metals with free (or protonated) ligands are intrinsically fast. Yet the observed rate of formation of metal complexes with strong ligands in seawater systems containing a mixture of ligands is remarkably slow. When copper is added to mixtures of natural and synthetic ligands, the equilibrium distribution of metal species is only established after hours or even days. At the calcium concentration of seawater, kinetic hindrance to the initial reaction of the stronger ligand with the added metal results in initial formation of copper complexes with the weaker ligands. Equilibrium metal speciation is attained slowly through a series of ligand and metal exchange reactions.

Observations of slow kinetics of coordination reactions in model systems demonstrate that re-equilibration of a natural system undergoing perturbations of metal or ligand concentrations (under natural or analytical conditions) cannot be assumed to be rapid. This study also suggests that the concentration of strong complexing agents in seawater may be underestimated in measurements of metal complexation that involve metal additions.

INTRODUCTION

Organic complexation of metals, particularly copper, is ubiquitous in natural waters (SUNDA and FERGUSON, 1983; HERING et al., 1987; SUNDA and HANSON, 1987; MOFFETT and ZIKA, 1987; CABANISS and SHUMAN, 1988; COALE and BRULAND, in press). The presence of organic complexing agents strongly influences metal reactivity and thus biogeochemical processes such as metal uptake by organisms (SUNDA and GUILLARD, 1976; ANDERSON and MOREL, 1978; ANDERSON and MOREL, 1982), sorption of metals onto surfaces (DAVIS and LECKIE, 1978; DAVIS, 1984), or metal redox reactions (WAITE and MOREL, 1984; STONE, 1986; TIPPING, 1986). In analytical measurements of metal complexation, in the study of biogeochemical processes in the presence of natural or synthetic ligands, and in modeling the interactions of metals with naturally-ocurring complexing agent (TURNER et al., 1985; FISH et al, 1986, DZOMBAK et al. 1986; CABANISS and SHUMAN, 1988), equilibrium (or pseudo-equilibrium) between complexing agents and dissolved metal species and rapid re-equilibration of the system after any perturbation of metal speciation have been assumed.

These assumptions, however, are not valid in complex systems containing mixtures of competing ligands and metals. In such cases, as is shown in this paper, slow attainment of equlibrium metal speciation is observed when the system is perturbed by addition of either metals or ligands. The reaction of strong ligands with transition metals is kinetically hindered in the presence of calcium at seawater concentrations. Thus, kinetically labile weak ligands react initially

with the metal. In the resulting pseudo-equilibrium, metal speciation is dominated by the weak rather than the strong ligands. Subsequent re-equilibration to give the thermodynamically favored strong ligand-metal complex proceeds slowly through a series of metal and ligand exchange reactions.

If the rates of metal coordination reactions in seawater are indeed slow, then the study of biogeochemical processes must consider explicitly the effect of complexation kinetics on the overall rates of such processes. In addition, rates of re-equilibration of complex systems have important implications for analytical measurements of metal complexation in which natural water samples are commonly perturbed by the addition of metals or synthetic ligands. An accurate estimation of the rates of metal coordination reactions in natural waters is required to understand and predict changes in metal reactivity in such systems.

BACKGROUND

The theory of coordination reaction kinetics has been extensively reviewed and empirical reaction mechanisms and rate constants have been compiled by MARGERUM et al. (1978). The rate of reaction of transition metals with protonated or free ligand species is predominantly controlled by water-loss from the inner coordination sphere of the metal (EIGEN and WILKINS, 1965). The reactions of alkaline earth ligand complexes with transition metals have also been studied and have been shown to proceed both through a dissociative mechanism and by direct attack of the incoming metal on the alkaline earth-ligand complex (CARR

and SWARTZFAGER, 1975, KUEMPEL and SCHAAP, 1968, HERING and MOREL, submitted (a)). For example, omitting protonated species for simplicity,

$$Cu + CaL \longrightarrow CuL + Ca$$

dissociative mechanism:

$$CaL \rightleftharpoons Ca + L$$

$$L + Cu \longrightarrow CuL$$

direct attack:

$$CaL + Cu \rightleftharpoons CaLCu \longrightarrow Ca + CuL$$

Previous results in this laboratory (HERING and MOREL, submitted (a)) have shown that the rate of copper complexation by EDTA (ethylenediaminetetraacetic acid) is dramatically decreased in the presence of seawater concentrations of calcium. This kinetic hindrance occurs because of direct competition between calcium and copper for the free (or protonated) ligand species produced as an intermediate in the dissociative mechanism and also because the direct attack of copper on the calcium complex is very slow compared to its reaction with free or protonated ligand species.

In this study, we examine the effect of alkaline earth metals on reactions of competing ligands with a transition metal. The strong ligand, L_s, has a higher affinity for both transition and alkaline earth metals than the weak ligand, L_w, (i.e.- $K_{CaL_s} >> K_{CaL_w}$ and $K_{CuL_s} >> K_{CuL_w}$). In the presence of calcium, the reaction with the thermodynamically favored ligand L_s is kinetically hindered and thus the initial distribution of metal-ligand species is far from equilibrium:

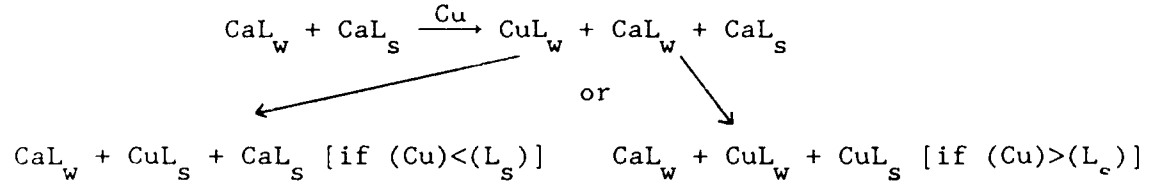

The time over which the equilibrium species distribution is attained will depend on the extent of the kinetic hindrance of the initial reaction of Cu with the strong ligand L_s and on the rate of exchange of CaL_s with CuL_w.

MATERIALS AND METHODS

All reagents were analytical grade and most were used without further purification. Aldrich humic acid and Suwannee Stream humic acid (obtained from the U.S. Geological Survey) were cleaned by re-precipitation from acid solution (HERING and MOREL, submitted (b)). The structure of the fluorescent reagent calcein (Sigma) and fluorescence quenching by copper have been described elsewhere (WALLACH and STECK, 1963; PRIBIL, 1982; SAARI and WEITZ, 1984). All experiments were conducted in acid-cleaned glass or polypropylene and care was taken in handling solutions to minimize trace metal contamination.

Kinetic experiments

The kinetics of metal complex formation and ligand exchange reactions were followed either by observing changes in inorganic copper concentrations by amperometric measurements or by following changes in the concentration of metal-ligand complexes by fluorescence measurements.

Amperometric measurements. Reaction of calcium complexes of NTA (nitrilotriacetic acid) and EDTA with copper were followed by measuring inorganic copper concentration over time. The mixture of ligands was pre-equilibrated with 0.01 M Ca. At t=0, an aliquot of the pre-formed Ca-ligand complexes was added to copper in electrolyte solution (0.5 M NaCl, 0.01 M $CaCl_2$, 0.002 M $NaHCO_3$) pre-equilibrated with the electrode system. Inorganic copper concentrations were determined from amperometric measurements of the reduction of Cu(II) to Cu(I) at 90 mV (relative to Ag/AgCl) as described in HERING et al. (1987) and HERING and MOREL (submitted(a)). The theory and application of the method (WAITE and MOREL, 1983) and the electrode system (MATSON et al., 1977) have been described in detail.

Fluorescence measurements. Fluorescence was measured with a Perkin-Elmer LS-5 fluorescence spectrophotometer in 1 cm quartz cuvettes. Fluorescence signals were integrated over 8 sec and then averaged over 1 min for each reading. Measurements were made at the following excitation/emission wavelengths (slit width 5 nm): 492/511 nm (calcein), 485/540 nm (Aldrich humic acid), 344/466 nm (Suwannee Stream humic acid).

Ligand exchange experiments were conducted either by adding aliquots of concentrated EDTA solutions to mixtures of calcein and copper in background medium of 0.1 M NaCl, 0.005 M HEPES (N-2-hydroxyethylpiperazine-N'-2-ethanesulphonic acid) buffer with 0 or 0.01 M $CaCl_2$ (pH $\approx$ 7.3) or by adding aliquots of copper to mixtures of ligands (either calcein/EDTA or humic acid/EDTA) in the same background

medium. For experiments involving additions of EDTA to solutions containing 0.01 M Ca, EDTA was added as the calcium bound form (i.e.- EDTA was pre-equilibrated with equimolar Ca).

For both calcein and humic acids, fluorescence is linearly related to concentration (over the concentration range of interest). For calcein, at the ligand-to-metal ratios used, fluorescence quenching is directly proportional to copper-binding. The quenching of natural humic acid fluorescence is also related to copper binding as has been shown by comparisons of ion-selective electrode and fluorescence quenching measurements in metal titration experiments (SAAR and WEBER, 1980; RYAN and WEBER, 1982; FISH, 1984; CABANISS and SHUMAN, 1986).

RESULTS

As shown in our previous work, the rate of reaction of EDTA with copper is markedly decreased in the presence of calcium. In seawater, the (pseudo first order) half-life for copper reacting with EDTA is ~2 h at 100 nM EDTA. Figure 1 shows the effect of addition of pre-formed calcium complexes of NTA and EDTA to inorganic copper at seawater calcium concentrations. The concentration of inorganic copper is quickly decreased to the level calculated for equilibrium with CaNTA alone, essentially behaving as though no EDTA were present. The subsequent slow decrease in inorganic copper concentration is consistent with reaction of the remaining inorganic copper with CaEDTA. Thus the kinetic hindrance to reaction of Cu with CaEDTA results in an initial distribution of metal-ligand species in which copper is complexed by the weaker rather than the stronger ligand.

Figure 1. Concentration of inorganic copper over time after addition of 62.5 nM CaNTA and 100 nM CaEDTA at t=0. (Δ) Cu_{init} = 37.5 nM. Electrolyte: 0.5 M NaCl, 0.01 M $CaCl_2$, 0.002 M $NaHCO_3$. (---) equilibrium concentration of inorganic copper calculated with NTA only. In the final equilibrium, copper is calculated to be ≈ 100% organically complexed.

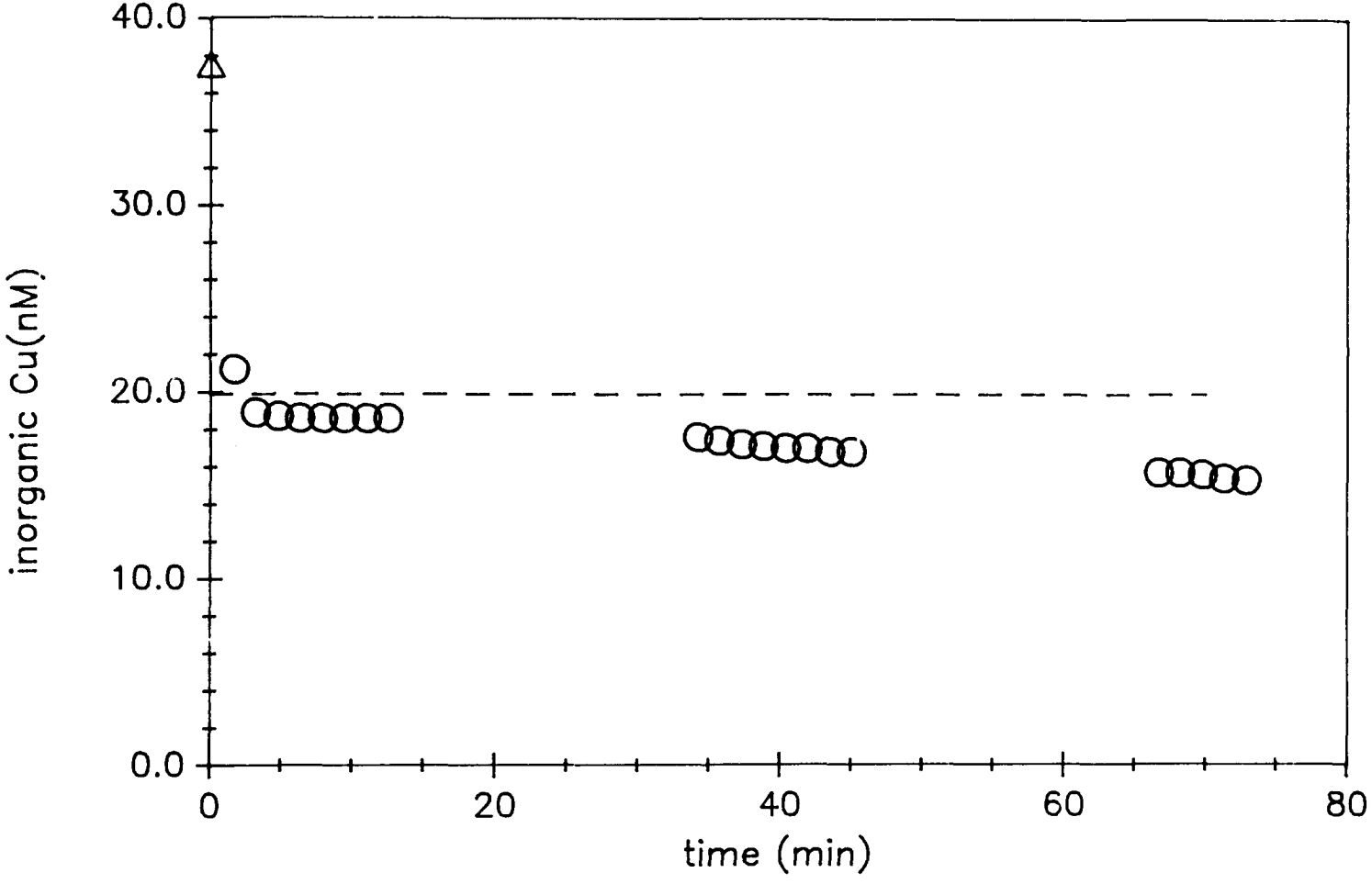
40.0
30.0
20.0
10.0
0.0
inorganic Cu(nM)
0
20
40
60
80
time (min)

Ligand exchange reactions were followed by using a fluorescent complexing agent, calcein; calcein fluorescence is quenched on binding to copper. The rate of exchange of copper from calcein to EDTA is very significantly decreased by calcium. Even at micromolar EDTA concentrations, the exchange reaction in the presence of calcium occurs on a time scale of hours to days (Fig. 2a,b). Addition of copper to a mixture of the two ligands (pre-equilibrated with calcium) results in an initial reaction predominantly with calcein (even with EDTA in 40-fold excess) followed by slow exchange to give the thermodynamically favored CuEDTA complex (Fig. 2b).

A similar effect is observed on the addition of copper to a mixture of humic acids and EDTA. In this case, quenching of the natural fluorescence of the humic acids is used as a qualitative measure of copper binding. No fluorescence quenching is observed upon addition of copper to the humic acid/EDTA mixture in the absence of calcium indicating fast formation of CuEDTA. In the presence of calcium, however, copper reacts initially with the humic acid (as shown by the immediate decrease in fluorescence) followed by a slow exchange with CaEDTA. This effect is observed for both commercial (Fig. 3) and Suwannee Stream (Fig. 4) humic acids.

DISCUSSION

Modeling metal coordination reaction kinetics

The exchange reaction between Cu-humate and CaEDTA may be modeled by assuming pseudo-equilibrium between Cu and humate ligands and

Figure 2. Ligand exchange experiments with calcein (a fluorescent complexing agent), EDTA, and Cu (50 nM total calcein, 30 nM total Cu in 0.1 M NaCl, 5mM HEPES, pH=7.28) (a) addition of 10μM EDTA at t=0 to pre-formed Cu-calcein complex (Δ ,∇) no Ca, (O) 0.01 M Ca (b) addition of 2 μM EDTA at t=0 to pre-formed Cu-calcein complex (Δ ,∇) no Ca, (O) 0.01 M Ca; ($\square$) addition of Cu at t=0 to calcein and EDTA pre-equilibrated with 0.01 M Ca.

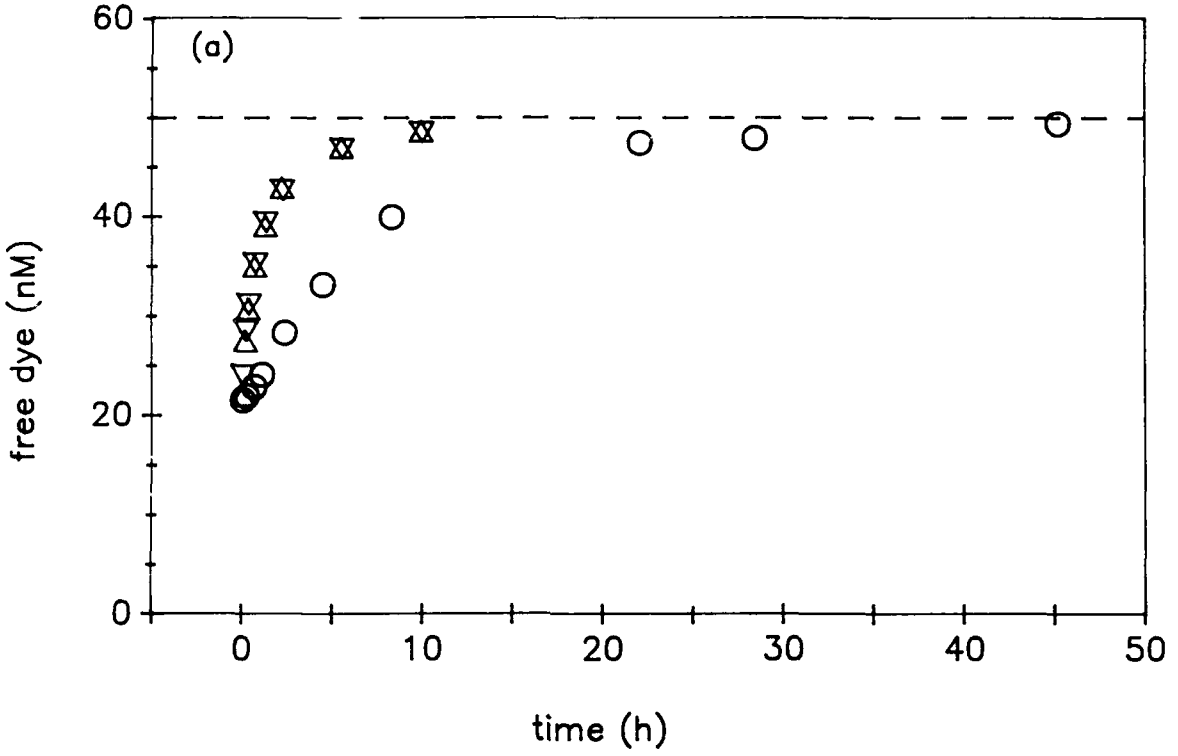
(a)
free dye (nM)
time (h)
0
20
40
60
0
10
20
30
40
50

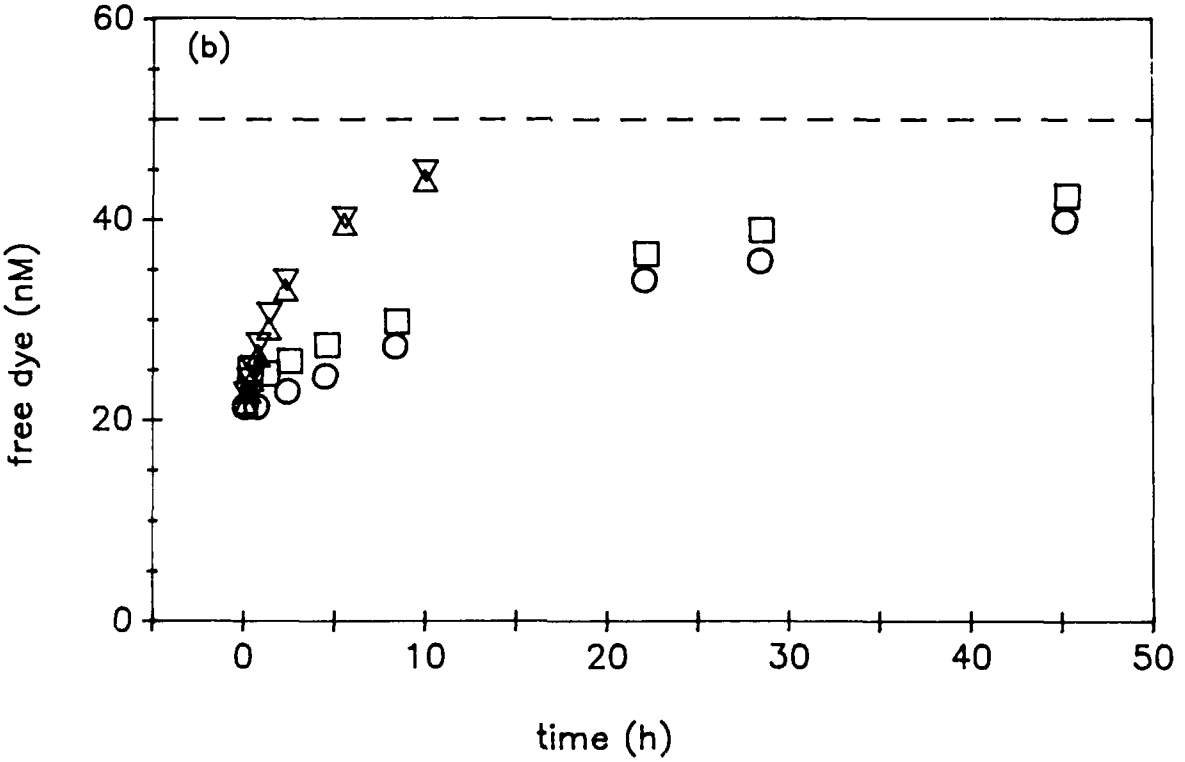
(b)
free dye (nM)
time (h)
0
20
40
60
0
10
20
30
40
50

Figure 3. Ligand exchange experiments with Aldrich humic acid (5.11 mg/L humic acid, total EDTA 2 μM, total Cu 2 μM in 0.1 M NaCl, 5 mM HEPES, pH= 7.35). (a) no Ca (b) 0.01 M Ca. Symbols: (□,◇) Cu added at t=0 to mixture of humic acid and EDTA, (○) humic acid and EDTA, no Cu, (△) humic acid and Cu, no EDTA.

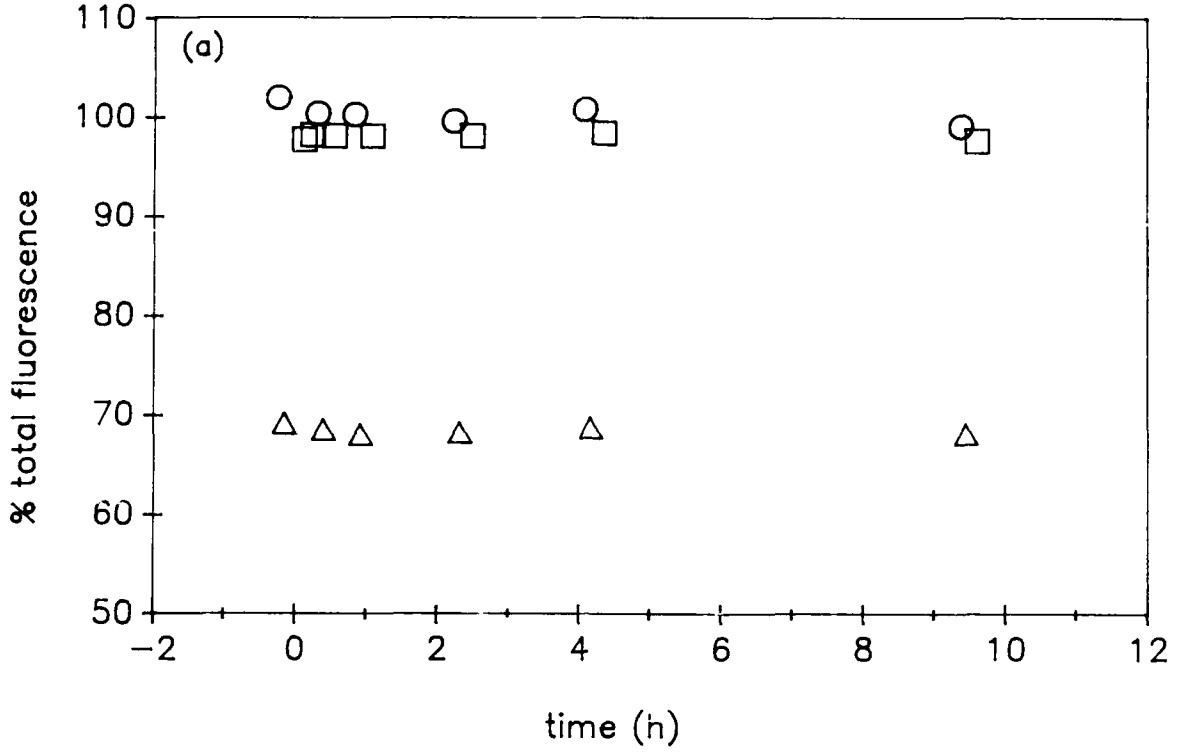
(a)
110
100
90
80
70
60
50
% total fluorescence
−2
0
2
4
6
8
10
12
time (h)

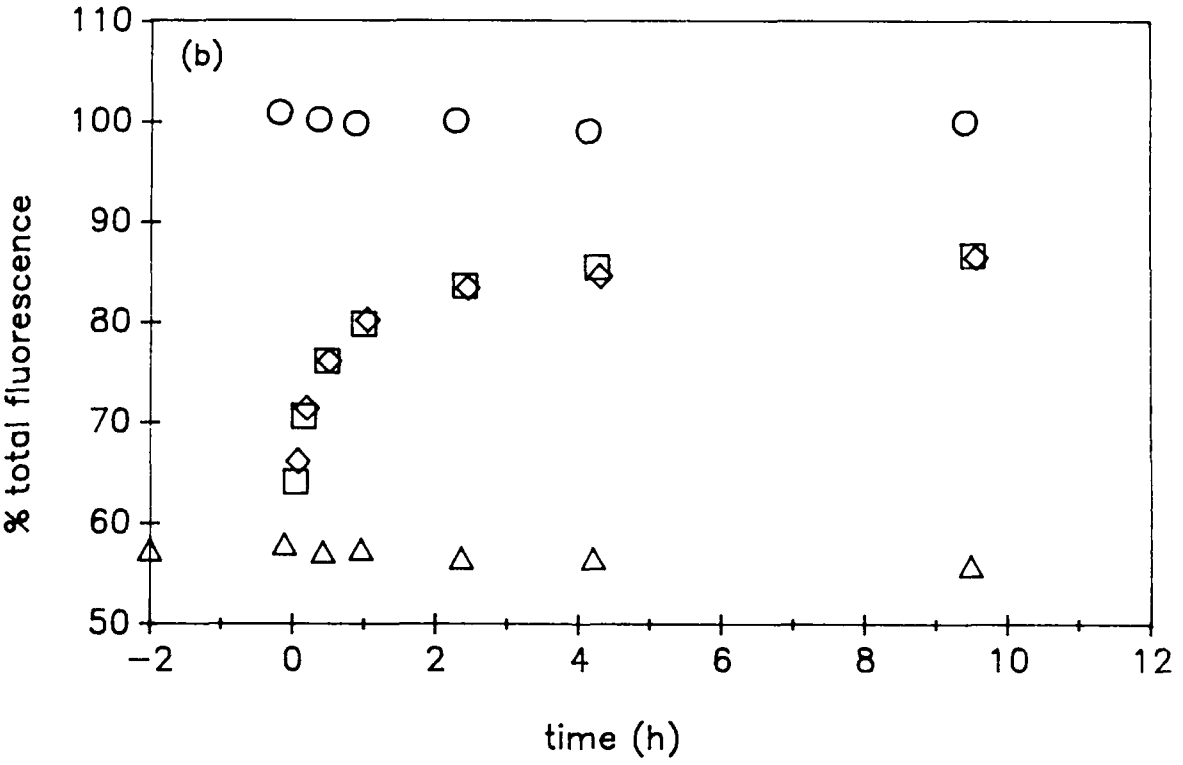
(b)
110
100
90
80
70
60
50
% total fluorescence
−2
0
2
4
6
8
10
12
time (h)

Figure 4. Ligand exchange experiments with Suwannee Stream humic acid (4.94 mg/L humic acid, total EDTA 2 μM, total Cu 2 μM in 0.1 M NaCl, 5 mM HEPES, pH= 7.39). (a) no Ca (b) 0.01 M Ca. Symbols: (□ , ◇) Cu added at t=0 to mixture of humic acid and EDTA, (○) humic acid and EDTA, no Cu, (△) humic acid and Cu, no EDTA. (——) calculated %free humate based on constants in Table I and model described in the Appendix.

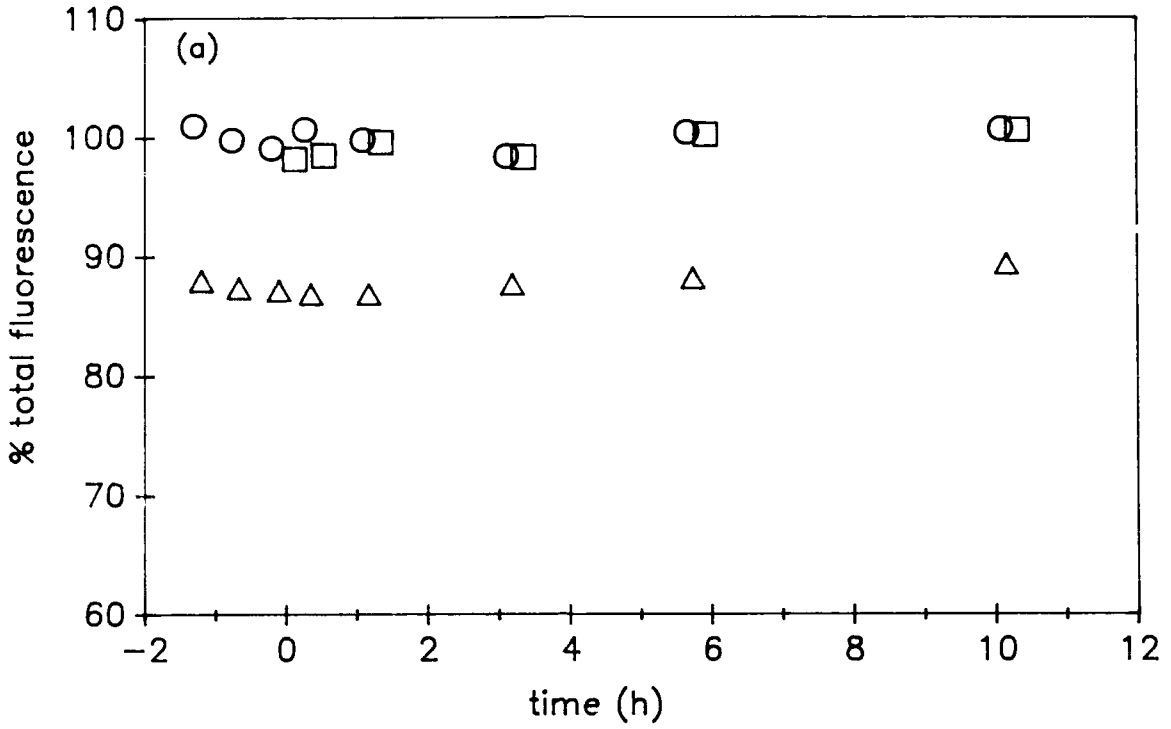
(a)
% total fluorescence
110
100
90
80
70
60
−2
0
2
4
6
8
10
12
time (h)

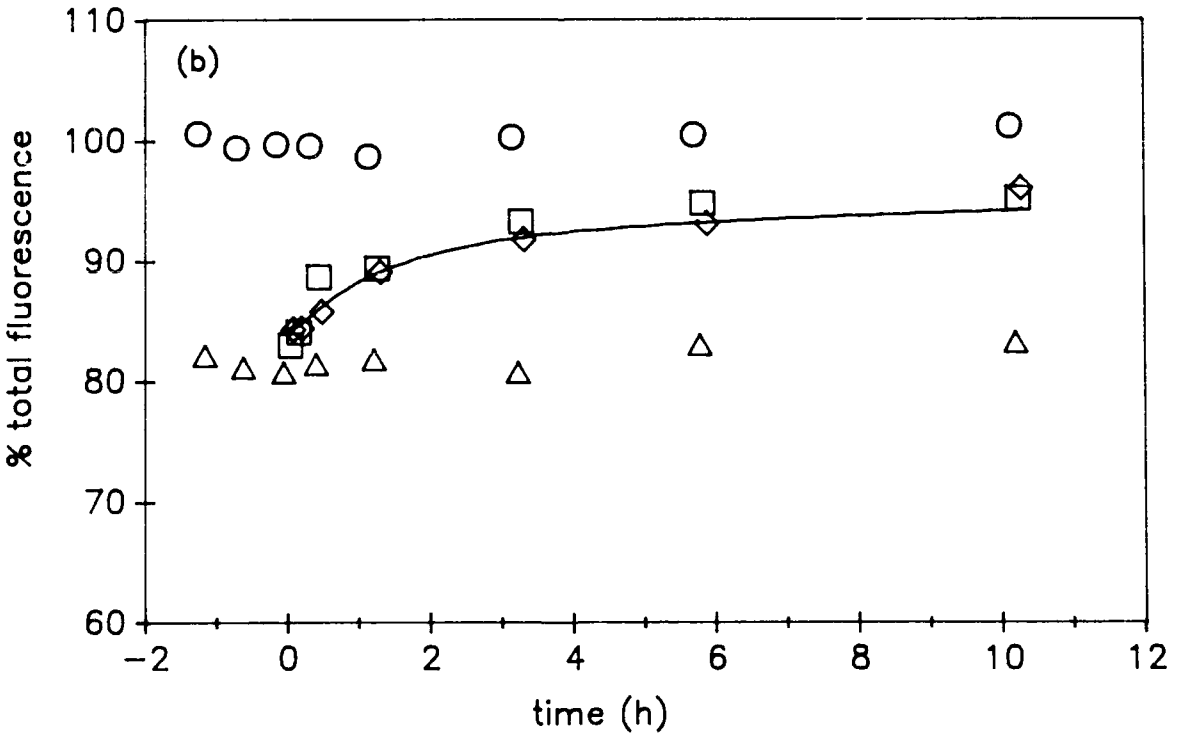
(b)
% total fluorescence
110
100
90
80
70
60
−2
0
2
4
6
8
10
12
time (h)

reaction of inorganic Cu with CaEDTA (see Appendix). The %free humate over time was predicted for the reaction of Cu with Suwannee Stream humic acid and EDTA for conditions of Fig. 4b (5 mg/L humic acid, 2 μM Cu_T, 2 μM $EDTA_T$, 0.01 M Ca_T, pH= 7.4) using equilibrium constants for Cu-binding by humic acid (modeled as discrete ligand sites) based on Cu titrations of Suwanee Stream humic acid (HERING and MOREL, submitted (b)) and kinetic constants for reaction of CaEDTA with inorganic Cu (HERING and MOREL, submitted (a)) (Table I).

The calculated %free humate is in agreement with the observed %fluorescence (Fig. 4b). Thus at high metal-to-humate loading, ligand exchange reactions may be modeled without any direct attack of EDTA species on humate-bound copper consistent with the observations of SHUMAN and co-workers (SHUMAN and MICHAEL, 1978; SHUMAN et al., 1983; OLSON and SHUMAN, 1983).

This model for the ligand exchange reaction between humate-bound copper and CaEDTA may also be applied to conditions that are not experimentally accessible. Figure 5 shows model predictions for lower Cu and EDTA concentrations and lower Cu-to-humate loading (1 mg/L humic acid, 10 nM Cu_T, 20 nM $EDTA_T$, 0.01 M Ca_T, pH=8.2, equilibrium and kinetic constants given in Table II). In this case, the back reaction of CuEDTA is included to allow the system to reach equilibrium. Equilibrium is attained in approximately 1 year. The slow progress of this reaction is due to the low inorganic Cu concentration available for reaction with CaEDTA when strong humate binding sites are in excess of total copper.

TABLE I. Constants used in modeling Fig.4 b.

ligand site	total conc.	log Cu stability constant*
Hum1	2.50×10^{-7} M	10.2
Hum2	1.00×10^{-6} M	8.4
Hum3	9.00×10^{-6} M	5.8

$$k_{Cu}^{CaEDTA} = 7.20 \times 10^{4}\ M^{-1} min^{-1}$$

[* These values are for conditional stability constants for the humate "ligands" with inorganic Cu (for pH = 7.4, inorganic Cu $\approx Cu^{2+}$).]

Figure 5. Results of the pseudo-equilibrium model for reaction of Cu-humate with CaEDTA showing calculated concentrations of CuEDTA (——) and Cu-humate species (---) CuHum1, (...) CuHum2 for total Cu= 10 nM, total EDTA= 20 nM, 1 mg/L humic acid, 0.01 M Ca, pH= 8.2, constants given in Table II.

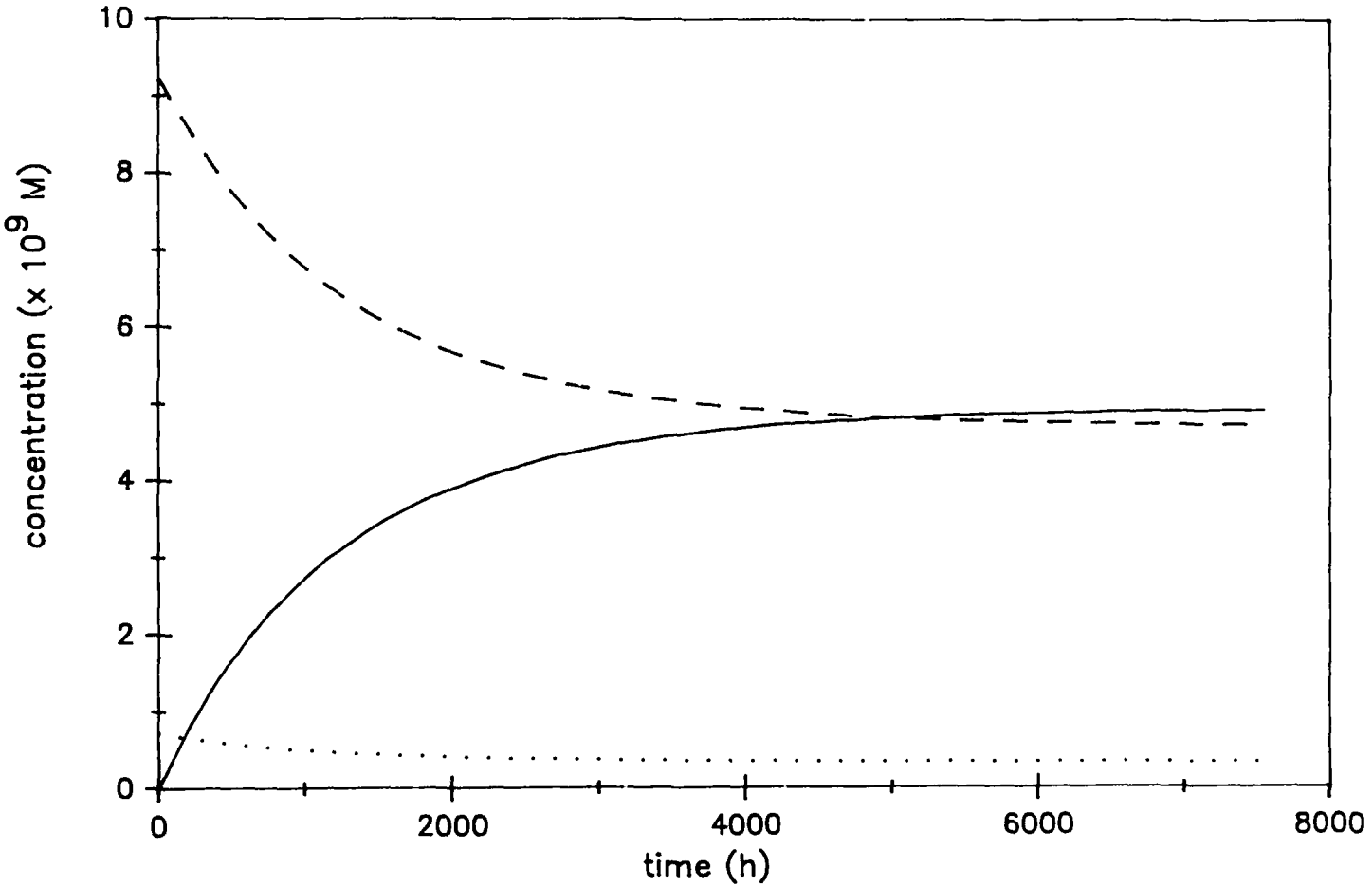
10
8
6
4
2
0
concentration (x 10^9 M)
0
2000
4000
6000
8000
time (h)

Table II. Constants used in modeling Fig. 5.

ligand site	total conc.	log Cu stability constant*
Hum1	5.00×10^{-8} M	9.6
Hum2	2.00×10^{-7} M	7.8
Hum3	1.80×10^{-6} M	5.2

$$k_{Cu}^{CaEDTA} = 5.82 \times 10^{4}\ M^{-1}min^{-1}$$
$$k_{Ca}^{CuEDTA} = 4.62 \times 10^{-4}\ M^{-1}min^{-1}$$

[* These values are for conditional stability constants for the humate "ligands" with inorganic Cu (for pH = 8.2, inorganic Cu $\approx 10^{1.4}\ Cu^{2+}$).]

In the calculation for Fig. 5, the discrete ligand representation of Cu-humate binding is used only to define the pseudo-equilibrium concentration of inorganic Cu. Such a pseudo-equilibrium description is obviously insufficient to model the progress of metal coordination reactions upon addition of Cu to the system. If, as a hypothetical case, the discrete ligand model is taken to describe actual humate Cu-binding sites, the initial reaction may be modeled by explicitly describing the formation (and dissociation) of Cu-humate species over some initial time and imposing the pseudo-equilibrium condition at later times (as described in the Appendix). Results of this model are shown in Fig. 6. In this model, the formation rates for all Cu-humate species (CuHum1, CuHum2, and CuHum3) are taken to be equal ($k_f = 10^7 M^{-1} sec^{-1}$) and dissociation rate constants for each Cu-humate complex are inversely proportional to their equilibrium stability constants. Thus the initial formation of Cu-humate species is determined by the concentrations of the free humate "ligands" and the initial reaction of Cu occurs at the weakest (most abundant) site. The time scale over which pseudo-equilibrium between Cu and humate species is attained is determined by the rate constant(s) for formation of Cu-humate species. In this example, such pseudo-equilibrium is attained in a few minutes. Figure 6 b shows the log of the inorganic Cu concentration over time. The shape of the curve reflects the change in Cu speciation over time as the reaction progresses toward the complexation of Cu by the stronger sites or ligands. Since the inorganic Cu concentration is quickly decreased by initial reaction with the humic acid, further progress of

Figure 6. Model of the initial reaction of Cu with humic acid and CaEDTA followed by pseudo-equilibrium exchange between Cu-humate and CaEDTA showing (a) calculated concentrations of inorganic Cu, Cu-humate species and CuEDTA as a function of the logarithm of time (in minutes) for the reaction of 10 nM Cu with 20 nM EDTA and 1 mg/L humic acid (0.01 M Ca, pH = 8.2, constants given in Table II) (b) logarithm of the inorganic Cu concentration as a function of the logarithm of time for the same conditions.

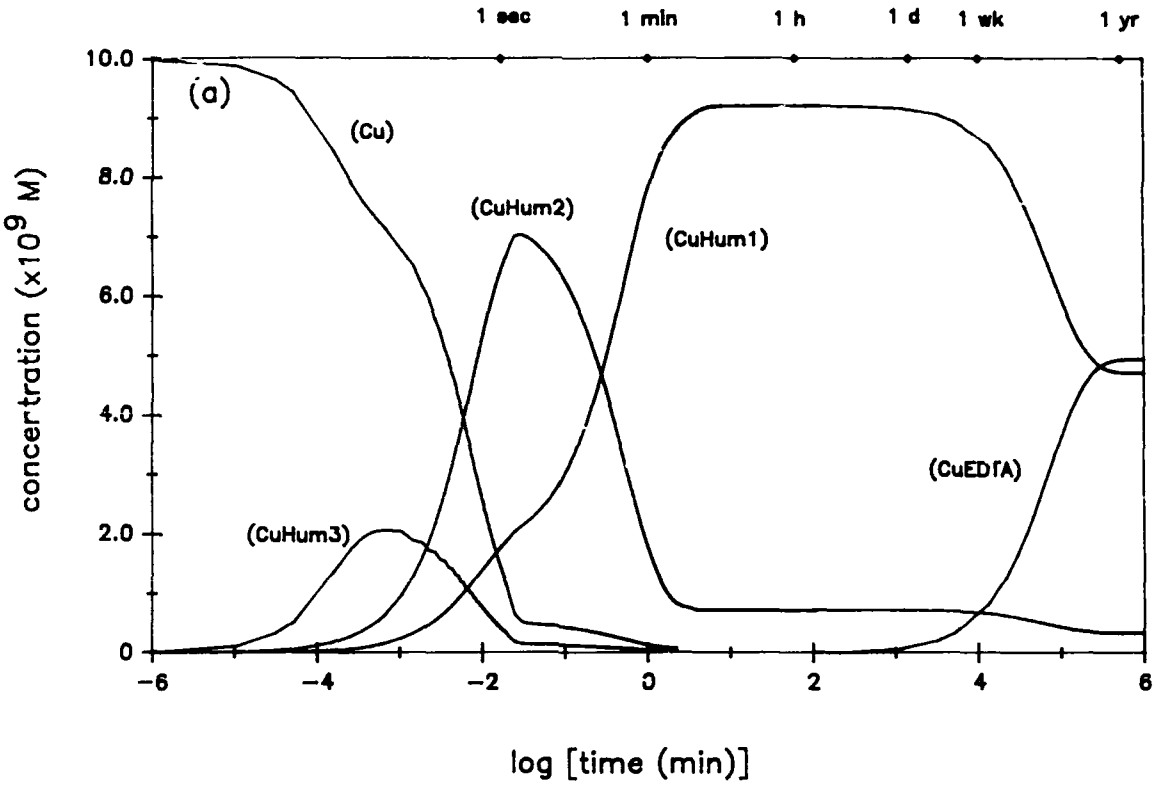
1 sec
1 min
1 h
1 d
1 wk
1 yr
10.0
8.0
6.0
4.0
2.0
0
(a)
(Cu)
(CuHum2)
(CuHum1)
(CuEDTA)
(CuHum3)
concertration (x10^9 M)
−6
−4
−2
0
2
4
6
log [time (min)]

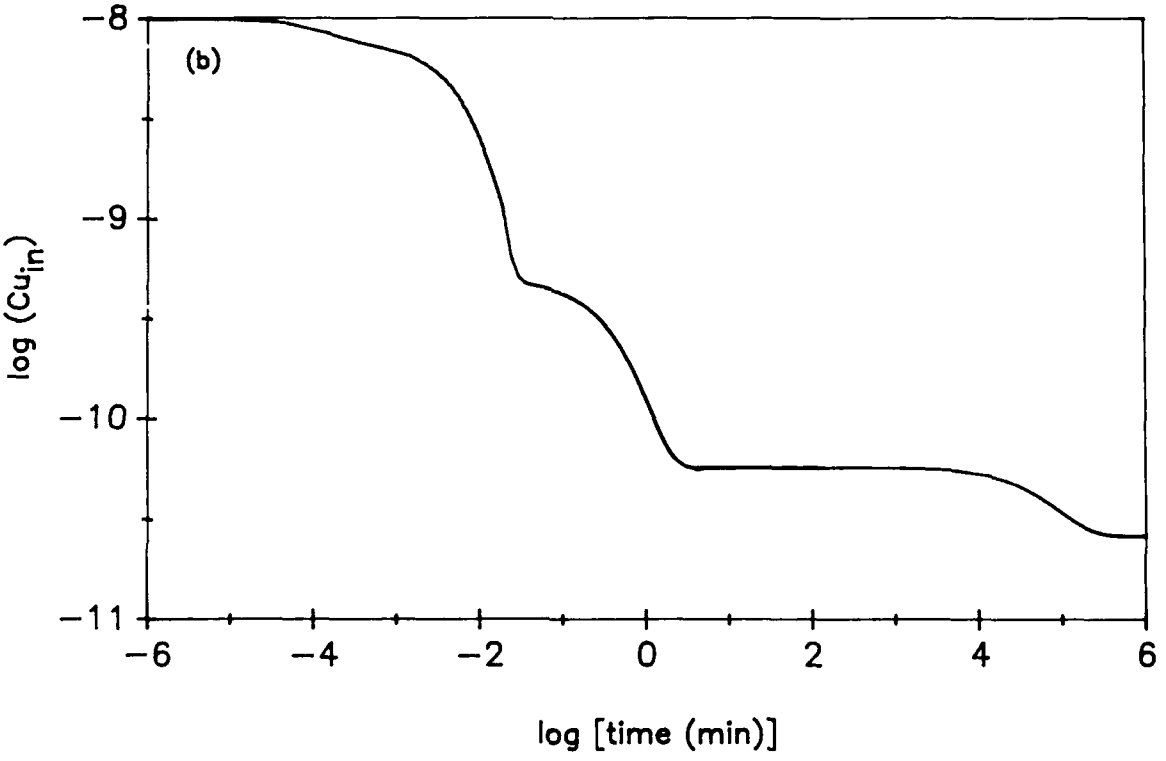
−8
−9
−10
−11
(b)
log (Cu$_{in}$)
−6
−4
−2
0
2
4
6
log [time (min)]

the reaction (i.e.- with strong ligands) may not be detectable by measurement of free or inorganic Cu if these species are already at or near the detection limit of the measurement techniques (regardless of complications due to the time scale of the reaction).

Rates and mechanisms of coordination reactions

The experimental results with model systems clearly show that when complex systems are perturbed by addition of either metal or ligands re-equilibration of metal speciation may be slow. In the reactions examined above, the slow attainment of equilibrium speciation is due to several factors. In systems with several competing metals and ligands, different kinetic reactivity of the ligands results in an initial pseudo-equilibrium condition in which the distribution of metal species is far from the equilibrium distribution. Metal speciation is initially dominated by the weaker ligands. The reaction pathways from the inital pseudo-equilibrium to the final equilibrium involve a series of metal and ligand exchange reactions. Thus even though the rate constants for many of the reactions involved are intrinsically fast (particularly for formation of metal complexes), the rate-limiting steps involved in double (i.e.- both ligand and metal) exchange reactions may be quite slow. The overall rate of formation of the thermodynamically favored complex will be slowest for low concentrations of the metal and strong ligand and for low ratios of strong-to-weak ligand concentrations.

Effects of different metals

In this study, we have examined reactions of a single transition metal, Cu, and only with the alkaline earth metal Ca as a competing

metal. The considerations raised in this paper, however, are clearly applicable to reactions of other metals and also to the competitive interactions of transition metals. The kinetic reactivity of metals in metal complex formation reactions is governed by the rate of water-loss from the metal. In this respect Cu is one of the most reactive of the transition metals. For kinetically inert metals [Cr(III) and to a lesser extent Fe(III) and Ni(II)] much longer equilibration times would be predicted. Ligand exchange reactions of Ni-humate species have been observed to occur over 10 days (LAVIGNE et al., 1987). In the case of competition between transition metals, predicted double exchange reactions would also be slower than the competitive reactions of transition and alkaline earth metals described above, largely because the dissociation of transition metal complexes is many orders of magnitude slower than the dissociation of alkaline earth metal complexes. Although a detailed discussion of transition metal competition is beyond the scope of this paper, it is clear that transition metal-bound ligands in complex systems will respond to metal additions even more sluggishly than alkaline earth metal-bound ligands.

Effects of ligand speciation

The initial ligand speciation in a natural system subject to perturbation will determine, to a large extent, the pathway for and rate of equilibration. The decrease observed in the reactivity of EDTA is due to the predominance of the calcium complex in EDTA speciation and to the intrinsic rate constants for the reaction of the calcium complex. For humic acids, calcium and copper do not appear to compete for the

same binding sites (HERING and MOREL, submitted (b)) and thus the kinetic reactivity of humic acids toward copper is not influenced by the presence of calcium (HERING and MOREL, submitted (a)). Competitive effects on humate-binding have been observed for the transition metals Cd and Cu (FISH, 1984). Thus the kinetic reactivity of humic acids to added metals will be influenced by the initial ligand speciation and particularly by the presence of pre-existing transition metal-humate complexes.

Analytical considerations

Observations of slow coordination reactions in model systems and predictions of the rates of such reactions at Cu-to-humate loadings reasonable for natural waters suggest kinetic artifacts that might affect determinations of Cu complexation, particularly in seawater. The measurement of metal complexation through metal titrations (typical equilibration times of minutes to hours) demonstrates the rapid formation of metal complexes with at least some natural complexing agents. Kinetic experiments with humic acids and EDTA suggest that strong complexing agents in seawater may be underestimated by metal-into-ligand titrations. Certainly EDTA itself, which has extensive industrial applications (MEANS et al., 1980) and has been measured in rivers (GARDINER, 1976) and groundwater (MEANS et al., 1978), would not be detectable by metal-into-ligand titrations. The question remains whether some natural complexing agents may also be undetectable, because of the time scale and the sensitivity of metal-into-ligand titration techniques. Analytical methods involving

addition of ligands (e.g.- MOFFETT and ZIKA, 1987; SUNDA and HANSON, 1987) should also be carefully scrutinized for artifacts due to slow kinetics of coordination reactions.

CONCLUSIONS

Slow equilibration was observed on the addition of copper to a mixture of natural and synthetic ligands in the presence of calcium at seawater concentrations. These observations are consistent with predictions from theory and show that some strong ligands may be undetectable in metal-into-ligand titrations of seawater samples.

In natural systems undergoing perturbations of metal speciation, it is possible that different ligands dominate metal speciation, i.e.- buffer free metal ion concentration, immediately after such perturbation and on longer time scales. Such slow equilibration would result in short-term non-equilibrium effects, for example, increased metal toxicity or chemical reactivity.

Generally, these results demonstrate that the assumption of rapid equilibration of ligands and metals in natural or laboratory systems with low concentrations of metals and ligands and seawater calcium concentrations is not valid. In particular, the effects of ligand speciation, the presence of competing metals, and possible reaction pathways should be considered in estimating the time scale over which equilibrium speciation will be reached.

REFERENCES

ANDERSON, D.M. and F.M.M. MOREL (1978) Copper sensitivity of *Gonyaulax tamarensis Limnol. Oceanogr.* **23**: 283-95.

ANDERSON, M.A. and F.M.M. MOREL (1982) The influence of aqueous iron chemistry on the uptake of iron by the coastal diatom *Thalassiosira weissflogii Limnol. Oceanogr.* **27**: 789-813.

CABANISS, S.E. and M.S. SHUMAN (1986) Combined Ion Selective Electrode and Fluorescence Quenching Detection for Copper Dissolved Organic Matter Titrations *Anal. Chem.* **58**: 398-401.

CABANISS, S.E. and M.S. SHUMAN (1988) Copper binding by dissolved organic matter: I. Suwannee River fulvic acid equilibria *Geochim. Cosmochim. Acta* **52**: 185-93.

CARR, J.D. and D.G. SWARTZFAGER (1975) Kinetics of the Ligand Exchange and Dissociation Reactions of Calcium-Aminocarboxylates *J. Am. Chem. Soc.* **97**: 315-21.

COALE, K.H. and K.W. BRULAND, *Limnol. Oceanogr.*, in press.

DAVIS, J.A. (1984) Complexation of trace metals by adsorbed natural organic matter *Geochim. Cosmochim. Acta* **48**: 679-91.

DAVIS, J.A. and J.O. LECKIE (1978) Effects of Adsorbed Complexing Ligands on Trace Metal Uptake by Hydrous Oxides *Environ. Sci. Technol.* **12**: 1309-15.

DZOMBAK, D.A., W. FISH and F.M.M. MOREL (1986) Metal-humate interactions. I. Discrete ligand and continous distribution models *Environ. Sci. Technol.* **20**: 669-75.

EIGEN. M. and R.G. WILKINS (1965) The Kinetics and Mechanism of Formation of Metal Complexes in *Mechanisms of Inorganic Reactions*, ed. R. KENT MURMANN, R.T.M. FRASER and J. BAUMAN. ACS Adv in Chem. Ser. 49: 55-80.

FISH, W. (1984) Ph.D. Thesis, Massachusetts Institute of Technology, Cambridge, MA.

FISH, W., D.A. DZOMBAK and F.M.M. MOREL (1986) Metal-humate interactions. II. Application and comparison of models *Environ. Sci. Technol.* **20**: 676-83.

GARDINER, J. (1976) Complexation of Trace Metals by Ethylenediamine tetraacetic acid (EDTA) in Natural Waters *Wat. Res.* **10**: 507-14.

HERING, J.G, W.G. SUNDA, R.F. FERGUSON and F.M.M. MOREL (1987) A field comparison of two methods for the determination of copper complexation: bacterial bioassay and fixed-potential amperometry *Mar. Chem.* **20**: 299-312.

HERING J.G. and F.M.M. MOREL (a) submitted to Environ. Sci. Technol.

HERING J.G. and F.M.M. MOREL (b) submitted to Environ. Sci. Technol.

KUEMPEL, J.R. and W.B. SCHAAP (1968) Cyclic Voltammetric Study of the Rate of Ligand Exchange between Cadmium Ion and Calcium Ethylendiaminetetraacetate *Inorg. Chem.* **7**: 2435-42.

LAVIGNE, J.A., C.H. LANGFORD and M.K.S. MAK (1987) Kinetic Study of Speciation of Nickel(II) Bound to a Fulvic Acid *Anal. Chem.* **59**: 2616-20.

MARGERUM, D.W., G.R. CAYLEY, D.C. WEATHERBURN, and G.K. PAGENKOPF (1974) Kinetics and Mechanism of Complex Formation and Ligand Exchange in *Coordination Chemistry* vol 2, ed. A. MARTELL. ACS Monograph 174.

MATSON, W., E. ZINK, R. VITUKEVITCH (1977) Programmable electrochemistry *Am. Lab.* **9**: 59-73.

MEANS, J.L., D.A. CRERAR, J.O. DUGUID (1978) Migration of Radioactive Wastes: Radionuclide Mobilization by Complexing Agents *Science* **200**: 1477-81.

MEANS, J.L., T. KUCAK, and D.A. CRERAR (1980) Relative degradation rates of NTA, EDTA, and DTPA and environmental implications *Environ. Poll. (Ser. B)* **1**: 45-60.

MOFFETT, J.W. and R.G. ZIKA (1987) Solvent extraction of copper acetylacetonate in studies of copper(II) speciation in seawater *Mar.Chem.* **21**: 303-13.

OLSON, D.L. and M.S. SHUMAN (1983) Kinetic Spectrum Method for Analysis of Simultaneous, First-Order Reactions and Application to Copper(II) Dissociation from Aquatic Macromolecules *Anal. Chem.* **55**: 1103-7.

PRIBIL, R. (1982) *Applied Complexometry*, Oxford: Pergammon Press.

RYAN, D.K. and J.H. WEBER (1982) Fluorescence Quenching Titration for Determination of Complexing Capacities and Stability Constants of Fulvic Acid *Anal. Chem.* **54**: 986-990.

SAAR, R.A and J.H. WEBER (1980) Comparison of Spectrofluorometry and Ion-Selective Electrode Potentiometry for Determination of Complexes between Fulvic Acid and Heavy-Metal Ions *Anal. Chem.* **52**: 2095-2100.

SAARI, L.A. and W.R. SEITZ (1984) Immobilized Calcein for Metal Ion Preconcentration *Anal. Chem.* **56**: 810-3.

SHUMAN, M.S. and L.C. MICHAEL (1978) Application of the Rotated Disk Electrode to Measurement of Copper Complex Dissociaiton Rate Constants in Marine Coastal Samples *Environ. Sci. Technol.* **12**: 1069-72.

SHUMAN, M.S., B.J. COLLINS, P. J. FITZGERALD, D.L. OLSON (1983) Distribution of Stability Constants and Dissociation Rate Constants Among Binding Sites on Estuarine Copper-Organic Complexes: Rotated Disk Electrode Studies and and Affinity Spectrum Analysis of Ion-Selective Electrode and Spectrophotometric Data in *Aquatic and Terrestrial Humic Materials* ed. R.F. CHRISTMANN and E.T. GJESSING. Ann Arbor, MI: Ann Arbor Science.

STONE, A.T. (1986) Adsorption of Organic Reductants and Subsequent Electron Transfer on Metal Oxide Surfaces in *Geochemical Processes at Mineral Surfaces* ed. J.A. DAVIES and K.F. HAYES, ACS Symp. Ser. 323.

SUNDA, W.G. and R.F. FERGUSON (1983) Sensitivity of natural bacterial communities to additions of copper and to cupric ion activity: a bioassay of copper complexation in seawater in *Trace Metals in Seawater*, ed. C.S. WONG, E. BOYLE, K.W. BRULAND, J.D. BURTON, and E.D. GOLDBERG. New York: Plenum Press, pp. 871-891.

SUNDA, W.G. and R.R. GUILLARD (1976) Relationship between cupric ion activity and the toxicity of copper to phytoplankton *J. Mar. Res.* **34**: 511-29.

SUNDA, W.G. and A.K. HANSON (1987) Measurement of free cupric ion concentration in seawater by a ligand competition technique involving copper sorption onto C_{18} SEP-PAK cartridges *Limnol. Oceanogr.* **32**: 537-51.

TURNER, D.R., M.S. VARNEY, M.WHITFIELD, R.F.C. MANTOURA, and J.P. RILEY (1985) Electrochemical studies of copper and lead complexation by fulvic acid. I. Potentiometric measurements and a critical comparison of metal binding models *Geochim. Cosmochim. Acta* **50**: 289-97.

WAITE, T.D. and F.M.M. MOREL (1983) Characterization of complexing agents in natural waters by copper(II)/ copper(I) amperometry *Anal. Chem.* **55**: 1268-74.

WAITE, T.D. and F.M.M. MOREL (1984) Photoreductive dissolution of colloidal iron oxides in natural waters *Environ. Sci. Technol.* **18**: 860-8.

WALLACH, D.F.H. and T.L. STECK (1963) Fluorescent Techniques in the Microdetermination of Metals in Biological Materials *Anal. Chem.* **35**: 1035-44.

WALLACH, D.F.H., D.M. SURGENOR, J. SODERBERG, E. DELANO (1959) Preparation and Properties of 3,6-Dihydroxy-2,4-bis-[N,N'-di-(carboxymethyl)-aminomethyl] fluoran *Anal. Chem.* **31**: 456-60.

APPENDIX- Kinetic models

Terms and Definitions

Cu_T	total copper concentration
$HumX_T$	total concentration of humate binding site X (X=1-3 for 3 ligand site types)
$(HumX)_t$	concentration of free humate binding site X at time = t
$(CuHumX)_t$	concentration of Cu-bound humate site X at time = t
K_x	conditional stability constant for binding of inorganic Cu at humate binding site X (X= 1-3)
K_{CuEDTA}	stability constant for CuEDTA complex
K_{CaEDTA}	stability constant for CaEDTA complex
k_{Cu}^{CaEDTA}	overall rate constant for metal exchange reaction of inorganic Cu with CaEDTA (at given pH and total Ca)
k_{Ca}^{CuEDTA}	overall rate constant for metal exchange reaction of Ca with CuEDTA (at given pH and total Ca)
k_{fx}	rate constant for formation of Cu complex with humate binding site X (X= 1-3)
k_{bx}	rate constant for dissociation of Cu complex with humate binding site X (X= 1-3)

Pseudo-equilibrium model

In this model, free Cu^{2+} concentration is taken to be controlled by pseudo-equilibrium with the humic acid (described as 3 discrete ligands). Initially,

for $Cu^* = Cu^{2+}$ + inorganic Cu complexes

$$Cu_T = (Cu^*) + (CuHum1) + (CuHum2) + (CuHum3)$$

$$(Cu^*) = \frac{Cu_T}{1 + \frac{K_1\ Hum1_T}{1+ K_1\ (Cu^*)} + \frac{K_2\ Hum2_T}{1+ K_2\ (Cu^*)} + \frac{K_3\ Hum3_T}{1 + K_3\ (Cu^*)}}$$

and $(CuEDTA)_o = 0.$

The concentration of EDTA species over time is described by

$$(CuEDTA)_{t+\Delta t} = (CuEDTA)_t + [\ k_{Cu}^{CaEDTA}\ (CaEDTA)_t\ (Cu^*)_t]\ \Delta t$$

$$(CaEDTA)_{t+\Delta t} = (CaEDTA)_t + [-k_{Cu}^{CaEDTA}\ (CaEDTA)_t\ (Cu^*)_t]\ \Delta t.$$

For the reaction proceeding to equilibrium a term for the back-reaction of CuEDTA is included. The rate constant for the back-reaction, k_{Ca}^{CuEDTA} is calculated from the forward rate constant and the Cu and Ca-EDTA stability constants. Thus

$$k_{Ca}^{CuEDTA} = k_{Cu}^{CaEDTA}\ K_{CaEDTA} / K_{CuEDTA}$$

and

$$(CuEDTA)_{t+\Delta t} = (CuEDTA)_t + [k_{Cu}^{CaEDTA}(CaEDTA)_t(Cu^*)_t - k_{Ca}^{CuEDTA}(CuEDTA)_t]\Delta t$$

The back-reaction term is also included in the expression for CaEDTA.

The Cu^* concentration over time is

$$(Cu^*)_{t+\Delta t} = \frac{Cu_T - (CuEDTA)_{t+\Delta t}}{1+ \frac{K_1Hum1_T}{1+K_1(Cu^*)_t} + \frac{K_2Hum2_T}{1+K_2(Cu^*)_t} + \frac{K_3Hum3_T}{1+K_3(Cu^*)_t}}$$

The concentrations of humic acid species over time are:

$$(HumX)_{t+\Delta t} = \frac{HumX_T}{1 + K_x\ (Cu^*)_{t+\Delta t}}$$

$$(CuHumX)_{t+\Delta t} = K_x\ (Cu^*)_{t+\Delta t}\ (HumX)_{t+\Delta t}$$

for the 3 ligand site types (X = 1-3) with total concentrations and conditional stability constants given in Tables I and II.

Initial reaction model

In the description of the initial reaction on addition of Cu to the humic acid/EDTA/Ca mixture, the reaction of inorganic Cu with each humate ligand is described expicitly. Then

$$(Cu^*)_{t+\Delta t} = (Cu^*)_t + \Big(-[k_{f1}(Hum1)_t + k_{f2}(Hum2)_t + k_{f3}(Hum3)_t](Cu^*)_t + k_{b1}(CuHum1)_t + k_{b2}(CuHum2)_t + k_{b3}(CuHum3)_t\Big)\Delta t$$

and

$$(HumX)_{t+\Delta t} = (HumX)_t + [-k_{fx}(HumX)_t(Cu^*)_t + k_{bx}(CuHumX)_t]\Delta t$$

$$(CuHumX)_{t+\Delta t} = (CuHumX)_t + [k_{fx}(HumX)_t(Cu^*)_t + k_{bx}(CuHumX)_t]\Delta t$$

where all formation rate constants for the reaction of inorganic Cu with humate species are taken to be the same ($k_{fx} = 6 \times 10^8$ $M^{-1}min^{-1}$). The dissociation rate constants are calcuated such that

$$k_{bx} = k_{fx} / K_{CuHumX}$$

for the Cu-humate stability constants given in Table II. For ease of calculation, pseudo-equilibrium conditions for the concentration of CuHum3 are imposed after 0.02 min as described in (i) above and the terms involving reaction of Hum3 and CuHum3 are eliminated from the equation describing the concentration of inorganic Cu over time.

CHAPTER SEVEN

SUMMARY

This thesis addresses several questions concerning metal complexation in natural waters, questions on the source and regulation of natural complexing agents and on the nature of their interactions with metals. Both the thermodynamics and kinetics of metal-humate interactions are examined.

CHAPTER 2: Some Effects of Biological Actvity on Complexation of Copper

Copper complexing agents are produced in phytoplankton cultures. In incubation studies of natural water samples, the extent of copper complexation is affected by biological cycling. The observed changes in copper complexation are consistent with ligand production associated with phytoplankton photosynthetic activity and loss of ligands by microbial degradation. In the field, strong correlations between phytoplankton abundance or photosynthetic activity and copper complexation was not observed. However, in the coastal ponds studied, biological cycling of natural complexing agents may be obscured by the contribution of refractory ligands, such as humic acids, to the observed copper complexation, by mixing of pond waters with coastal seawater, or by the natural balance between biological production and degradation (resulting in overall steady-state level of copper complexation).

CHAPTER 3: Humic Acid Complexation of Calcium and Copper

Information on the structure of natural ligands and on the physical-chemical nature of metal-ligand interactions cannot be deduced from models of metal-ligand binding because none of the models provide a unique representation of the observed interactions. The combined information from individual metal titrations for Ca and Cu and from Cu titrations in the presence of Ca (as a competing metal) provide additional constraints to modeling metal-ligand binding. Although, the individual metal titrations can be modeled by metal binding at discrete sites (with a consistent concentration of metal-binding sites per weight humic acid), the lack of competition between Ca and Cu demonstrates that both metals cannot be bound at the same sites. Thus metal binding at discrete sites must involve different sites for alkaline earth and transition metals or the nature of binding for these different metals must also be different.

CHAPTER 4: Kinetics of Trace Metal Complexation: The Role of Alkaline Earth Metals

In seawater, trace metal complexation reactions with natural ligands occur perforce in the presence of an overwhelming concentration of competing alkaline earth metals. Experiments with the model ligands EDTA and NTA show that the rate of reaction of calcium-bound ligands with copper is governed by the affinity of the ligand for the alkaline earth metal. The dominant pathway for the metal-exchange reaction is affected by the calcium concentration since metal exchange through a

dissociative pathway is inhibited at high calcium concentrations while the interchange pathway is unaffected by the presence of calcium. These considerations apply if Ca and Cu are bound at the same sites. For humic acid, no effect of Ca on the kinetics of Cu complexation was observed consistent with the lack of competition in metal binding documented in Chapter 3.

CHAPTER 5: Kinetics of Trace Metal Complexation: Ligand Exchange Reactions

For metals, such as copper, that occur in natural waters as organic complexes, the rate of biogeochemical processes will be influenced by the kinetics of complex dissociation and ligand exchange reactions. This chapter investigates the rates of those coordination reactions (which may be thought of as precursor reactions). Experiments with the model ligands NTA and EDTA demonstrate that both dissociative and interchange pathways are involved in ligand exchange reactions at environmental ligand and metal concentrations. Both of these mechanisms are likely to be important in the reaction of Cu-humate species at the Cu-to-humate loadings typical of estuarine and coastal waters. The rate constants for the dissociative reaction of Cu-humate species provide information on the concentration of Cu binding sites and on the affinity of the sites for Cu.

CHAPTER 6: Slow Coordination Reactions in Aquatic Systems

In complicated systems (i.e.- mixtures of competing metals and ligands), the overall rates of the "simple" complexation reactions

studied in chapters 4 and 5 are dramatically retarded. In the presence of a mixture of ligands and metals, the apparent complexation reaction of an added metal occurs through a series of double- (i.e.- metal- and ligand-) exchange reactions. Thus strong ligands are slow to react due to the effect of competing metals and the initial speciation of the metal is governed by the weaker ligands in the system. The rate of re-equilibration of metal and ligand speciation can be extremely slow depending on the concentrations and relative proportions of the reacting species.

APPENDIX A

A FIELD COMPARISON OF TWO METHODS FOR THE DETERMINATION OF COPPER COMPLEXATION: BACTERIAL BIOASSAY AND FIXED-POTENTIAL AMPEROMETRY

(co-authors: W.G. Sunda, R.L. Ferguson, F.M.M. Morel)

ABSTRACT

Complexation of copper added to seawater was determined by bacterial bioassay and fixed-potential amperometry. Consistent results were obtained by these two fundamentally different methods. The results of this study support the validity of both techniques and the field applicability of fixed-potential amperometry.

The intercomparison studies were performed on samples collected at the N.Y.C. sewage sludge dumpsite and in relatively unpolluted coastal waters. In this limited study. the calculated free cupric ion concentrations at ambient total copper concentrations were similar at both sites.

INTRODUCTION

Complexing characteristics* of natural waters have been determined for several transition metals (e.g., Cu, Zn, Fe, Cd) with a variety of electrochemical, chromatographic and bioassay techniques for measuring "reactive" and "unreactive" metal fractions (see Table II for references). [*We avoid here the expression "complexing capacity" which has evolved to designate some elusive total ligand concentration.]

Copper has been the most extensively studied metal since it forms stronger complexes than most other divalent transition metals and can be analyzed by a number of different techniques.

Measurements of copper complexation in natural waters are highly controversial. All available techniques are subject to theoretical or practical limitations and most researchers view existing measurements in seawater as qualitative rather than quantitative indications of copper speciation. This lack of confidence is exacerbated by the inadequate validation of practically all techniques. The ability to measure copper complexation accurately in model laboratory systems containing well defined complexing agents is a necessary (though not a sufficient) attribute of any acceptable technique. Yet, the most often used technique, anodic stripping voltammetry (ASV), fails to measure properly the complexation of copper and other metals in simple NTA solutions (Tuschall and Brezonik, 1981; Shuman et al.,1982; Goncalves et al., 1987). Even for those techniques that seem to work well in model systems, the jump from Cu-NTA buffered systems to natural samples is a large one. The acceptability of the quantitative results cannot be sustained by oceanographic consistency arguments alone: artifacts are just as likely as actual copper speciation to be correlated with broad physical, chemical or biological trends.

Here we report on the comparison of two totally different techniques, utilized side by side to measure copper complexation during a short cruise in the New York Bight. Fixed potential amperometry and bacterial bioassay have each been shown previously to provide accurate measurement of copper speciation in well defined laboratory systems

(Waite and Morel. 1983; Sunda and Ferguson, 1983). In addition, each of these methods has been successfully compared with potentiometric measurements in freshwater samples containing natural chelating agents and relatively high copper concentrations (Fish and Morel, 1985; Sunda et al., 1984). Although potentiometric measurements undoubtedly provide the most reliable measurement of copper speciation, the use of Cu^{2+}-sensitive electrodes is limited to total Cu concentrations in excess of 0.1 μM and to low salinity samples - see Westall et al., 1979.

The remarkable agreement we report here between amperometry and bioassay measurements at low copper concentrations and with fresh natural seawater samples does much to enhance our confidence in the validity of the measurements and to justify the distinct assumptions on which each technique is based. At the same time, we point out that, in their present state of development, neither of these methods is sensitive enough to measure directly the actual free cupric ion concentration or activity in seawater. The necessary extrapolation provides only an upper limit for that much sought after parameter.

MATERIALS AND METHODS

Samples were collected at the N.Y.C. sewage sludge disposal site in the N.Y. Bight at Christiansen Basin ($40^{o}25'$ N, $73^{o}44'$ W) and off Montauk Point ($40^{o}50'$ N, $71^{o}50'$ W). Both stations were sampled on two days: Montauk Point on Feb. 7, 1984 and Feb. 8, 1984 and Christiansen Basin on Feb. 9, 1984 and Feb. 11, 1984. Sampling occurred between 0800-1400 h. Samples were taken at 15-20 m at approximately the 1% light level. The Christiansen Basin site was not sampled during sludge

dumping. Samples were filtered for total copper analysis and fixed-potential amperometry through 0.4 μm Nuclepore filters under positive pressure. Precautions were taken during sampling and sample handling to avoid trace metal contamination as described by Sunda and Ferguson (1983). Total copper concentrations were determined by the Co-APDC coprecipitation method described by Boyle et al. (1981). Total copper measurements were made on filtered samples from Montauk Point and Christiansen Basin and on one unfiltered sample from Christiansen Basin (collected Feb. 11). Unfiltered Montauk Point samples were not available for total metal analysis. For these samples total copper was assumed to equal the dissolved concentration. Based on previous measurements of dissolved and particulate copper in coastal waters, total copper should be only slightly underestimated by this approximation (Huizenga and Kester, 1983). Total copper concentration for the unfiltered Feb. 9 Christiansen Basin sample was estimated from the measured filterable concentration and the ratio of filterable/total copper determined for the Feb. 11 sample.

Microbiological parameters determined at both sites included the number of bacterial cells (assayed by acridine orange direct counts (AODC)) and the abundance of colony forming units (CFU). CFU has been used as an index of the abundance of bacteria with the ability to grow rapidly after nutrient enrichmemt (Ferguson et al., 1984, Torrella and Morita, 1981).

Fixed-potential Amperometery

Theory and application of measurement of inorganic Cu(II)

concentration by fixed-potential amperometry in high chloride medium have been described by Waite and Morel (1983). The current produced by the reduction of Cu(II) inorganic species to Cu(I) chloride complexes in the vicinity of a graphite electrode is measured at 90mV (relative to Ag/AgCl). (NB - the concentration of Cu(I) produced in the bulk solution is negligible.) The current is integrated (over 35 sec) and corrected by subtracting the current generated (over 35 sec) without stirring. The "unstirred current" is due to non-mass transport-limited phenomena (Matson et al., 1977). Measurements were repeated until electrode response stabilized (~5-15 min).

The amperometric measurements were made with an Environmental Science Associates Model 3040 Charge Transfer Analyzer equipped with a pyrolytic graphite working electrode, Pt counterelectrode, and Ag/AgCl, saturated NaCl reference electrode. The Charge Transfer Analyzer and electrode systems have been described in detail by Matson et al. (1977). Electrode response was calibrated using an organic-free electrolyte solution (0.5 M NaCl, 0,01 M $CaCl_2$, 2mM $NaHCO_3$). Natural water smnples were equilibrated with added Cu for 10 min before amperometric measurements. Both filtered and unfiltered samples were titrated. Typical titrations are shown in Figure 1.

Bacterial Bioassay

Ihe theory and application of free cupric ion concentration measurements by bacterial bioassays have been described by Gillespie and Vaccaro (1978), Sunda and Gillespie (1979) and Sunda and Ferguson (1983). The technique is based on the modulation of copper toxicity to

Figure 1. (a) Reproducibilty of amperometric measurements illustrated by duplicate titrations of an aged sample: samples collected at Christiansen Basin (Feb. 9), analyzed (○) Feb. 25, (□) Feb. 28, and effects of filtration: samples collected at Christiansen Basin (Feb. 11), (▲) filtered, (●) unfiltered. (b) Variations in copper complexation at Montauk Point: results from amperometric titration, (○) Feb. 7, (△) Feb. 8, (□) Feb. 7, analyzed Feb. 21.

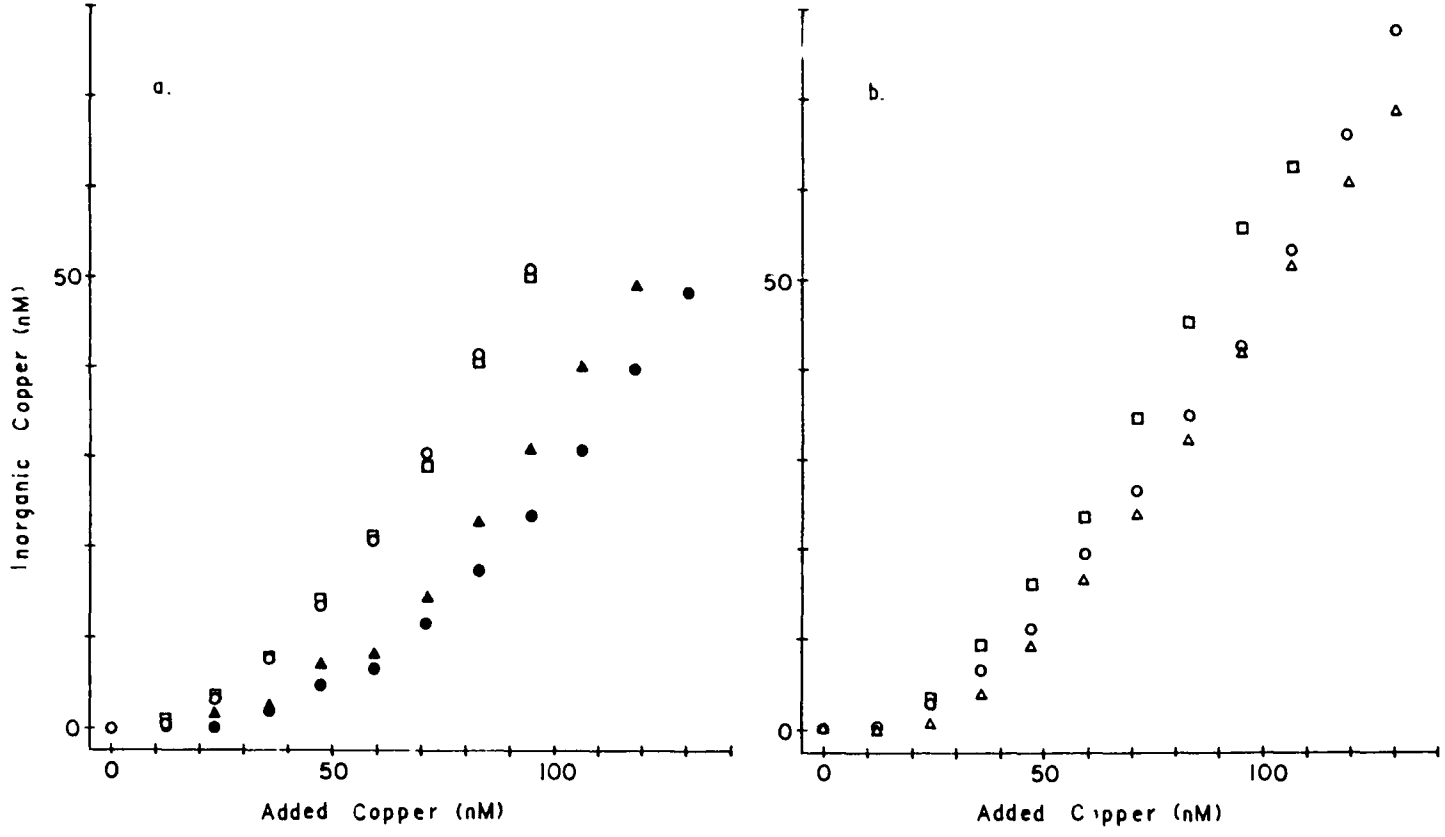
a.
b.
Inorganic Copper (nM)
Added Copper (nM)
Added Copper (nM)
0
50
100
0
50
0
50
100

aquatic microorganisms by the free cupric ion concentration (or activity). In this study, the natural bacterial population was used (Sunda and Ferguson, 1983) and its response calibrated with Cu-NTA cupric ion buffers (i.e., pre-equilibrated solutions of $CuSO_4$ and NTA).

Subsamples of unfiltered seawater were spiked with concentrated solutions of $CuSO_4$ ± NTA (final NTA concentration 0, 1 or 4 μM). After 4 h (4.5 h for Christiansen Basin samples), 1-2 nM of a mixture of ^3H-labelled amino acids or 10 nM of ^{14}C-labelled glucose was added. After an additional hour (0.5 h at Christiansen Basin due to the higher in situ concentration of bacteria), the suspended bacteria were killed with formalin and collected on 0.2 μM Nuclepore filters. Uptake of labelled substrate was determined by liquid scintillation counting of the filters. The data were corrected for blanks obtained by adding formaldehyde at the beginning of the radiolabel incubation period.

Data Treatment

Free cupric ion concentrations, (Cu^{2+}), were calculated from amperometric titration and bacterial bioassay data. For the amperometric data, measured integrated current (stirred - unstirred response) was converted to reducible copper based on calibration of electrode response in an organic free electrolyte solution. The free cupric ion concentration was then calculated assuming all reducible copper to be free or inorganically complexed. The ratio α = (Cu^{2+})/(inorganic Cu(II)) is pH-dependent and equals $10^{-1.4}$ at pH=8.2 and $10^{-1.2}$ at pH = 8.0. These values for α were determined by biosssay and from inorganic speciation models (Sunda et al., 1984). A pH of 8.2

was assumed for the Montauk Point station in the absence of appropriately calibrated absolute pH measurements at the Montauk Point and Christiansen Basin stations. The relative difference of 0.2 pH units between the two stations was measured on freshly collected samples.

The calculation of (Cu^{2+}) from bacterial bioassay data is somewhat intricate and has been described in detail previously (Sunda and Ferguson, 1983).

(1) Data for uptake of radiolabeled glucose were normalized to the maximum value at the same NTA concentration (0, 1 μM, and 4 μM) to account for the effect of the chelator by itself. (This was not necessary for uptake of amino acids.)

(2) The concentration of CuNTA in buffered media was taken to equal the total copper concentration (at given total NTA) minus the total copper concentration at which equal substrate incorporation occurred in seawater without added NTA [as shown in Fig. 2a, ($CuNTA^-$) equals total copper at point B minus total copper at Point A]. Thus, ($CuNTA^-$) equals the copper concentration added to the buffered system corrected for copper complexation by natural ligands.

(3) The response of the natural bacterial populations was calibrated by calculating (Cu^{2+}) in the NTA buffers using experimentally derived values for ($CuNTA^-$).

$$(Cu^{2+} = \frac{(CuNTA^-)}{K_{eff}(\text{free NTA})}$$

$$(\text{free NTA}) = (\text{Total NTA}) - (CuNTA^-)$$

$$K_{eff} = 10^{8.45}$$

Figure 2. (a) Effect of additions of copper and cupric ion buffers (copper and NTA) on the rate of incorporation of tritium-labled amino acids by natural bacterial populations. Data are shown for seawater collected from Christiansen Basin (○) no NTA added; (△) 1 μM NTA added; (□) 4 μM NTA added. (b) Rate of amino acid incorporation as a function of pCu as determined from the addition of (△) 1 μM NTA and (□) 4 μM NTA for Christiansen Basin; (— - —) corresponding curve for Montauk Point (data not shown).

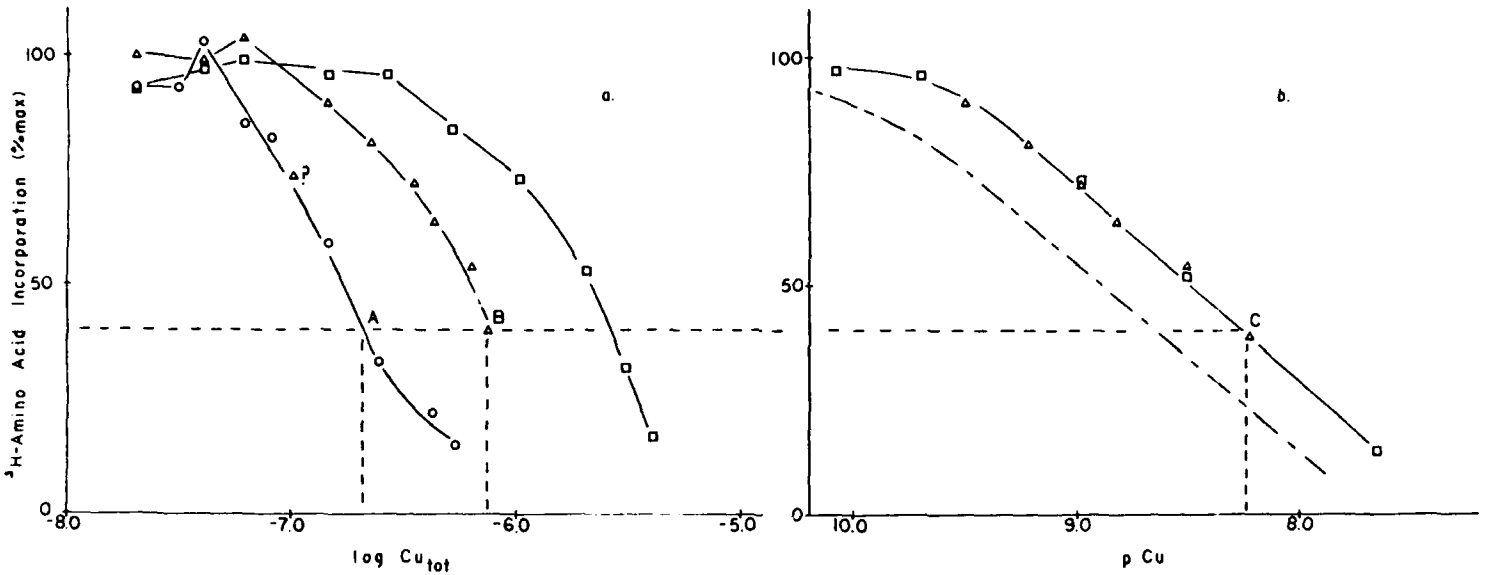
100
50
0
^{3}H-Amino Acid Incorporation (%max)
a.
A
B
A?
-8.0
-7.0
-6.0
-5.0
log Cu_{tot}
b.
C
10.0
9.0
8.0
p Cu

(4) Finally, (Cu^{2+}) was obtained for each addition of copper (without NTA) as that yielding the same (relative) uptake of label as in the NTA buffers (i.e., in Figure 2a and b, the pCu at point A is the same as the pCu calculated for point C).

Modeling

For purposes of comparison, the copper titration curves were modeled assuming complexation by discrete ligands. Although the corresponding stability constants (K_i) and ligand concentrations (L_{iT}) are only fitting parameters (Dzombak et al., 1986; Fish et al., 1986), they are useful for extrapolating the data to ambient copper concentrations and for comparing with previous studies.

The data fitting procedure was constrained by choosing the minimum number of (and weakest) ligands required to fit the data. Two ligands were necessary such that:

$$Cu_T = \frac{(Cu^{2+})}{\alpha} + \frac{K_1 L_{1T} (Cu^{2+})}{1 + K_1 (Cu^{2+})} + \frac{K_2 L_{2T} (Cu^{2+})}{1 + K_2 (Cu^{2+})}$$

The stability constants are conditional constants for a given pH in seawater. The fitting routine FITEQL (Westall, 1982) was used to obtain constants and ligand concentrations.

Interpretation of the results of the copper titrations are subject to two principal limitations. Because of analytical detection limits, stability constants for the strong ligands cannot be unambiguously defined, but can only be constrained by minimum values. Also, as is typical of such titrations, the natural ligands were never completely titrated (some of the added copper was always measured as bound) and the

total ligand concentration may consequently be underestimated. Free cupric ion concentrations were calculated by extrapolation of the data to ambient total copper concentrations with the derived constants and ligand concentrations. These values should be considered upper estimates of the actual free cupric ion concentration in the samples.

RESULTS

Comparison of Methods

The central result of this study is the remarkable agreement between the two sets of measurements. As seen in Figure 3, the free cupric ion concentrations calculated from amperometric titration and bacterial bioassay data at known total copper concentrations are the same within the precision of the data. All the data for each site were combined since only small variations were observed among the amperometric titrations of the various samples (vide infra).

In samples from both the polluted and the unpolluted sites, the ambient free cupric ion concentration was always below the detection limit of either technique. Measurable responses, either copper reduction or inhibition of substrate uptake by bacteria, were only observed on addition of copper (~10-20 nM) to samples.

Variations among samples

The amperometric data shown in Fig. 3 were obtained with samples collected over several days and subject to some differences in sample pretreatment (i.e., filtration and length of storage before analysis).

Figure 3. Cupric ion concentrations derived from copper titrations as a function of total copper at (a) Montauk Point ($\alpha = 10^{-1.4}$, salinity 32) and (b) Christiansen Basin ($\alpha = 10^{-1.2}$, salinity 31.8). Solid symbols, bioassay data: (■) 1 μM and (◆) 4 μM NTA (glucose used in bioassay, Feb. 9 sample); (▲) 1 μM and (■) 4 μM NTA (amino acids used in bioassay (a) Feb. 7 sample and (b) Feb. 11 sample). Open symbols, amperometry data: (a) (○), (◇) filtered Feb. 7 sample, (□) filtered Feb. 8 sample, (▽) unfiltered Feb. 8 sample analyzed Feb. 10; (b) (△) filtered Feb. 9 sample, (◇) filtered Feb. 11 sample, (○) unfiltered Feb. 11 sample. (Solid lines give the relationship between free cupric ion concentration and total copper based on inorganic complexation only.)

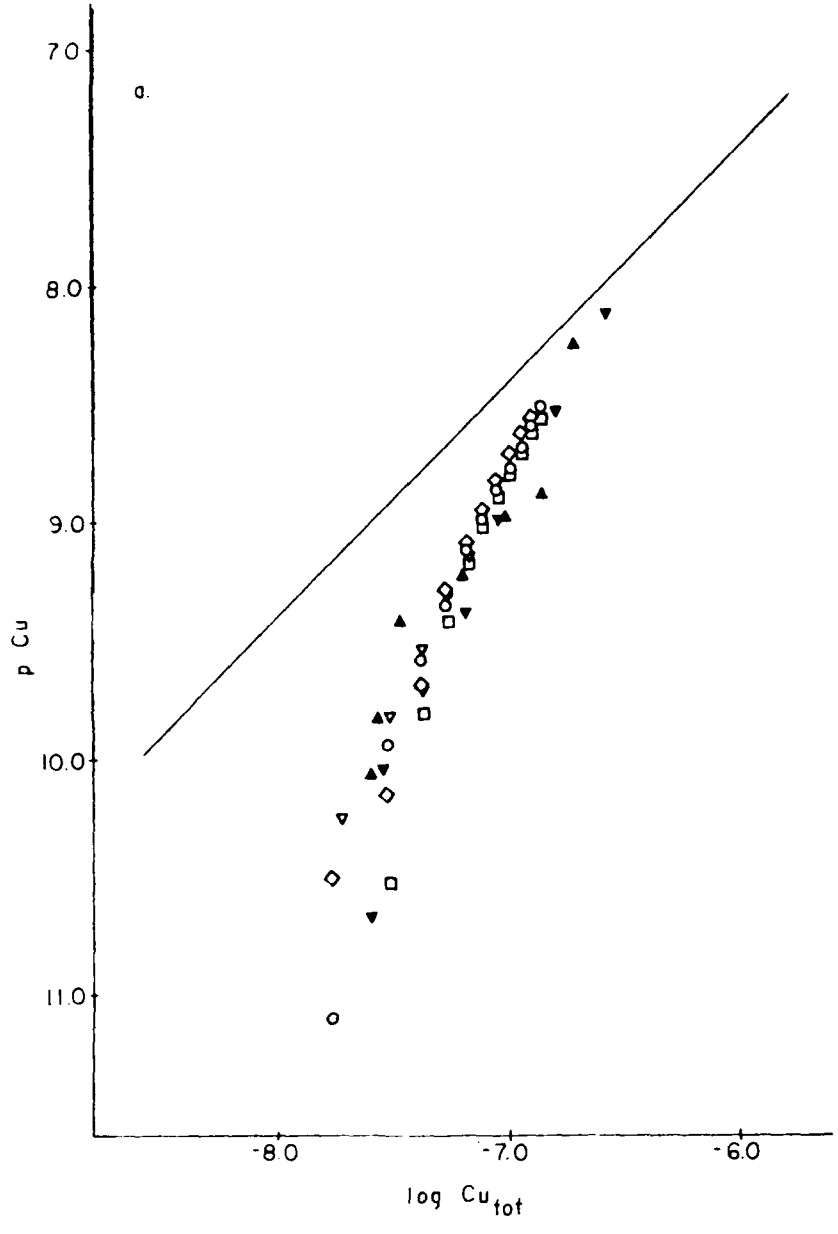
a.
7.0
8.0
9.0
10.0
11.0
p Cu
-8.0
-7.0
-6.0
log Cu tot

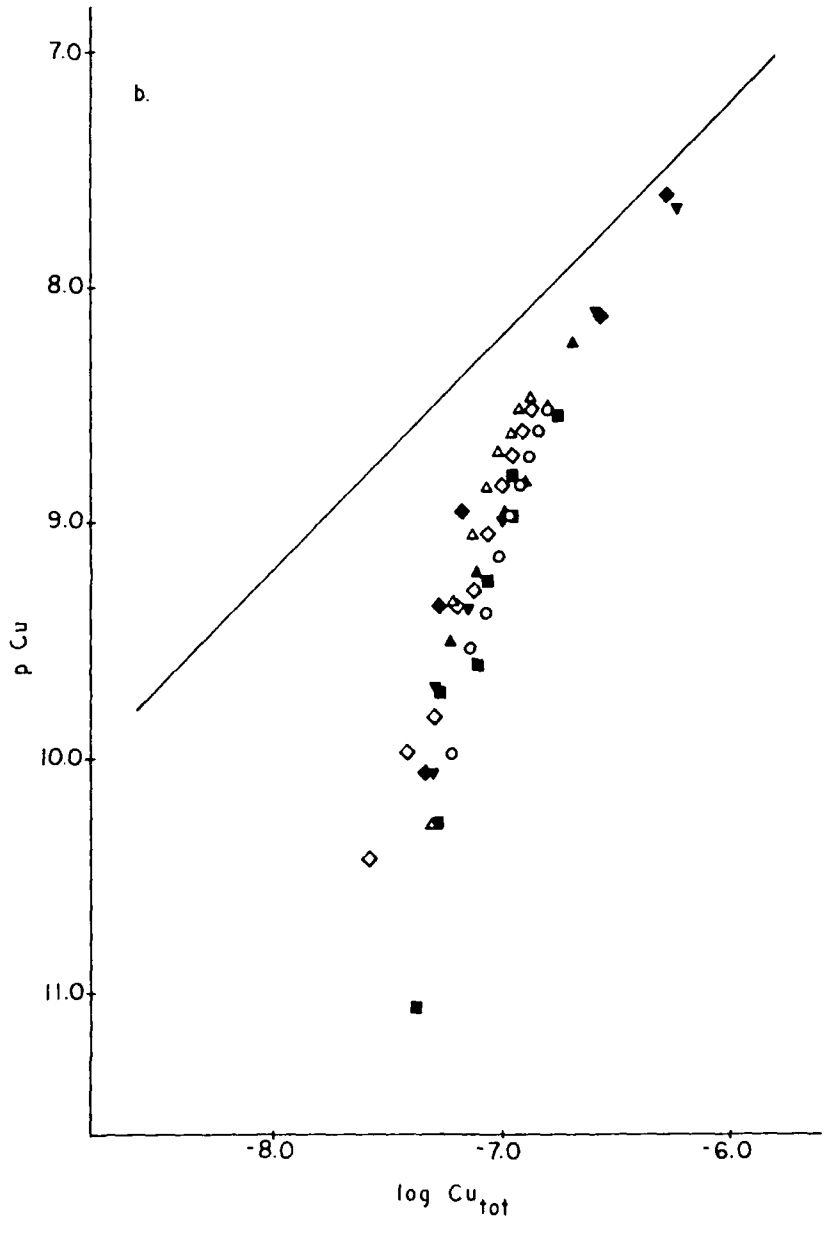
b.
7.0
8.0
9.0
10.0
11.0
p Cu
-8.0
-7.0
-6.0
log Cu tot

The excellent reproducibility of amperometric titrations of an aged sample (Fig. 1a) suggests that the variations in freshly collected samples are real. Despite the number of variables (collection time, sample pretreatment, etc.) and the limited number of samples, the data do indicate that the effects of sampling over intervals of 1-2 days (particularly at Montauk Point- Figure 1b) and removal of suspended particles and particulate copper by filtration (Figure 1a) are small. Storage of samples (unfiltered for 2 d shown in Fig. 3a or filtered for 2 weeks shown in Fig. 1b) resulted in a slight decrease in complexation of added copper.

A direct comparison of the pooled titration data for the two sites show slightly more complexation of copper at Christiansen Basin than at Montauk Point. If the data are plotted as pCu vs. added copper, the data from Montauk Point and Christiansen Basin are virtually superimposable. Additional organic complexation in the Christiansen Basin roughly compensates for the larger ambient total copper and the lower inorganic complexation (due to lower pH) in these samples as compared to the Montauk Point samples. Bioassay data suggest that natural bacterial population at Montauk Point was more sensitive to free cupric ion concentration than at Christiansen Basin as indicated by the 0.4 difference in pCu at 50% inhibition (Figure 2b).

Total copper

Total copper concentrations in filtered Montauk Point samples were 5.1 nM (Feb. 7) and 6.7 nM (Feb. 8) consistent with literature values for coastal waters off Massachusetts, not far from Montauk Point (Boyle

et al., 1984). Concentrations of 13.3 and 14.5 nM were measured in filtered Christiansen Basin samples (Feb. 9 and Feb. 11). The Feb. 11 unfiltered smnple contained 23.5 nM total copper. Total copper concentration of 21 nM was estimated for the Feb. 9 unfiltered sample.

Bacterial counts

Similar numbers of bacterial cells ($x \pm S.D.$) were determined by AODC at both sites: $8.4 \pm 1.3 \times 10^5$ cells/ml at Christisnsen Basin and $6.6 \pm 1.3 \times 10^5$, cells/ml at Montauk Point. However the ratio of CFU/AODC was elevated at Christiansen Basin (1.5% vs. 0.3%). CFU/AODC ratios exceeding 1% have been found under enriched conditions such as oil-polluted seawater as compared with 0.01% in oceanic water (Pfaender et al., 1980).

Model ligands

For both Montauk Point and Christiansen Basin, the data could be modeled using the same stability constants ($10^{9.1}$ and $10^{11.7}$) and similar concentrations of the weak ligand (50 nM at Montauk Point and 70 nM at Christiansen Basin). As seen in Table I, an approximately two-fold higher concentration of strong ligand was required to model the Christiansen Basin data (50 nM) than for the Montauk Point data (20nM).

Ambient (Cu^{2+})

As a result of the detection limits of the analytical techniques, it is not possible to extrapolate unambiguously from the available data to (Cu^{2+}) at ambient total copper concentrations; only higher limits can

Table I. Discrete ligands fit to amperometric data (a) weakest ligands (b) stronger ligands chosen so that calculated ambient pCu is the same for both sites.

	$\log K_1$	$\log K_2$	L_{1T}(nM)	L_{2T}(nM)
(a)				
Montauk Point	11.7	9.1	20	50
Christiansen Basin	11.7	9.1	50	68
(b)				
Montauk Point	12.1	9.3	18	49
Christiansen Basin	12.5	9.1	49	69

be calculated. With our estimates of stability constants and ligand concentrations, the calculated pCu for Christiansen Basin is lower [(Cu^{2+}) higher] than at Montauk Point: 11.8 vs. 12.2 (Figure 4). However, this difference is small (comparable to the difference in pCu of +0.2 due to the higher pH at Montauk Point) and both sites may well have the same ambient pCu. Stronger ligands (see Table I and Figure 4), which also provide a good fit of the data yield an extrapolated ambient pCu of 12.5 for both Christiansen Basin and Montauk Point.

DISCUSSION

The two techniques compared in this study are fundamentally different. They differ in the parameter measured, conditions for calibration, time of equilibration of samples to added copper, and underlying premises. Fixed-potential amperometry measures the total inorganic concentration of Cu(II) and the measured response (i.e., integrated current) is calibrated in the absence of organic ligands. The ambient bacterial community bioassay measures the reactivity of copper as quantified by the free cupric ion concentration and is internally calibrated with NTA. Thus, the results of the two methods are entirely independent.

The close agreement between techniques supports the validity of each individual method and indicates both that the basic premises on which they rely are correct and that they are minimally affected by potential interferences. The amperometric method assumes that no significant labile copper-organic complexes are reduced. This assumption is important only for strong organic ligands since at low

Figure 4. Cupric ion concentrations derived from amperometric titration data (a) for Montauk Point Feb. 7 and (b) Christiansen Basin Feb. 11 (unfiltered) as a function of total copper (●). Also shown are modeled curves computed from ligand concentrations and stability constants in Table I: (——) using weakest ligands adequate to fit data; (---) using stronger ligands. Note that available data can only define a minimum pCu at ambient total Cu concentration.

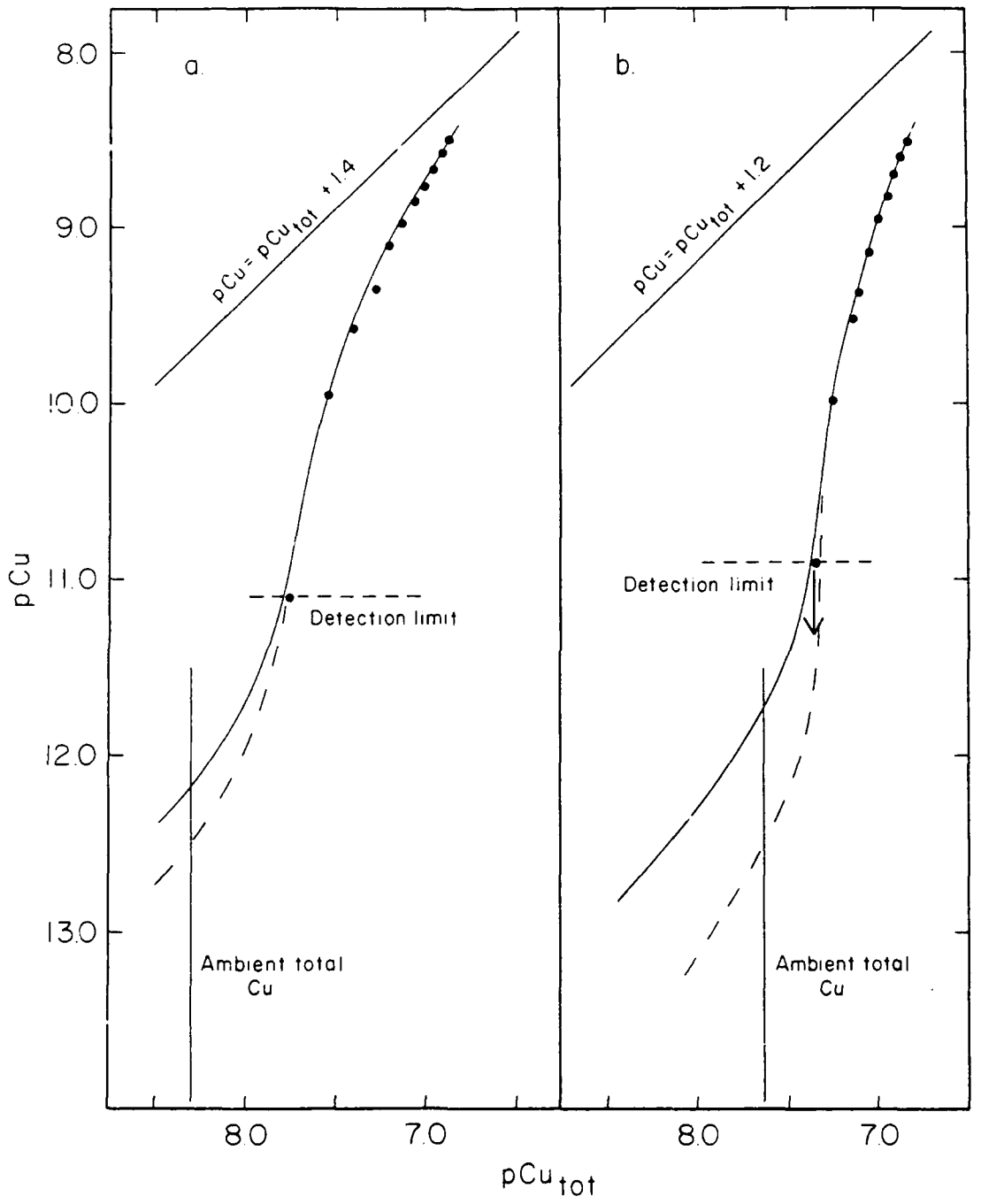
a.
b.
8.0
9.0
10.0
11.0
12.0
13.0
pCu
pCu = pCu_tot + 1.4
pCu = pCu_tot + 1.2
Detection limit
Detection limit
Ambient total Cu
Ambient total Cu
8.0
7.0
8.0
7.0
pCu_tot

copper concentrations weak ligands cannot influence copper speciation. The bacterial bioassay presupposes that substrate uptake by bacteria is not affected by copper complexed to NTA or to natural ligands. This premise is supported by the agreement of results obtained with varying NTA concentrations. A possible interference in the bacterial bioassay is the effect of toxic metals other than copper on the microbial community. The toxicity of the ambient free ion concentration of such metals may be neglected since addition of a large excess of NTA (at low copper added) did not result in enhanced substrate uptake. Displacement of such metals from natural ligand complexes by added copper is unlikely to be important until all available ligands are titrated. The basic premises have been confirmed in laboratory systems (Waite and Morel, 1983; Sunda and Gillespie, 1979). Our results suggest that these premises are equally correct for field samples and demonstrate the general applicability of the two techniques.

In interpreting and modeling the data from both techniques, we have assumed equilibrium between ligands and added metal. The time scales of equilibration used for the two methods were different-- ~ 20 min for the amperometric titration vs. 5 h for bioassay. In previous studies, no difference in bioassay results was observed for equilibration times of 2 and 5 h (Sunda and Ferguson, 1983). A small decrease in copper complexation was observed by amperometry on storage of a filtered (not bacteria-free) sample for 14 days (Figure 1b). Thus, changes in natural ligand concentration over 5 h may be neglected. The equilibration times might also have affected the results if the added copper was not fully equilibrated with the natural ligands at short equilibration times. The

correspondence of results from amperometry and bioassay indicated that a relatively fast (pseudo) equilibrium was reached on these time scales.

Questions as to the uniqueness and meaning of ligand concentrations and stability constants notwithstanding, these parameters provide at least some basis for comparison with previously published results (shown in Table II). Our total ligand coocentrations at Montauk Point (70nM) and Christiansen Basin (120nM) are within the range of 60-220 nM previously reported for coastal waters. Our weak ligand stability constant ($10^{9.1}$) agrees well with the values ($10^{8.9}$ - $10^{9.2}$) determined previously in coastal waters by bacterial bioassay (Sunda and Ferguson, 1983; Anderson et al., 1984), differential pulse anodic stripping voltammetry (jet-stream Hg-film electrode) (Kramer and Duinker, 1984) and C_{18}-SEP-PAK sorption with internal cupric ion calibration (Sunda and Hanson, 1987). Low concentrations of strong ligands (log $K_c \approx$ 11-12) could be detected only by the more sensitive of the techniques.

Despite the very limited scope of this study, it is interesting to speculate on the effect of anthropogenic inputs to the sludge dumpsite. The extent of pollution at Christiansen Basin is evidenced by elevated total copper concentrations and by differences in microbiological parameters. Titration data indicate, however, that copper was more complexed at Christiansen Basin than at Montauk Point. As a result, the estimated free cupric ion concentrations are roughly similar at both sites (pCu ca. 11.8 to 12.2) and within the range suggested for unpolluted coastal waters (11.3-12.5) (Sunda and Hanson, 1987). Even with the uncertainty in calculated ambient values the similarity of (Cu^{2+}) at a polluted site with unpolluted marine waters is striking

Table II. Total ligand concentrations, conditional stability constants and calculated ambient pCu (adapted from Sunda and Hanson, submitted).

Sampling location	pH	pCu	L_1 (nM)	L_2 (nM)	log K_1	log K_2	Technique	Reference
Christiansen Basin	8.0	11.8	50	68	11.7	9.1	Fixed-potential amperometry	This paper
Montauk Point	8.2	12.2	20	50	11.7	9.1[4]	"	"
Naragansett Bay	8.0	12.5	50	100	12.4	10.0	RPLC with cupric ion calibration	Sunda and Hanson (submitted)
"	8.0	12.1	20	100	> 12	~10	"	"
Coastal Peru	8.2	11.4	4.5	70	12.3	9.2	"	"
Vineyard Sound	7.8-8.1	---	*	90-220	*	9.0-9.2	Cupric ion bioassay	Anderson et al. (1984)
Lower Newport River Estuary	8.2	---	*	110-300	*	8.7-9.6	"	Sunda et al. (1984)
Cape San Blas, Florida	8.2	11.5	13	30	11.2	9.0	"	Sunda and Ferguson (1983)
Missippi River Plume	8.1	11.3	20	130	11.1	8.9	"	"
Irish Sea	8.2	---	--	60-150	--	10.0-10.4	Cu adsorption onto MnO_2	van den Berg (1982)
North Sea	7.9-8.2	---	*	80-103	*	8.9-9.1[+]	DPASV with jet-stream Hg film electrode	Kramer and Duinker (1984)
South Atlantic	7.7	---	11	33	12.2	10.2	Cathodic stripping voltammetry of Cu-catechol complexes	van den Berg (1984)
Southeastern Gulf of Mexico	8.2	---	5	15	≥ 12	9.8	Cupric ion bioassay	Sunda and Ferguson (1983)
Atlantic	--	---	31	87	9.9	9.0	Cu adsorption onto MnO_2	van den Berg et al. (1984)
Atlantic	--	---	60	120	9.7	8.6	DPASV	"

*Technique was not sufficiently sensitive to detect low concentrations of strong ligand.

+Computed from the operational ligand concentration and ratios of free cupric ion to inorganic copper species of $10^{-1.1}$ to $10^{-1.3}$ for pH 7.9 to 8.1.

(Table II). At Christiansen Basin, sewage effluent and sludge input are likely sources of the observed ligands (Sposito et al.,1979; Jardim and Allen, 1984). However, it is also possible that organisms "actively" contribute complexing agents to their environment in response to increased metal concentrations.

Certainly many interesting environmental and ecological questions concerning metal speciation in natural waters remain unanswered. Although direct measurement of ambient free cupric ion concentration must await more sensitive techniques, the methods we have compared do appear to provide valid field measurements of copper complexation and may profitably be used to address such issues.

ACKNOWLEDGEMENTS

We wish to thank Dr. W, Matson (Environmental Science Associates) for the loan of electrochemical instrumentation. E. Callahan (Massachusetts Institute of Technology) for performing total coppper analyses, Dr. A. Palumbo (University of Tennessee) and C. Currin (National Marine Fisheries, Beaufort) for assisting with the bioassays, and the officers and crew of the R/V "Researcher". This research was supported by two contracts from the Ocean Assessments Division, National Ocean Services, NOAA (F.M.- grant NA79 AA-D-00077), by NSF grant# OCE-8317532, and by International Copper Research Association (INCRA) project No. 364A.

REFERENCES

Anderson, D.M., J.S. Lively, R.F.Vaccaro (1984) J. Mar. Res. 42: 677-95.

Boyle, E.A., S.S. Huested, and S.P. Jones (1981) J. Geophys. Res. 86: 8048-66.

Boyle, E.A., D.F. Reid, S.S. Huested, and J.G. Hering (1984) Earth Planet. Sci. Lett. 69: 69-87.

Dzombak, D.A., W. Fish and F.M.M. Morel (1986) Environ. Sci. Technol. 20: 669-75.

Ferguson, R.L., E.N. Buckley, and A.V. Palumbo (1984) Appl. Environ. Microbiol. 47: 48-55.

Fish, W. and F.M.M. Morel (1983) Can. J. Fish. Aquat. Sci. 40: 1270-7.

Fish, W., D.A. Dzombak and F.M.M. Morel (1986) Environ. Sci. Technol. 20: 676-83.

Gillespie, P.A. and R.F. Vaccaro (1978) Limnol. Oceanogr. 23: 543-8.

Goncalves, M., L. Sigg, and W. Stumm (1987) J. Total Environ. 60: 105-19.

Huizenga, D.L. and D.R. Kester (1983) Mar. Chem 13: 281-91.

Jardim, W.F. and H.E. Allen (1984) in Complexation of Trace Metals in Natural Waters, ed. C.J.M. Kramer and J.C. Duinker. The Hague: Nijhoff/Junk pub, pp. 1-15.

Kramer, C.J.M. and J.C. Duinker (1984) in Complexation of Trace Metals in Natural Waters, ed. C.J.M. Kramer and J.C. Duinker. The Hague: Nijhoff/ Dr. W. Junk Publishers, pp. 217-238.

Matson, W., E. Zink, R. Vitukevitch (1977) Am. Lab. 9: 59-73.

Pfaender, F.K., E.N. Buckley, R.L. Ferguson (1980) in Proc. Symp. on preliminary results from the 1979 Researcher/Pierce IXTOC-I cruise. U.S. Dept. of Commerce, NOAA Office of Marine Pollution Assessment, Boulder, CO, pp. 545-550

Shuman, M.S., P.L. Brezonik, and J.R. Tuschall (1982) Anal. Chem 54: 998-1001.

Sposito, G., K.M. Holtzclaw, and C.S. Le Vesque-Madure (1979) Soil Sci. Soc. Am. J. 43: 1148-55.

Sunda, W.G. and R.F. Ferguson (1983) in Trace Metals in Seawater, ed. C.S. Wong, E. Boyle, K.W. Bruland, J.D. Burton, and E.D. Goldberg. New York: Plenum Press, pp. 871-891.

Sunda, W.G. and P.A. Gillespie (1979) J. Mar. Res. 37: 761-77.

Sunda,W.G. and A.K. Hanson (1987) Limnol. Oceanogr. 32: 537-51.

Sunda, W.G., D. Klaveness, A.V. Palumbo (1984) in Trace Metal Complexation in Natural Waters, ed. C.J.M. Kramer and J.C. Duinker. The Hague: Martinus Nijhoff/ Dr. W. Junk Pub.

Torella, F. and R.Y. Morita (1981) Appl. Environ. Microbiol. 41: 518-527.

Tuschall, J.R., and P.L. Brezonik (1981) Anal. Chem. 53: 1986-9.

van den Berg, C.M.G. (1982) Mar. Chem 11:323-42.

van den Berg, C.M.G. (1984) Mar. Chem. 15: 1268-74.

van den Berg, C.M.G., P.M. Buckley, S. Dharmvanij in Complexation of Trace Metals in Natural Waters, ed. C.J.M. Kramer and J.C. Duinker The Hague: Nijhoff/Junk Pub. pp. 213-6.

Waite, T.D. and F.M.M. Morel (1983) Anal. Chem. 55: 1268-74.

Westall, J.C. (1982) Technical Report, Dept. of Chem., Oregon State University, Corvallis, OR.

Westall, J.C., F.M.M. Morel, and D.N. Hume (1979) Anal. Chem 51: 1792-8.

APPENDIX B

DETERMINATION OF METAL COMPLEXATION USING A FLUORESCENT LIGAND

ABSTRACT

In this analytical method, measurement of fluorescence is used to determine speciation of a fluorescent ligand. The fluorescence of the ligand is quenched on formation of metal complexes with paramagnetic metal cations, in this case Cu^{2+}. Thus observed fluorescence may be used as a measure of unbound ligand and stability constants for metal-ligand complexes may be deduced from measurement of fluorescence at varying ligand-to-metal ratios.

This paper describes the application of this theory with a commercially available fluorescent ligand and estimates stability constants for 1:1 and 2:1 Cu-ligand complexes and for a ternary complex formed with NTA. Difficulties in the application of the technique arising from complicated ligand speciation are discussed.

INTRODUCTION

The reagent used in this study, Calcein (fluorexone), was first synthesized in 1956 by the condensation of fluorescein (Figure 1) with aminodiacetic acid and formaldehyde. The condensation product is fluorescent as is the parent compound and also possesses the metal complexing capability associated with the aminodiacetate functionalities. The general fluorescence characteristics of Calcein are well established. The reagent is fluorescent between pH 3 and 11.

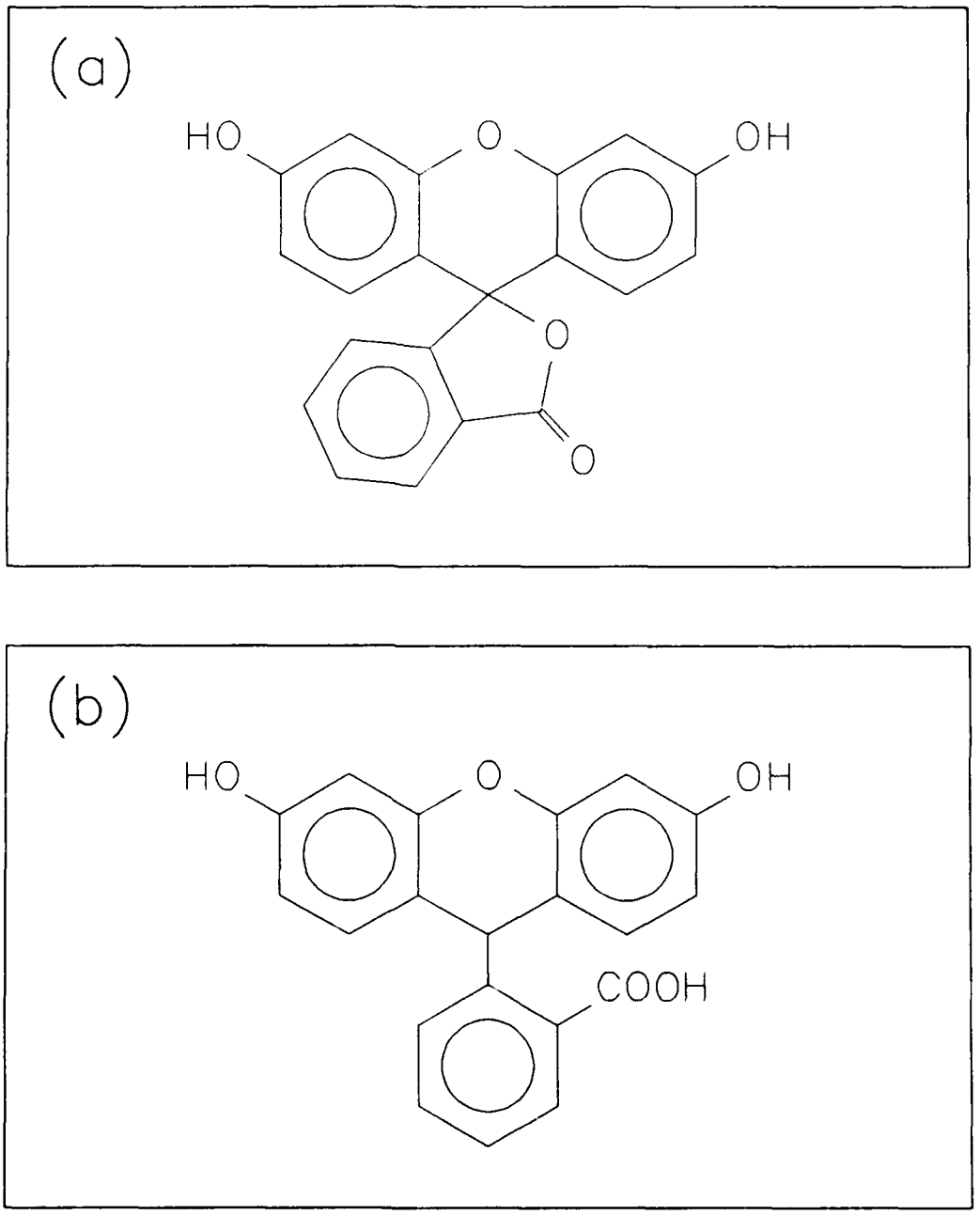

Figure 1. Structures of fluorescein reported by (a) Wallach et al. (1959) and (b) Markuszewski (1976).

Some metal complexes, particularly alkali and alkaline earth metal complexes are also fluorescent. Complexes with paramagnetic transition metals (Cu^{2+}, Co^{2+}, Ni^{2+}, Mn^{2+}) are not fluorescent (Pribil, 1982; Wallach and Steck, 1963; Markuszewski, 1976).

Some disagreement remains in the literature as to the structure of Calcein. Wallach et al. (1959) proposed an asymmetrically substituted structure (Figure 2a) based on their observed pK_a's for the phenolic hydroxy groups (see Table I). They reported quite different pK_a's for the two phenolic -OH groups, 5.4 and 9.0. They attributed the lower pK_a to the labilizing influence of the proximate aminodiacetate groups. However a symmetrical structure for Calcein has also been proposed based on observed pK_a's, H-nmr (Markuszewski, 1976), and C-13-nmr (Martin, 1977). Markuszewski reported pK_a's for the two phenolic hydroxy groups of 4.58 and 6.19 (both lower than the typical pK_a of ~9). He attributed the lability of the protons to a triple zwitterionic structure (Figure 2b).

Stability constants for Calcein complexes with some alkaline earth and transition metals have been reported (Table II). Both 1:1 and 2:1 metal-ligand complexes have been observed although the agreement in reported stability constants for Cu-Calcein complexes is not good.

Despite these uncertainties as to the structure and properties of Calcein, it has been used as an analytical reagent mostly for calcium (Diehl and Ellingboe, 1956; Kepner and Hercules, 1963; Bandrowski and Benson, 1972) but also for cadmium (Hefley and Jaselskis, 1974) and copper. Tovar-Grau et al. (1983) measured copper concentrations by fluorescence quenching of Calcein in the micromolar range. Saari and

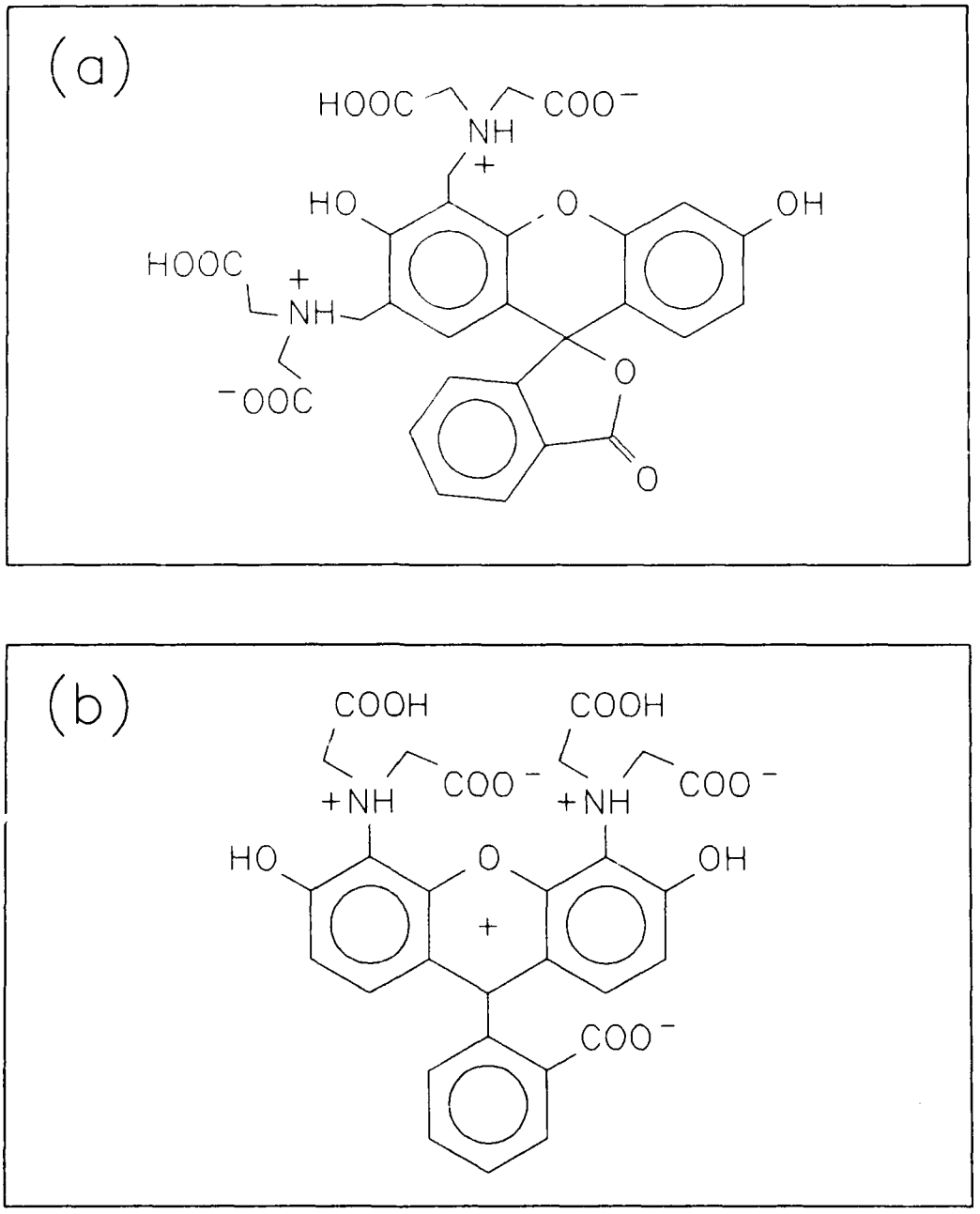

Figure 2. Structures of Calcein reported by (a) Wallach et al. (1959) and (b) Markuszewski (1976).

TABLE I. Stability constants for Calcein protonation

	reference	
	Markuszewski	Wallach et al.
pK_1	2.74	< 3
pK_2	3.53	< 4
pK_3	4.58	5.4
pK_4	6.19	9.0
pK_5	9.88	10.5
pK_6	11.64	> 12

$$\text{for } K_1 = \frac{(H^+)(H_5Cal^-)}{(H_6Cal)}$$

TABLE II. Stability constants for some metal complexes of Calcein

Metal ion	log K	"type K"	reference
Ba^{2+}	5.57±0.08	$K_2 = \frac{(M_2L)}{(ML)(M)}$	Wallach and Steck (63)
Sr^{2+}	5.86±0.04	"	"
Ca^{2+}	6.63±0.09	"	"
Mg^{2+}	7.90±0.2	"	"
Cu^{2+}	8.27	K_{CuH_2L}	Miyahara (77)
	12.3	K_{CuL}^{cond} (pH 7)	Saari and Weitz (84)
	12.8	" (pH 7.3)	this work
	28.97	β_{Cu_2L}	Miyahara (77)
	20.8	β_{Cu_2L} (50% EtOH)	Markuszewski
	24.5	$\beta_{Cu_2L}^{cond}$ (pH=7.3)	this work

Weitz (1984) have suggested that Calcein immobilized on cellulose could be used for preconcentration of metal ions or in an optical sensor.

It is clear that application of Calcein as an analytical reagent for determining metal concentrations and speciation and binding constants of competing ligands, a more detailed understanding of the complexing proerties of the analytical reagent is required.

EXPERIMENTAL SECTION

Materials: All reagents were analytical grade and most were used without further purification. For some experiments NaCl solutions were prepared by dilution of 5 M NaCl solutions pretreated with Chelex resin to reduce metal contamination. [Chelex 100 resin was cleaned with 3 M NH_4OH, rinsed extensively and reconverted to the Na^+-form before use to minimize leaching of organic chelators from the resin.] All solutions were buffered with 1 mM PO_4 (pH = 7.4 ± 0.2) except for the kinetic experiment which was buffered to pH = 7.3 with 5 mM HEPES (N-2-hydroxyethylpiperazine-N'-2-ethanesulphonic acid). Calcein (obtained from Sigma, >95% pure) was used as recieved. The only significant contamination reported in Calcein is unreacted fluorescein (Tovar-Grau et al., 1983). The absence of any residual fluorescence in the presence of excess copper indicated that fluorescein contamination is not significant. Stock solutions of Calcein (0.001 M in 0.01 M KOH) were stored in the dark at 4^{o} C for not more than 2 months (as suggested by Wallach et al., 1959). Calcein Blue, used in one experiment, was also used as received from Sigma. The stock solution was prepared the day preceding the experiment as decomposition of the reagent in solution

has been noted in the literature (Brittain, 1987).

Amperometric experiments: The theory and analytical methodology for measurement of inorganic copper by fixed-potential amperometry has been described previously (Waite and Morel, 1983; Hering et al, 1987; Hering and Morel, submitted; Matson et al., 1977). Amperometric titrations were performed by the addition of aliquots of stock copper solution to Calcein (at concentrations of 37.5 or 50 nM) in 170 mL of 0.5 M NaCl, 1 mM PO_4 at pH 7.35).

Fluorescence quenching experiments: Calcein fluorescence was measured on a Perkin-Elmer LS-5 Fluorescence spectrophotometer (excitation wavelength 492 nm, emission wavelength 511 nm). Fluorescence signals were integrated over 8 sec and then averaged over ~1 min. For most of the fluorescence quenching experiments (with or without a competing ligand) experiments were performed by spiking 10.00 ± 0.02 g aliquots of buffer (with or without the competing ligand) with appropriate volumes of copper and Calcein (concentrations $1\text{-}10\text{x}10^{-5}$M prepared from 0.01 (Cu) or 0.001 (Calcein) M stock solutions). All solutions, including calibration solutions, were stored in the dark at room temperature for ~4 h before fluorescence measurements. Experiments were routinely performed in acid leached ~15 mL polyethylene flip-top vials. The same protocol was followed with ~50 mL Teflon centrifuge tubes for comparison.

For one Calcein calibration curve (at high concentrations, $>10^{-7}$ M), aliquots of the reagent were added to 100 mL of 0.1 M NaCl/0.001 M PO_4 buffer. Aliquots of solution removed for fluorescence measurements were recombined with the remaining solution to minimize volume changes during the procedure.

For the kinetics experiment, solution of pre-equlibrated NTA/Cu or Calcein/Cu were prepared in 100 mL acid-washed glass volumetric flasks. Calibration flasks with Calcein and NTA were similarly prepared. The kinetic experiments were begun ("t=0") by spiking the experimental flasks with a small volume of the competing ligand. Over time aliquots were removed for fluorescence measurements. All flasks were foil-wrapped to exclude light and stored at room temperature.

Modeling: Stability constants for copper-Calcein complexes were obtained using FITEQL (Westall, 1982). All constants are reported as pH- (and ionic strength) dependent conditional constants. Due to the formation of more than one copper-Calcein complex, the FITEQL solutions do not represent unique descriptions of the experimental data (for any individual data set). The inclusion of information from several types of experiments precludes a simplistic optimization for any individual experiment (as described below). Constants for inorganic copper complexes and NTA species were taken from the MINEQL (Westall et al., 1976) data base. Predicted free Calcein vs. Cu curves based on FITEQL constants were also generated using MINEQL.

RESULTS AND DISCUSSION

Calcein fluorescence: Calcein fluorescence was observed to be linear with concentration up to ~200 nM. In the micromolar range very large deviations from linearity were observed probably due to re-absorbance of the fluoresced light (Figure 3).

Some difficulties arise in determining the calibration curve for Calcein at low concentrations probably due to copper contamination in

Figure 3. Fluorescence vs, Calcein concentration (above 100 nM Calcein).

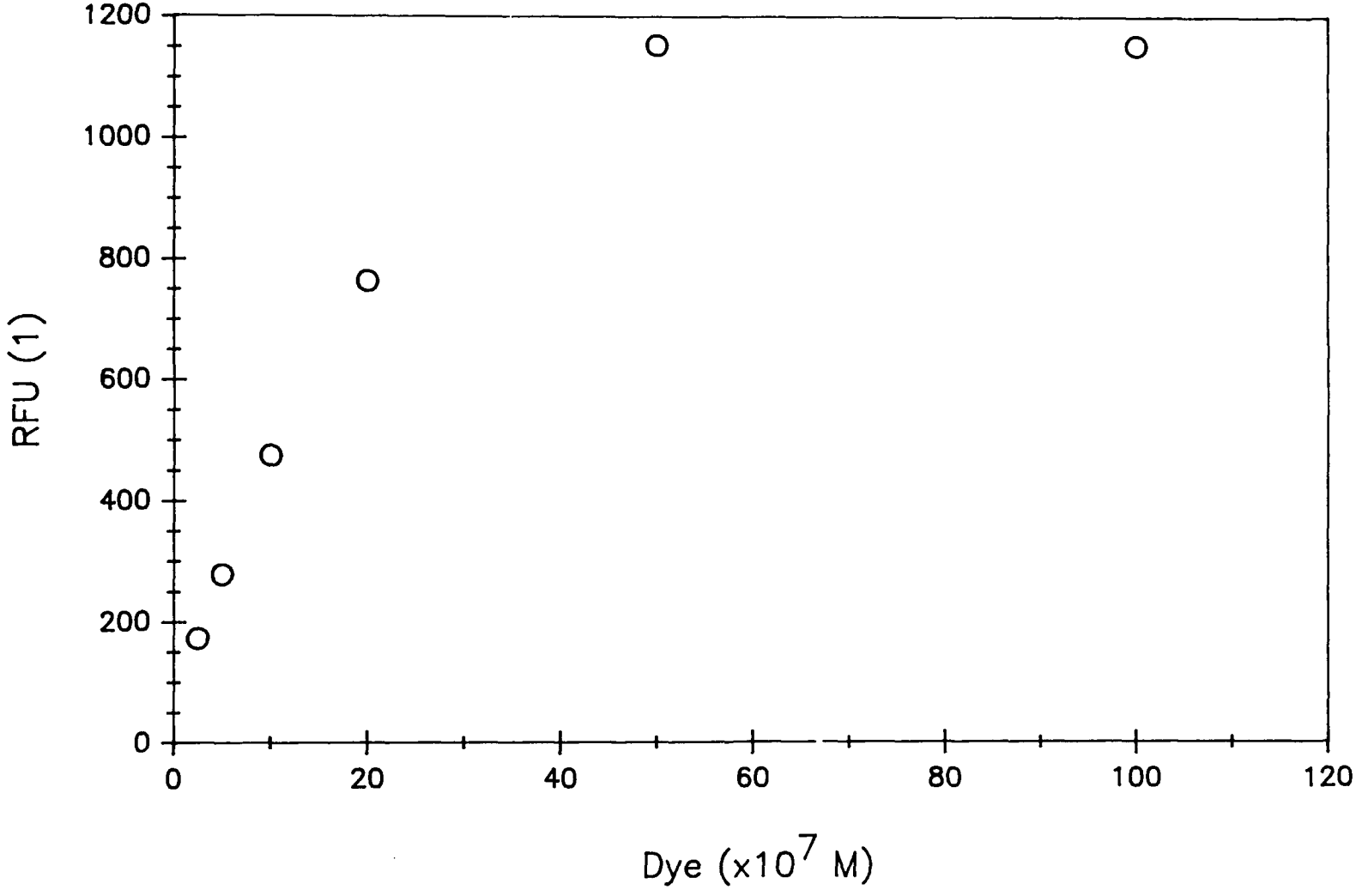
1200
1000
800
600
400
200
0
RFU (1)
0
20
40
60
80
100
120
Dye (x10^7 M)

media or on container surfaces. The difference in calibration curves with varying concentrations of ligands is difficult to interpret since the calibration curves with no added NTA do not show what might be the expected effect of copper contamination (i.e.- the same slope as curves with added NTA but an offset in the intercept) but rather a decrease in the slope (Figure 4). NTA itself does not contribute to the fluorescence signal. It has also been noted that the stability of Calcein fluorescence over the course of several hours was influenced by the presence of NTA (Figure 5). Calibration curves obtained in polyethylene and Teflon were identical (Figure 6). Unfortunately, the uncertainty in the interpretation of calibration curves creates a significant error in the interpretation of ligand competition experiments (to be discussed later).

Calcein-copper binding: Copper binding by Calcein was studied by observing fluorescence quenching as a function of added copper and by measuring inorganic copper as a function of added copper by fixed-potential amperometry. Fluorescence quenching data show a linear decrease in fluorescence (i.e.- free Calcein) with added Cu to ~0.5:1 metal-to-ligand ratios. No residual fluorescence is observed at >3:1 metal-to-ligand ratios (Figure 7). The quenching curves are consistent with the formation of a non-fluorescent 1:1 Cu-Calcein complex with a conditional stability constant of $\sim 10^{9.0}$. However, this interpretation is inconsistent with the amperometric data and the ligand-competition data (to be discussed later). The amperometric data (Figure 8) show more copper complexation than can be accounted for by the formation of a 1:1 complex. Both fluorescence quenching and amperometric data can be

Figure 4. Fluorescence vs. Calcein concentration. Symbols: (O) no NTA, (Δ) 10 μM NTA.

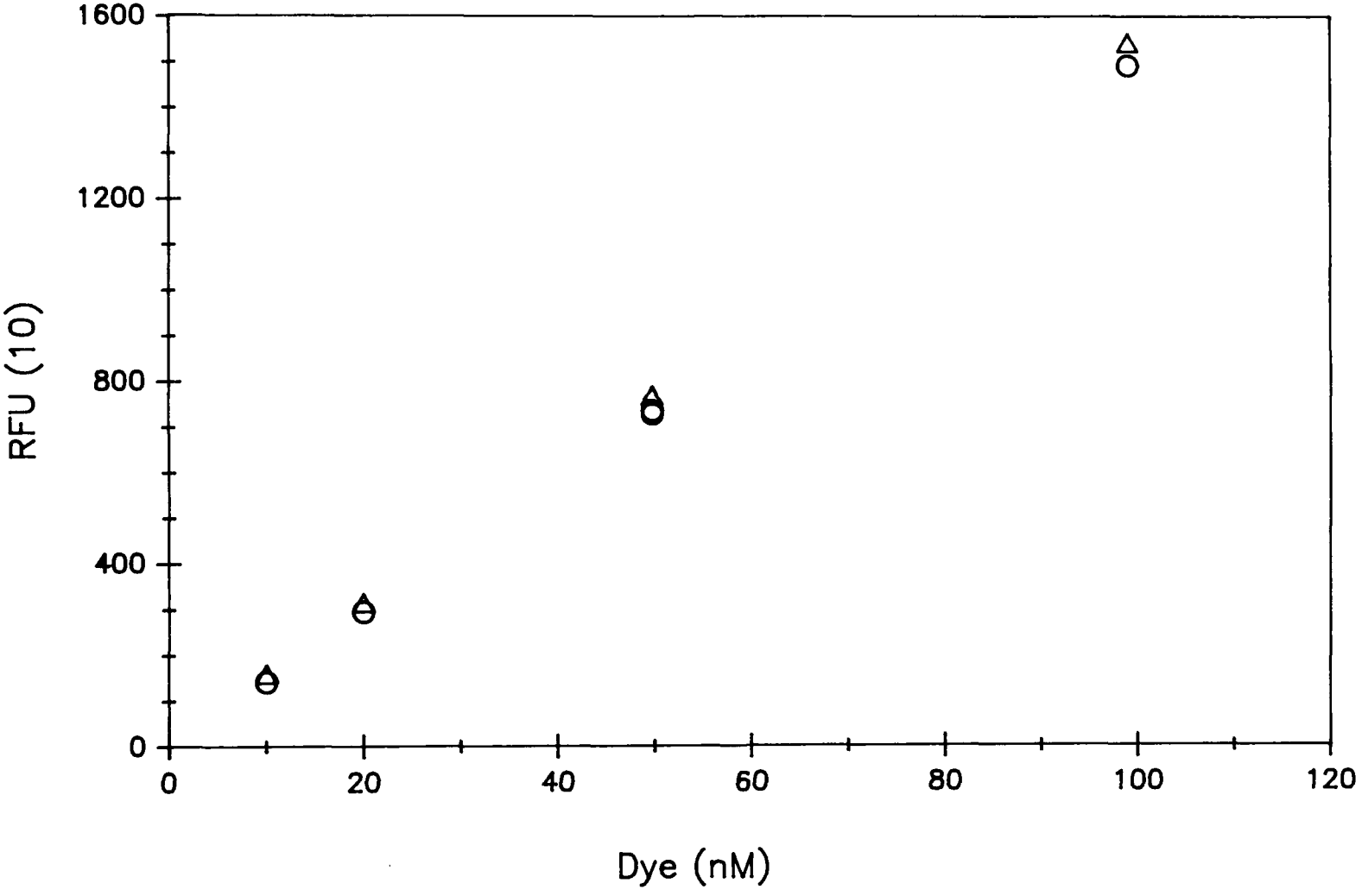
1600
1200
800
400
0
RFU (10)
0
20
40
60
80
100
120
Dye (nM)

Figure 5. Changes in fluorescence over time for Calcein solutions. (a) Fluorescence as a function of time for 1 μM NTA (open symbols) and 10 μM NTA (closed symbols). Calcein concentration (○, ●) 10 nM, (△, ▲) 20 nM, (□, ■) 50 nM, (▽, ▼) 100 nM. (b) and (c) Fluorescence vs. Calcein concentrations for (b) 1 μM NTA and (c) 10 μM NTA. Approximate times (from (a)): (○) 0 h, (△) 1.5 h, (□) 3.5 h (◇) 6-7 h.

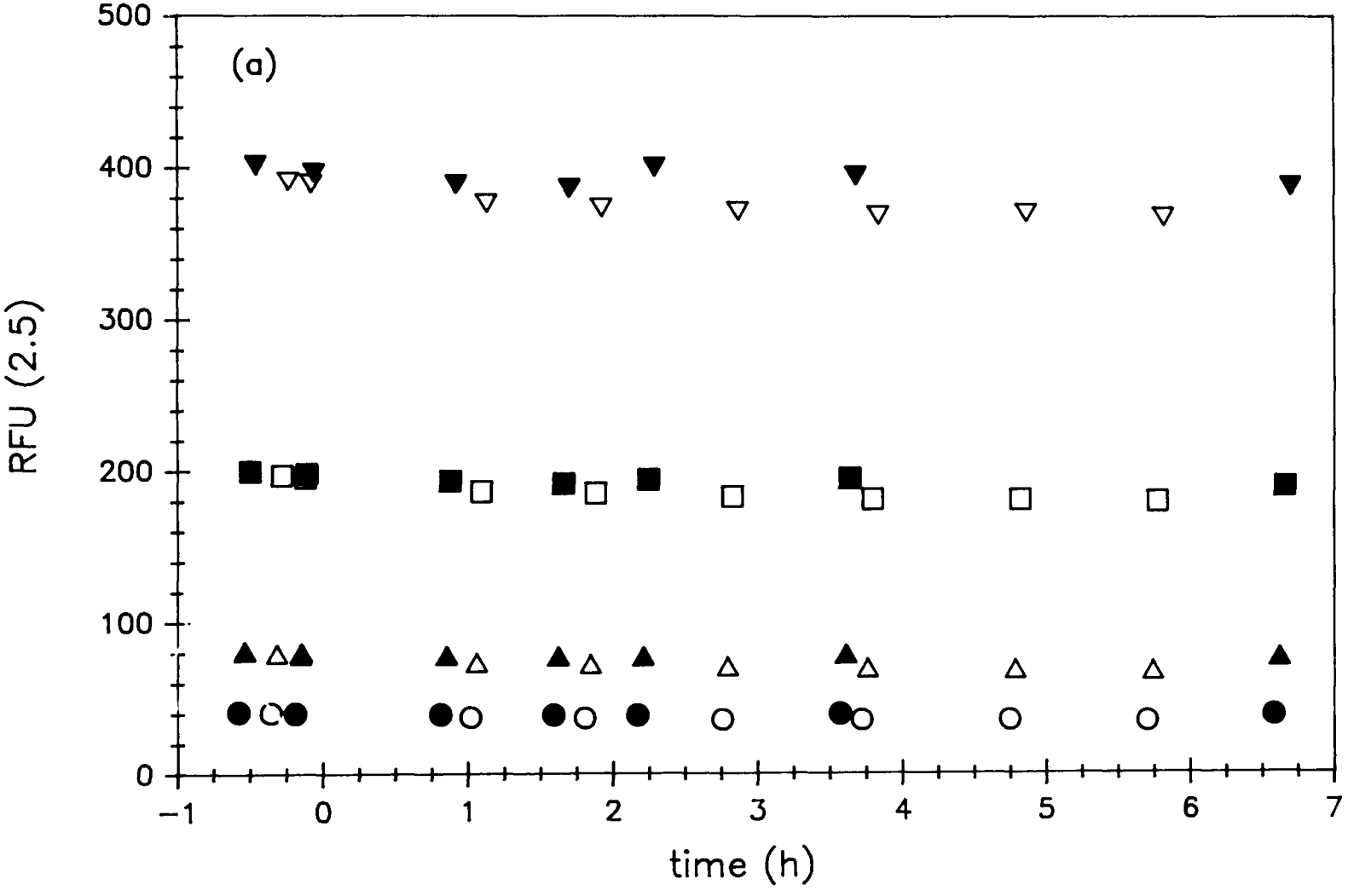
(a)
500
400
300
200
100
0
RFU (2.5)
−1
0
1
2
3
4
5
6
7
time (h)

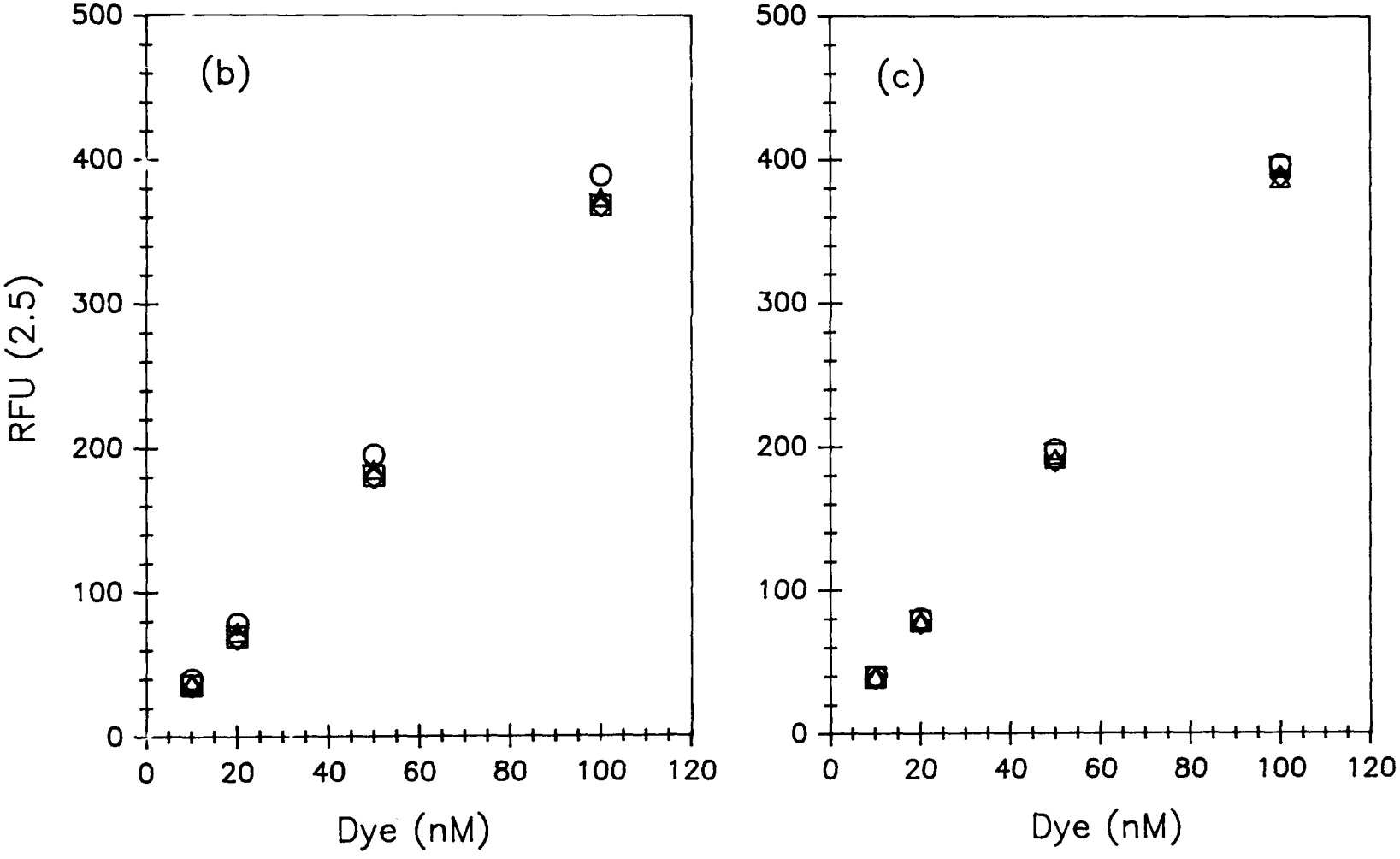
(b)
(c)
RFU (2.5)
Dye (nM)
Dye (nM)
0
100
200
300
400
500
0
20
40
60
80
100
120

Figure 6. Fluorescence vs. Calcein concentration for samples in polyethylene (O) and Teflon (□).

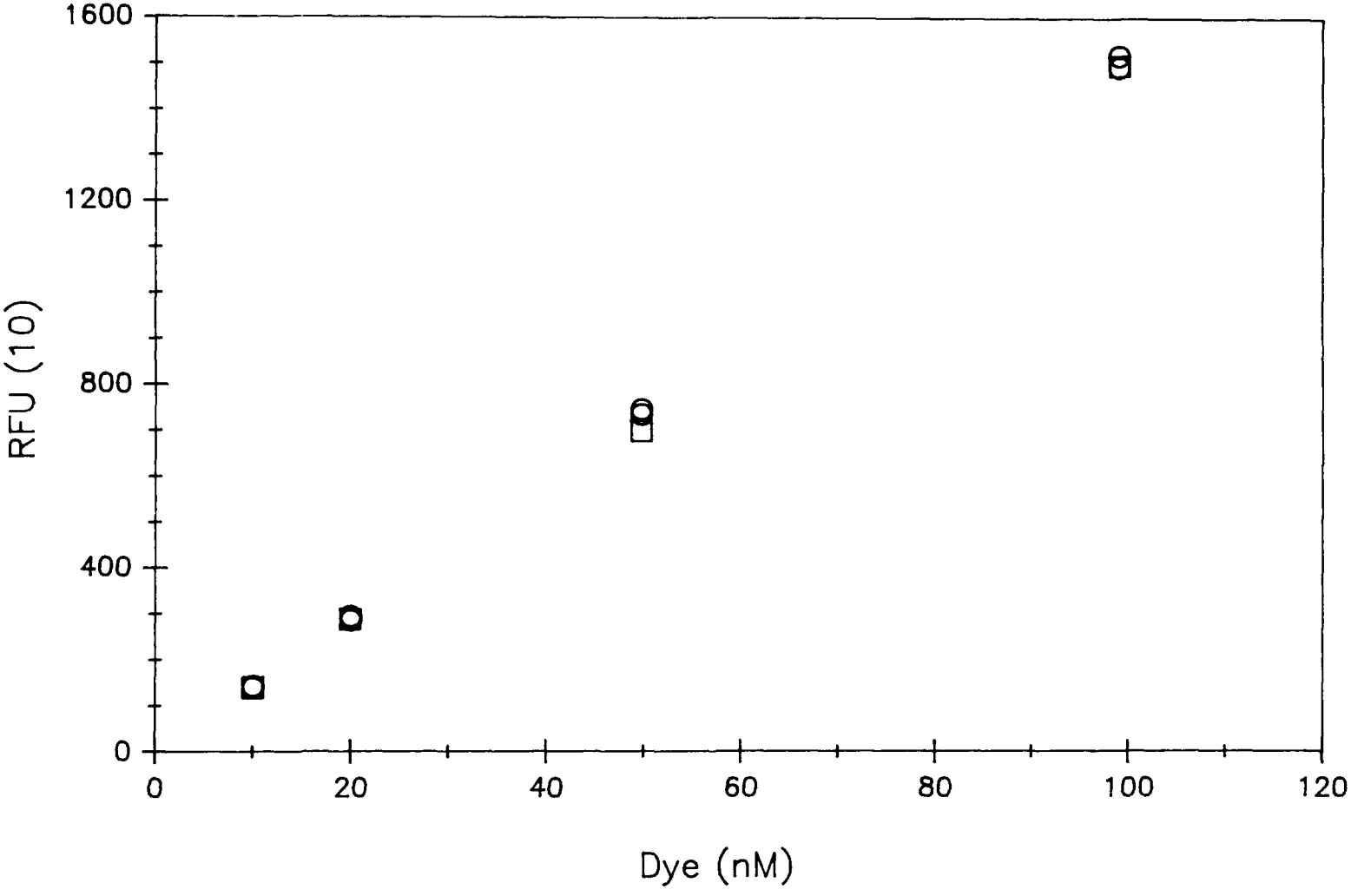
1600
1200
800
400
0
RFU (10)
0
20
40
60
80
100
120
Dye (nM)

Figure 7. Effects of copper concentration on free Calcein. (——) model fit for $K_{CuD} = 10^{12.8}$, $K_{Cu_2D} = 10^{24.6}$; (---) model fit for $K_{CuD} = 10^{12.8}$, $K_{Cu_2D} = 10^{24.5}$. [The different symbols correspond to separate data sets. Differences may be due to varying levels of Cu contamination.]

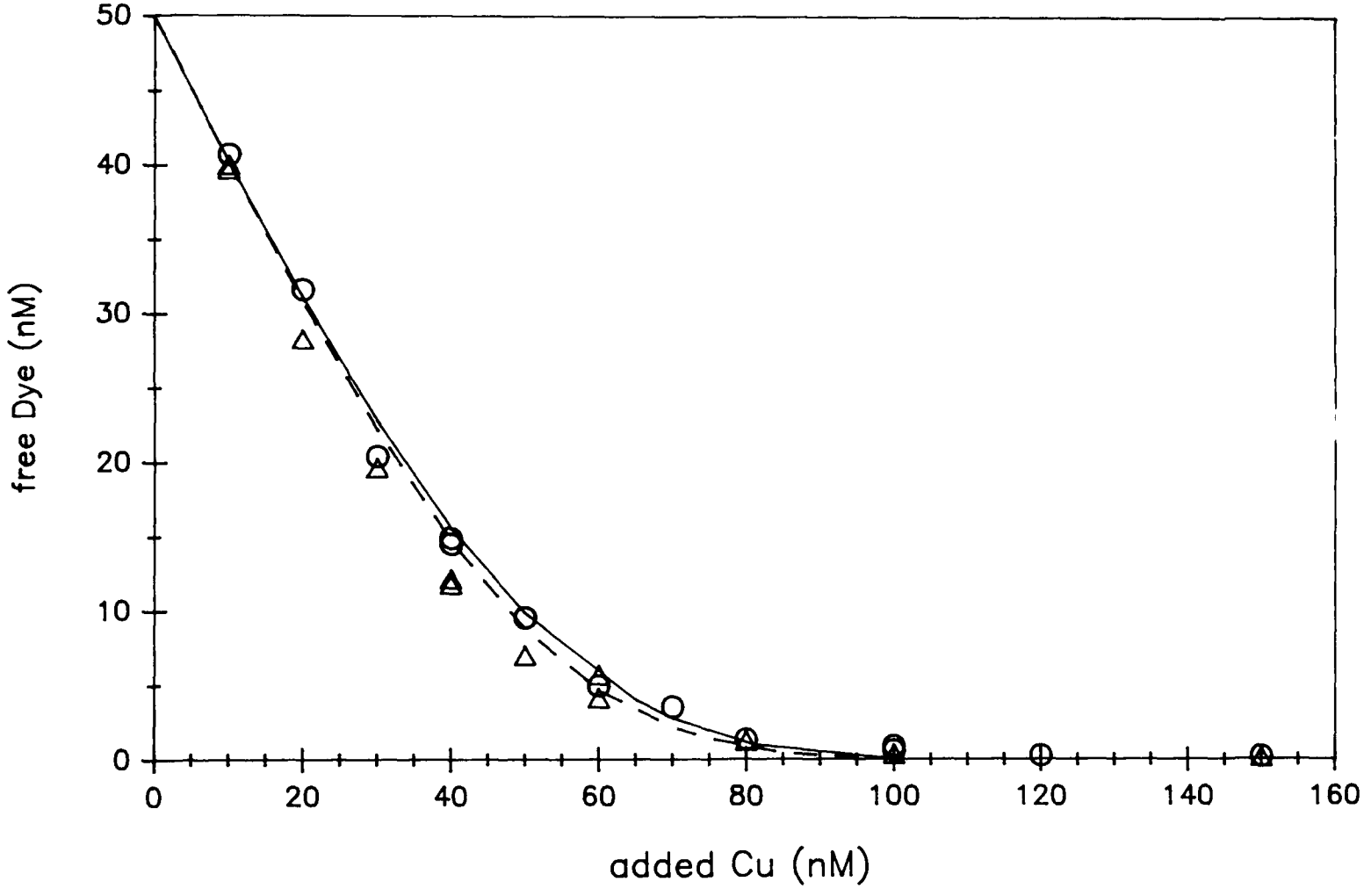
50
40
30
20
10
0
free Dye (nM)
0
20
40
60
80
100
120
140
160
added Cu (nM)

Figure 8. Amperometric Cu titrations of Calcein. Calcein concentrations: (O) 37.5 nM, (Δ) 50 nM.

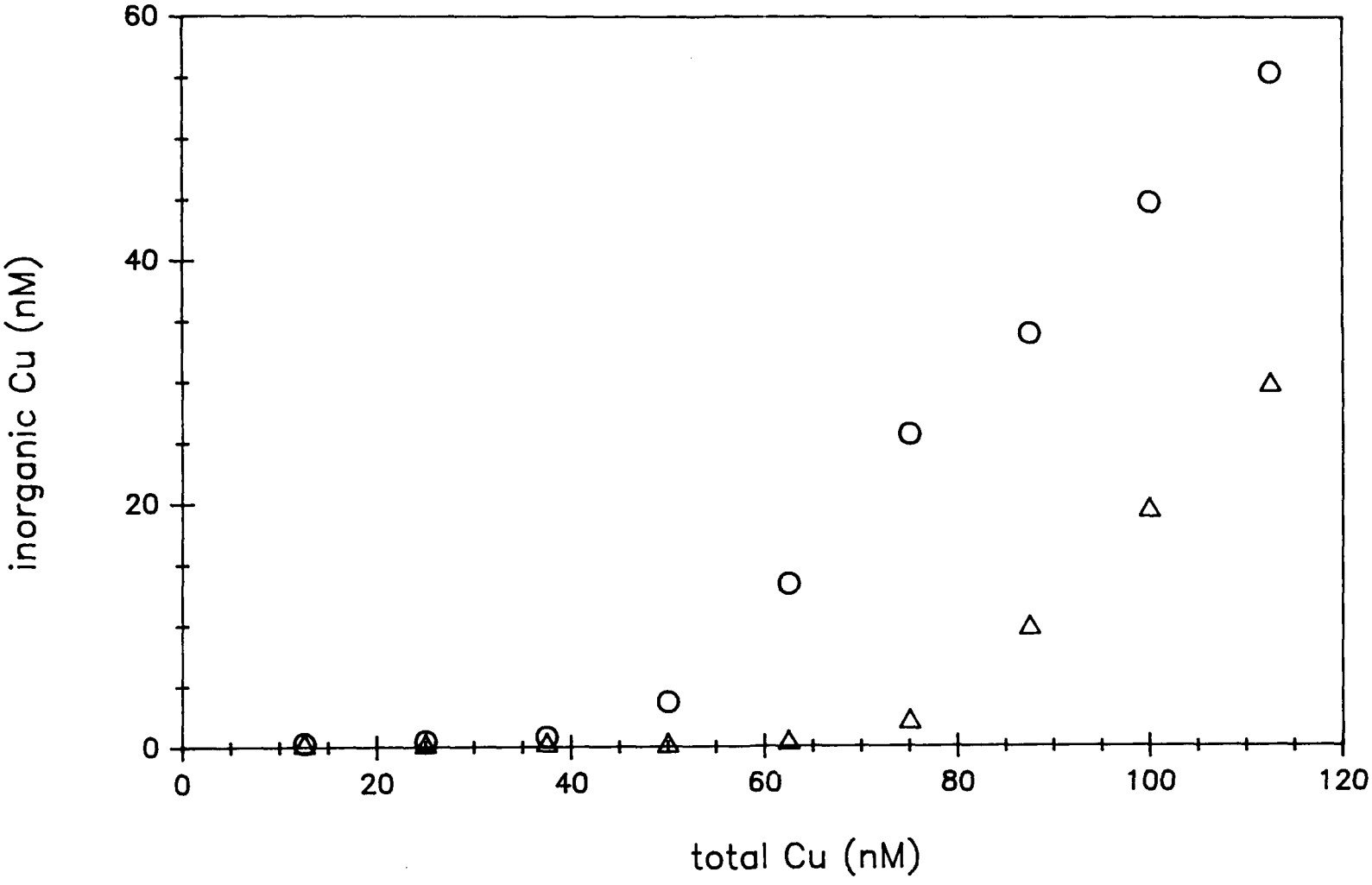
60
40
20
0
0
20
40
60
80
100
120
inorganic Cu (nM)
total Cu (nM)

qualitatively resolved by including formation of a 2:1 Cu-Calcein complex. The fluorescence quenching data indicate the relative strengths of the stability constants for the 2:1 and 1:1 complexes, however, they cannot be used to determine unique values for these constants. The model fit shown with the data (in Fig. 7) imposes a conditional stability constant for the 1:1 complex of $10^{12.8}$ (based on ligand-competition experiments) and uses a value for $K_{Cu_2Calcein}$ based on the optimization of the fit to the fluorescence quenching data using FITEQL. These constants, however, are not entirely consistent with the amperometric titration data; a model fit of the titration experiment significantly overpredicts the observed complexation. This discrepancy may be due to some dissociation of the 2:1 complex during the electrochemical measurement.

Calcein-copper binding- ligand competition fluorescence quenching: Information on Calcein -copper binding can also be obtained by observing fluorescence quenching in the presence of competing ligands (cf. Saari and Weitz, 1984).

Comparison of fluorescence quenching of both Calcein and Calcein Blue in the same solutions indicates similar strength of binding (Figure 9a,b). Since Calcein Blue (structure shown in Figure 10) has only one aminodiacetate functionality (Pribil, 1982), this concordance in binding strengths indicates that the binding of copper by Calcein involves only a single aminodiacetate group (as suggested by Markuszewski, 1976). However since the binding constants of Calcein Blue are not well established, this information cannot be interpreted quantitatively.

Calcein fluorescence quenching was also measured in the presence of

Figure 9. Measurements of free Calcein and free Calcein Blue in solutions containing Calcein, Calcein Blue and Cu.

(a) Concentration of free Calcein as a function of total Cu for $Calcein_T$= 50 nM and (□) $Calcein\ Blue_T$= 50 nM, (○) $Calcein\ Blue_T$= 20 nM.

(b) Concentration of free Calcein Blue as a function of total Cu for $Calcein\ Blue_T$= 50 nM and (□) $Calcein_T$= 50 nM, (○) $Calcein_T$ = 20 nM.

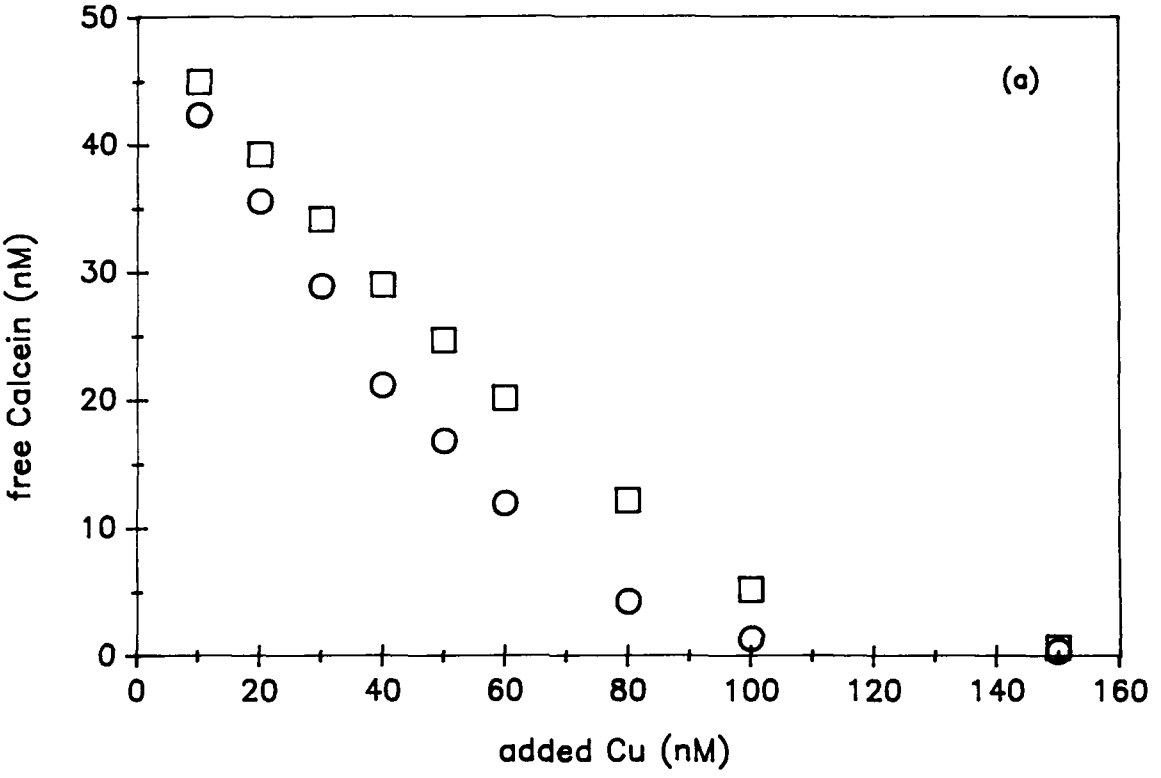
(a)
free Calcein (nM)
added Cu (nM)
0
10
20
30
40
50
0
20
40
60
80
100
120
140
160

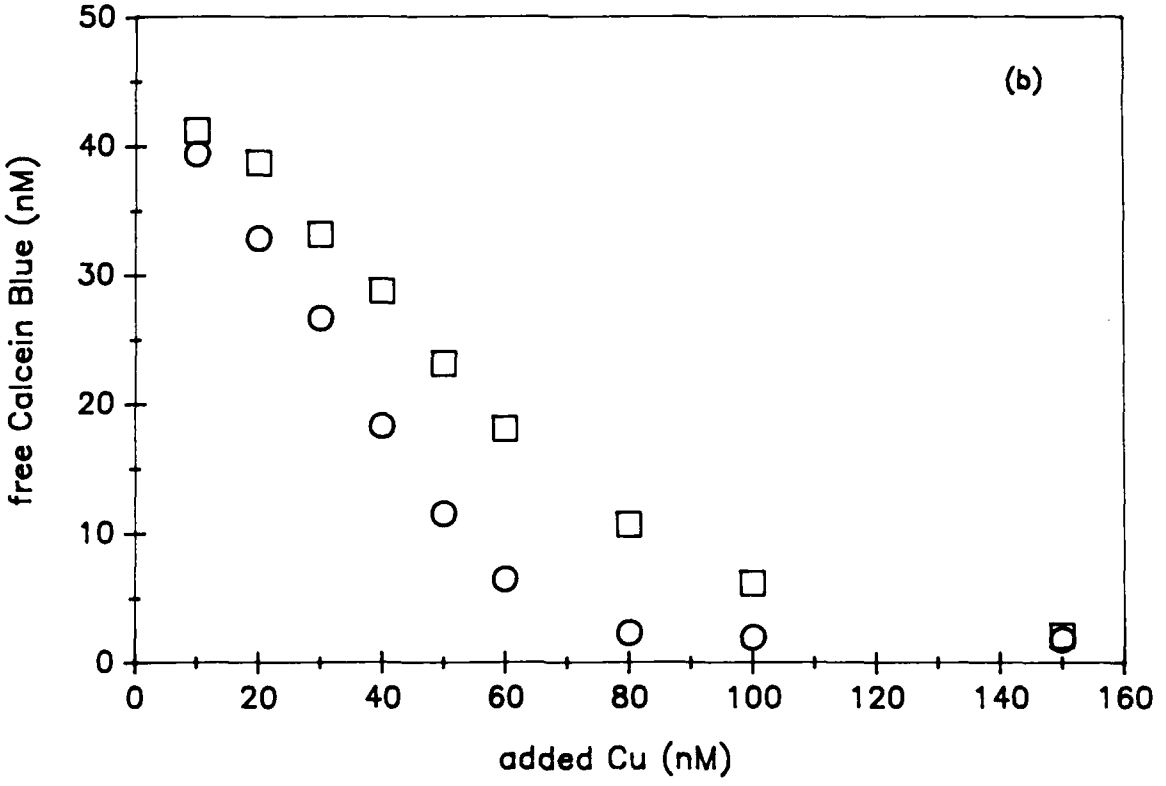
(b)
free Calcein Blue (nM)
added Cu (nM)
0
10
20
30
40
50
0
20
40
60
80
100
120
140
160

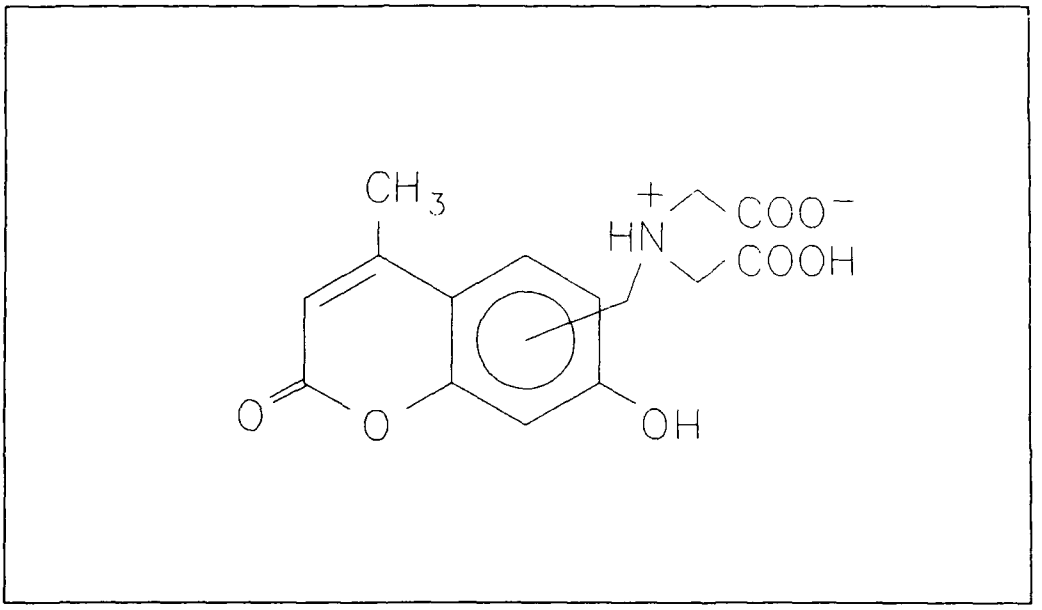

Figure 10. Structure of Calcein Blue (Pribil, 1982).

varying concentrations of NTA and ethylenediamine. It is clear from these experiments that the conditional stability constant for Cu-Calcein exceeds that of CuNTA. Figure 11 shows the results of ligand competition experiments with 10^{-5} M NTA, 10^{-7} M calcein, and 10^{-7} M Cu. Equilibrium is attained in ~4 h. The observed equilibrium value is consistent with a conditional stability constants for Cu-Calcein of $\sim 10^{12.8}$.

Examination of ligand-competition fluorescence quenching with a range of added Cu suggests more complicated ligand speciation. Comparison of model fits with data shown in Figures 12 a and b show that the observed quenching at high Cu is significantly less than expected. This discrepancy can be resolved by inclusion of a stable ternary complex (NTACuCalcein) that is also (at least partially) fluorescent. Such a species would be expected to contribute significantly to the overall Calcein speciation at high NTA concentrations and at high Cu-to-Calcein ratios. Figure 12 shows the calculated concentrations of free Calcein and the ternary complex (with a stability constant of $10^{20.4}$). It is assumed that the ternary complex is as fluorescent as free Calcein. The discrepancies between the calculated values for the two data sets may be due to a reduced quantum efficiency for the ternary complex as compared with the free ligand. Although it is somewhat counter-intuitive to suggest that such a ternary complex would be fluorescent, kinetic data suggest formation of a fluorescent ternary complex with EDTA as an intermediate. For the reaction of Cu-Calcein with excess EDTA, the deviations from linearity in the plot of ln(Cu-Calcein) vs. time could be due to initial formation of a fluorescent ternary intermediate (Fig. 13).

Figure 11. Concentration of free Calcein over time for (Δ , ∇) 100 nM Calcein added to pre-equilibrated Cu/NTA (Cu_T= 100 nM, NTA_T= 10 μM) at t=0 and (O , $\square$) 10 μM NTA added to pre-equilibrated Cu/ Calcein (Cu_T= 100 nM, $Calcein_T$= 100 nM) at t=0. (——) Equilibrium value for free Calcein for K_{CuD}= $10^{12.8}$, K_{Cu_2D}= $10^{24.6}$, (---) equilibrium value for free Calcein neglecting Cu_2D.

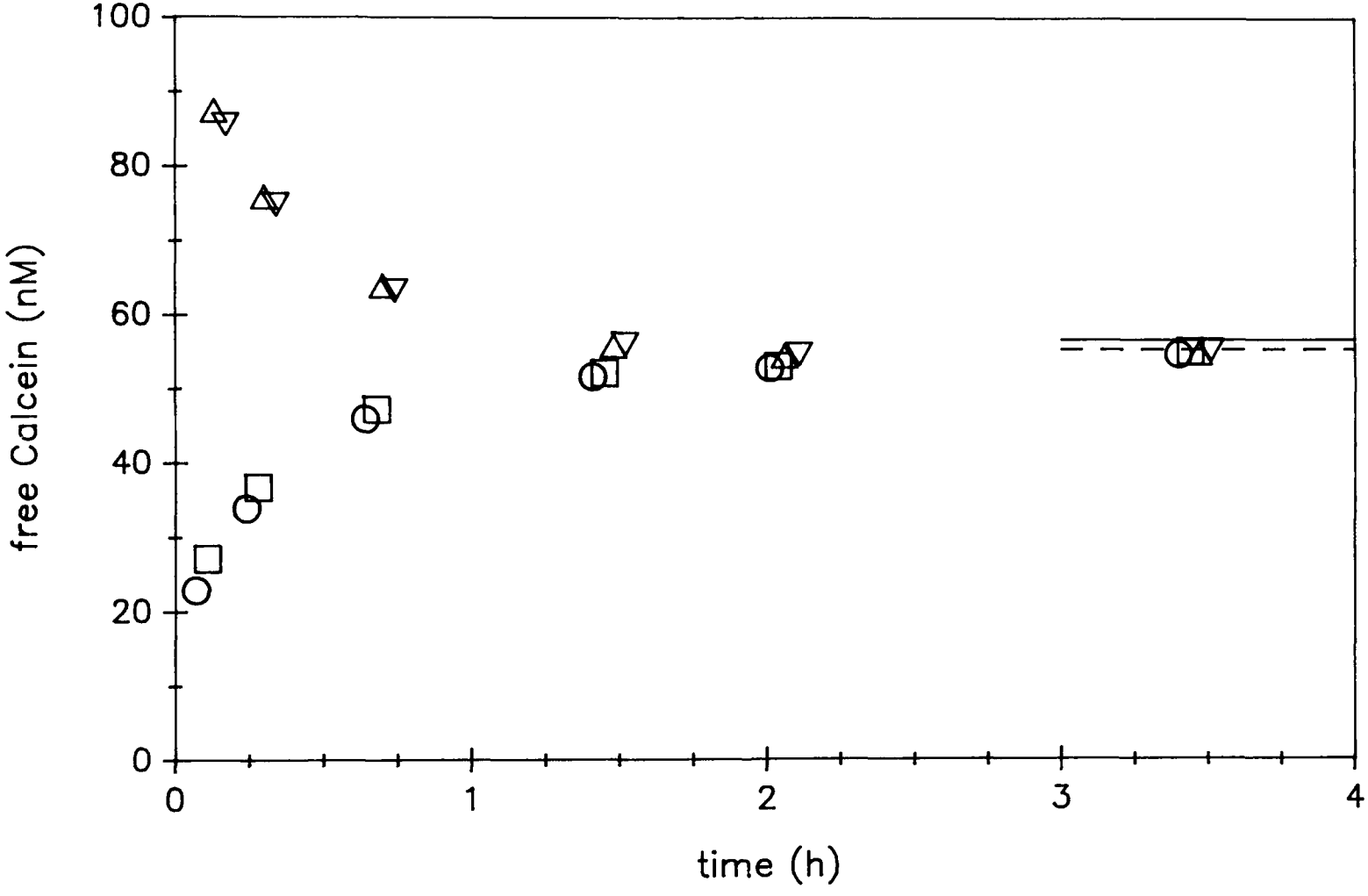
100
80
60
40
20
0
free Calcein (nM)
0
1
2
3
4
time (h)

Figure 12. Effect of Cu on Calcein speciation in the presence of (a) 10 μM NTA and (b) 1 μM NTA. Symbols are fluorescence normalized using calibration curves and corresponds to free dye concentration assuming that no other dye species contributes to the observed fluorescence. Lines show model fits based on constants $K_{CuD} = 10^{12.8}$, $K_{Cu_2D} = 10^{24.5}$, $K_{NTACuD} = 10^{20.4}$. (....) predicted concentration of free dye, (----) predicted concentration of NTACuD, (——) sum of predicted concentrations of these two species.

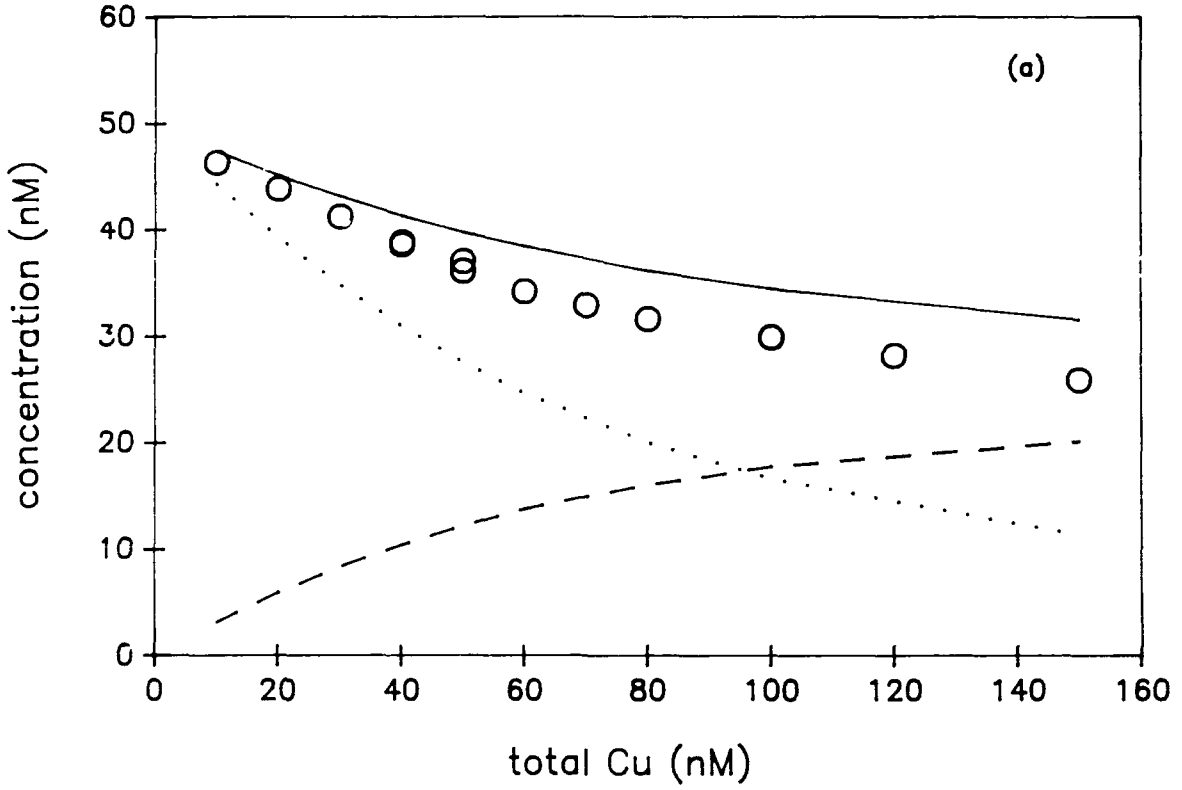
(a)
concentration (nM)
total Cu (nM)
0
10
20
30
40
50
60
0
20
40
60
80
100
120
140
160

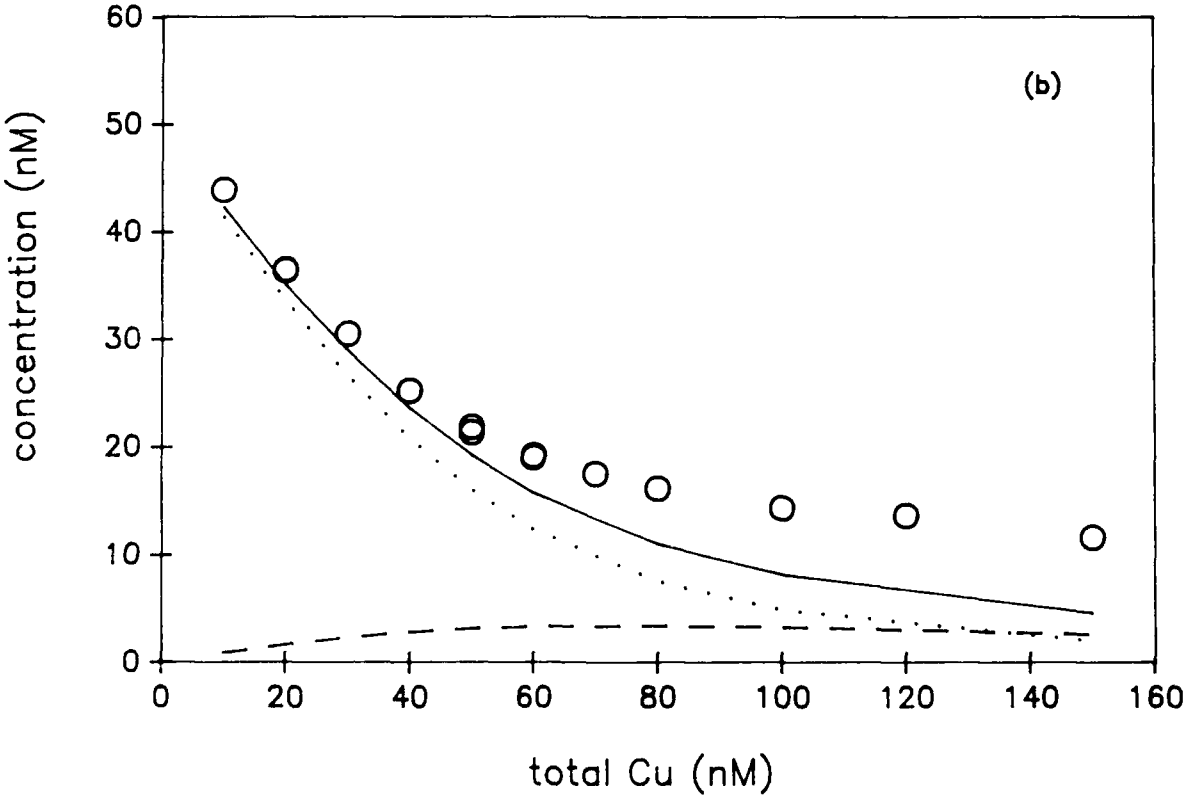
(b)
concentration (nM)
total Cu (nM)
0
10
20
30
40
50
60
0
20
40
60
80
100
120
140
160

Figure 13. Ligand exchange experiments with Calcein, EDTA and Cu (50 nM total Calcein, 30 nM total Cu in 0.1 M NaCl, 5 mM HEPES, pH = 7.3) (a) addition of EDTA at t=0 to pre-formed Cu-Calcein complex. Symbols: (△ ,▽) 2 μM EDTA; (□ ,◇) 10 μM EDTA. (b) logarithmic transform of calculated CuD concentration vs. time (symbols as above).

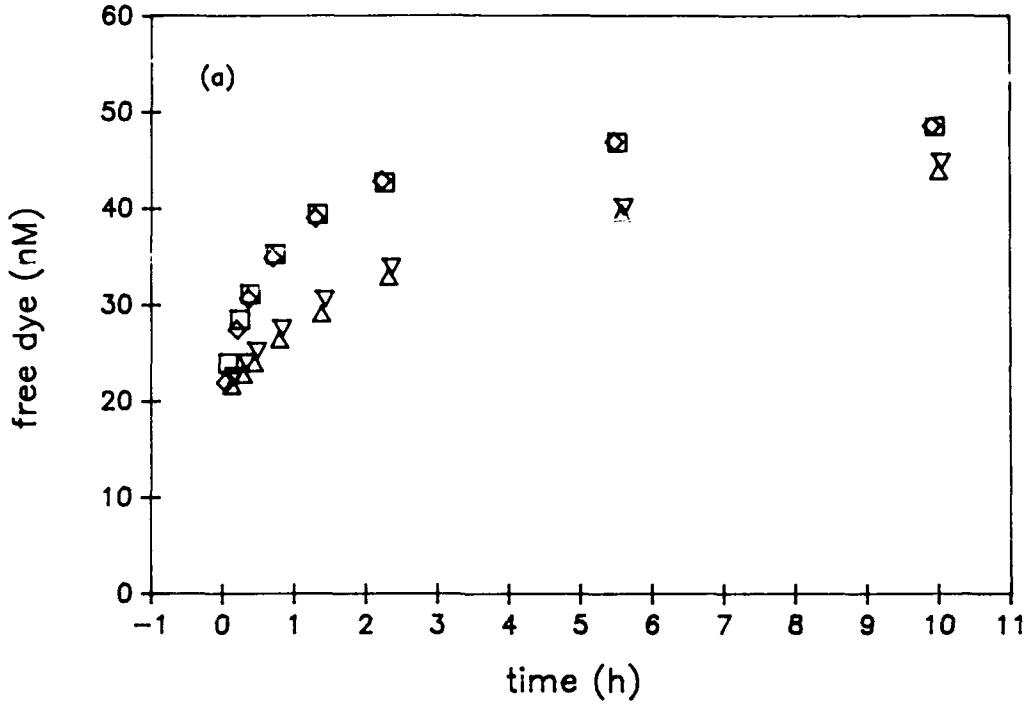
(a)
free dye (nM)
time (h)
0
10
20
30
40
50
60
−1
0
1
2
3
4
5
6
7
8
9
10
11

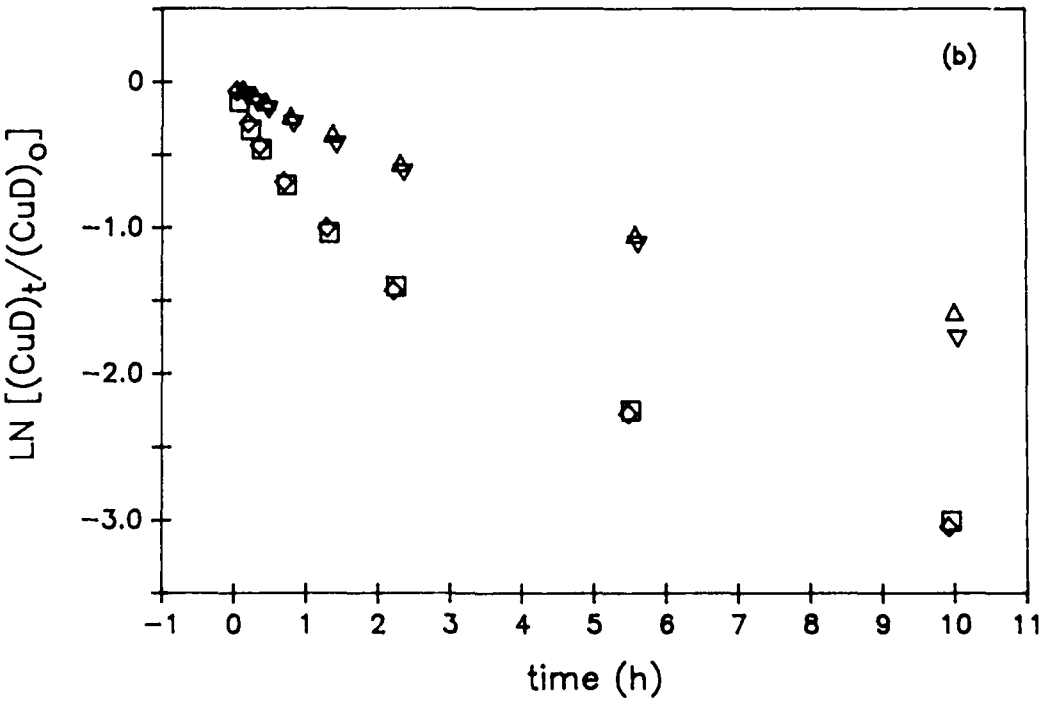
(b)
LN [(CuD)t/(CuD)o]
time (h)
0
−1.0
−2.0
−3.0
−1
0
1
2
3
4
5
6
7
8
9
10
11

Comments on reproducibility and consistency of results: Although all ligand-competition fluorescence quenching experiments agree qualitatively, it has not been possible to fit all the data with a single set of conditional stability constants. While reproducibilty of data for a single experiment is excellent, some discrepancies are apparent in comparing different data sets. It is likely that some of these discrepancies are due to difficulties in obtaining accurate calibration curves as described above. Variations in levels of copper contamination may also contribute to observed discrepancies. Although the results suggest complicated ligand speciation, the available information is insufficient to provide a complete description of ligand and metal speciation in this system.

CONCLUSION

Fluorescent complexing agents are a powerful tool for determining ligand and metal speciation. Application of this technique, however, is difficult due to problems in accurately calibrating the fluorescence-Calcein concentration relationship and to complicated ligand speciation.

With these caveats, the conditional stability constants for Cu-Calcein binding may be estimated from fluorescence quenching, amperometric and ligand competition experiments. Our results demonstrate formation of both 1:1 and 2:1 CuCalcein complexes and suggest the formation of a fluorescent ternary complex.

REFERENCES

Bandrowski, J.F. and C.L. Benson (1972) Clin. Chem. 18: 1411-1414.

Brittain, H.G. (1987) Anal. Chem. 59: 1122-5.

Diehl,H. and J.L. Ellingboe (1956) Anal. Chem. 5: 882-4.

Hefley, A.J. and B. Jaselskis (1974) Anal. Chem. 46: 2036-8.

Hering J.G. and F.M.M. Morel, submitted to Environ. Sci. Technol.

Hering, J.G, W.G. Sunda, R.F. Ferguson and F.M.M. Morel (1987) Mar. Chem. 20: 299-312.

Kepner,B. and D.M. Hercules (1963) Anal. Chem. 35: 1238-40.

Markuszewski, R. (1976) Ph.D. Thesis. Iowa State University, Ames, Iowa.

Martin, D.B. (1977) Ph.D Thesis. Iowa State University. Ames, Iowa.

Matson, W., E. Zink, R. Vitukevitch (1977) Am. Lab. 9: 59-73.

Miyahara, T. (1977) Bunseki Kagaku 26: 615-20 (Chem. Abst. 88:28,490a).

Pribil, R. (1982) Applied Complexometry, Oxford: Pergammon Press.

Saari, L.A. and W.R. Weitz (1984) Anal. Chem. 56: 810-3.

Tovar-Grau, J., C.L. Graham, and M.B. Hayes (1983) Anal. Proc. 20: 125-7.

Waite, T.D. and F.M.M. Morel (1983) Anal. Chem. 55: 1268-74.

Wallach, D.F.H. and T.L. Steck (1963) Anal. Chem 35: 1035-44.

Wallach, D.F.H., D.M. Surgenor, J. Soderberg, E. Delano (1959) Anal. Chem. 31: 456-60.

Westall, J.C. (1982) Technical Report, Dept. of Chem., Oregon State University, Corvallis, OR.

Westall, J.C., J.L. Zachary and F.M.M. Morel (1976) R.M. Parsons Laboratory, Technical Note 18, Massachusetts Institute of Technology, Cambridge, MA.

APPENDIX C

ANCILLARY DATA FOR CHAPTER FOUR

Experimental protocol is given in the text of Chapter 4.

METAL EXCHANGE EXPERIMENTS DATA SUMMARY
MEXDAT.WK1

CALCIUM EXPERIMENTS METEX 1-15

METEX1	
DATE	2/12/86
log CaT	-5.0
pH	8.5
CuT	25 nM
CaEDTA T	112.5 nM
analysis	2nd ord
# pts	6
% rxn	76

time (min)	Cu (nM)
0	
1.7	16.6
3.2	12.8
4.7	10.2
6.1	8.5
7.6	7.1
9.1	6
10.5	5.3
12	4.7

METEX2	
DATE	3/23/86
log CaT	-5.0
pH	8.2
CuT	37.5 nM
CaEDTA T	75 nM
analysis	2nd ord
# pts	4
% rxn	67

time (min)	Cu (nM)
0	
1.7	22.5
3.2	17.8
4.7	15.1
6.2	12.8
7.7	11.3
9.2	10.1
10.7	9.4
12.2	8.6
13.7	7.9

METEX3	
DATE	1/6/86
log CaT	-5.0
pH	7.9
CuT	37.5 nM
CaEDTA T	128 nM
analysis	2nd ord
# pts	3
% rxn	86

time (min)	Cu (nM)
0	
1.5	12.4
3	7
4.4	4.8
5.9	3.7
7.3	3.2
8.7	2.7
10.2	2.4
11.6	2.2

METEX4	
DATE	1/5/86(b)
log CaT	-4.9
pH	7.9
CuT	25 nM
CaEDTA T	150 nM
analysis	2nd ord
# pts	3
% rxn	85

time (min)	Cu (nM)
0	
1.6	10.9
3.1	5.7
4.6	3.7
6.1	2.7
7.7	2.1
9.1	1.8
10.6	1.5
12.1	1.4

METEX5	
DATE	2/24/86
log CaT	-4.5
pH	8.2
*CuT	37.5 nM
CaEDTA T	750 nM
analysis	2nd ord
# pts	5
% rxn	64

time (min)	Cu (nM)
0	
1.7	26.4
3.2	21
4.7	17.6
6.2	14.8
7.7	12.8
9	11.5
10.7	10.1
12.2	9.1
13.7	8.1
15.2	7.3
16.7	6.8
18.2	6.2

* apparent initial Cu 36.9 nM

METEX6	
DATE	2/22/86
log CaT	-4.0
pH	8.3
CuT	37.5 nM
CaEDTA T	750 nM
analysis	1st ord
# pts	5
% rxn	86

time (min)	Cu (nM)
0	
1.7	20.5
3.3	13.3
4.8	9.2
6.4	6.8
7.9	5.4
9.5	4.3
11.1	3.7
12.6	3.3
14.2	2.7
15.7	2.6
17.3	2.1
18.7	2.1

METEX7	
DATE	3/22/86
log CaT	-3.8
pH	8.2
CuT	37.5 nM
CaEDTA T	375 nM
analysis	1st ord
# pts	8
% rxn	74

time (min)	Cu (nM)
0	
1.7	28.6
3.2	24.2
4.7	20.4
6.2	17.2
7.7	14.9
9.2	12.8
10.7	11.3
12.2	9.9
13.7	8.7
15.2	7.8
16.7	7
18.2	6.4
19.7	5.7

METEX8	
DATE	2/25/86
log CaT	-3.4
pH	8.2
CuT	37.5 nM
CaEDTA T	750 nM
analysis	1st ord
# pts	8
% rxn	78

time (min)	Cu (nM)
0	
1.7	27.4
3.2	23.2
4.7	19
6.2	15.7
7.7	13.4
9.2	11.1
10.7	9.6
12.2	8.3
13.7	7.2
15.2	6.4

METEX9

DATE	2/10/86
log CaT	-3.0
pH	8.3
CuT	25 nM
CaEDTA T	112.5 nM
analysis	1st ord
# pts	14
% rxn	20

time (min)	Cu (nM)
0	
3.1	23.7
4.6	23.3
6	22.7
7.5	22.5
9	22.3
10.4	21.9
11.9	21.7
13.3	21.5
14.8	21.2
16.2	20.7
17.7	20.3
19.2	20.1
20.7	20.1
22.1	19.9
23.6	19.5
25	19.1
26.5	19.1
28	18.7
29.4	18.5

METEX10

DATE	2/13/86
log CaT	-3.0
pH	8.2
CuT	25 nM
CaEDTA T	750 nM
analysis	1st ord
# pts	14
% rxn	72

time (min)	Cu (nM)
0	
1.7	21.6
3.2	19.7
4.7	18.1
6.1	16.5
7.6	15.2
9.1	13.9
10.6	12.9
12	12
14.9	10.2
16.4	9.6
17.9	8.8
19.3	8.3
20.8	7.6
22.3	7.2
23.8	6.9

METEX11

DATE	2/28/86
log CaT	-2.5
pH	8.2
CuT	37.5 nM
CaEDTA T	750 nM
analysis	1st ord
# pts	13
% rxn	60

time (min)	Cu (nM)
0	
1.7	32.9
3.2	30.9
4.7	28.7
6.2	26.6
7.7	24.9
9.1	23.1
10.6	21.8
12.1	20.3
13.6	19.1
15.1	17.7
16.6	16.5
18.1	15.8
19.5	14.9
21	13.9
22.5	13.1
24	12.5
25.5	11.7
26.9	11.2
28.5	10.7

METEX12

DATE	1/31/86
log CaT	-2.0
pH	8.2
CuT	25 nM
CaEDTA T	750 nM
analysis	1st ord
# pts	13
% rxn	56

time (min)	Cu (nM)
0	
1.7	22.9
3.2	21.1
4.7	19.6
6.2	18.2
7.7	17.3
9.3	16.2
10.8	15.2
12.3	14.3
13.8	13.6
15.3	12.8
16.8	12.3
18.4	11.8
19.9	10.9
21.4	10.5
22.9	9.7
24.5	9.2

METEX13

DATE	2/9/86
log CaT	-2.0
pH	8.3
CuT	25 nM
CaEDTA T	112.5 nM
analysis	1st ord
# pts	27
% rxn	27

time (min)	Cu (nM)
0	
1.6	25.2
3.1	24
4.5	23.8
6	23.6
7.5	23.2
8.9	22.8
10.4	22.6
11.9	22.5
13.3	22.2
14.8	22
16.2	21.8
17.7	21.4
19.1	21.2
20.6	21.1
25	20.5
26.5	20.3
27.9	20
29.4	20
30.8	17.4
32.3	19.4
33.8	19.1
35.2	19.1
36.7	18.9
38.2	18.9
39.6	18.6
41.1	18.4
42.5	18.3

METEX14

DATE	7/24/85
log CaT	-2.0(SSW)
pH	8.3
CuT	37.5 nM
CaEDTA T	1250 nM
analysis	1st ord
# pts	8
% rxn	60

time (min)	Cu (nM)
0	
1.7	32.1
3.2	28.2
4.8	24.8
6.3	22.2
7.8	20
9.4	17.9
10.9	16.3
12.4	15
14	13.5
15.5	12.6
17.1	11.5
18.6	10.6
20.1	9.8

METEX15

DATE	7/30/85
log CaT	-2.0(SSW)
pH	8.3
CuT	37.5 nM
CaEDTA T	125 nM
analysis	1st ord
# pts	13
% rxn	27

time (min)	Cu (nM)
0	
1.6	36.8
3.2	35.9
4.7	35.2
6.3	34.8
7.8	34.2
9.7	33.7
10.9	33.1
12.5	32.7
14	32.2
31.8	29.3
33.3	28.5
34.9	28.3
36.5	27.7

MAGNESIUM EXPERIMENTS METEX 16-25

METEX16

DATE	3/12/86
log MgT	-3.85
pH	8.2
*CuT	37.5 nM
MgEDTA T	62.5 nM
analysis	2nd ord
# pts	2
% rxn	65

time (min)	Cu (nM)
0	
1.7	15.5
3.2	12.2
4.7	10
6.2	8.8
7.7	8
9.2	8.1
10.7	7.2

* apparent initial Cu 36.7 nM

METEX17

DATE	3/13/86-a
log MgT	-3.8
pH	8.2
CuT	37.5 nM
MgEDTA T	62.5 nM
analysis	2nd ord
# pts	2
% rxn	75

time (min)	Cu (nM)
0	
1.7	14.6
3.2	9.8
4.7	7.5
6.2	6
7.7	5.2
9.2	4.6
10.7	3.9

METEX19

DATE	3/15/86
log MgT	-3.5
pH	8.2
*CuT	37.5 nM
MgEDTA T	62.5 nM
analysis	2nd ord
# pts	2
% rxn	65

time (min)	Cu (nM)
0	
1.7	16.9
3.2	12.1
4.7	9.4
6.2	7.5
7.7	6.4
9.2	5.8
10.7	5

*apparent initial Cu 36.3 nM

METEX20

DATE	3/18/86
log MgT	-3.0
pH	8.2
CuT	37.5 nM
MgEDTA T	62.5 nM
analysis	2nd ord
# pts	6
% rxn	56

time (min)	Cu (nM)
0	
1.7	26.2
3.2	22.7
4.7	20.4
6.2	18.6
7.7	17.3
9.3	16.3
10.8	15.7
12.3	15.1
13.8	14.5
15.3	14.2

METEX21	
DATE	3/13/86-b
log MgT	-2.5
pH	8.2
CuT	37.5 nM
MgEDTA T	62.5 nM
analysis	2nd ord
# pts	5
% rxn	53

time (min)	Cu (nM)
0	
1.7	29.7
3.2	26.2
4.7	22.9
6.2	20.6
7.7	18.6
9.2	17
10.7	15.6
12.2	14.4
13.7	13.3
15.2	12.7

METEX22	
DATE	3/4/86-b
log MgT	-1.9
pH	8.3
*CuT	37.5 nM
MgEDTA T	62.5 nM
analysis	2nd ord
# pts	14
% rxn	44

time (min)	Cu (nM)
0	
1.7	27.9
3.2	26.6
4.7	24.8
6.2	23.6
7.7	22.6
9.2	21.3
10.7	20
12	19.2
13.6	18.5
15.2	17.8
16.6	16.8
18.1	16.3
19.6	15.9

* apparent initial Cu 31.5 nM

METEX23	
DATE	3/4/86-a
log MgT	-1.6
pH	8.2
*CuT	37.5 nM
MgEDTA T	62.5 nM
analysis	2nd ord
# pts	16
% rxn	53

time (min)	Cu (nM)
0	
3.3	28.2
4.7	26.4
6.2	24.9
7.7	23.6
9.2	22.3
10.7	21
12.2	19.8
13.7	18.9
15.2	18.1
16.7	17.4
18.2	16.7
19.7	16.2
21.1	15.5
32.6	14.9
34.1	14.4

* apparent initial Cu 34.3 nM

METEX24

DATE	3/3/86
log MgT	-1.3
pH	8.2
*CuT	37.5 nM
MgEDTA T	62.5 nM
analysis	2nd ord
# pts	20
% rxn	53

time (min)	Cu (nM)
0	
1.7	31.2
3.2	29.8
4.7	28.1
6.2	26.7
7.7	25.7
9.2	24.5
10.6	23.6
12.1	22.6
13.6	21.6
15.1	20.8
16.6	19.9
18.1	19.4
19.6	18.7
21	18.1
22.5	17.5
24	16.7
25.5	16.3
27	15.9
28.5	15.4

* apparent initial Cu 35.0 nM

METEX25

DATE	8/20/85
log MgT	-1.3
pH	8.0
CuT	37.5 nM
MgEDTA T	62.5 nM
analysis	2nd ord
# pts	19
% rxn	72

time (min)	Cu (nM)
0	
1.6	33.6
3.2	31
4.7	28.1
6.3	25.4
7.9	23.7
9.4	21.9
11	20.4
12.5	19.2
14.1	18.3
15.7	17.1
17.2	16.3
18.8	15.7
20.3	14.6
21.8	13.9
23.5	13.7
25	12.8
26.5	12.3
28.1	11.9
29.6	11.4

APPENDIX D

ANCILLARY DATA FOR CHAPTER FIVE

Experimental protocol is given in the text of Chapter 5.

LIGAND EXCHANGE 10/22 A
CuNTA + D to CuD + NTA
Dye(BD) 1.00E-07
Cu(BD) 1.00E-07
NTA(BD) 2.00E-06

time (sec)	RFU(10)	D (obs) nM
0.00E+00		
2.00E+01	7.57E+02	5.19E+01
3.00E+01	7.59E+02	5.21E+01
4.00E+01	7.64E+02	5.24E+01
5.00E+01	7.52E+02	5.16E+01
6.00E+01	7.45E+02	5.11E+01
7.00E+01	7.57E+02	5.20E+01
9.00E+01	7.51E+02	5.15E+01
1.00E+02	7.54E+02	5.17E+01
1.10E+02	7.55E+02	5.18E+01
1.20E+02	7.46E+02	5.12E+01
1.30E+02	7.34E+02	5.03E+01
1.40E+02	7.33E+02	5.03E+01
1.50E+02	7.36E+02	5.05E+01
1.60E+02	7.17E+02	4.92E+01
1.70E+02	7.23E+02	4.96E+01
1.80E+02	7.17E+02	4.92E+01
1.90E+02	7.12E+02	4.89E+01
2.00E+02	7.06E+02	4.85E+01
2.10E+02	7.06E+02	4.85E+01
2.20E+02	7.06E+02	4.85E+01
2.30E+02	7.09E+02	4.86E+01
2.40E+02	7.08E+02	4.86E+01
2.50E+02	7.00E+02	4.80E+01
2.60E+02	7.04E+02	4.83E+01
2.70E+02	7.00E+02	4.80E+01
2.80E+02	7.00E+02	4.81E+01
2.90E+02	6.99E+02	4.80E+01
3.00E+02	6.91E+02	4.74E+01
3.10E+02	6.87E+02	4.71E+01
3.20E+02	6.95E+02	4.77E+01
3.30E+02	6.95E+02	4.77E+01
3.40E+02	6.87E+02	4.71E+01
3.50E+02	6.93E+02	4.75E+01
3.60E+02	6.92E+02	4.75E+01

LIGAND EXCHANGE 10/22 B
CuNTA + D to CuD + NTA
Dye(BD) 1.00E-07
Cu(BD) 1.00E-07
NTA(BD) 3.00E-06

time (sec)	RFU(10)	D (obs) nM
0.00E+00		
2.00E+01	7.60E+02	5.22E+01
3.00E+01	7.47E+02	5.13E+01
4.00E+01	7.42E+02	5.09E+01
5.00E+01	7.40E+02	5.07E+01
6.00E+01	7.42E+02	5.09E+01
7.00E+01	7.45E+02	5.11E+01
8.00E+01	7.42E+02	5.09E+01
9.00E+01	7.47E+02	5.13E+01
1.00E+02	7.49E+02	5.14E+01
1.10E+02	7.51E+02	5.15E+01
1.20E+02	7.45E+02	5.11E+01
1.30E+02	7.46E+02	5.12E+01
1.40E+02	7.41E+02	5.08E+01
1.50E+02	7.37E+02	5.06E+01
1.60E+02	7.31E+02	5.02E+01
1.70E+02	7.21E+02	4.95E+01
1.80E+02	7.23E+02	4.96E+01
1.90E+02	7.29E+02	5.00E+01
2.00E+02	7.28E+02	5.00E+01
2.10E+02	7.30E+02	5.01E+01
2.20E+02	7.23E+02	4.96E+01
2.40E+02	7.19E+02	4.93E+01
2.50E+02	7.27E+02	4.99E+01
2.60E+02	7.17E+02	4.92E+01
2.70E+02	7.16E+02	4.91E+01
2.80E+02	7.21E+02	4.95E+01
2.90E+02	7.17E+02	4.92E+01
3.00E+02	7.19E+02	4.93E+01
3.10E+02	7.14E+02	4.90E+01
3.20E+02	7.11E+02	4.88E+01
3.30E+02	7.12E+02	4.88E+01
3.40E+02	7.08E+02	4.86E+01
3.50E+02	7.10E+02	4.87E+01
3.60E+02	7.10E+02	4.87E+01

LIGAND EXCHANGE 10/22 C
CuNTA + D to CuD + NTA
Dye(BD) 1.00E-07
Cu(BD) 1.00E-07
NTA(BD) 4.00E-06

time (sec)	RFU(10)	D (obs) nM
0.00E+00		
2.00E+01	7.91E+02	5.43E+01
3.00E+01	7.92E+02	5.44E+01
4.00E+01	7.88E+02	5.41E+01
5.00E+01	7.93E+02	5.44E+01
6.00E+01	7.89E+02	5.42E+01
7.00E+01	7.88E+02	5.41E+01
8.00E+01	7.85E+02	5.39E+01
9.00E+01	7.80E+02	5.36E+01
1.00E+02	7.74E+02	5.31E+01
1.10E+02	7.72E+02	5.30E+01
1.20E+02	7.70E+02	5.29E+01
1.30E+02	7.73E+02	5.31E+01
1.40E+02	7.65E+02	5.25E+01
1.50E+02	7.66E+02	5.26E+01
1.60E+02	7.67E+02	5.26E+01
1.70E+02	7.65E+02	5.25E+01
1.80E+02	7.57E+02	5.19E+01
1.90E+02	7.59E+02	5.21E+01
2.00E+02	7.59E+02	5.21E+01
2.10E+02	7.54E+02	5.17E+01
2.20E+02	7.52E+02	5.16E+01
2.30E+02	7.60E+02	5.22E+01
2.40E+02	7.52E+02	5.16E+01
2.50E+02	7.50E+02	5.15E+01
2.60E+02	7.47E+02	5.13E+01
2.70E+02	7.52E+02	5.16E+01
2.80E+02	7.38E+02	5.06E+01
2.90E+02	7.39E+02	5.07E+01
3.00E+02	7.43E+02	5.10E+01
3.10E+02	7.40E+02	5.08E+01
3.20E+02	7.37E+02	5.06E+01
3.30E+02	7.36E+02	5.05E+01
3.40E+02	7.33E+02	5.03E+01
3.50E+02	7.30E+02	5.01E+01
3.60E+02	7.27E+02	4.99E+01

LIGAND EXCHANGE 10/22 D
CuNTA + D to CuD + NTA
Dye(BD) 2.00E-07
Cu(BD) 1.00E-07
NTA(BD) 2.00E-06

time (sec)	RFU scale	D (obs)
	5.00E+00	nM
0.00E+00		
2.00E+01	8.11E+02	1.11E+02
3.00E+01	8.12E+02	1.11E+02
4.00E+01	8.02E+02	1.10E+02
5.00E+01	8.08E+02	1.11E+02
6.00E+01	7.90E+02	1.08E+02
7.00E+01	7.81E+02	1.07E+02
8.00E+01	7.84E+02	1.08E+02
9.00E+01	7.86E+02	1.08E+02
1.00E+02	7.75E+02	1.06E+02
1.10E+02	7.76E+02	1.06E+02
1.20E+02	7.76E+02	1.07E+02
1.30E+02	7.85E+02	1.08E+02
1.40E+02	7.74E+02	1.06E+02
1.50E+02	7.72E+02	1.06E+02
1.60E+02	7.67E+02	1.05E+02
1.70E+02	7.64E+02	1.05E+02
1.80E+02	7.66E+02	1.05E+02
1.90E+02	7.64E+02	1.05E+02
2.00E+02	7.58E+02	1.04E+02
2.30E+02	7.51E+02	1.03E+02
2.40E+02	7.51E+02	1.03E+02
2.50E+02	7.39E+02	1.01E+02
2.60E+02	7.48E+02	1.03E+02
2.70E+02	7.47E+02	1.03E+02
2.80E+02	7.46E+02	1.02E+02
2.90E+02	7.29E+02	1.00E+02
3.00E+02	7.38E+02	1.01E+02
3.10E+02	7.35E+02	1.01E+02
3.20E+02	7.34E+02	1.01E+02
3.30E+02	7.41E+02	1.02E+02
3.40E+02	7.37E+02	1.01E+02
3.50E+02	7.34E+02	1.01E+02
3.60E+02	7.35E+02	1.01E+02

LIGAND EXCHANGE 10/22 E
CuNTA + D to CuD + NTA
Dye(BD) 2.00E-07
Cu(BD) 1.00E-07
NTA(BD) 3.00E-06

time (sec)	RFU(5)	
0.00E+00		
2.00E+01	7.44E+02	1.02E+02
3.00E+01	7.53E+02	1.03E+02
4.00E+01	7.52E+02	1.03E+02
5.00E+01	7.50E+02	1.03E+02
6.00E+01	7.43E+02	1.02E+02
7.00E+01	7.43E+02	1.02E+02
8.00E+01	7.36E+02	1.01E+02
9.00E+01	7.55E+02	1.04E+02
1.00E+02	7.50E+02	1.03E+02
1.10E+02	7.48E+02	1.03E+02
1.20E+02	7.42E+02	1.02E+02
1.30E+02	7.33E+02	1.01E+02
1.40E+02	7.28E+02	9.99E+01
1.50E+02	7.19E+02	9.87E+01
1.60E+02	7.21E+02	9.90E+01
1.70E+02	7.21E+02	9.89E+01
1.80E+02	7.21E+02	9.90E+01
1.90E+02	7.15E+02	9.81E+01
2.00E+02	7.21E+02	9.89E+01
2.10E+02	7.21E+02	9.89E+01
2.20E+02	7.19E+02	9.87E+01
2.30E+02	7.09E+02	9.73E+01
2.40E+02	7.14E+02	9.80E+01
2.50E+02	7.14E+02	9.80E+01
2.60E+02	7.11E+02	9.75E+01
2.70E+02	7.12E+02	9.77E+01
2.80E+02	7.09E+02	9.73E+01
2.90E+02	7.10E+02	9.74E+01
3.00E+02	7.07E+02	9.70E+01
3.10E+02	7.05E+02	9.67E+01
3.20E+02	7.06E+02	9.68E+01
3.30E+02	7.05E+02	9.67E+01
3.40E+02	7.02E+02	9.63E+01
3.50E+02	6.99E+02	9.59E+01
3.60E+02	6.91E+02	9.48E+01

LIGAND EXCHANGE 10/22 F
CuNTA + D to CuD + NTA
Dye(BD) 2.00E-07
Cu(BD) 1.00E-07
NTA(BD) 4.00E-06

time (sec)	RFU(5)	D (obs) nM
0.00E+00		
2.00E+01	7.91E+02	1.09E+02
3.00E+01	7.82E+02	1.07E+02
4.00E+01	7.76E+02	1.06E+02
5.00E+01	7.71E+02	1.06E+02
6.00E+01	7.70E+02	1.06E+02
7.00E+01	7.69E+02	1.06E+02
8.00E+01	7.64E+02	1.05E+02
9.00E+01	7.59E+02	1.04E+02
1.00E+02	7.68E+02	1.05E+02
1.10E+02	7.64E+02	1.05E+02
1.20E+02	7.61E+02	1.04E+02
1.30E+02	7.65E+02	1.05E+02
1.40E+02	7.66E+02	1.05E+02
1.50E+02	7.61E+02	1.04E+02
1.60E+02	7.62E+02	1.05E+02
1.70E+02	7.56E+02	1.04E+02
1.80E+02	7.55E+02	1.04E+02
1.90E+02	7.54E+02	1.03E+02
2.00E+02	7.51E+02	1.03E+02
2.10E+02	7.47E+02	1.03E+02
2.20E+02	7.46E+02	1.02E+02
2.30E+02	7.42E+02	1.02E+02
2.40E+02	7.44E+02	1.02E+02
2.50E+02	7.40E+02	1.02E+02
2.60E+02	7.41E+02	1.02E+02
2.70E+02	7.35E+02	1.01E+02
2.80E+02	7.35E+02	1.01E+02
2.90E+02	7.32E+02	1.01E+02
3.00E+02	7.32E+02	1.01E+02
3.10E+02	7.35E+02	1.01E+02
3.20E+02	7.39E+02	1.01E+02
3.30E+02	7.34E+02	1.01E+02
3.40E+02	7.34E+02	1.01E+02
3.50E+02	7.32E+02	1.00E+02
3.60E+02	7.27E+02	9.98E+01

LIGAND EXCHANGE 10/22 G
CuNTA + D to CuD + NTA
Dye(BD) 2.00E-08
Cu(BD) 1.00E-07
NTA(BD) 3.00E-07

time (sec)	RFU(20)	D (obs) nM
0.00E+00		
2.00E+01	2.38E+02	8.16E+00
3.00E+01	2.29E+02	7.85E+00
4.00E+01	2.35E+02	8.06E+00
5.00E+01	2.28E+02	7.83E+00
6.00E+01	2.27E+02	7.79E+00
7.00E+01	2.30E+02	7.88E+00
8.00E+01	2.27E+02	7.[illegible]00
9.00E+01	2.25E+02	7.[illegible]+00
1.00E+02	2.21E+0[illegible]	[illegible]+00
1.10E+02	2.16E+02	[illegible]E+00
1.20E+02	2.16E+02	7.41E+00
1.30E+02	2.15E+02	7.36E+00
1.40E+02	2.14E+02	7.33E+00
1.50E+02	2.09E+02	7.18E+00
1.60E+02	2.07E+02	7.10E+00
1.70E+02	2.09E+02	7.17E+00
1.80E+02	2.05E+02	7.05E+00
1.90E+02	2.06E+02	7.08E+00
2.00E+02	2.02E+02	6.93E+00
2.10E+02	2.01E+02	6.89E+00
2.20E+02	2.01E+02	6.89E+00
2.30E+02	1.97E+02	6.77E+00
2.40E+02	1.95E+02	6.70E+00
2.50E+02	1.97E+02	6.75E+00
2.60E+02	1.97E+02	6.75E+00
2.70E+02	1.91E+02	6.54E+00
2.80E+02	1.90E+02	6.52E+00
2.90E+02	1.86E+02	6.39E+00
3.00E+02	1.83E+02	6.29E+00
3.10E+02	1.81E+02	6.21E+00
3.20E+02	1.82E+02	6.26E+00
3.30E+02	1.82E+02	6.25E+00
3.40E+02	1.77E+02	6.06E+00
3.50E+02	1.77E+02	6.06E+00
3.60E+02	1.75E+02	6.01E+00

LIGAND EXCHANGE 10/22 H

CuNTA + D to CuD + NTA
Dye(BD) 2.00E-08
Cu(BD) 1.00E-07
NTA(BD) 4.50E-07

time (sec)	RFU(20)	
0.00E+00		
2.00E+01	2.82E+02	9.67E+00
3.00E+01	2.77E+02	9.49E+00
4.00E+01	2.78E+02	9.55E+00
5.00E+01	2.77E+02	9.50E+00
6.00E+01	2.72E+02	9.32E+00
7.00E+01	2.73E+02	9.35E+00
8.00E+01	2.73E+02	9.37E+00
9.00E+01	2.75E+02	9.44E+00
1.00E+02	2.71E+02	9.30E+00
1.10E+02	2.72E+02	9.32E+00
1.20E+02	2.71E+02	9.29E+00
1.30E+02	2.67E+02	9.17E+00
1.40E+02	2.68E+02	9.21E+00
1.50E+02	2.66E+02	9.13E+00
1.60E+02	2.63E+02	9.04E+00
1.70E+02	2.63E+02	9.04E+00
1.80E+02	2.64E+02	9.06E+00
1.90E+02	2.62E+02	8.98E+00
2.00E+02	2.58E+02	8.85E+00
2.10E+02	2.55E+02	8.76E+00
2.20E+02	2.52E+02	8.63E+00
2.30E+02	2.48E+02	8.52E+00
2.40E+02	2.47E+02	8.47E+00
2.50E+02	2.46E+02	8.44E+00
2.60E+02	2.44E+02	8.38E+00
2.70E+02	2.46E+02	8.44E+00
2.80E+02	2.42E+02	8.31E+00
2.90E+02	2.42E+02	8.30E+00
3.00E+02	2.39E+02	8.21E+00
3.10E+02	2.40E+02	8.22E+00
3.[illegible]E+02	2.41E+02	8.26E+00
3.30E+02	2.38E+02	8.16E+00
3.40E+02	2.34E+02	8.04E+00
3.50E+02	2.33E+02	8.00E+00
3.60E+02	2.32E+02	7.97E+00

IIGAND EXCHANGE 10/22 J
CuNTA + D to CuD + NTA
Dye(BD) 4.00E-08
Cu(BD) 1.00E-07
NTA(BD) 3.00E-07

time (sec)	RFU(10)	D (obs) nM
0.00E+00		
2.00E+01	2.92E+02	2.00E+01
3.00E+01	2.85E+02	1.95E+01
4.00E+01	2.83E+02	1.94E+01
5.00E+01	2.82E+02	1.93E+01
6.00E+01	2.79E+02	1.91E+01
7.00E+01	2.76E+02	1.89E+01
8.00E+01	2.74E+02	1.88E+01
9.00E+01	2.72E+02	1.86E+01
1.00E+02	2.70E+02	1.85E+01
1.10E+02	2.68E+02	1.84E+01
1.20E+02	2.61E+02	1.79E+01
1.30E+02	2.61E+02	1.79E+01
1.40E+02	2.53E+02	1.74E+01
1.50E+02	2.55E+02	1.75E+01
1.60E+02	2.52E+02	1.73E+01
1.70E+02	2.48E+02	1.70E+01
1.80E+02	2.48E+02	1.70E+01
1.90E+02	2.46E+02	1.69E+01
2.00E+02	2.45E+02	1.68E+01
2.10E+02	2.42E+02	1.66E+01
2.20E+02	2.42E+02	1.66E+01
2.30E+02	2.40E+02	1.65E+01
2.40E+02	2.35E+02	1.61E+01
2.50E+02	2.36E+02	1.62E+01
2.50E+02	2.35E+02	1.61E+01
2.70E+02	2.32E+02	1.59E+01
2.80E+02	2.30E+02	1.58E+01
2.90E+02	2.29E+02	1.57E+01
3.00E+02	2.27E+02	1.56E+01
3.10E+02	2.25E+02	1.54E+01
3.20E+02	2.22E+02	1.53E+01
3.30E+02	2.20E+02	1.51E+01
3.40E+02	2.19E+02	1.50E+01
3.50E+02	2.21E+02	1.52E+01
3.60E+02	2.16E+02	1.48E+01

LIGAND EXCHANGE 10/22 K
CuNTA + D to CuD + NTA
Dye(BD) 4.00E-08
Cu(BD) 1.00E-07
NTA(BD) 4.50E-07

time (sec)	RFU(10)	D (obs) nM
0.00E+00		
2.00E+01	2.91E+02	1.99E+01
3.00E+01	2.89E+02	1.99E+01
4.00E+01	2.88E+02	1.97E+01
5.00E+01	2.84E+02	1.95E+01
6.00E+01	2.84E+02	1.95E+01
7.00E+01	2.81E+02	1.93E+01
8.00E+01	2.84E+02	1.95E+01
9.00E+01	2.78E+02	1.91E+01
1.00E+02	2.74E+02	1.88E+01
1.10E+02	2.73E+02	1.87E+01
1.20E+02	2.71E+02	1.86E+01
1.30E+02	2.69E+02	1.85E+01
1.40E+02	2.67E+02	1.83E+01
1.50E+02	2.65E+02	1.82E+01
1.60E+02	2.65E+02	1.82E+01
1.70E+02	2.64E+02	1.81E+01
1.80E+02	2.62E+02	1.80E+01
1.90E+02	2.57E+02	1.76E+01
2.00E+02	2.57E+02	1.76E+01
2.10E+02	2.55E+02	1.75E+01
2.20E+02	2.53E+02	1.73E+01
2.30E+02	2.53E+02	1.74E+01
2.40E+02	2.49E+02	1.71E+01
2.50E+02	2.47E+02	1.70E+01
2.60E+02	2.49E+02	1.71E+01
2.70E+02	2.45E+02	1.68E+01
2.80E+02	2.46E+02	1.69E+01
2.90E+02	2.46E+02	1.69E+01
3.00E+02	2.44E+02	1.68E+01
3.10E+02	2.44E+02	1.67E+01
3.20E+02	2.43E+02	1.67E+01
3.30E+02	2.42E+02	1.66E+01
3.40E+02	2.41E+02	1.65E+01
3.50E+02	2.40E+02	1.65E+01
3.60E+02	2.37E+02	1.63E+01

LIGAND EXCHANGE 10/22 L
CuNTA + D to CuD + NTA
Dye(BD) 4.00E-08
Cu(BD) 1.00E-07
NTA(BD) 6.00E-07

time (sec)	RFU(10)	D (obs) nM
0.00E+00		
2.00E+01	2.99E+02	2.05E+01
3.00E+01	2.98E+02	2.04E+01
4.00E+01	2.93E+02	2.01E+01
5.00E+01	2.94E+02	2.02E+01
6.00E+01	2.92E+02	2.00E+01
7.00E+01	2.93E+02	2.01E+01
8.00E+01	2.89E+02	1.98E+01
9.00E+01	2.86E+02	1.96E+01
1.00E+02	2.83E+02	1.94E+01
1.10E+02	2.83E+02	1.94E+01
1.20E+02	2.84E+02	1.95E+01
1.30E+02	2.81E+02	1.93E+01
1.40E+02	2.81E+02	1.93E+01
1.50E+02	2.76E+02	1.90E+01
1.60E+02	2.74E+02	1.88E+01
1.70E+02	2.73E+02	1.87E+01
1.80E+02	2.73E+02	1.87E+01
1.90E+02	2.68E+02	1.84E+01
2.00E+02	2.70E+02	1.86E+01
2.10E+02	2.68E+02	1.84E+01
2.20E+02	2.69E+02	1.84E+01
2.30E+02	2.69E+02	1.85E+01
2.40E+02	2.65E+02	1.82E+01
2.50E+02	2.63E+02	1.80E+01
2.60E+02	2.64E+02	1.81E+01
2.70E+02	2.60E+02	1.78E+01
2.80E+02	2.58E+02	1.77E+01
2.90E+02	2.59E+02	1.77E+01
3.00E+02	2.56E+02	1.76E+01
3.10E+02	2.57E+02	1.77E+01
3.20E+02	2.59E+02	1.77E+01
3.30E+02	2.54E+02	1.75E+01
3.40E+02	2.55E+02	1.75E+01
3.50E+02	2.54E+02	1.74E+01
3.60E+02	2.53E+02	1.73E+01

LIGAND EXCHANGE 9/30 #1A
CuNTA + D to CuD + NTA

init para Cu(bd)	data time(sec)	RFU	D (obs) nM
1.00E-07	0.00E+00		
dye(bd)	2.30E+01	5.12E+02	8.31E+00
2.00E-08	3.70E+01	4.70E+02	7.63E+00
lig(bd)	4.90E+01	4.53E+02	7.36E+00
1.20E-07	5.90E+01	4.39E+02	7.12E+00
	6.90E+01	4.25E+02	6.90E+00
	8.00E+01	3.98E+02	6.45E+00
	9.00E+01	3.82E+02	6.20E+00
	1.00E+02	3.66E+02	5.93E+00
cal slope	1.10E+02	3.48E+02	5.64E+00
6.16E+01	1.20E+02	3.33E+02	5.41E+00
	1.30E+02	3.15E+02	5.11E+00
	1.45E+02	3.01E+02	4.88E+00
	1.57E+02	2.93E+02	4.75E+00
	1.69E+02	2.82E+02	4.58E+00
	1.81E+02	2.69E+02	4.36E+00
	1.90E+02	2.63E+02	4.26E+00
	1.99E+02	2.56E+02	4.15E+00
	2.10E+02	2.45E+02	3.97E+00
	2.20E+02	2.33E+02	3.78E+00
	2.30E+02	2.31E+02	3.75E+00
	2.40E+02	2.18E+02	3.53E+00
	2.49E+02	2.18E+02	3.53E+00
	2.59E+02	2.04E+02	3.32E+00
	2.69E+02	2.04E+02	3.31E+00
	2.80E+02	1.96E+02	3.18E+00
	2.90E+02	1.93E+02	3.14E+00
	3.00E+02	1.87E+02	3.03E+00
	3.10E+02	1.78E+02	2.89E+00
	3.20E+02	1.75E+02	2.84E+00
	3.30E+02	1.69E+02	2.74E+00
	3.40E+02	1.68E+02	2.73E+00
	3.50E+02	1.58E+02	2.56E+00
	3.60E+02	1.57E+02	2.54E+00

LIGAND EXCHANGE 9/30 #1B

CuNTA + D to CuD + NTA

init para	data		D (obs)
Cu(bd)	time(sec)	RFU	nM
1.00E-07	0.00E+00		
dye(bd)	1.80E+01	5.37E+02	8.72E+00
2.00E-08	2.70E+01	5.01E+02	8.13E+00
lig(bd)	3.80E+01	4.80E+02	7.79E+00
1.20E-07	5.00E+01	4.43E+02	7.19E+00
	6.00E+01	4.32E+02	7.01E+00
	7.00E+01	4.09E+02	6.63E+00
	8.00E+01	3.96E+02	6.43E+00
	9.00E+01	3.90E+02	6.32E+00
cal slope	1.00E+02	3.73E+02	6.05E+00
6.16E+01	1.12E+02	3.49E+02	5.66E+00
	1.35E+02	3.24E+02	5.26E+00
	1.45E+02	3.12E+02	5.06E+00
	1.57E+02	3.00E+02	4.87E+00
	1.69E+02	2.83E+02	4.60E+00
	1.80E+02	2.65E+02	4.30E+00
	1.90E+02	2.55E+02	4.14E+00
	2.01E+02	2.49E+02	4.04E+00
error	2.10E+02	2.42E+02	3.92E+00
0.00E+00	2.20E+02	2.36E+02	3.83E+00
	2.30E+02	2.30E+02	3.73E+00
	2.40E+02	2.25E+02	3.65E+00
	2.50E+02	2.17E+02	3.51E+00
	2.60E+02	2.11E+02	3.42E+00
	2.70E+02	2.02E+02	3.27E+00
	2.80E+02	1.96E+02	3.18E+00
	2.90E+02	1.94E+02	3.15E+00
	3.00E+02	1.91E+02	3.09E+00
	3.10E+02	1.82E+02	2.96E+00
	3.20E+02	1.78E+02	2.88E+00
	3.30E+02	1.73E+02	2.80E+00
	3.39E+02	1.72E+02	2.79E+00
	3.49E+02	1.64E+02	2.66E+00
	3.60E+02	1.55E+02	2.51E+00

LIGAND EXCHANGE 9/30 #2

CuNTA + D to CuD + NTA

init para	data 9/30#2		D (obs)
Cu(bd)	time(sec)	RFU	nM
1.00E-07	0.00E+00		
dye(bd)	1.60E+01	5.35E+02	8.69E+00
2.00E-08	2.70E+01	5.24E+02	8.51E+00
lig(bd)	3.80E+01	5.01E+02	8.13E+00
1.60E-07	5.00E+01	4.79E+02	7.77E+00
	6.00E+01	4.70E+02	7.62E+00
	7.00E+01	4.51E+02	7.32E+00
	8.00E+01	4.39E+02	7.12E+00
	9.00E+01	4.27E+02	6.92E+00
cal slope	1.00E+02	4.29E+02	6.95E+00
6.16E+01	1.10E+02	4.13E+02	6.71E+00
	1.20E+02	3.98E+02	6.46E+00
	1.30E+02	4.02E+02	6.53E+00
	1.40E+02	3.95E+02	6.41E+00
	1.50E+02	3.82E+02	6.20E+00
	1.60E+02	3.78E+02	6.13E+00
	1.69E+02	3.70E+02	6.00E+00
	1.80E+02	3.62E+02	5.87E+00
	1.90E+02	3.65E+02	5.93E+00
	1.99E+02	3.52E+02	5.71E+00
	2.10E+02	3.48E+02	5.65E+00
	2.20E+02	3.44E+02	5.59E+00
	2.30E+02	3.29E+02	5.33E+00
	2.40E+02	3.34E+02	5.42E+00
	2.50E+02	3.33E+02	5.40E+00
	2.60E+02	3.22E+02	5.23E+00
	2.70E+02	3.18E+02	5.16E+00
	2.79E+02	3.12E+02	5.06E+00
	2.89E+02	3.00E+02	4.87E+00
	3.00E+02	3.00E+02	4.87E+00
	3.10E+02	2.93E+02	4.75E+00
	3.20E+02	2.88E+02	4.67E+00
	3.30E+02	2.76E+02	4.48E+00
	3.40E+02	2.71E+02	4.39E+00
	3.50E+02	2.60E+02	4.23E+00
	3.60E+02	2.65E+02	4.30E+00

LIGAND EXCHANGE 9/30 #3

CuNTa + D to CuD + NTA		
Dye(BD)	2.00E-08	
Cu(BD)	1.00E-07	
NTA(BD)	2.40E-07	
time (sec)	RFU(40)	
0.00E+00		
1.50E+01	5.66E+02	9.31E+00
2.60E+01	5.62E+02	9.23E+00
3.70E+01	5.61E+02	9.22E+00
4.80E+01	5.67E+02	9.32E+00
5.90E+01	5.53E+02	9.09E+00
7.00E+01	5.45E+02	8.96E+00
8.00E+01	5.34E+02	8.78E+00
9.10E+01	5.30E+02	8.72E+00
1.01E+02	5.24E+02	8.61E+00
1.10E+02	5.14E+02	8.45E+00
1.20E+02	5.06E+02	8.31E+00
1.31E+02	4.97E+02	8.17E+00
1.40E+02	4.89E+02	8.04E+00
1.50E+02	4.85E+02	7.98E+00
1.78E+02	4.76E+02	7.82E+00
1.88E+02	4.62E+02	7.59E+00
1.99E+02	4.51E+02	7.41E+00
2.10E+02	4.44E+02	7.29E+00
2.20E+02	4.48E+02	7.36E+00
2.30E+02	4.46E+02	7.34E+00
2.40E+02	4.28E+02	7.04E+00
2.49E+02	4.18E+02	6.87E+00
2.59E+02	4.27E+02	7.01E+00
2.70E+02	4.31E+02	7.08E+00
2.80E+02	4.32E+02	7.10E+00
2.90E+02	4.26E+02	7.00E+00
3.01E+02	4.08E+02	6.70E+00
3.11E+02	4.06E+02	6.67E+00
3.21E+02	3.97E+02	6.52E+00
3.31E+02	3.99E+02	6.56E+00
3.41E+02	3.95E+02	6.49E+00
3.50E+02	3.86E+02	6.35E+00
3.60E+02	3.86E+02	6.34E+00

LIGAND EXCHANGE 9/30 #4
CuNTA + D to CuD + NTA
Dye(BD) 2.00E-08
Cu(BD) 1.00E-07
NTA(BD) 4.00E-07

time (sec)	RFU(40)	
0.00E+00		
1.90E+01	5.49E+02	9.03E+00
3.00E+01	5.39E+02	8.87E+00
4.00E+01	5.37E+02	8.83E+00
5.00E+01	5.36E+02	8.80E+00
6.00E+01	5.30E+02	8.71E+00
7.00E+01	5.19E+02	8.53E+00
8.00E+01	5.20E+02	8.54E+00
9.00E+01	5.06E+02	8.31E+00
1.00E+02	5.11E+02	8.40E+00
1.10E+02	5.09E+02	8.37E+00
1.20E+02	5.08E+02	8.35E+00
1.30E+02	4.94E+02	8.11E+00
1.40E+02	5.05E+02	8.29E+00
1.50E+02	4.81E+02	7.90E+00
1.60E+02	4.84E+02	7.96E+00
1.70E+02	4.77E+02	7.84E+00
1.80E+02	4.75E+02	7.80E+00
1.90E+02	4.69E+02	7.71E+00
2.00E+02	4.69E+02	7.71E+00
2.10E+02	4.56E+02	7.49E+00
2.20E+02	4.58E+02	7.53E+00
2.30E+02	4.57E+02	7.51E+00
2.40E+02	4.58E+02	7.52E+00
2.50E+02	4.59E+02	7.54E+00
2.60E+02	4.50E+02	7.40E+00
2.70E+02	4.44E+02	7.31E+00
2.80E+02	4.50E+02	7.40E+00
2.90E+02	4.42E+02	7.27E+00
3.00E+02	4.39E+02	7.21E+00
3.10E+02	4.43E+02	7.29E+00
3.20E+02	4.39E+02	7.21E+00
3.30E+02	4.38E+02	7.19E+00
3.40E+02	4.30E+02	7.07E+00
3.50E+02	4.29E+02	7.05E+00
3.60E+02	4.18E+02	6.87E+00
3.70E+02	4.17E+02	6.85E+00
3.80E+02	4.23E+02	6.95E+00
3.90E+02	4.15E+02	6.82E+00
4.01E+02	3.98E+02	6.54E+00
4.10E+02	3.95E+02	6.49E+00
4.20E+02	4.05E+02	6.65E+00

LIGAND EXCHANGE 9/30 #6
CuNTA + D to CuD + NTA

init para Cu(bd)	data time(sec)	RFU	D (obs) nM
1.00E-07	0.00E+00		
dye(bd)	1.60E+01	5.56E+02	1.80E+01
4.00E-08	2.60E+01	5.35E+02	1.74E+01
lig(bd)	3.70E+01	5.11E+02	1.66E+01
1.20E-07	4.90E+01	4.83E+02	1.57E+01
	5.90E+01	4.72E+02	1.53E+01
	7.00E+01	4.55E+02	1.48E+01
	8.20E+01	4.36E+02	1.41E+01
	9.20E+01	4.24E+02	1.38E+01
cal slope	1.03E+02	4.08E+02	1.33E+01
3.08E+01	1.12E+02	3.98E+02	1.29E+01
	1.28E+02	3.81E+02	1.24E+01
	1.39E+02	3.78E+02	1.23E+01
	1.50E+02	3.65E+02	1.18E+01
	1.60E+02	3.61E+02	1.17E+01
	1.69E+02	3.49E+02	1.13E+01
	1.80E+02	3.40E+02	1.10E+01
	1.90E+02	3.27E+02	1.06E+01
	2.00E+02	3.21E+02	1.04E+01
	2.10E+02	3.17E+02	1.03E+01
	2.20E+02	3.06E+02	9.92E+00
	2.30E+02	2.97E+02	9.64E+00
	2.40E+02	2.91E+02	9.45E+00
	2.50E+02	2.85E+02	9.25E+00
	2.60E+02	2.82E+02	9.15E+00
	2.70E+02	2.74E+02	8.90E+00
	2.80E+02	2.69E+02	8.72E+00
	2.90E+02	2.61E+02	8.48E+00
	3.00E+02	2.60E+02	8.42E+00
	3.10E+02	2.51E+02	8.14E+00
	3.20E+02	2.49E+02	8.08E+00
	3.30E+02	2.47E+02	8.02E+00
	3.40E+02	2.45E+02	7.96E+00
	3.50E+02	2.38E+02	7.73E+00
	3.60E+02	2.37E+02	7.69E+00

LIGAND EXCHANGE 9/30 #7
CuNTA + D to CuD + NTA

init para Cu(bd)	data time(sec)	RFU	D (obs) nM
1.00E-07	0.00E+00		
dye(bd)	1.80E+01	6.00E+02	1.95E+01
4.00E-08	2.90E+01	5.95E+02	1.93E+01
lig(bd)	4.00E+01	5.84E+02	1.89E+01
1.60E-07	5.00E+01	5.78E+02	1.88E+01
	6.00E+01	5.65E+02	1.83E+01
	7.00E+01	5.48E+02	1.78E+01
	8.00E+01	5.38E+02	1.75E+01
	9.10E+01	5.21E+02	1.69E+01
cal slope	1.01E+02	5.11E+02	1.66E+01
3.08E+01	1.16E+02	4.94E+02	1.60E+01
	1.30E+02	4.89E+02	1.59E+01
	1.40E+02	4.83E+02	1.57E+01
	1.50E+02	4.76E+02	1.55E+01
	1.60E+02	4.65E+02	1.51E+01
	1.70E+02	4.61E+02	1.50E+01
	1.80E+02	4.53E+02	1.47E+01
	1.90E+02	4.43E+02	1.44E+01
	2.10E+02	4.39E+02	1.42E+01
	2.22E+02	4.17E+02	1.35E+01
	2.36E+02	4.06E+02	1.32E+01
	2.50E+02	3.92E+02	1.27E+01
	2.60E+02	3.84E+02	1.24E+01
	2.70E+02	3.81E+02	1.24E+01
	2.80E+02	3.72E+02	1.21E+01
	2.90E+02	3.63E+02	1.18E+01
	3.00E+02	3.60E+02	1.17E+01
	3.10E+02	3.58E+02	1.16E+01
	3.20E+02	3.54E+02	1.15E+01
	3.30E+02	3.54E+02	1.15E+01
	3.40E+02	3.45E+02	1.12E+01
	3.50E+02	3.46E+02	1.12E+01
	3.60E+02	3.43E+02	1.11E+01

LIGAND EXCHANGE 9/30 #8
CuNTA + D to CuD + NTA

init para	data		D (obs)
Cu(bd)	time(sec)	RFU	nM
1.00E-07	0.00E+00		
dye(bd)	2.00E+01	5.59E+02	1.81E+01
4.00E-08	3.00E+01	5.55E+02	1.80E+01
lig(bd)	4.00E+01	5.45E+02	1.77E+01
2.40E-07	5.00E+01	5.36E+02	1.74E+01
	6.00E+01	5.38E+02	1.75E+01
	7.00E+01	5.24E+02	1.70E+01
	8.00E+01	5.22E+02	1.69E+01
	9.00E+01	5.15E+02	1.67E+01
cal slope	1.00E+02	5.14E+02	1.67E+01
3.08E+01	1.10E+02	5.11E+02	1.66E+01
	1.20E+02	4.98E+02	1.62E+01
	1.30E+02	4.86E+02	1.58E+01
	1.40E+02	4.77E+02	1.55E+01
	1.50E+02	4.70E+02	1.53E+01
	1.60E+02	4.72E+02	1.53E+01
	1.70E+02	4.56E+02	1.48E+01
	1.80E+02	4.50E+02	1.46E+01
	1.90E+02	4.47E+02	1.45E+01
	2.00E+02	4.41E+02	1.43E+01
	2.10E+02	4.42E+02	1.43E+01
	2.20E+02	4.38E+02	1.42E+01
	2.30E+02	4.27E+02	1.39E+01
	2.40E+02	4.34E+02	1.41E+01
	2.50E+02	4.25E+02	1.38E+01
	2.60E+02	4.22E+02	1.37E+01
	2.70E+02	4.19E+02	1.36E+01
	2.80E+02	4.14E+02	1.34E+01
	2.90E+02	4.08E+02	1.32E+01
	3.00E+02	4.08E+02	1.32E+01
	3.10E+02	3.96E+02	1.29E+01
	3.20E+02	3.95E+02	1.28E+01
	3.30E+02	3.91E+02	1.27E+01
	3.40E+02	3.90E+02	1.27E+01
	3.50E+02	3.87E+02	1.26E+01
	3.60E+02	3.79E+02	1.23E+01

LIGAND EXCHANGE 9/30 #9
CuNTA + D to CuD + NTA
Dye(BD) 4.00E-08
Cu(BD) 1.00E-07
NTA(BD) 4.00E-07

time (sec)	RFU(20)	D (obs) nM
0.00E+00		
2.00E+01	5.92E+02	1.95E+01
3.00E+01	5.87E+02	1.93E+01
4.00E+01	5.83E+02	1.92E+01
5.00E+01	5.75E+02	1.89E+01
6.10E+01	5.68E+02	1.87E+01
7.10E+01	5.72E+02	1.88E+01
8.00E+01	5.66E+02	1.86E+01
9.00E+01	5.56E+02	1.83E+01
1.00E+02	5.53E+02	1.82E+01
1.20E+02	5.47E+02	1.80E+01
1.30E+02	5.37E+02	1.77E+01
1.40E+02	5.31E+02	1.74E+01
1.50E+02	5.32E+02	1.75E+01
1.60E+02	5.25E+02	1.73E+01
1.70E+02	5.13E+02	1.69E+01
1.80E+02	5.13E+02	1.69E+01
1.89E+02	5.08E+02	1.67E+01
2.00E+02	5.00E+02	1.64E+01
2.10E+02	5.04E+02	1.66E+01
2.20E+02	5.02E+02	1.65E+01
2.30E+02	4.97E+02	1.63E+01
2.40E+02	4.90E+02	1.61E+01
2.50E+02	4.98E+02	1.64E+01
2.60E+02	4.87E+02	1.60E+01
2.70E+02	4.89E+02	1.61E+01
2.80E+02	4.84E+02	1.59E+01
2.90E+02	4.82E+02	1.59E+01
3.00E+02	4.78E+02	1.57E+01
3.10E+02	4.77E+02	1.57E+01
3.20E+02	4.72E+02	1.55E+01
3.30E+02	4.67E+02	1.53E+01
3.40E+02	4.65E+02	1.53E+01
3.50E+02	4.64E+02	1.52E+01
3.60E+02	4.60E+02	1.51E+01
3.70E+02	4.52E+02	1.49E+01
3.80E+02	4.55E+02	1.49E+01
3.90E+02	4.51E+02	1.48E+01
4.00E+02	4.50E+02	1.48E+01
4.10E+02	4.45E+02	1.46E+01
4.20E+02	4.41E+02	1.45E+01

LIGAND EXCHANGE 9/30 #11
CuNTA + D to CuD + NTA

init para	data		D (obs)
Cu(bd)	time(sec)	RFU	nM
1.00E-07	0.00E+00		
dye(bd)	2.00E+01	5.86E+02	3.80E+01
8.00E-08	3.00E+01	5.74E+02	3.72E+01
lig(bd)	4.00E+01	5.55E+02	3.60E+01
1.20E-07	5.00E+01	5.47E+02	3.55E+01
	6.00E+01	5.39E+02	3.50E+01
	7.00E+01	5.33E+02	3.46E+01
	8.00E+01	5.27E+02	3.42E+01
	9.00E+01	5.21E+02	3.38E+01
cal slope	1.00E+02	5.06E+02	3.29E+01
1.54E+01	1.10E+02	4.98E+02	3.24E+01
	1.20E+02	4.80E+02	3.12E+01
	1.30E+02	4.68E+02	3.04E+01
	1.40E+02	4.62E+02	3.00E+01
	1.50E+02	4.55E+02	2.95E+01
	1.60E+02	4.45E+02	2.89E+01
	1.70E+02	4.43E+02	2.87E+01
	1.80E+02	4.25E+02	2.76E+01
	1.90E+02	4.24E+02	2.75E+01
	2.00E+02	4.18E+02	2.71E+01
	2.09E+02	4.12E+02	2.67E+01
	2.20E+02	4.08E+02	2.65E+01
	2.30E+02	3.96E+02	2.57E+01
	2.40E+02	3.94E+02	2.56E+01
	2.50E+02	3.88E+02	2.52E+01
	2.60E+02	3.90E+02	2.53E+01
	2.70E+02	3.88E+02	2.52E+01
	2.80E+02	3.80E+02	2.47E+01
	2.90E+02	3.76E+02	2.44E+01
	3.00E+02	3.68E+02	2.39E+01
	3.10E+02	3.53E+02	2.29E+01
	3.20E+02	3.59E+02	2.33E+01
	3.30E+02	3.57E+02	2.32E+01
	3.40E+02	3.55E+02	2.30E+01
	3.50E+02	3.52E+02	2.28E+01
	3.60E+02	3.47E+02	2.25E+01

LIGAND EXCHANGE 9/30 #12
CuNTA + D to CuD + NTA

init para	data		D (obs)
Cu(bd)	time(sec)	RFU	nM
1.00E-07	0.00E+00		
dye(bd)	1.90E+01	5.83E+02	3.78E+01
8.00E-08	3.00E+01	5.62E+02	3.64E+01
lig(bd)	4.00E+01	5.52E+02	3.58E+01
1.60E-07	5.00E+01	5.46E+02	3.55E+01
	6.00E+01	5.40E+02	3.50E+01
	7.00E+01	5.39E+02	3.50E+01
	8.00E+01	5.31E+02	3.44E+01
	9.00E+01	5.15E+02	3.35E+01
cal slope	1.00E+02	5.16E+02	3.35E+01
1.54E+01	1.10E+02	5.07E+02	3.29E+01
	1.20E+02	5.00E+02	3.24E+01
	1.30E+02	4.98E+02	3.23E+01
	1.40E+02	4.90E+02	3.18E+01
	1.50E+02	4.86E+02	3.15E+01
	1.60E+02	4.74E+02	3.08E+01
	1.70E+02	4.70E+02	3.05E+01
	1.80E+02	4.70E+02	3.05E+01
	1.90E+02	4.63E+02	3.00E+01
	2.00E+02	4.55E+02	2.96E+01
	2.10E+02	4.43E+02	2.88E+01
	2.20E+02	4.34E+02	2.82E+01
	2.30E+02	4.31E+02	2.80E+01
	2.40E+02	4.15E+02	2.69E+01
	2.50E+02	4.14E+02	2.68E+01
	2.60E+02	4.06E+02	2.64E+01
	2.70E+02	4.06E+02	2.63E+01
	2.80E+02	4.01E+02	2.60E+01
	2.90E+02	3.97E+02	2.58E+01
	3.00E+02	3.96E+02	2.57E+01
	3.10E+02	3.93E+02	2.55E+01
	3.20E+02	3.90E+02	2.53E+01
	3.30E+02	3.86E+02	2.51E+01
	3.40E+02	3.84E+02	2.49E+01
	3.50E+02	3.86E+02	2.50E+01
	3.60E+02	3.85E+02	2.50E+01

LIGAND EXCHANGE 9/30 #13
CuNTA + D to CuD + NTA

init para	data		D (obs)
Cu(bd)	time(sec)	RFU	nM
1.00E-07	0.00E+00		
dye(bd)	2.00E+01	5.93E+02	3.85E+01
8.00E-08	3.00E+01	5.89E+02	3.82E+01
lig(bd)	4.00E+01	5.90E+02	3.83E+01
2.40E-07	5.00E+01	5.69E+02	3.69E+01
	6.00E+01	5.64E+02	3.66E+01
	7.00E+01	5.73E+02	3.72E+01
	8.00E+01	5.40E+02	3.51E+01
	9.00E+01	5.44E+02	3.53E+01
cal slope	1.00E+02	5.39E+02	3.50E+01
1.54E+01	1.10E+02	5.34E+02	3.47E+01
	1.20E+02	5.37E+02	3.49E+01
	1.30E+02	5.14E+02	3.34E+01
	1.40E+02	5.23E+02	3.39E+01
	1.50E+02	5.18E+02	3.36E+01
	1.60E+02	5.05E+02	3.28E+01
	1.70E+02	5.14E+02	3.33E+01
	1.80E+02	4.99E+02	3.24E+01
	1.90E+02	4.98E+02	3.23E+01
	2.00E+02	4.90E+02	3.18E+01
	2.10E+02	4.78E+02	3.10E+01
	2.20E+02	4.77E+02	3.09E+01
	2.30E+02	4.64E+02	3.01E+01
	2.40E+02	4.68E+02	3.04E+01
	2.50E+02	4.66E+02	3.02E+01
	2.60E+02	4.66E+02	3.03E+01
	2.70E+02	4.68E+02	3.03E+01
	2.80E+02	4.68E+02	3.03E+01
	2.90E+02	4.60E+02	2.99E+01
	3.00E+02	4.65E+02	3.02E+01
	3.10E+02	4.60E+02	2.99E+01
	3.20E+02	4.55E+02	2.96E+01
	3.30E+02	4.55E+02	2.96E+01
	3.40E+02	4.46E+02	2.89E+01
	3.50E+02	4.47E+02	2.90E+01
	3.60E+02	4.35E+02	2.82E+01

LIGAND EXCHANGE 9/30 #14
CuNTA + D to CuD + NTA

init para	data		D (obs)
Cu(bd)	time(sec)	RFU	nM
1.00E-07	0.00E+00		
dye(bd)	2.00E+01	5.90E+02	3.83E+01
8.00E-08	3.00E+01	5.83E+02	3.78E+01
lig(bd)	4.00E+01	5.77E+02	3.74E+01
4.00E-07	5.00E+01	5.68E+02	3.69E+01
	6.00E+01	5.69E+02	3.69E+01
	7.00E+01	5.63E+02	3.65E+01
	8.00E+01	5.55E+02	3.60E+01
	9.00E+01	5.56E+02	3.61E+01
cal slope	1.00E+02	5.42E+02	3.52E+01
1.54E+01	1.10E+02	5.34E+02	3.47E+01
	1.20E+02	5.35E+02	3.47E+01
	1.30E+02	5.36E+02	3.48E+01
	1.40E+02	5.34E+02	3.46E+01
	1.50E+02	5.27E+02	3.42E+01
	1.60E+02	5.22E+02	3.39E+01
	1.70E+02	5.24E+02	3.40E+01
	1.80E+02	5.04E+02	3.27E+01
	1.90E+02	5.11E+02	3.31E+01
	2.00E+02	5.07E+02	3.29E+01
	2.10E+02	4.98E+02	3.23E+01
	2.20E+02	5.00E+02	3.24E+01
	2.30E+02	4.91E+02	3.19E+01
	2.40E+02	4.88E+02	3.17E+01
	2.50E+02	4.86E+02	3.15E+01
	2.60E+02	4.74E+02	3.07E+01
	2.70E+02	4.71E+02	3.06E+01
	2.80E+02	4.68E+02	3.04E+01
	2.90E+02	4.63E+02	3.00E+01
	3.00E+02	4.61E+02	2.99E+01
	3.10E+02	4.60E+02	2.99E+01
	3.20E+02	4.60E+02	2.99E+01
	3.30E+02	4.51E+02	2.93E+01
	3.40E+02	4.52E+02	2.94E+01
	3.50E+02	4.43E+02	2.88E+01
	3.60E+02	4.41E+02	2.87E+01
	3.70E+02	4.45E+02	2.89E+01
	3.80E+02	4.47E+02	2.90E+01
	3.89E+02	4.49E+02	2.91E+01
	4.00E+02	4.42E+02	2.87E+01
	4.10E+02	4.38E+02	2.84E+01
	4.20E+02	4.46E+02	2.90E+01

LIGAND EXCHANGE 9/30 #16
CuNTA + D to CuD + NTA

init para	data		D (obs)
Cu(bd)	time(sec)	RFU	nM
1.00E-07	0.00E+00		
dye(bd)	2.00E+01	7.69E+02	9.99E+01
2.00E-07	3.00E+01	7.69E+02	9.98E+01
lig(bd)	4.00E+01	7.61E+02	9.87E+01
1.20E-07	5.00E+01	7.58E+02	9.84E+01
	6.00E+01	7.48E+02	9.71E+01
	7.00E+01	7.46E+02	9.68E+01
	8.00E+01	7.33E+02	9.51E+01
	9.00E+01	7.20E+02	9.35E+01
cal slope	1.00E+02	7.21E+02	9.36E+01
7.70E+00	1.10E+02	7.19E+02	9.34E+01
	1.20E+02	7.09E+02	9.21E+01
	1.30E+02	6.93E+02	8.99E+01
	1.40E+02	6.91E+02	8.97E+01
	1.50E+02	6.87E+02	8.91E+01
	1.60E+02	6.80E+02	8.83E+01
	1.70E+02	6.76E+02	8.78E+01
	1.80E+02	6.70E+02	8.70E+01
	1.90E+02	6.70E+02	8.70E+01
	2.00E+02	6.55E+02	8.51E+01
	2.10E+02	6.49E+02	8.43E+01
	2.20E+02	6.54E+02	8.49E+01
	2.30E+02	6.53E+02	8.48E+01
	2.40E+02	6.46E+02	8.39E+01
	2.50E+02	6.43E+02	8.34E+01
	2.60E+02	6.38E+02	8.28E+01
	2.70E+02	6.37E+02	8.27E+01
	2.80E+02	6.37E+02	8.27E+01
	2.90E+02	6.32E+02	8.20E+01
	3.00E+02	6.26E+02	8.12E+01
	3.10E+02	6.32E+02	8.21E+01
	3.20E+02	6.17E+02	8.01E+01
	3.30E+02	6.25E+02	8.12E+01
	3.40E+02	6.14E+02	7.97E+01
	3.50E+02	6.22E+02	8.08E+01
	3.60E+02	6.16E+02	7.99E+01

LIGAND EXCHANGE 9/30 #17
CuNTA + D

init para	data		D (obs)
Cu(bd)	time(sec)	RFU	nM
1.00E-07	0.00E+00		
dye(bd)	2.00E+01	7.66E+02	9.94E+01
2.00E-07	3.00E+01	7.70E+02	9.99E+01
lig(bd)	4.00E+01	7.50E+02	9.73E+01
1.60E-07	5.00E+01	7.49E+02	9.72E+01
	6.00E+01	7.47E+02	9.70E+01
	7.00E+01	7.39E+02	9.59E+01
	8.00E+01	7.29E+02	9.47E+01
	9.00E+01	7.19E+02	9.33E+01
cal slope	1.00E+02	7.09E+02	9.20E+01
7.70E+00	1.10E+02	7.08E+02	9.19E+01
	1.20E+02	7.03E+02	9.13E+01
	1.29E+02	6.87E+02	8.92E+01
	1.40E+02	6.89E+02	8.94E+01
	1.50E+02	6.87E+02	8.92E+01
	1.60E+02	6.87E+02	8.91E+01
	1.70E+02	6.72E+02	8.73E+01
	1.80E+02	6.69E+02	8.69E+01
	1.90E+02	6.70E+02	8.69E+01
	2.00E+02	6.66E+02	8.65E+01
	2.10E+02	6.61E+02	8.58E+01
	2.20E+02	6.62E+02	8.59E+01
	2.30E+02	6.48E+02	8.41E+01
	2.40E+02	6.42E+02	8.33E+01
	2.50E+02	6.39E+02	8.30E+01
	2.60E+02	6.43E+02	8.34E+01
	2.70E+02	6.37E+02	8.27E+01
	2.80E+02	6.31E+02	8.19E+01
	2.90E+02	6.30E+02	8.18E+01
	3.00E+02	6.35E+02	8.24E+01
	3.10E+02	6.36E+02	8.26E+01
	3.20E+02	6.35E+02	8.24E+01
	3.30E+02	6.26E+02	8.12E+01
	3.40E+02	6.26E+02	8.13E+01
	3.50E+02	6.15E+02	7.98E+01
	3.60E+02	6.17E+02	8.01E+01

LIGAND EXCHANGE 9/30 #18
CuNTA + D to CuD + NTA

init para	data		D (obs)
Cu(bd)	time(sec)	RFU	nM
1.00E-07	0.00E+00		
dye(bd)	2.00E+01	7.63E+02	9.90E+01
2.00E-07	3.00E+01	7.54E+02	9.79E+01
lig(bd)	4.00E+01	7.55E+02	9.80E+01
2.40E-07	5.00E+01	7.39E+02	9.60E+01
	6.00E+01	7.29E+02	9.47E+01
	7.00E+01	7.16E+02	9.30E+01
	8.00E+01	7.17E+02	9.31E+01
	9.00E+01	7.10E+02	9.22E+01
cal slope	1.02E+02	7.03E+02	9.13E+01
7.70E+00	1.11E+02	6.94E+02	9.01E+01
	1.20E+02	6.96E+02	9.03E+01
	1.31E+02	7.01E+02	9.11E+01
	1.40E+02	6.97E+02	9.04E+01
	1.50E+02	6.82E+02	8.86E+01
	1.60E+02	6.80E+02	8.83E+01
	1.70E+02	6.81E+02	8.84E+01
	1.80E+02	6.75E+02	8.76E+01
	1.90E+02	6.62E+02	8.60E+01
	2.00E+02	6.63E+02	8.61E+01
	2.10E+02	6.57E+02	8.52E+01
	2.20E+02	6.55E+02	8.50E+01
	2.30E+02	6.45E+02	8.37E+01
	2.40E+02	6.49E+02	8.42E+01
	2.50E+02	6.51E+02	8.45E+01
	2.60E+02	6.46E+02	8.39E+01
	2.70E+02	6.41E+02	8.31E+01
	2.79E+02	6.34E+02	8.23E+01
	2.90E+02	6.37E+02	8.27E+01
	3.00E+02	6.40E+02	8.30E+01
	3.10E+02	6.32E+02	8.20E+01
	3.20E+02	6.39E+02	8.29E+01
	3.30E+02	6.23E+02	8.09E+01
	3.40E+02	6.20E+02	8.05E+01
	3.50E+02	6.23E+02	8.09E+01
	3.60E+02	6.15E+02	7.99E+01

LIGAND EXCHANGE 11/19 A
CuNTA + D to CuD + NTA

init para	data		D(obs)
Cu(bd)	time(sec)	RFU	nM
1.00E-07	0.00E+00		
dye(bd)	2.00E+01	2.79E+02	9.09E+01
2.00E-07	3.00E+01	2.75E+02	8.96E+01
lig(bd)	4.00E+01	2.69E+02	8.78E+01
1.40E-07	5.00E+01	2.68E+02	8.75E+01
	6.00E+01	2.69E+02	8.76E+01
	7.00E+01	2.61E+02	8.51E+01
	9.00E+01	2.55E+02	8.32E+01
	1.00E+02	2.53E+02	8.25E+01
cal slope	1.10E+02	2.51E+02	8.17E+01
3.07E+00	1.20E+02	2.47E+02	8.07E+01
	1.30E+02	2.44E+02	7.95E+01
	1.40E+02	2.42E+02	7.88E+01
	1.50E+02	2.39E+02	7.80E+01
	1.60E+02	2.37E+02	7.73E+01
	1.70E+02	2.36E+02	7.70E+01
	1.80E+02	2.39E+02	7.78E+01
	1.90E+02	2.34E+02	7.64E+01
	2.00E+02	2.31E+02	7.52E+01
	2.10E+02	2.30E+02	7.50E+01
	2.20E+02	2.28E+02	7.44E+01
	2.30E+02	2.24E+02	7.32E+01
	2.40E+02	2.22E+02	7.24E+01
	2.50E+02	2.22E+02	7.25E+01
	2.60E+02	2.18E+02	7.10E+01
	2.70E+02	2.21E+02	7.21E+01
	2.80E+02	2.21E+02	7.21E+01
	2.90E+02	2.17E+02	7.09E+01
	3.00E+02	2.17E+02	7.08E+01
	3.10E+02	2.14E+02	6.98E+01
	3.20E+02	2.16E+02	7.05E+01
	3.30E+02	2.13E+02	6.94E+01
	3.40E+02	2.10E+02	6.86E+01
	3.50E+02	2.11E+02	6.88E+01
	3.60E+02	2.08E+02	6.77E+01

LIGAND EXCHANGE 11/19 B
CuNTA + D to CuD + NTA

init para	data		D (obs)
Cu(bd)	time(sec)	RFU	nM
1.00E-07	0.00E+00		
dye(bd)	2.00E+01	4.54E+02	1.48E+02
3.00E-07	3.00E+01	4.51E+02	1.47E+02
lig(bd)	4.00E+01	4.49E+02	1.46E+02
1.40E-07	5.00E+01	4.42E+02	1.44E+02
	6.00E+01	4.38E+02	1.43E+02
	7.00E+01	4.36E+02	1.42E+02
	8.00E+01	4.35E+02	1.42E+02
	9.00E+01	4.35E+02	1.42E+02
cal slope	1.00E+02	4.34E+02	1.42E+02
3.07E+00	1.10E+02	4.33E+02	1.41E+02
	1.20E+02	4.30E+02	1.40E+02
	1.30E+02	4.25E+02	1.39E+02
	1.40E+02	4.20E+02	1.37E+02
	1.50E+02	4.22E+02	1.38E+02
	1.60E+02	4.14E+02	1.35E+02
	1.70E+02	4.12E+02	1.34E+02
	1.80E+02	4.09E+02	1.33E+02
	1.90E+02	4.07E+02	1.33E+02
	2.00E+02	4.06E+02	1.33E+02
	2.10E+02	4.03E+02	1.31E+02
	2.20E+02	4.01E+02	1.31E+02
	2.30E+02	3.98E+02	1.30E+02
	2.40E+02	3.94E+02	1.28E+02
	2.50E+02	3.94E+02	1.28E+02
	2.60E+02	3.87E+02	1.26E+02
	2.70E+02	3.85E+02	1.26E+02
	2.80E+02	3.83E+02	1.25E+02
	2.90E+02	3.85E+02	1.26E+02
	3.00E+02	3.81E+02	1.24E+02
	3.10E+02	3.80E+02	1.24E+02
	3.20E+02	3.79E+02	1.24E+02
	3.30E+02	3.77E+02	1.23E+02
	3.40E+02	3.73E+02	1.22E+02
	3.50E+02	3.72E+02	1.21E+02
	3.60E+02	3.71E+02	1.21E+02

LIGAND EXCHANGE 11/19 C
CuNTA + D to CuD + NTA

data		D (obs)
time(sec)	RFU	nM
0.00E+00		
2.00E+01	4.44E+02	1.45E+02
3.00E+01	4.40E+02	1.43E+02
4.00E+01	4.35E+02	1.42E+02
5.00E+01	4.30E+02	1.40E+02
6.00E+01	4.23E+02	1.38E+02
7.00E+01	4.19E+02	1.37E+02
8.00E+01	4.16E+02	1.36E+02
9.00E+01	4.14E+02	1.35E+02
1.20E+02	4.06E+02	1.32E+02
1.30E+02	4.03E+02	1.31E+02
1.40E+02	3.98E+02	1.30E+02
1.50E+02	3.93E+02	1.28E+02
1.60E+02	3.93E+02	1.28E+02
1.70E+02	3.90E+02	1.27E+02
1.80E+02	3.90E+02	1.27E+02
1.90E+02	3.87E+02	1.26E+02
2.00E+02	3.83E+02	1.25E+02
2.10E+02	3.83E+02	1.25E+02
2.20E+02	3.78E+02	1.23E+02
2.30E+02	3.78E+02	1.23E+02
2.40E+02	3.78E+02	1.23E+02
2.50E+02	3.77E+02	1.23E+02
2.60E+02	3.79E+02	1.24E+02
2.70E+02	3.78E+02	1.23E+02
2.80E+02	3.78E+02	1.23E+02
2.90E+02	3.75E+02	1.22E+02
3.00E+02	3.73E+02	1.22E+02
3.10E+02	3.69E+02	1.20E+02
3.20E+02	3.64E+02	1.19E+02
3.30E+02	3.63E+02	1.18E+02
3.40E+02	3.62E+02	1.18E+02
3.50E+02	3.59E+02	1.17E+02
3.60E+02	3.58E+02	1.17E+02

LIGAND EXCHANGE 11/19 D
CuNTA + D to CuD + NTA

init para	data		D (obs)
Cu(bd)	time(sec)	RFU	nM
1.00E-07	0.00E+00		
dye(bd)	2.00E+01	3.02E+02	1.97E+02
4.00E-07	3.00E+01	3.01E+02	1.96E+02
lig bd)	4.00E+01	2.95E+02	1.92E+02
1.40E-07	5.00E+01	2.91E+02	1.90E+02
	6.00E+01	2.89E+02	1.88E+02
	7.00E+01	2.83E+02	1.85E+02
	8.00E+01	2.83E+02	1.85E+02
	9.00E+01	2.79E+02	1.82E+02
cal slope	1.00E+02	2.78E+02	1.81E+02
1.53E+00	1.10E+02	2.73E+02	1.78E+02
	1.20E+02	2.74E+02	1.79E+02
	1.30E+02	2.73E+02	1.78E+02
	1.40E+02	2.77E+02	1.81E+02
	1.50E+02	2.71E+02	1.77E+02
	1.60E+02	2.76E+02	1.80E+02
	1.70E+02	2.72E+02	1.77E+02
	1.80E+02	2.72E+02	1.77E+02
	1.90E+02	2.68E+02	1.75E+02
	2.00E+02	2.69E+02	1.75E+02
	2.10E+02	2.67E+02	1.74E+02
	2.20E+02	2.65E+02	1.73E+02
	2.30E+02	2.64E+02	1.72E+02
	2.40E+02	2.64E+02	1.72E+02
	2.50E+02	2.61E+02	1.70E+02
	2.60E+02	2.63E+02	1.71E+02
	2.70E+02	2.61E+02	1.70E+02
	2.80E+02	2.62E+02	1.71E+02
	2.90E+02	2.61E+02	1.70E+02
	3.00E+02	2.56E+02	1.67E+02
	3.10E+02	2.57E+02	1.68E+02
	3.20E+02	2.58E+02	1.68E+02
	3.30E+02	2.57E+02	1.68E+02
	3.40E+02	2.55E+02	1.66E+02
	3.50E+02	2.55E+02	1.66E+02
	3.60E+02	2.54E+02	1.65E+02

LIGAND EXCHANGE 11/19 E
CuNTA + D to CuD + NTA

init para	data		D (obs)
Cu(bd)	time(sec)	RFU	nM
1.00E-07	0.00E+00		
dye(bd)	2.00E+01	2.99E+02	1.95E+02
4.00E-07	3.00E+01	2.97E+02	1.94E+02
lig(bd)	4.00E+01	2.95E+02	1.92E+02
1.40E-07	5.00E+01	2.89E+02	1.89E+02
	6.00E+01	2.92E+02	1.91E+02
	7.00E+01	2.87E+02	1.87E+02
	8.00E+01	2.85E+02	1.86E+02
	9.00E+01	2.82E+02	1.84E+02
cal slope	1.00E+02	2.81E+02	1.83E+02
1.53E+00	1.10E+02	2.79E+02	1.82E+02
	1.20E+02	2.79E+02	1.82E+02
	1.30E+02	2.75E+02	1.79E+02
	1.40E+02	2.74E+02	1.79E+02
	1.50E+02	2.72E+02	1.77E+02
	1.60E+02	2.70E+02	1.76E+02
	1.70E+02	2.68E+02	1.74E+02
	1.80E+02	2.67E+02	1.74E+02
	1.90E+02	2.68E+02	1.75E+02
	2.00E+02	2.66E+02	1.74E+02
	2.10E+02	2.68E+02	1.74E+02
	2.20E+02	2.66E+02	1.73E+02
	2.30E+02	2.63E+02	1.71E+02
	2.40E+02	2.60E+02	1.69E+02
	2.50E+02	2.59E+02	1.69E+02
	2.60E+02	2.58E+02	1.68E+02
	2.70E+02	2.56E+02	1.67E+02
	2.80E+02	2.57E+02	1.67E+02
	2.90E+02	2.57E+02	1.68E+02
	3.00E+02	2.54E+02	1.65E+02
	3.10E+02	2.52E+02	1.65E+02
	3.20E+02	2.52E+02	1.64E+02
	3.30E+02	2.50E+02	1.63E+02
	3.40E+02	2.50E+02	1.63E+02
	3.50E+02	2.49E+02	1.63E+02
	3.60E+02	2.49E+02	1.62E+02

LIGAND EXCHANGE 11/19 F
CuNTA + D to CuD + NTA

init para	d ta		D (obs)
Cu(bd)	time(sec)	RFU	nM
1.00E-07	0.00E+00		
dye(bd)	2.00E+01	3.64E+02	2.38E+02
5.00E-07	3.00E+01	3.65E+02	2.38E+02
lig(bd)	4.00E+01	3.64E+02	2.38E+02
1.40E-07	5.00E+01	3.53E+02	2.30E+02
Pmix	7.00E+01	3.51E+02	2.29E+02
4.80E-01	8.00E+01	3.51E+02	2.29E+02
alpha	9.00E+01	3.48E+02	2.27E+02
8.00E-01	1.00E+02	3.46E+02	2.26E+02
cal slope	1.10E+02	3.45E+02	2.25E+02
1.53E+00	1.20E+02	3.43E+02	2.23E+02
kassoc	1.30E+02	3.42E+02	2.23E+02
4.81E+02	1.40E+02	3.43E+02	2.24E+02
alphabl	1.50E+02	3.41E+02	2.22E+02
1.31E-03	1.60E+02	3.39E+02	2.21E+02
	1.70E+02	3.39E+02	2.21E+02
	1.80E+02	3.37E+02	2.20E+02
	1.90E+02	3.36E+02	2.19E+02
	2.00E+02	3.40E+02	2.22E+02
	2.10E+02	3.39E+02	2.21E+02
	2.20E+02	3.36E+02	2.19E+02
	2.30E+02	3.35E+02	2.19E+02
	2.40E+02	3.32E+02	2.17E+02
	2.50E+02	3.35E+02	2.18E+02
	2.60E+02	3.34E+02	2.18E+02
	2.70E+02	3.30E+02	2.15E+02
	2.80E+02	3.26E+02	2.13E+02
	2.90E+02	3.30E+02	2.15E+02
	3.00E+02	3.29E+02	2.14E+02
	3.10E+02	3.27E+02	2.13E+02
	3.20E+02	3.25E+02	2.12E+02
	3.30E+02	3.28E+02	2.14E+02
	3.40E+02	3.22E+02	2.10E+02
	3.50E+02	3.20E+02	2.09E+02
	3.60E+02	3.20E+02	2.08E+02

LIGAND EXCHANGE 11/19 G
CuNTA + D to CuD + NTA

init para Cu(bd)	data time(sec)	RFU	D (obs) nM
2.00E-07	0.00E+00		
dye(bd)	2.00E+01	2.89E+02	9.43E+01
2.00E-07	3.00E+01	2.87E+02	9.36E+01
lig(bd)	4.00E+01	2.77E+02	9.03E+01
2.80E-07	5.00E+01	2.71E+02	8.85E+01
	6.00E+01	2.65E+02	8.63E+01
	7.00E+01	2.54E+02	8.27E+01
	8.00E+01	2.47E+02	8.05E+01
	9.00E+01	2.40E+02	7.84E+01
cal slope	1.00E+02	2.36E+02	7.70E+01
3.07E+00	1.10E+02	2.35E+02	7.68E+01
	1.20E+02	2.28E+02	7.43E+01
	1.30E+02	2.24E+02	7.32E+01
	1.40E+02	2.23E+02	7.26E+01
	1.50E+02	2.16E+02	7.05E+01
	1.60E+02	2.10E+02	6.85E+01
	1.70E+02	2.05E+02	6.69E+01
	1.80E+02	2.03E+02	6.61E+01
	1.90E+02	1.99E+02	6.49E+01
	2.00E+02	1.95E+02	6.34E+01
	2.10E+02	1.91E+02	6.23E+01
	2.20E+02	1.89E+02	6.15E+01
	2.30E+02	1.85E+02	6.03E+01
	2.40E+02	1.81E+02	5.92E+01
	2.50E+02	1.80E+02	5.88E+01
	2.60E+02	1.81E+02	5.90E+01
	2.70E+02	1.79E+02	5.83E+01
	2.80E+02	1.73E+02	5.65E+01
	2.90E+02	1.71E+02	5.58E+01
	3.00E+02	1.68E+02	5.47E+01
	3.10E+02	1.66E+02	5.42E+01
	3.20E+02	1.68E+02	5.47E+01
	3.30E+02	1.61E+02	5.26E+01
	3.40E+02	1.62E+02	5.30E+01
	3.50E+02	1.58E+02	5.17E+01
	3.60E+02	1.59E+02	5.19E+01

LIGAND EXCHANGE 11/19 H
CuNTA + D to CuD + NTA

init para Cu(bd)	data time(sec)	RFU	D (obs) nM
2.00E-07	0.00E+00		
dye(bd)	2.00E+01	4.47E+02	1.46E+02
3.00E-07	3.00E+01	4.41E+02	1.44E+02
lig(bd)	4.00E+01	4.22E+02	1.38E+02
2.80E-07	5.00E+01	4.18E+02	1.36E+02
	6.00E+01	4.08E+02	1.33E+02
	7.00E+01	3.99E+02	1.30E+02
	8.00E+01	3.90E+02	1.27E+02
	9.00E+01	3.86E+02	1.26E+02
cal slope	1.00E+02	3.79E+02	1.24E+02
3.07E+00	1.10E+02	3.74E+02	1.22E+02
	1.20E+02	3.69E+02	1.20E+02
	1.30E+02	3.64E+02	1.19E+02
	1.40E+02	3.55E+02	1.16E+02
	1.50E+02	3.51E+02	1.14E+02
	1.60E+02	3.45E+02	1.13E+02
	1.70E+02	3.39E+02	1.11E+02
	1.80E+02	3.35E+02	1.09E+02
	1.90E+02	3.27E+02	1.07E+02
	2.00E+02	3.20E+02	1.04E+02
	2.10E+02	3.20E+02	1.04E+02
	2.20E+02	3.13E+02	1.02E+02
	2.30E+02	3.10E+02	1.01E+02
	2.40E+02	3.07E+02	1.00E+02
	2.50E+02	3.02E+02	9.86E+01
	2.60E+02	3.02E+02	9.84E+01
	2.70E+02	3.00E+02	9.79E+01
	2.80E+02	2.96E+02	9.64E+01
	2.90E+02	2.92E+02	9.53E+01
	3.00E+02	2.90E+02	9.46E+01
	3.10E+02	2.87E+02	9.35E+01
	3.20E+02	2.83E+02	9.22E+01
	3.30E+02	2.79E+02	9.09E+01
	3.40E+02	2.78E+02	9.08E+01
	3.50E+02	2.73E+02	8.91E+01
	3.60E+02	2.73E+02	8.91E+01

LIGAND EXCHANGE 11/19 I
CuNTA + D to CuD + NTA

init para Cu(bd)	data time(sec)	RFU	D (obs) nM
2.00E-07	0.00E+00		
dye(bd)	2.00E+01	4.48E+02	1.46E+02
3.00E-07	3.00E+01	4.35E+02	1.42E+02
lig(bd)	4.00E+01	4.24E+02	1.38E+02
2.80E-07	5.00E+01	4.19E+02	1.37E+02
	6.00E+01	4.16E+02	1.36E+02
	7.00E+01	4.05E+02	1.32E+02
	8.00E+01	4.04E+02	1.32E+02
	9.00E+01	3.96E+02	1.29E+02
cal slope	1.00E+02	3.92E+02	1.28E+02
3.07E+00	1.10E+02	3.89E+02	1.27E+02
	1.20E+02	3.81E+02	1.24E+02
	1.30E+02	3.72E+02	1.21E+02
	1.40E+02	3.68E+02	1.20E+02
	1.50E+02	3.67E+02	1.20E+02
	1.60E+02	3.62E+02	1.18E+02
	1.70E+02	3.52E+02	1.15E+02
	1.80E+02	3.48E+02	1.13E+02
	1.90E+02	3.43E+02	1.12E+02
	2.00E+02	3.39E+02	1.11E+02
	2.10E+02	3.29E+02	1.07E+02
	2.20E+02	3.21E+02	1.05E+02
	2.30E+02	3.21E+02	1.05E+02
	2.40E+02	3.21E+02	1.05E+02
	2.50E+02	3.17E+02	1.03E+02
	2.60E+02	3.12E+02	1.02E+02
	2.70E+02	3.10E+02	1.01E+02
	2.80E+02	3.05E+02	9.94E+01
	2.90E+02	3.03E+02	9.89E+01
	3.00E+02	2.97E+02	9.70E+01
	3.10E+02	2.97E+02	9.67E+01
	3.20E+02	2.95E+02	9.63E+01
	3.30E+02	2.92E+02	9.51E+01
	3.40E+02	2.90E+02	9.47E+01
	3.50E+02	2.86E+02	9.34E+01
	3.60E+02	2.81E+02	9.15E+01

LIGAND EXCHANGE 11/19 J
CuNTA + D to CuD + NTA

init para Cu(bd)	data time(sec)	RFU	D (obs) nM
2.00E-07	0.00E+00		
dye(bd)	2.00E+01	2.85E+02	1.86E+02
4.00E-07	3.00E+01	2.83E+02	1.85E+02
lig(bd)	4.00E+01	2.74E+02	1.79E+02
2.80E-07	5.00E+01	2.66E+02	1.73E+02
	6.00E+01	2.64E+02	1.72E+02
	7.00E+01	2.57E+02	1.68E+02
	8.00E+01	2.52E+02	1.64E+02
	9.00E+01	2.42E+02	1.58E+02
cal slope	1.00E+02	2.38E+02	1.55E+02
1.53E+00	1.10E+02	2.34E+02	1.53E+02
	1.20E+02	2.31E+02	1.50E+02
	1.30E+02	2.30E+02	1.50E+02
	1.40E+02	2.28E+02	1.49E+02
	1.50E+02	2.23E+02	1.45E+02
	1.60E+02	2.22E+02	1.45E+02
	1.70E+02	2.19E+02	1.43E+02
	1.80E+02	2.17E+02	1.41E+02
	1.90E+02	2.17E+02	1.42E+02
	2.00E+02	2.15E+02	1.40E+02
	2.10E+02	2.14E+02	1.40E+02
	2.20E+02	2.11E+02	1.38E+02
	2.30E+02	2.10E+02	1.37E+02
	2.40E+02	2.07E+02	1.35E+02
	2.50E+02	2.06E+02	1.34E+02
	2.60E+02	2.03E+02	1.33E+02
	2.70E+02	1.99E+02	1.30E+02
	2.80E+02	1.99E+02	1.30E+02
	2.90E+02	1.96E+02	1.28E+02
	3.00E+02	1.93E+02	1.26E+02
	3.10E+02	1.90E+02	1.24E+02
	3.20E+02	1.88E+02	1.22E+02
	3.30E+02	1.87E+02	1.22E+02
	3.40E+02	1.85E+02	1.21E+02
	3.50E+02	1.84E+02	1.20E+02
	3.60E+02	1.84E+02	1.20E+02

LIGAND EXCHANGE 11/19 K
CuNTA + D to CuD + NTA

init para Cu(bd)	data time(sec)	RFU	D (obs) nM
2.00E-07	0.00E+00		
dye(bd)	2.00E+01	2.95E+02	1.92E+02
4.00E-07	3.00E+01	2.86E+02	1.87E+02
lig(bd)	4.00E+01	2.79E+02	1.82E+02
2.80E-07	5.00E+01	2.74E+02	1.79E+02
	6.00E+01	2.67E+02	1.74E+02
	7.00E+01	2.69E+02	1.76E+02
	8.00E+01	2.68E+02	1.75E+02
	9.00E+01	2.64E+02	1.72E+02
cal slope	1.00E+02	2.62E+02	1.71E+02
1.53E+00	1.10E+02	2.60E+02	1.70E+02
	1.20E+02	2.55E+02	1.67E+02
	1.30E+02	2.52E+02	1.64E+02
	1.40E+02	2.49E+02	1.62E+02
	1.50E+02	2.47E+02	1.61E+02
	1.60E+02	2.45E+02	1.60E+02
	1.70E+02	2.43E+02	1.59E+02
	1.80E+02	2.41E+02	1.57E+02
	1.90E+02	2.38E+02	1.55E+02
	2.00E+02	2.35E+02	1.53E+02
	2.10E+02	2.34E+02	1.53E+02
	2.20E+02	2.27E+02	1.48E+02
	2.30E+02	2.15E+02	1.40E+02
	2.40E+02	2.18E+02	1.42E+02
	2.50E+02	2.23E+02	1.45E+02
	2.60E+02	2.17E+02	1.41E+02
	2.70E+02	2.20E+02	1.43E+02
	2.80E+02	2.15E+02	1.40E+02
	2.90E+02	2.15E+02	1.40E+02
	3.00E+02	2.07E+02	1.35E+02
	3.10E+02	2.06E+02	1.34E+02
	3.20E+02	2.04E+02	1.33E+02
	3.30E+02	2.03E+02	1.32E+02
	3.40E+02	2.03E+02	1.32E+02
	3.50E+02	2.01E+02	1.31E+02
	3.60E+02	2.00E+02	1.30E+02

LIGAND EXCHANGE 11/19 L
CuNTA + D to CuD + NTA

init para Cu(bd)	data time(sec)	RFU	D (obs) nM
2.00E-07	0.00E+00		
dye(bd)	2.00E+01	3.75E+02	2.44E+02
5.00E-07	3.00E+01	3.67E+02	2.39E+02
lig(bd)	4.00E+01	3.70E+02	2.41E+02
2.80E-07	5.00E+01	3.66E+02	2.39E+02
Fmix	6.00E+01	3.53E+02	2.30E+02
5.07E-01	7.00E+01	3.47E+02	2.26E+02
alpha	8.00E+01	3.43E+02	2.24E+02
2.00E-01	9.00E+01	3.37E+02	2.20E+02
cal slope	1.00E+02	3.33E+02	2.17E+02
1.53E+00	1.10E+02	3.29E+02	2.14E+02
kassoc	1.20E+02	3.29E+02	2.14E+02
4.81E+03	1.30E+02	3.23E+02	2.11E+02
alphakl	1.40E+02	3.21E+02	2.09E+02
1.31E-03	1.50E+02	3.20E+02	2.09E+02
	1.60E+02	3.21E+02	2.10E+02
	1.70E+02	3.22E+02	2.10E+02
	1.80E+02	3.19E+02	2.08E+02
	1.90E+02	3.12E+02	2.04E+02
	2.00E+02	3.11E+02	2.03E+02
	2.10E+02	3.08E+02	2.01E+02
	2.20E+02	3.05E+02	1.99E+02
	2.30E+02	3.01E+02	1.96E+02
	2.40E+02	2.99E+02	1.95E+02
	2.50E+02	3.02E+02	1.97E+02
	2.60E+02	3.01E+02	1.97E+02
	2.70E+02	2.98E+02	1.94E+02
	2.80E+02	2.95E+02	1.92E+02
	2.90E+02	2.93E+02	1.91E+02
	3.00E+02	2.93E+02	1.91E+02
	3.20E+02	2.82E+02	1.84E+02
	3.30E+02	2.80E+02	1.82E+02
	3.50E+02	2.81E+02	1.83E+02
	3.60E+02	2.76E+02	1.80E+02

LIGAND EXCHANGE 8/24 #1
CuNTA + D to CuD + NTA

Dye(BD)	2.00E-08
Cu(BD)	1.00E-07
NTA(BD)	1.60E-07

time (sec)	RFU(30)	D (obs) nM
0.00E+00		
1.80E+01	3.91E+02	8.10E+00
2.90E+01	3.86E+02	8.00E+00
3.90E+01	3.75E+02	7.78E+00
5.10E+01	3.60E+02	7.46E+00
6.20E+01	3.44E+02	7.13E+00
7.10E+01	3.51E+02	7.28E+00
8.20E+01	3.26E+02	6.76E+00
9.20E+01	3.30E+02	6.84E+00
1.02E+02	3.12E+02	6.47E+00
1.11E+02	3.11E+02	6.44E+00
1.21E+02	3.09E+02	6.41E+00
1.31E+02	2.97E+02	6.16E+00
1.41E+02	2.99E+02	6.20E+00
1.51E+02	2.95E+02	6.12E+00
1.61E+02	2.87E+02	5.95E+00
1.70E+02	2.81E+02	5.82E+00
1.80E+02	2.74E+02	5.68E+00
1.90E+02	2.67E+02	5.54E+00
1.99E+02	2.65E+02	5.48E+00
2.09E+02	2.59E+02	5.38E+00
2.20E+02	2.47E+02	5.13E+00
2.30E+02	2.42E+02	5.01E+00
2.40E+02	2.38E+02	4.94E+00
2.50E+02	2.32E+02	4.81E+00
2.59E+02	2.23E+02	4.62E+00
2.69E+02	2.25E+02	4.67E+00
2.80E+02	2.22E+02	4.61E+00
2.90E+02	2.21E+02	4.58E+00
3.00E+02	2.17E+02	4.49E+00
3.10E+02	2.10E+02	4.35E+00
3.20E+02	2.08E+02	4.30E+00
3.29E+02	2.09E+02	4.33E+00
3.40E+02	2.03E+02	4.21E+00
3.50E+02	2.01E+02	4.16E+00
3.60E+02	2.00E+02	4.14E+00
3.70E+02	1.92E+02	3.98E+00
3.80E+02	1.92E+02	3.99E+00
3.90E+02	1.89E+02	3.91E+00
4.00E+02	1.83E+02	3.78E+00

LIGAND EXCHANGE 8/24 #2
CuNTA + D to CuD + NTA

init para Cu(bd)	data time(sec)	RFU	D (obs) nM
1.00E-07	0.00E+00		
dye(bd)	1.50E+01	7.21E+02	2.22E+01
4.00E-08	2.60E+01	7.06E+02	2.17E+01
lig(bd)	3.70E+01	6.42E+02	1.98E+01
1.60E-07	4.90E+01	6.22E+02	1.91E+01
	6.00E+01	6.20E+02	1.91E+01
	7.00E+01	6.25E+02	1.92E+01
	8.00E+01	6.19E+02	1.90E+01
	9.10E+01	6.16E+02	1.89E+01
cal slope	1.01E+02	6.00E+02	1.85E+01
3.25E+01	1.12E+02	5.94E+02	1.83E+01
	1.21E+02	5.74E+02	1.76E+01
	1.30E+02	5.70E+02	1.75E+01
	1.40E+02	5.72E+02	1.76E+01
	1.50E+02	5.60E+02	1.72E+01
	1.60E+02	5.57E+02	1.71E+01
	1.70E+02	5.49E+02	1.69E+01
	1.80E+02	5.40E+02	1.66E+01
	1.90E+02	5.30E+02	1.63E+01
	2.00E+02	5.37E+02	1.65E+01
	2.10E+02	5.27E+02	1.62E+01
	2.20E+02	5.23E+02	1.61E+01
	2.30E+02	5.18E+02	1.59E+01
	2.40E+02	5.07E+02	1.56E+01
	2.50E+02	4.99E+02	1.53E+01
	2.60E+02	4.97E+02	1.53E+01
	2.70E+02	5.00E+02	1.54E+01
	2.80E+02	4.88E+02	1.50E+01
	2.90E+02	4.80E+02	1.48E+01
	3.00E+02	4.72E+02	1.45E+01
	3.10E+02	4.71E+02	1.45E+01
	3.20E+02	4.67E+02	1.43E+01
	3.30E+02	4.53E+02	1.39E+01
	3.40E+02	4.47E+02	1.38E+01
	3.50E+02	4.27E+02	1.31E+01
	3.60E+02	4.37E+02	1.34E+01
	3.70E+02	4.36E+02	1.34E+01
	3.80E+02	4.28E+02	1.32E+01
	3.90E+02	4.27E+02	1.31E+01
	4.00E+02	4.19E+02	1.29E+01
	4.10E+02	4.14E+02	1.27E+01
	4.20E+02	4.15E+02	1.28E+01
	4.30E+02	4.05E+02	1.24E+01
	4.40E+02	4.00E+02	1.23E+01
	4.50E+02	4.05E+02	1.24E+01
	4.60E+02	4.02E+02	1.24E+01
	4.72E+02	3.96E+02	1.22E+01
	4.82E+02	3.94E+02	1.21E+01
	4.92E+02	3.89E+02	1.20E+01
	5.05E+02	3.83E+02	1.18E+01
	5.16E+02	3.78E+02	1.16E+01
	5.25E+02	3.78E+02	1.16E+01
	5.35E+02	3.74E+02	1.15E+01
	5.45E+02	3.65E+02	1.12E+01
	5.55E+02	3.66E+02	1.13E+01
	5.65E+02	3.62E+02	1.11E+01
	5.75E+02	3.50E+02	1.08E+01
	5.85E+02	3.52E+02	1.08E+01
	5.95E+02	3.39E+02	1.04E+01
	6.05E+02	3.38E+02	1.04E+01

LIGAND EXCHANGE 8/24 #3
CuNTA + D to CuD + NTA

init para	data		
Cu(bd)	time(sec)	RFU	
1.00E-07	0.00E+00		
dye(bd)	1.70E+01	8.45E+02	5.20E+01
1.00E-07	2.90E+01	8.20E+02	5.04E+01
lig(bd)	4.00E+01	7.95E+02	4.89E+01
1.60E-07	5.30E+01	7.83E+02	4.82E+01
	6.20E+01	7.60E+02	4.68E+01
	7.20E+01	7.50E+02	4.61E+01
	8.10E+01	7.62E+02	4.69E+01
	9.00E+01	7.53E+02	4.63E+01
cal slope	1.00E+02	7.44E+02	4.58E+01
1.63E+01	1.10E+02	7.31E+02	4.49E+01
	1.20E+02	7.26E+02	4.47E+01
	1.30E+02	7.24E+02	4.45E+01
	1.40E+02	7.14E+02	4.39E+01
	1.50E+02	7.01E+02	4.31E+01
	1.60E+02	6.94E+02	4.27E+01
	1.70E+02	6.86E+02	4.22E+01
	1.80E+02	6.79E+02	4.18E+01
	1.91E+02	6.65E+02	4.09E+01
	2.00E+02	6.67E+02	4.10E+01
	2.10E+02	6.61E+02	4.07E+01
	2.20E+02	6.54E+02	4.02E+01
	2.30E+02	6.47E+02	3.98E+01
	2.40E+02	6.43E+02	3.95E+01
	2.50E+02	6.33E+02	3.90E+01
	2.60E+02	6.25E+02	3.84E+01
	2.70E+02	6.26E+02	3.85E+01
	2.80E+02	6.13E+02	3.77E+01
	2.90E+02	6.08E+02	3.74E+01
	3.00E+02	6.02E+02	3.70E+01
	3.10E+02	5.97E+02	3.67E+01
	3.20E+02	5.92E+02	3.64E+01
	3.30E+02	5.89E+02	3.62E+01
	3.40E+02	5.86E+02	3.60E+01
	3.50E+02	5.77E+02	3.55E+01
	3.60E+02	5.71E+02	3.51E+01
	3.70E+02	5.68E+02	3.49E+01
	3.80E+02	5.65E+02	3.48E+01
	3.90E+02	5.58E+02	3.43E+01
	4.00E+02	5.53E+02	3.40E+01
	4.10E+02	5.51E+02	3.39E+01
	4.20E+02	5.46E+02	3.36E+01
	4.30E+02	5.43E+02	3.34E+01
	4.40E+02	5.40E+02	3.32E+01
	4.50E+02	5.35E+02	3.29E+01
	4.60E+02	5.29E+02	3.25E+01
	4.72E+02	5.23E+02	3.22E+01
	4.82E+02	5.26E+02	3.23E+01
	4.90E+02	5.20E+02	3.20E+01
	5.00E+02	5.14E+02	3.16E+01
	5.10E+02	5.13E+02	3.15E+01
	5.20E+02	5.08E+02	3.13E+01
	5.30E+02	5.09E+02	3.13E+01
	5.40E+02	5.00E+02	3.08E+01
	5.50E+02	4.96E+02	3.05E+01
	5.60E+02	4.94E+02	3.04E+01
	5.70E+02	4.87E+02	3.00E+01
	5.80E+02	4.84E+02	2.97E+01
	5.90E+02	4.83E+02	2.97E+01
	6.00E+02	4.84E+02	2.98E+01

LIGAND EXCHANGE 8/24 #4
CuNTA + D to CuD + NTA

init para	data		D (obs)
Cu(bd)	time(sec)	RFU	nM
1.00E-07	0.00E+00		
dye(bd)	1.50E+01	7.97E+02	9.80E+01
2.00E-07	2.70E+01	7.97E+02	9.80E+01
lig(bd)	3.90E+01	7.88E+02	9.70E+01
1.60E-07	5.00E+01	7.91E+02	9.72E+01
	6.00E+01	7.88E+02	9.69E+01
	7.00E+01	7.81E+02	9.61E+01
	8.00E+01	7.77E+02	9.55E+01
	9.00E+01	7.74E+02	9.52E+01
cal slope	1.01E+02	7.63E+02	9.39E+01
8.13E+00	1.11E+02	7.54E+02	9.27E+01
	1.20E+02	7.43E+02	9.13E+01
	1.30E+02	7.32E+02	9.00E+01
	1.40E+02	7.32E+02	9.01E+01
	1.50E+02	7.25E+02	8.91E+01
	1.60E+02	7.21E+02	8.87E+01
	1.70E+02	7.04E+02	8.65E+01
	1.80E+02	7.39E+02	9.09E+01
	1.91E+02	7.30E+02	8.98E+01
	2.00E+02	7.25E+02	8.92E+01
	2.10E+02	7.19E+02	8.84E+01
	2.20E+02	7.15E+02	8.80E+01
	2.30E+02	7.08E+02	8.71E+01
	2.40E+02	7.10E+02	8.73E+01
	2.52E+02	6.64E+02	8.16E+01
	2.61E+02	6.66E+02	8.19E+01
	2.71E+02	6.59E+02	8.10E+01
	2.81E+02	6.70E+02	8.25E+01
	2.91E+02	6.54E+02	8.05E+01
	3.00E+02	6.52E+02	8.02E+01

LIGAND EXCHANGE 11/2 A
CuNTA + D to CuD + NTA

init para	data		D (obs)
Cu(bd)	time(sec)	RFU	nM
1.00E-07	0.00E+00		
dye(bd)	2.00E+01	6.52E+02	1.08E+02
2.00E-07	3.00E+01	6.46E+02	1.07E+02
lig(bd)	4.00E+01	6.39E+02	1.06E+02
1.20E-07	5.00E+01	6.28E+02	1.04E+02
	6.00E+01	6.28E+02	1.04E+02
	7.00E+01	6.27E+02	1.04E+02
	8.00E+01	6.33E+02	1.05E+02
	9.00E+01	6.30E+02	1.04E+02
cal slope	1.00E+02	6.24E+02	1.03E+02
6.04E+00	1.12E+02	6.15E+02	1.02E+02
	1.22E+02	6.09E+02	1.01E+02
	1.40E+02	5.96E+02	9.87E+01
	1.50E+02	5.86E+02	9.70E+01
	1.60E+02	5.85E+02	9.68E+01
	1.70E+02	5.74E+02	9.50E+01
	1.80E+02	5.71E+02	9.45E+01
	1.90E+02	5.66E+02	9.37E+01
	2.00E+02	5.64E+02	9.34E+01
	2.10E+02	5.59E+02	9.26E+01
	2.20E+02	5.47E+02	9.06E+01
	2.30E+02	5.52E+02	9.14E+01
	2.40E+02	5.49E+02	9.09E+01
	2.50E+02	5.45E+02	9.02E+01
	2.60E+02	5.43E+02	9.00E+01
	2.70E+02	5.42E+02	8.97E+01
	2.80E+02	5.40E+02	8.94E+01
	2.90E+02	5.33E+02	8.83E+01
	3.00E+02	5.34E+02	8.85E+01
	3.10E+02	5.28E+02	8.74E+01
	3.20E+02	5.23E+02	8.66E+01
	3.30E+02	5.22E+02	8.64E+01
	3.40E+02	5.19E+02	8.59E+01
	3.50E+02	5.16E+02	8.55E+01
	3.60E+02	5.15E+02	8.53E+01

LIGAND EXCHANGE 11/2 B
CuNTA + D to CuD + NTA

init para	data		D (obs)
Cu(bd)	time(sec)	RFU	nM
1.00E-07	0.00E+00		
dye(bd)	2.00E+01	4.82E+02	1.59E+02
3.00E-07	3.00E+01	4.78E+02	1.58E+02
lig(bd)	4.00E+01	4.79E+02	1.59E+02
1.20E-07	5.00E+01	4.79E+02	1.58E+02
	6.00E+01	4.81E+02	1.59E+02
	7.00E+01	4.73E+02	1.57E+02
	8.00E+01	4.73E+02	1.57E+02
	9.00E+01	4.67E+02	1.55E+02
cal slope	1.00E+02	4.64E+02	1.54E+02
3.02E+00	1.10E+02	4.61E+02	1.53E+02
	1.20E+02	4.58E+02	1.52E+02
	1.30E+02	4.55E+02	1.51E+02
	1.40E+02	4.55E+02	1.51E+02
	1.50E+02	4.55E+02	1.51E+02
	1.60E+02	4.55E+02	1.51E+02
	1.70E+02	4.57E+02	1.51E+02
	1.80E+02	4.59E+02	1.52E+02
	1.90E+02	4.56E+02	1.51E+02
	2.00E+02	4.53E+02	1.50E+02
	2.10E+02	4.53E+02	1.50E+02
	2.20E+02	4.49E+02	1.49E+02
	2.30E+02	4.47E+02	1.48E+02
	2.40E+02	4.44E+02	1.47E+02
	2.50E+02	4.42E+02	1.46E+02
	2.60E+02	4.39E+02	1.46E+02
	2.70E+02	4.39E+02	1.45E+02
	2.80E+02	4.39E+02	1.45E+02
	2.90E+02	4.39E+02	1.45E+02
	3.00E+02	4.38E+02	1.45E+02
	3.10E+02	4.36E+02	1.44E+02
	3.20E+02	4.35E+02	1.44E+02
	3.30E+02	4.31E+02	1.43E+02
	3.40E+02	4.32E+02	1.43E+02
	3.50E+02	4.27E+02	1.41E+02
	3.60E+02	4.27E+02	1.41E+02

LIGAND EXCHANGE 11/2 C
CuNTA + D to CuD + NTA

init para	data		D (obs)
Cu(bd)	time(sec)	RFU	nM
1.00E-07	0.00E+00		
dye(bd)	2.00E+01	6.25E+02	2.07E+02
4.00E-07	3.00E+01	6.19E+02	2.05E+02
lig(bd)	4.00E+01	6.16E+02	2.04E+02
1.20E-07	5.00E+01	6.13E+02	2.03E+02
	6.00E+01	6.10E+02	2.02E+02
	7.00E+01	6.07E+02	2.01E+02
	8.00E+01	6.06E+02	2.01E+02
	9.00E+01	5.97E+02	1.98E+02
cal slope	1.00E+02	5.95E+02	1.97E+02
3.02E+00	1.10E+02	5.94E+02	1.97E+02
	1.20E+02	5.89E+02	1.95E+02
	1.30E+02	5.90E+02	1.95E+02
	1.40E+02	5.87E+02	1.94E+02
	1.50E+02	5.83E+02	1.93E+02
	1.60E+02	5.78E+02	1.92E+02
	1.70E+02	5.76E+02	1.91E+02
	1.80E+02	5.73E+02	1.90E+02
	1.90E+02	5.72E+02	1.89E+02
	2.00E+02	5.73E+02	1.90E+02
	2.10E+02	5.68E+02	1.88E+02
	2.20E+02	5.63E+02	1.87E+02
	2.30E+02	5.63E+02	1.87E+02
	2.40E+02	5.67E+02	1.88E+02
	2.50E+02	5.59E+02	1.85E+02
	2.60E+02	5.58E+02	1.85E+02
	2.70E+02	5.58E+02	1.85E+02
	2.80E+02	5.53E+02	1.83E+02
	2.90E+02	5.52E+02	1.83E+02
	3.00E+02	5.54E+02	1.83E+02
	3.10E+02	5.51E+02	1.82E+02
	3.20E+02	5.50E+02	1.82E+02
	3.30E+02	5.46E+02	1.81E+02
	3.40E+02	5.48E+02	1.81E+02
	3.50E+02	5.45E+02	1.81E+02
	3.60E+02	5.44E+02	1.80E+02

LIGAND EXCHANGE 11/2 D
CuNTA + D to CuD + NTA

init para	data		D (obs)
Cu(bd)	time(sec)	RFU	nM
1.00E-07	0.00E+00		
dye(bd)	2.00E+01	7.90E+02	2.62E+02
5.00E-07	3.00E+01	7.86E+02	2.60E+02
lig(bd)	4.00E+01	7.75E+02	2.57E+02
1.20E-07	5.00E+01	7.60E+02	2.52E+02
	6.00E+01	7.58E+02	2.51E+02
	7.00E+01	7.58E+02	2.51E+02
	8.00E+01	7.58E+02	2.51E+02
	9.00E+01	7.52E+02	2.49E+02
cal slope	1.00E+02	7.52E+02	2.49E+02
3.02E+00	1.10E+02	7.44E+02	2.47E+02
	1.20E+02	7.51E+02	2.49E+02
	1.30E+02	7.55E+02	2.50E+02
	1.40E+02	7.50E+02	2.48E+02
	1.50E+02	7.48E+02	2.48E+02
	1.60E+02	7.55E+02	2.50E+02
	1.70E+02	7.54E+02	2.50E+02
	1.80E+02	7.54E+02	2.50E+02
	1.90E+02	7.51E+02	2.49E+02
	2.00E+02	7.50E+02	2.48E+02
	2.10E+02	7.43E+02	2.46E+02
	2.20E+02	7.38E+02	2.45E+02
	2.30E+02	7.40E+02	2.45E+02
	2.40E+02	7.39E+02	2.45E+02
	2.50E+02	7.32E+02	2.42E+02
	2.60E+02	7.33E+02	2.43E+02
	2.70E+02	7.27E+02	2.41E+02
	2.80E+02	7.27E+02	2.41E+02
	2.90E+02	7.19E+02	2.38E+02
	3.00E+02	7.20E+02	2.38E+02
	3.10E+02	7.13E+02	2.36E+02
	3.20E+02	7.13E+02	2.36E+02
	3.30E+02	7.15E+02	2.37E+02
	3.40E+02	7.08E+02	2.34E+02
	3.50E+02	7.06E+02	2.34E+02
	3.60E+02	7.07E+02	2.34E+02

LIGAND EXCHANGE 10/7/86 F
CuD + EDTA to CuEDTA + D
D (BD) 140 nM
Cu (BD) 100 nM
EDTA (BD) 1000nM

time(sec)	RFU(10)	D (obs) nM
0		
20	357.4	24.28649
30	357.5	24.29328
40	353.9	24.04865
50	355.5	24.15737
60	354.7	24.10301
70	357.4	24.28649
80	359.1	24.40201
90	366.6	24.91166
230	363.5	24.70100
240	359	24.39521
250	368.2	25.02038
260	363.8	24.72139
270	364.5	24.76895
280	365.3	24.82332
290	362.4	24.62625
300	362.4	24.62625
310	363.1	24.67382
320	362.9	24.66023
330	368.7	25.05436
510	378.2	25.69991
520	376.3	25.57080
530	380.2	25.83582
540	377.6	25.65914
550	378.8	25.74069
560	378.6	25.72709
570	379.1	25.76107
580	378.9	25.74748
590	378.2	25.69991
600	382.4	25.98532
610	384.2	26.10763
620	378.7	25.73389
630	383.3	26.04648
840	385.2	26.17559
850	383.9	26.08725
863	376.7	25.59798
880	382.4	25.98532
890	382.9	26.01929
900	384.5	26.12802
910	384.1	26.10084
920	381.2	25.90377
930	384.1	26.10084

LIGAND EXCHANGE 10/7/86 G
CuD + EDTA to CuEDTA + D
D (BD) 140 nM
Cu (BD) 100 nM
EDTA (BD) 2000nM

time(sec)	RFU(10)	D (obs) nM
0		
20	349.2	23.72927
30	347.3	23.60016
40	344.6	23.41668
50	348.7	23.69529
60	344.5	23.40989
70	347.4	23.60695
80	350.7	23.83120
90	347.1	23.58657
260	357.7	24.30687
270	359.4	24.42239
280	357.8	24.31367
290	359.8	24.44957
300	356	24.19135
310	360.6	24.50394
320	364.7	24.78254
330	367.6	24.97961
550	373.2	25.36015
560	373.9	25.40771
570	376.6	25.59119
580	375.9	25.54362
590	377.8	25.67273
600	378	25.68632
610	381.9	25.95134
620	378.5	25.72030
630	376.2	25.56401
830	387.6	26.33867
840	389.1	26.44060
850	388.9	26.42701
860	390.3	26.52215
870	391	26.56972
880	392.3	26.65805
890	393.5	26.73960
900	392.2	26.65126
910	391.8	26.62408
920	394.2	26.78717
930	391.5	26.60369
940	400	27.18129
950	398.8	27.09975
960	395.4	26.86871
1160	398.7	27.09296
1170	403.3	27.40554
1180	405.4	27.54824

LIGAND EXCHANGE 10/8/86 A
CuD + EDTA to CuEDTA + D
D (BD) 140 nM
Cu (BD) 100 nM
EDTA (BD) 2000 nM

time(sec)	RFU(10)	D (obs) nM
0		
20	355	24.09818
30	355.4	24.12523
40	349.8	23.74519
50	354.4	24.05745
60	359.2	24.38329
70	361.9	24.56657
80	359.6	24.41044
90	358.1	24.30861
210	364.6	24.74985
220	365.2	24.79058
230	364.2	24.72270
240	364.1	24.71591
250	363.7	24.68876
260	368.2	24.99423
270	363.7	24.68876
280	365.9	24.83810
290	366.8	24.89919
300	369.1	25.05532
310	367.2	24.92634
320	369.2	25.06211
520	370.1	25.12320
530	371.9	25.24539
540	370.7	25.16393
550	370.5	25.15035
560	370.5	25.15035
570	371.8	25.23860
580	375.2	25.46940
590	366.4	24.87204
600	363.8	24.69554
610	367.9	24.97386
620	370	25.11641
810	374.4	25.41509
820	376.2	25.53728
830	378	25.65947
840	377.7	25.63911
850	382.8	25.98531
860	381.7	25.91063
870	380.6	25.83596
880	377.6	25.63232
890	373.6	25.36079
900	380.1	25.80202
910	390.5	26.50800
920	384.3	26.08713
930	383.8	26.05319
1160	386.2	26.21610
1170	382.6	25.97173
1180	386.3	26.22289
1190	386.2	26.21610
1200	387	26.27041
1210	386.6	26.24326
1220	388.3	26.35866
1230	391.3	26.56230

LIGAND EXCHANGE 10/8/86 B
CuD + EDTA to CuEDTA + D
D (BD) 140 nM
Cu (BD) 100 nM

EDTA (BD) 4000 nM

time(sec)	RFU(10)	D (obs) nM
0		
20	345.5	23.45330
30	349.1	23.69767
40	353.3	23.98278
50	355.2	24.11176
60	354.2	24.04387
70	346.3	23.50760
80	352.8	23.94884
90	355.9	24.15927
240	371.9	25.24539
250	369.1	25.05532
260	369	25.04853
270	369.3	25.06890
280	369.9	25.10962
290	372.7	25.29969
300	375.4	25.48298
310	373.8	25.37437
320	375.8	25.51013
330	376	25.52371
520	384	26.06676
530	384.4	26.09392
540	387.1	26.27720
550	382.6	25.97173
560	388.5	26.37223
570	390.5	26.50800
580	389.8	26.46048
590	387.3	26.29078
600	389.7	26.45369
610	391.2	26.55552
620	391.9	26.60303
840	399.8	27.13930
850	397.8	27.00354
860	403.8	27.41083
870	402.4	27.31580
880	404.1	27.43120
890	398.9	27.07821
900	405.7	27.53981
910	403.7	27.40404
920	404.7	27.47193
1120	413.8	28.08965
1130	414.6	28.14396
1140	408.5	27.72988
1150	412.8	28.02177
1160	412.2	27.98104
1170	414.9	28.16432
1180	410.3	27.85207
1190	415.9	28.23221
1200	414.4	28.13038
1210	413.4	28.06250
1220	419.7	28.49016
1230	416.3	28.25936

LIGAND EXCHANGE 10/8/86 C
CuD + EDTA to CuEDTA + D

D (BD) 140 nM
Cu (BD) 100 nM
EDTA (BD) 8000 nM

time(sec)	RFU(10)	D (obs) nM
0		
20	335.5	22.84453
30	340.9	23.14324
40	339.8	23.06856
50	345.3	23.44195
60	344.8	23.40801
70	346.3	23.50984
80	345.9	23.48268
90	347.5	23.59131
230	360.3	24.46028
240	366	24.84725
250	367.6	24.95587
260	370.9	25.17990
270	375.6	25.49898
280	369	25.05091
290	357.3	24.25661
300	364	24.71147
310	363.1	24.65037
320	365.7	24.82688
330	372.4	25.28173
530	393.4	26.70739
540	380.9	25.85879
550	394.1	26.75492
560	407.6	27.67141
570	407	27.63068
580	403.2	27.37270
590	404.6	27.46775
600	403.8	27.41344
610	409.3	27.78682
620	406.8	27.61710
630	411	27.90224
830	407.8	27.68499
840	411.3	27.92260
850	422.5	28.68295
860	408.5	27.73251
870	427.4	29.01561
880	422.4	28.67617
890	417.9	28.37067
900	421.8	28.63543
910	421.2	28.59470
920	430.2	29.20570
930	436.8	29.65376
940	435.1	29.53835
1110	441.9	30
1120	438.9	29.79633
1130	444.4	30.16972
1140	456.5	30.99117
1150	452.3	30.70604
1160	451.6	30.65852
1170	446.7	30.32586
1180	447.3	30.36659
1190	448.5	30.44806
1200	446.3	30.29871
1210	447.7	30.39375
1220	449.7	30.52953
1230	447.1	30.35302

LIGAND EXCHANGE 10/8/86 D
CuD + EDTA to CuEDTA + D
D (BD) 280 nM
Cu (BD) 200 nM
EDTA (BD) 2000 nM

time(sec)	RFU(5)	D (obs) nM
0		
20	322.9	43.83833
30	320.9	43.56680
40	322.6	43.79760
50	320.8	43.55322
60	327.1	44.40854
70	321.8	43.68899
80	309.3	41.99193
90	305.3	41.44887
220	317	43.03732
230	317.5	43.10520
240	317.9	43.15950
250	319.7	43.40388
260	325.2	44.15058
270	323.7	43.94694
280	325.3	44.16416
290	322.9	43.83833
300	328.5	44.59861
310	325.1	44.13701
320	329.4	44.72080
330	324.5	44.05555
530	342.6	46.51289
540	340	46.15990
550	344.3	46.74369
560	344.5	46.77084
570	346.7	47.06952
580	350.4	47.57185
590	345.8	46.94733
600	352.3	47.82980
610	350.3	47.55827
620	348.8	47.35463
630	343.8	46.67580
830	345.8	46.94733
840	340.9	46.28209
850	353.4	47.97914
860	348.9	47.36820
870	347	47.11025
880	349.7	47.47681
890	345.2	46.86587
900	343	46.56719
910	346.9	47.09667
920	352.3	47.82980
930	351.2	47.68046
940	345.6	46.92018
1120	359.9	48.86161
1130	367.7	49.92057
1140	362.9	49.26890
1150	367.1	49.83911
1160	365.3	49.59474
1170	365.1	49.56759
1180	360.3	48.91592
1190	367.7	49.92057
1200	368.7	50.05634
1210	367.5	49.89342
1220	367.6	49.90700
1230	369.3	50.13780

LIGAND EXCHANGE 10/7/86 E
CuD + EDTA to CuEDTA + D
D (BD) 140 nM
Cu (BD) 100 nM
EDTA (BD) 500 nM

time(sec)	RFU(10)	D (obs) nM
0		
20	322.2	21.89453
30	317.8	21.59554
40	322.6	21.92171
50	323	21.94889
60	325.2	22.09839
70	328.2	22.30225
80	319	21.67708
90	321.1	21.81978
230	334.6	22.73715
240	328.4	22.31584
250	331.8	22.54688
260	328.5	22.32264
270	335.9	22.82549
280	332.5	22.59445
290	339.1	23.04294
300	335.4	22.79151
310	330	22.42457
320	330.1	22.43136
330	334.3	22.71677
520	346.2	23.52541
530	347.3	23.60016
540	341	23.17205
550	345.6	23.48464
560	347.9	23.64093
570	344.1	23.38271
580	342.1	23.24680
500	345.4	23.47105
600	338.1	22.97499
610	342.4	23.26719
620	342.3	23.26039
630	347.1	23.58657
900	345.9	23.50502
910	346.6	23.55259
920	345.9	23.50502
930	343.5	23.34194
940	350.2	23.79722
950	346.3	23.53220
960	344.5	23.40989
1190	409.7	27.84044
1200	407.2	27.67056
1210	409.7	27.84044
1220	406	27.58901
1230	403.9	27.44631
1240	403.9	27.44631
1440	412.7	28.04430
1450	416.1	28.27534
1460	415.9	28.26175
1470	418.5	28.43843
1480	421.1	28.61511
1500	421	28.60831
1510	413	28.06469
1520	415.6	28.24136
1530	420	28.54036
1700	423.2	28.75781
1710	427.4	29.04321
1720	429.5	29.18592
1730	429.6	29.19271
1740	425.5	28.91410
1750	425.7	28.92769
1760	428.4	29.11117
1770	430.8	29.27425
1780	425.1	28.88692
1790	428.1	29.09078
1800	432.1	29.36259
1810	428.5	29.11796
1820	430.9	29.28105

LIGAND EXCHANGE 10/8/86 E
CuD + EDTA to CuEDTA + D
D (BD) 280 nM
Cu (BD) 200 nM
EDTA (BD) 4000 nM

time(sec)	RFU(5)	D (obs) nM
20	319.3	43.34957
30	319.9	43.43103
40	318.6	43.25454
50	320.1	43.45819
60	318.6	43.25454
70	318.7	43.26812
80	321.8	43.68899
90	323	43.85190
230	338.8	45.99698
240	338.8	45.99698
250	338.4	45.94268
260	340.7	46.25493
270	339.6	46.10559
280	338.9	46.01056
290	336.9	45.73903
300	344.4	46.75726
310	342.5	46.49931
560	363.4	49.33679
570	364.9	49.54043
580	366.6	49.77123
590	366.2	49.71693
600	365.8	49.66262
610	366.4	49.74408
620	364.7	49.51328
630	368.3	50.00203
820	383.7	52.09280
830	376.5	51.11530
840	378.1	51.33252
850	379.1	51.46829
860	385.3	52.31003
870	383.1	52.01134
880	385.5	52.33718
890	381.3	51.76697
900	376.7	51.14245
910	384.7	52.22857
920	386.1	52.41864
930	385.5	52.33718
1170	399.4	54.22430
1180	397.1	53.91205
1190	398.7	54.12927
1200	396.1	53.77628
1210	394.9	53.61337
1220	396.9	53.88489
1230	394.6	53.57264
1240	398.1	54.04781
1250	398.5	54.10212
1260	400.4	54.36007

LIGAND EXCHANGE 10/8/86 F
CuD + EDTA to CuEDTA + D
D (BD) 280 nM
Cu (BD) 200 nM
EDTA (BD) 8000 nM

time(sec)	RFU(5)	D (obs) nM
20	303.7	41.23165
30	311	42.22273
40	316.7	42.99659
50	319.6	43.39030
60	322.3	43.75687
70	324.8	44.09628
80	323.6	43.93336
90	331.5	45.00590
220	332.7	45.16882
230	333.6	45.29101
240	334.3	45.38604
250	336.7	45.71188
260	338.6	45.96983
270	341.7	46.39070
280	349.2	47.40893
290	356.1	48.34571
300	361.1	49.02453
310	354.6	48.14206
320	355.2	48.22352
330	358.2	48.63081
340	363.5	49.35036
540	380.4	51.64478
550	384.4	52.18784
560	381.9	51.84843
570	377.7	51.27822
580	384.3	52.17426
590	384.6	52.21499
600	387.4	52.59513
610	388.8	52.78520
620	389.9	52.93454
630	393.5	53.42329
640	392.8	53.32826
820	408.4	55.44618
830	399.5	54.23788
840	402.2	54.60445
850	396.4	53.81701
860	401.6	54.52299
870	401.8	54.55014
880	408.7	55.48691
890	412.6	56.01640
900	412.6	56.01640
910	412.7	56.02997
920	411.6	55.88063
930	414.3	56.24719
1120	419	56.88529
1130	421.4	57.21112
1140	420.4	57.07536
1150	426.4	57.88994
1160	427.6	58.05286
1170	431.1	58.52804
1180	428	58.10717
1190	429	58.24293
1200	431.9	58.63665
1210	439	59.60058
1220	434	58.92175
1230	433.2	58.81314
1240	431.7	58.60950

LIGAND EXCHANGE 1/22/88 IIA
CuD + NTA to CuNTA + D
D (final) 100 nM
Cu (final) 100 nM
NTA (final) 10 μM

time (h)	D (obs) nM
0.07	22.85
0.24	33.87
0.64	45.93
1.41	51.62
2.01	52.82
3.40	54.70

LIGAND EXCHANGE 1/22/88 IIB
CuD + NTA to CuNTA + D
D (final) 100 nM
Cu (final) 100 nM
NTA (final) 10 μM

time (h)	D (obs) nM
0.11	27.06
0.28	36.77
0.68	47.23
1.45	52.13
2.04	53.07
3.44	55.09

DOCUMENT LIBRARY

August 21, 1987

Distribution List for Technical Report Exchange

Attn: Stella Sanchez-Wade
Documents Section
Scripps Institution of Oceanography
Library, Mail Code C-075C
La Jolla, CA 92093

Hancock Library of Biology &
Oceanography
Alan Hancock Laboratory
University of Southern California
University Park
Los Angeles, CA 90089-0371

Gifts & Exchanges
Library
Bedford Institute of Oceanography
P.O. Box 1006
Dartmouth, NS, B2Y 4A2, CANADA

Office of the International
Ice Patrol
c/o Coast Guard R & D Center
Avery Point
Groton, CT 06340

Library
Physical Oceanographic Laboratory
Nova University
8000 N. Ocean Drive
Dania, FL 33304

NOAA/EDIS Miami Library Center
4301 Rickenbacker Causeway
Miami, FL 33149

Library
Skidaway Institute of Oceanography
P.O. Box 13687
Savannah, GA 31416

Institute of Geophysics
University of Hawaii
Library Room 252
2525 Correa Road
Honolulu, HI 96822

Library
Chesapeake Bay Institute
4800 Atwell Road
Shady Side, MD 20876

MIT Libraries
Serial Journal Room 14E-210
Cambridge, MA 02139

Director, Ralph M. Parsons Laboratory
Room 48-311
MIT
Cambridge, MA 02139

Marine Resources Information Center
Building E38-320
MIT
Cambridge, MA 02139

Library
Lamont-Doherty Geological
Observatory
Colombia University
Palisades, NY 10964

Library
Serials Department
Oregon State University
Corvallis, OR 97331

Pell Marine Science Library
University of Rhode Island
Narragansett Bay Campus
Narragansett, RI 02882

Working Collection
Texas A&M University
Dept. of Oceanography
College Station, TX 77843

Library
Virginia Institute of Marine Science
Gloucester Point, VA 23062

Fisheries-Oceanography Library
151 Oceanography Teaching Bldg.
University of Washington
Seattle, WA 98195

Library
R.S.M.A.S.
University of Miami
4600 Rickenbacker Causeway
Miami, FL 33149

Maury Oceanographic Library
Naval Oceanographic Office
Bay St. Louis
NSTL, MS 39522-5001

50272-101

REPORT DOCUMENTATION PAGE	1. REPORT NO. WHOI-88-22	2.	3. Recipient's Accession No.

4. Title and Subtitle

The Kinetics and Thermodynamics of Copper Complexation in Aquatic Systems

5. Report Date June 1988

6.

7. Author(s)

Janet G. Hering

8. Performing Organization Rept. No. WHOI-88-22

9. Performing Organization Name and Address

The Woods Hole Oceanographic Institution
Woods Hole, Massachusetts 02543, and
The Massachusetts Institute of Technology
Cambridge, Massachusetts 02139

10. Project/Task/Work Unit No.

11. Contract(C) or Grant(G) No.

(C) N00014-86-K-0325

(G)

12. Sponsoring Organization Name and Address

Through MIT:
The National Science Foundation; NOAA; and the Office of Naval Research

13. Type of Report & Period Covered Ph.D. Thesis

14.

15. Supplementary Notes

This thesis should be cited as: Janet G. Hering, 1988. The Kinetics and Thermodynamics of Copper Complexation in Aquatic Systems Ph.D., MIT/WHOI, WHOI-88-22.

16. Abstract (Limit: 200 words)

Copper complexation is ubiquitous in natural waters. Yet, many questions remain on the chemistry and biogeochemistry of naturally-occurring complexing agents. This thesis examines the sources and extent of biological cycling of such complexing agents and also the physical-chemical nature of their interactions with copper.

Investigations of copper complexation in coastal ponds and coordinated laboratory studies suggest that both labile, biogenic and refractory ligands contribute to the observed copper complexation. Culture and incubation experiments demonstrate ligand production associated with phytoplankton photosynthetic activity and suggest microbial degradation of complexing agents. However in the coastal ponds studied, the biological cycling of natural complexing agents is obscured possibly due to contributions of refractory ligands to the observed copper complexation, mixing of pond waters with coastal seawater, or to the natural balance between biological production and degradation.

The physical-chemical nature of interactions of humic acids with copper was studied by examining both the thermodynamics and kinetics of these interactions. Extensive studies of the kinetics of metal- and ligand-exchange reactions with well-defined ligands under natural water conditions (i.e.- low concentrations of reacting species and the presence of competing metals and ligands) provide a mechanistic framework for examining the kinetics of metal-humate complexation reactions.

Study of the kinetics of copper-for-calcium metal-exchange reactions and metal titration experiments (individual metal titrations with calcium or copper and copper titrations in the presence of calcium as a competing metal) show that alkaline earth and transition metals do not compete for the same humate metal-binding sites.

17. Document Analysis a. Descriptors

1 copper
2. complexation
3. kinetics

b. Identifiers/Open-Ended Terms

c. COSATI Field/Group

18. Availability Statement

Approved for publication; distribution unlimited.

19. Security Class (This Report) UNCLASSIFIED

20. Security Class (This Page)

21. No. of Pages 308

22. Price

(See ANSI-Z39.18) *See Instructions on Reverse*

OPTIONAL FORM 272 (4-77)
(Formerly NTIS-35)
Department of Commerce